UNDERSTANDING ALTERED IMMUNE RESPONSES TO INFLUENZA B VIRUSES

by

THOMAS ROWE

(Under the Direction of Ted M. Ross)

ABSTRACT

The vast majority of influenza studies focus on influenza A viruses (IAV); however, influenza B viruses (IBV) represent nearly one quarter of all influenza cases and are generally responsible for most cases late in the influenza season. The ferret is the gold standard animal model for influenza research in that it can readily be infected with influenza clinical samples, has similar course of disease, generate similar immune responses following infection and vaccination, and can transmit infectious virus to other ferrets and humans. Antibodies generated following infection of ferrets with human influenza viruses are used in surveillance to distinguish antigenic drift and cross-reactivity between vaccine viruses and circulating strains. IAVs generate robust antibody responses in ferrets, whereas IBVs require an additional booster dose over 85% of the time to generate equivalent antibody titers.

This PhD investigates the disparity between IAV and IBV in ferret immune responses following infection and interventions to improve immune responses to IBV. Initial in vitro studies in primary, differentiated ferret nasal epithelial cell cultures reveal that delays in pro-inflammatory cytokines and interferons may play an important role in

communication with other immune cells to allow for generation of robust antibody responses. Subsequent in vivo studies confirmed suppressed innate responses including reduced pro-inflammatory cytokines and interferons (IFN) in the serum. Compared to IAV infection, weak, delayed antibody levels were seen following IBV infection. The addition of adjuvanted ferret IFN was able to stimulate innate immune responses resulting in increased antibody levels in both IBV infected and vaccinated animals compared to untreated animals. These studies confirmed the low and delayed adaptive immune responses by IBV and provide further evidence that initial innate responses, especially IFN and proinflammatory responses play an important role in developing robust antibody responses. This work adds additional ferret immune reagents to aid in unraveling immune processes following infection with new and emerging respiratory viruses and the development of improved countermeasures quickly to address public health needs.

INDEX WORDS: influenza B, ferret, innate, interferon, antibody response

UNDERSTANDING ALTERED IMMUNE RESPONSES TO INFLUENZA B VIRUSES

by

THOMAS ROWE

B.S., The University of Georgia, 1986

M.S., Georgia Institute of Technology, 1999

A Dissertation Submitted to the Graduate Faculty of The University of Georgia in Partial Fulfillment of the Requirements for the Degree

DOCTOR OF PHILOSOPHY

ATHENS, GEORGIA

2024

UNDERSTANDING ALTERED IMMUNE RESPONSES TO INFLUENZA B VIRUSES

by

THOMAS ROWE

Major Professor:	Ted M. Ross
Committee:	Kim Klonowski
	Stephen M. Tompkins
	Wendy T. Watford
	David E. Wentworth

Electronic Version Approved:

Ron Walcott
Vice Provost for Graduate Education and Dean of the Graduate School
The University of Georgia
May 2024

DEDICATION

"The important thing is to never stop questioning; curiosity has its own reason for existing" Albert Einstein.

I dedicate this dissertation to my wife Abby for standing by me and putting up with my messy office and long evenings working on this dissertation or papers or having to go into the lab many nights and weekends for experimental timepoints. You can now say "you call him Dr. Rowe!", or just Thomas :). You made it through with me, whew. I love you.

I also dedicate this dissertation to my parents Gene (Poppy/Padre) and Gerda (Mommy/Madre) who were with me from day 1 and always for supporting my science dream from an early age from my first science experiments and fascination with biology to helping me obtain my B.S. degree at UGA those many years ago. Thank you for your sacrifices, I love you both and glad you are here with me to see me finally finish my degree. To my children Matthew, Emily, Stephanie, and John. I don't know if you remember a time when I WASN'T in school.

……and to Sam, you were a good boy.

ACKNOWLEDGEMENTS

I would like to thank Dr. Tom Voss for being a good friend and supporting my decision to return to school after a long absence, talking science with me, as well as keeping me excited about science. Third try is the charm! I would also like to thank my committee for listening to my often-long presentations and keeping me on point and focused. I would especially like to thank Dr. Dave Wentworth for allowing me to take on this endeavor for a PhD, agreeing that it was a worthwhile project and allowing me to use lab space and resources. Dr. Ted Ross for being an excellent major professor on my committee, especially for always being there to listen to my ideas and guiding me in the right direction. You are a good friend and stellar virologist!

Thank you to my colleagues at CDC, especially to Gaby Jasso and Yasuko Hatta for helping with ferret "wrangling", to Ansley Smith for helping me in the lab and keeping my cells alive, and to Melissa Lange for running HI's for me. Also, my fellow current and former students at UGA, especially Alex Richardson for collaborating with me to tease out ferret immune responses from ferret samples, Michael Carlock and Dr. James Allen for valuable discussions and collaborations and Dr. Greg Kirchenbaum for helpful discussions and always questioning (that's a good thing).

Thank you, Joanna LaBresh at Kingfisher Biotech for collaboration and generating ferret interferons, especially IFNλ3. It works great! Ashley Fletcher and Dr. Laurie Stephen from Ampersand Biosciences for their collaboration and development of ferret

multiplex assays to evaluate many ferret serum and nasal wash samples to help understand immune responses. Dr. Xinxia Peng and Tammy Tollison at NC State for collaborations on single cell RNA-seq for ferrets. Looking forward to the complete gene annotations.

Thank you all.

TABLE OF CONTENTS

Page

LIST OF ABBREVIATIONS

ABBREVIATION	DEFINITION
#K	Thousand. # indicates number, i.e. 20K = 20,000
AAALAC	Association for Assessment and Accreditation of Laboratory Animal Care International
ADCC	Antibody-Dependent Cell-mediated Cytotoxicity
ALI	Air-Liquid Interface
APCs	Antigen presenting cells [i.e. macrophages, dendritic cells(DC)]
ANOVA	Analysis of Variance
ASC	Antibody Secreting Cells
bax	B-Cell Lymphoma 2 Associated X gene
BCIP/NBT	5-bromo-4-chloro-3-indolyl phosphate (**BCIP**)/nitro blue tetrazolium (**NBT**)
BCL-2	B-Cell Lymphoma 2 gene
BHQ1	Black-Hole Quencher 1
BR	Influenza B/Brisbane/60/2008 virus (B-Victoria lineage)
BSA	Bovine Serum Albumin
CA	Influenza A/California/07/2009 virus (H1N1pdm09 subtype)
CC	Cell Control
CCL2	Chemokine (C-C motif) Ligand 2 gene
cRNA	Complementary RNA (positive sense)

ABBREVIATION	DEFINITION
C_T	Cycle Threshold
CXCL10	Chemokine interferon-gamma inducible protein 10kDa
D#	Day (# = value), i.e. D3 = day 3
DAMP	Damage-Associated Molecular Pattern
DC	Dendritic Cell
DMEM	Dulbecco's Modified Eagle Medium
DMSO	Dimethyl Sulfoxide
DNA	Deoxyribonucleic Acid
EC	Epithelial Cell
EDTA	Ethylenediaminetetracetic Acid
ELISA	Enzyme Linked Immunosorbant Assay
ELISpot	Enzyme-linked Immunosorbant Spot Assay
EXPRES	Expression (fold gene expression)
F/T	Freeze/Thaw
FAM	Fluorescein Amidites (fluorescent dye in oligonucleotide synthesis)
FBS	Fetal Bovine Serum
FFA	Focus Forming Assay
FFU	Focus Forming Units
fIFNx	Ferret Interferon X [X = alpha (α) "A", beta (ß) "B", gamma (γ) "G", or lambda (λ) "L" or "L3"]
FNEC	Ferret Nasal Epithelial Cells

ABBREVIATION	DEFINITION
FOXP3	Forkhead Box Protein 3 gene
FRA	Focus Reduction Assay
GAPDH	Glyceraldehyde-3-phosphate dehydrogenase gene (housekeeping gene)
GMT	Geometric Mean Titer
GRANA or *Granzyme A*	Granzyme A gene
HA	hemagglutinin
HAI	Hemagglutinin Inhibition Assay
HEK	Human Embryonic Kidney (HEK 293 cell line)
HI	Hemagglutinin Inhibition Assay
hIFNx	Human Interferon X [X = alpha (α) "A", beta (ß) "B", gamma (γ) "G", or lambda (λ) "L" or "L3"]
HIV	Human Immunodeficiency Virus
hNEC	Human Nasal Epithelial Cells
Hr	Hour
IACUC	Institutional Animal Care and use Committee
IAV	Influenza A Virus
IBV	Influenza B Virus
IFNA	Interferon alpha (α) gene
IFNB	Interferon beta (ß) gene
IFNG	Interferon gamma (γ) gene

ABBREVIATION	DEFINITION
IFNL	Interferon lambda (λ) gene
IFNL3	Interferon lambda 3(λ) gene
IFNx	Interferon X [X = alpha (α) "A", beta (ß) "B", gamma (γ) "G", or lambda (λ) "L" or "L3"] protein
Ig	Immunoglobulin
IL-12p40 (IL-12p40)	Interleukin-12 p40 subunit gene (protein)
IL-17 (IL-17)	Interleukin-17 gene (protein)
IL-1B	Interleukin-1 beta gene
IL-2 (IL-2)	Interleukin-2 gene (protein)
IL-4 (IL-4)	Interleukin-4 gene (protein)
IL-6 (IL-6)	Interleukin-6 gene (protein)
IP-10 (IP-10)	Interleukin-10 gene (protein)
IRF	Interferon Regulatory Factor gene
ISG	Interferon-Stimulated Gene
KS	Influenza A/Kansas/14/2017 virus (H3N2 subtype)
LAIV	Live-attenuated Influenza Virus
LCMV	Lymphocytic Choriomeningitis Virus
LNA A	Locked Nucleic Acid (A=adenine)
LPS	Lipopolysaccharides (Gram negative cell wall component)
LRT	Lower Respiratory Tract
M1	Influenza Matrix 1 gene

ABBREVIATION	DEFINITION
MCP-1 (MCP-1)	Monocyte chemoattractant Protein-1 gene (protein)
MDCK	Madin Darby Canine Kidney
MEM	Modified Eagle Medium
MHC-I	Major Histocompatibility Complex-I
MHC-II	Major Histocompatibility Complex-II
mL	Milliliter
MO	Month
MOCK	Mock (Vehicle or phosphate buffered saline)
MOI	Multiplicity of Infection
mRNA	Messenger Ribonucleic Acid
NA	Influenza Neuraminidase Gene or protein
N/A	Not applicable
NEAA	Non-essential Amino Acids
nG/mL	nanograms per milliliter
NHP	Non-human Primate
NLR	Nucleotide Oligomerization Domain-like receptors
NOD	Nucleotide Oligomerization Domain
NS1	Influenza Nonstructural Protein 1 encoded by NS gene
NT	Nasal Turbinate
NW	Nasal Wash
PAMP	Pathogen-associated Molecular Patterns
PBMC	Peripheral Blood Mononuclear Cells

ABBREVIATION	DEFINITION
PBS	Phosphate Buffered Saline
PBST	Phosphate Buffered Saline with Tween
PCR	Polymerase Chain Reaction
PEG	Polyethylene Glycol
pG/mL	picograms per milliliter
PH	Influenza B/Phuket/3073/2013 virus (B-Yamagata lineage)
pInoc	Post Inoculation
PRR	Pathogen Recognition Receptor
qRT-PCR	Real-Time Quantitative Reverse Transcription Polymerase Chain Reaction
r	Correlation Coefficient (R>0 = Direct Correlation; r<0 Inverse or Negative Correlation)
RANTES	Regulated upon Activation, Normal T cell Expressed and Secreted gene
RBC	Red blood cell (erythrocytes)
RDE	Receptor Destroying Enzyme
rHA	Recombinant Hemagglutinin Protein
RIG-I	Retinoic acid-inducible gene I
RII	Relative Inactivity Index (Measure of lethargy)
RNA	Ribonucleic Acid
SARS-CoV2	Severe Acute Respiratory Syndrome Coronavirus 2
SDS	Sodium Dodecyl Sulfate

ABBREVIATION	DEFINITION
SEAP	Secreted Embryonic Alkaline Phosphatase
SFU	Spot Forming Units
SM	Sooty mangabey (*Cercocebus atys*), Old World non-human primate
SOCS3	Suppressor Of Cytokine Signaling 3 gene
SST	Serum Separator Tube
STAT1	Signal Transducer and Activator of Transcription 1 gene
STAT2	Signal Transducer and Activator of Transcription 2 gene
STAT3	Signal Transducer and Activator of Transcription 3 gene
STD	Standard
Teff	Effector T-cells
Tfh	Follicular Helper T cells
TfR	Transferrin Receptor
TGFB (TGFB1)	Transforming Growth Factor Beta 1 gene
Th1	T-helper 1 response
Th2	T-helper 2 response
TNF	Tumor Necrosis Factor
TPCK	N-alpha-tosyl-l-phenylalanyl chloromethyl ketone (chymotrypsin inhibitor)
TRBC	Turkey Red Blood Cells (erythrocytes)
Treg	Regulatory T-cells
*TSLP (*TSLP)	Thymic Stromal Lymphopoietin gene (Protein)

ABBREVIATION	DEFINITION
TYK2	Tyrosine Kinase 2 gene
URT	Upper Respiratory Tract
USP18	Ubiquitin-Specific Peptidase 18 gene
VAL	Valine amino acid
VC	Virus Control
VE	Vaccine Efficacy
VGM-T	Virus Growth Medium with TPCK-Trypsin
vRNA	Viral RNA (negative sense)
WHO	World Health Organization
Wk	Week

LIST OF TABLES

Page

LIST OF FIGURES

Page

CHAPTER 1

INTRODUCTION

Most influenza studies focus on influenza A viruses (IAV); however, influenza B viruses (IBV) represent nearly one quarter of all influenza cases and are generally responsible for most cases late in the influenza season [1]. Even though IBV co-circulates with IAV, little is known about the antibody and cellular responses following IBV infection [2]. Currently, a hemagglutination inhibition (HI) titer of 1:40 correlates with protection of influenza vaccines administered to healthy adults corresponding to a 50% reduction in risk of contracting influenza virus [3]; however this risk reduction requires an HI titer of at least 1:110 in children [4]. The conventional titer of 1:40 seen in adults was only associated with 22% protection in children. Consequently, low HI antibody titers of <1:160 following initial influenza infection or vaccination may indicate an inadequate immune response to fully protect from subsequent exposure to virus. This low antibody response could be due to a delay or suppression in initial innate immune signals following infection in the host. Since there exists significant similarity in the infection and disease course of IAV and IBV in both humans and ferrets, understanding the mechanism of immune responses in the IBV-infected ferret may aid in better understanding human IBV infection. Innate immune responses in ferrets have only focused on influenza A viruses where an association between innate immune responses

and transmission and virulence has been found [5]. In order to understand the altered immune responses to IBV, a review of influenza and animal models used is warranted.

INFLUENZA A AND B VIRUSES

Influenza viruses can cause mild to severe respiratory infections in humans and remain a major public health problem worldwide. According to the World Health Organization seasonal influenza viruses cause around one billion cases each year including 3 – 5 million severe illnesses. Additionally, influenza causes between 290,000 and 650,000 deaths annually with 99% of deaths in children under 5 years of age with influenza-related lower respiratory tract infections in developing countries [6]. Influenza viruses belong to the virus family *Orthomyxoviridae* and are characterized by a negative sense, segmented single-strand RNA genome. Three different genera, influenza A, B, and C have been known to infect humans. Influenza A viruses (IAV) are further classified into subtypes based on the antigenicity of their hemagglutinin (HA) and neuraminidase (NA) surface proteins [7]. Viruses of all known subtypes HA (H1 – H16) and NA (N1 – N9) are maintained in wild aquatic birds. Two additional HA and NA subtypes have been discovered, H17N10 [8] and H18N11 [9]; however, these are only found in bats and have not been found to be able to transmit to humans [10].

B viruses (IBV) are classified according to their lineage. IBV is divided into two lineages based on their HA protein: B-Victoria and B-Yamagata which have diverged from a common lineage in the late 1970s [11] and have cocirculated until the 2020s. However, B-Yamagata lineage viruses infections have declined dramatically since the COVID-19 pandemic and have not shown to circulate currently [12, 13]. Contrary to

IAV, IBV is not known to cause pandemics mostly due to its limited host range. Both IAV and IBV co-circulate in humans and are responsible for most of the diagnosed cases of seasonal influenza each year. Since influenza viruses have segmented genomes, reassortment of primarily their surface proteins are an important mechanism for their diversity. Since IAV animal reservoir is birds, primarily waterfowl, reassortant viruses between avian and human viruses have led to the emergence of several pandemics in the past century. Reassortant events resulting in emergent human pandemics are primarily through the introduction of HA, and to a lesser extent NA gene, derived from the avian reservoir and internal genes from a human virus. However, the 2009 H1N1 pandemic (H1N1pdm09) was the result of a triple reassortment event with avian, human and swine genes [14, 15]. The reassortment usually occurs within a "mixing-vessel" species which has both human (α2,6-linked sialic acid) and avian (α2,3-linked sialic acid) receptors in the respiratory tract [16]. Susceptibility of humans coupled with introduction of a new HA and/or NA in an immunological naïve population has resulted in pandemics of IAV in humans. This reassortment primarily occurs by IAV are given the greatest attention due to their infrequent infections from zoonotic transmission from animals which give rise to pandemic viruses through genetic reassortment, known as antigenic shift, as well as sustained antigenic drift, transmission, and severity of disease.

Wild aquatic birds are the main reservoir for IAV which can cause pandemics when new subtypes have been reassorted and introduced into humans usually through an animal intermediary, such as the pig. Influenza A viruses are divided into subtypes based on two surface proteins, hemagglutinin (HA) and neuraminidase (NA). All known subtypes of IAV have been found in birds (H1-H16 and N1-N9), except H17N10 and

H18N11 which have only been found in bats [8]. Once IAV is introduced into humans these viruses cause seasonal epidemics through antigenic drift of the hemagglutinin (HA) and neuraminidase (NA) genes [7]. The origins of IBV in humans is unclear but was first isolated around 1940 and has later divided into two clear lineages by 1983, the Yamagata-like and Victoria-like [11]. IBV has not been demonstrated to cause pandemics. Unlike IAVs, IBVs do not have a known animal reservoir and do not pose the same pandemic risks as IAVs and have therefore received less attention. However, IBVs represent approximately 25% of all cases late in the influenza season [1] and result in increased mortality in children compared to adults [17]. IBVs have stably adapted to humans, which are proposed to be the reservoir for these viruses, and may only have infected other species such as dogs, pigs, and seals by reverse zoonotic events [18-20]. Since the IBV reservoir appears to be mammalian, and potentially humans, questions exist about the persistence of IBV in humans, including: 1) Could IBV persistence be due to a defect in the human innate and subsequent adaptive immune responses? and 2) Can these deficiencies be overcome through modified vaccines to provide broader and/or more robust protection? To answer these unknowns and develop better vaccines and interventions to IBVs, it is important to understand how these viruses evade the immune system and alter innate and adaptive immune responses.

An example of an animal reservoir is the e Sooty mangabey (SM) non-human primate which is a natural reservoir for simian immunodeficiency virus (SIV) and does not develop disease following SIV infection [21]. In contrast, Black and Rhesus macaques (RM) infected with SIV leads to development of immunodeficiency and persistent virus replication [22, 23]. Infection of SM with SIV results in reduced IFNα

production by plasmacytoid dendritic cells, whereas RM activate the innate responses to produce IFNα, IL-10 and TNFα [24]. Other immunological differences include suppression and delay of innate immune responses in rodent reservoirs for Hantaviruses [25, 26] and reduced IFNα responses leading to attenuated adaptive immune responses in SM reservoir for yellow fever virus [27].

IBV infections generally induce milder disease than IAV infections in humans; however, IBV is the most prominent circulating type of influenza every four to five years and carry higher risks of hospitalizations than IAV infections in HIV-infected individuals [28]. During the 2010-2011 influenza season, IBV was responsible for 38% of pediatric deaths [29] and in a Canadian study from 2004-2013 found that significantly higher mortality rates following IBV infection compared to IAV was observed in children younger than 16 years of age [17]. The vaccine effectiveness of influenza B is low in susceptible populations such as children between 9-17 years of age (28% effective for B-Yamagata lineage) [30]. Since children have greater morbidity and mortality to IBV compared to IAV infections, their immunological development may play a role in their responses to IBV in this age group. Several factors in early life immune responses are different from adults and include: 1) neonatal CD4+ and CD8+ T cells produce decreased IFNγ and TNFα upon exposure to pathogenic bacteria, 2) cord blood contains increased CD4+CD25+ regulatory T cells (Treg) that may inhibit adaptive immune responses, 3) Increased levels of IL-4/IL-10/IL-13/ TGFß in cord blood compared to adults, and 4) neonatal plasma inhibits TLR-mediated generation of pro-inflammatory cytokines [31]. Treg effects on anti-influenza antibody responses have shown that TGFß as well as CD4+Foxp3+ Treg cells may act as checkpoints between antibody production after

vaccination as shown by lower antibody titers to influenza B component in a human vaccine study of healthy young adults 35.6±12.5 years [32]. These early life immune responses are biased against pro-inflammatory responses while favoring immune suppression which may take time to mature into adult responses thus allowing IBV to cause severe morbidity and mortality in younger populations due to innate and adaptive immune disparities.

IBV may have adapted to mammals and potentially humans as the natural reservoir. There are some key differences between IBV and IAV that support the theory of humans as the primary host for IBV [33]. Differences in HA-specifics and immune evasion between IBV and IAV support this theory. Human influenza viruses (IAV and IBV strains) preferentially bind to α2,6 linked-linked sialic acids [34] and avian IAV strains preferentially bind to α2,3 linked-sialic acids [35, 36]. However, younger individuals demonstrate more common and severe IBV Victoria-lineage infections than Yamagata-lineage [37]; also, among IBVs, only B-Victoria lineage has been linked with binding to α2,3 linked-sialic acid residues [38]. Taken together, this difference could be associated with more common B-Victoria lineage viral infections in younger individuals than with B-Yamagata lineage viruses, and the bias of B-HA binding to α2,6 linked-sialic residues may reduce transmission in younger individuals whose URT contains more α2,3 linked-sialic acid residues [33]. Other differences in HA and IBV replication may also play a role in humans as the reservoir for IBV. pH required for B-HA activation and membrane fusion is lower (pH 5.4 – 5.6)than for avian IAV (pH 5.7 – 5.8) and the optimal replication temperature for IBV is 33°C and it is significantly reduced at 39°C [39].

Differences in immune evasion by IBV may also contribute to humans as the reservoir. One major difference between IAV and IBV is the lack of alternative polymerase proteins encoded in the PB1 and PA genes. IAV PB1-F2 [40] and PA-X [41] have immunomodulatory functions for IAV in suppressing cytokine and IFN responses [42]; however, these proteins are absent in IBV. During infection, host cells produce IFN to activate host IFN stimulating genes (ISGs) and limit host gene expression [43]. IBV NS1 protein has been shown to interfere with human IFN signaling by preventing upstream activation of host ISGs, thus suppressing host responses and ensuring virus persistence [44]. In addition to avoiding innate immune detection inside the cell, the virus must also be able to evade any adaptive immune response to infected cells. After IBV infection, cell lines expressing different HLA-alleles showed significant decreases in MHC-I surface expression compared to IAV infection [45]. Taken together, these differences and others not uncovered at this time, contribute to the establishment of humans, or another mammal as the reservoir for IBVs. A comparison of IAV and IBV is summarized [2] in Table 1.1.

Table 1.1: Comparison of IAV and IBV

	INFLUENZA A (IAV)	**INFLUENZA B (IBV)**
Host Range	• Multiple animal reservoirs & possible animal hosts • Known reservoir = Avian (waterfowl)	• No established animal reservoirs • Known reservoir = Humans (sole reservoir?)

	INFLUENZA A (IAV)	INFLUENZA B (IBV)
Phylogenetics	• Subtyped by HA & NA (ex. H1N1pdm09, H3N2)	• 2 lineages according to HA (Victoria & Yamagata)
Epidemiology	• ↑Severity in children & **elderly**	• ↑Severity in children & **adolescents**
Clinical Presentation	• Symptoms: sore throat, coughing, fever, nasal discharge • Avian strains lead to severe disease and ↑ mortality	• Symptoms: sore throat, coughing, fever, nasal discharge • Can cause severe complications in children
Virology	• 8 negative sense RNA segments & >13 known proteins • Unique proteins: (PB1-F2, PB1-N40, PA-X)	• 8 negative sense RNA segments & 11 known proteins • Unique proteins: NB
Immunology	• Generally strong IFN-αß and cytokine response • HA is major Ab target • Major CD8+ T-cell antigens	• Strong IFN-αß and cytokine response (details unclear) • HA is major Ab target

	INFLUENZA A (IAV)	INFLUENZA B (IBV)
	=M1 & NP • 2 strains in annual vaccine (H3N2/H1N1pdm09)	• Major CD8+ T-cell antigens unknown • 1 or 2 strains in annual vaccine depending on formulation
Antivirals	• Adamantanes = **effective** • NAIs = effective, but resistance detected	• Adamantanes = **ineffective** • NAIs = effective, but resistance detected (without apparent fitness cost in some instances)

INFLUENZA VIRUS LIFE CYCLE

A general overview of influenza virus infection of the host cell and replication can be broken down into four main steps: 1) Virus attachment and entry into the host cell, 2) Transport of the viral genome into the nucleus and replication, 3) Viral assembly and packaging, and 4) Virus budding and release from the cell. Virus replication steps are reviewed in Dou et al. [46]. Each step is described below for a clearer understanding of how influenza viruses invade the cell and replicate. Functions of IBV proteins are listed in table 1.2 (Adapted from van de Sandt et al. [47]).

Virus attachment and fusion

Influenza binds sialic acids attached to galactose on the surface of airway epithelial cells. The viral HA binds to cell surface glycoproteins containing terminal SA residues linked to galactose in either a α2,3-linkage or α2,6-linkage. Most avian influenza viruses usually have preferential tropism for N-acetylneuraminic acid linked to galactose in an α2,3 configuration (α2,3-SA), while human influenza A viruses preferentially recognize N-acetylneuraminic acid linked to galactose in an α2,6 configuration (α2,6-SA) [48, 49]. This binding preference is one of the major determinants for controlling viral tropism and host species specificity [50, 51]. It was originally thought that birds only expressed α2,3-SA "avian receptor" in their respiratory and intestinal tracts, whereas humans only expressed α2,6-SA "human receptor" in their respiratory tracts. Pigs serve as the primary "mixing-vessel" for influenza pandemics since they express both α2,3-SA and α2,6-SA on their epithelial cells which could produce reassortant viruses between avian and human viruses, thus introducing new "pandemic" viruses into the human population [52]. More recently, this paradigm has shifted due to the findings that humans have both α2,3-SA and α2,6-SA receptors on their cells in both the URT and LRT [53]. Even though humans have both receptors, the distribution of these receptors may play a role in host specificity. In humans α2,6-SA>α2,3-SA and avian hosts α2,3>α2,6-SA [34]. As in humans, ferrets show similar tissue distributions of receptors: α2,6-SA>α2,3-SA with α2,6-SA being found throughout the respiratory tract and α2,3-SA in the lamina propria and to a lesser extent in the alveoli [54]. Recently it has been reported from virion motion studies, that influenza NA may play a role in virus binding by facilitating

penetration through the mucous layer to reach susceptible cells and that a second sialic acid binding site (2sbs) within NA may contribute to virus attachment and facilitate virion rolling and encounter with an internalization receptor [55, 56].

HA-mediated binding to the receptor triggers endocytosis of the virion in either a clathrin-dependent manner [57, 58] or by micropinocytosis [59, 60]. Once inside the cell, the virus is trafficked to the endosome. The endosome has a low pH which activates the influenza ion channel M2 [61] (BM2 for IBV [62]) that triggers the fusion of the viral and endosomal membrane by causing a conformational change in HA to expose the HA2 fusion peptide to insert into the endosomal membrane [63]. M2 is embedded in the virus membrane and functions as an ion channel, which when open inside the endosome results in uncoating and release of the packaged viral ribonucleoproteins (vRNPs) particles from viral matrix protein (M1); this allows for transfer of the vRNPs into the cytoplasm following HA fusion [64, 65]. A total of eight vRNP complexes are transferred, one complex for each viral gene segment. Each vRNP consists of one viral RNA gene segment, which is encapsidated by viral nucleoprotein (NP), and carrying polymerase proteins (PB1, PB2, PA) [66].

Transport of the viral genome into the nucleus and replication

Unlike virus entry and fusion, vRNP transport to the nucleus is dependent on host cell machinery and transport pathways. Uncoated vRNPs, with exposed nuclear localization signals, bind to cellular importin adapter proteins (IMPα). IMPα in turn recognizes importin transport receptor (IMPß) to form a complex. This vRNP-IMPα/ß complex docks at the nuclear pore complex on the nuclear membrane and is transported

into the nucleus where Ran-GTP binds to IMPß facilitating vRNP release to initiate transcription and replication [67].

Inside the nucleus, the trimeric viral RNA-dependent RNA polymerase complex, consisting of polymerase basic protein 1 (PB1), polymerase basic protein 2 (PB2) and polymerase acidic protein (PA) subunits are responsible for the transcription and replication of viral RNA genomic segments [68]. Replication of the viral genome involves two major steps: transcription of complementary RNA (cRNA), followed by transcription of new viral RNA (vRNA) using the cRNAs as templates [46]. Viral mRNA transcription from the vRNA templates is primed using 5'capped RNA's cleaved from host cell mRNA, thereby making it much easier and more efficient than cRNA and vRNA transcription. The viral polymerase complex obtains the primers from the host through a mechanism termed "cap snatching" [69]. The viral polymerase PB2 subunit binds to 5' caps of nascent host transcripts and the PA subunit endonuclease domain cleaves 10-13 nucleotides downstream of the 5' cap. This bound 5' cap is then rotated to position the cap into the PB1 catalytic center where it is extended using the vRNA as a template. Each completed transcript is poly-adenylated through a reiterative "stuttering" process when the polymerase encounters a short poly-U sequence at the 5' end of the vRNA [70]. During the virus lifecycle, mRNA synthesis occurs before cRNA and vRNA transcription, and mRNA transcription is more abundant since primer use significantly increases its initiation efficiency. These initial mRNAs are transcribed by vRNP-associated polymerases and exported from the nucleus for translation by cytoplasmic ribosomes [71]. For replication of the genomic RNA the viral polymerase complex initiates transcription of the positive sense cRNA upon base pairing of ATP and GTP

with the complimentary nucleotides on the 3' end of the vRNA. The A-G dinucleotide formation locks the vRNA template in the active site of PB1 followed by elongation of the cRNA transcript . Viral NP molecules bind to the newly synthesized vRNA as it exits the polymerase, promoting cRNP assembly. cRNP formation is complete after transcription termination and binding of a newly viral polymerase. vRNA transcription occurs in the same manner as cRNA synthesis

Viral assembly and packaging

Virus protein synthesis is dependent on the translation machinery of the host. Following nuclear export is divided between cytosolic ribosomes (for PB1, PB2, PA, NP, NS1, NS1 and M1) and the endoplasmic reticulum (ER) associated ribosomes (for HA, NA and M2[BM2]) [72]. Nuclear import signals on newly synthesized NP and polymerase proteins (PB1, PB2, and PA) target these to the nucleus by IMPα/ß as in the initial vRNP. These imported proteins assist in viral mRNA transcription and vRNA replication. NP monomers bind to vRNAs and cRNAs to assemble into vRNPs and cRNPs respectively. Additionally, the viral RNA-binding protein NS1 is synthesized early and also imported into the nucleus. Once in the nucleus it can act as an inhibitor of IFN-signaling to reduce host innate responses [73]. NS1 has also been reported to contribute to viral mRNA nuclear export through linkage of viral transcripts to cellular nuclear export components [74]. vRNPs are trafficked from the cytoplasm towards the plasma membrane for virus assembly by Rab11, which facilitates assembly by associating with the viral PB2, thus ensuring new virions incorporate vRNPs that carry a polymerase [75].

Influenza membrane proteins that are part of the virus envelope, HA, NA, and M2, are synthesized by ribosomes associated with the ER. After the vRNPs have exited the nucleus, they need to form viral particles and leave the cell. vRNPs nuclear export occurs in a CRM1(chromosomal maintenance 1)-dependent manner [76]. This process involves two viral proteins matrix protein (M1) and nuclear export protein (NEP) known as nonstructural protein 2 (NS2). CRM1 recognizes two nuclear export signals near the N-terminus of NEP, while the C-terminal hairpin of NEP associates with the N-terminal nuclear localization signal of M1. The M1, in turn binds to a C-terminal region of the NP component of the vRNP in a "daisy chain" arrangement [76]. vRNPs are exported through the nucleus into the cytoplasm. After leaving the nucleus vRNPs associate with Rab11-containing endosomes for trafficking to the apical side of the cell [75].

Packaging of IAV vRNAs is better studied than IBV and for IAV each vRNA is believed to have a specific packaging signal that differentiates it from other vRNA segments resulting in packaging of eight vRNA segments into each virus particle [77, 78]. This model is supported for IAV and IBV by electron microscopy and multicolor single-molecule fluorescent in situ hybridization [79]. Packaging signals have been identified in the 5' and 3' non-coding and coding regions of some of the viral segments [80, 81]; however, some still remain elusive [82]. Similar to IAV, the 5' and 3' termini of the HA of IBV were shown to have packaging signals [83].

Virus budding and release from the cell

Since influenza is an enveloped virus, it uses the host cell plasma membrane to form viral particles. Influenza viruses are enriched in cholesterol and sphingolipids and

bud from distinct apical plasma membrane regions known as “rafts” [84]. Viral particles bud from the apical side of polarized cells [85]. HA, NA, M1, and M2 localize to distinct regions of the plasma membrane followed by delivery of vRNPs by Rab11 and localize to the budding site by binding to viral M1 protein [86, 87]. To bud from the cell surface, the virus must induce curvature of the membrane and then constrict the ends of the membrane to help facilitate membrane excision. This is induced by protein crowding on one leaflet of the bilayer followed by association of curved or “bending” proteins with the bilayer, accumulation of cone shaped lipids in one leaflet of the bilayer or the cytoskeleton (reviewed in Jarsh et al. 2016 [88]). Following accumulation of proteins on the membrane surface and vRNPs which are linked to the M1 viral protein, scission occurs to excise the completed virus from the plasma membrane. One of the major functions of NA is to remove sialic acids from both cellular receptors and newly synthesized HA and NA on nascent virions that have been sialylated as part of the host glycosylation process [89]. Viral NA facilitates viral release by cleaving SA to prevent virus aggregation and HA binding back to the host cell, allowing for efficient release of virus and spread to new target cells [90].

Table 1.2: Influenza B proteins and functions

RNA SEGMENT	PROTEIN	AA	FUNCTION
1	PB2	770	**Virus replication** – component of RNA pol; cap-binding
2	PB1	752	**Virus replication** – catalytic subunit of RNA pol; RNA elongation
3	PA	726	**Virus replication** – component of RNA pol; cap-snatching

RNA SEGMENT	PROTEIN	AA	FUNCTION
			endonuclease subunit
4	HA	584	**Virus attachment** – surface glycoprotein receptor; receptor binding/membrane fusion; Antigenic determinant
5	NP	560	**RNA encapsidation, nuclear targeting, RNA transcription** – Encapsidation of viral genomic RNA; RNA synthesis, nuclear import vRNA
6	NA NB	486 100	**Virus release from cell** – surface glycoprotein; NA activity, virus release after budding; antigenic determinant Ion channel activity; function unknown
7	M1 BM2	248 109	**Membrane stability** – role in assembly and budding **Virus uncoating** – ion channel activity; essential for uncoating, role in virus budding
8	NS1 NS2/NEP	281 122	**Non-structural protein** – regulation vRNA pol complex, interferes with antiviral state of cell (IFN antagonist) **Nuclear export** – role in nuclear export RNP, regulates transcription and replication

IMMUNE RESPONSES FOLLOWING INFLUENZA INFECTION

Immune responses to IAV have been widely studied; however, this is not the case for IBV. In order to understand altered immune responses to IBV, one must first review general immune responses to viruses. The immune response following influenza infection consists of two phases. Reaction to infection is initiated by the innate immune response followed by the adaptive immune response. The innate immune response occurs within

minutes following infection and an effective response can limit early virus replication by secretion of cytokines with antiviral activity such as type I IFN, recruit antigen-presenting cells to the site of infection to enhance the response including phagocytosis of infected cells, and release of IFN and other cytokines to provide alarm signals to activate cells of both the innate and adaptive immune system such as DC, NK and T-cells prior to development of an adaptive response [91]. The adaptive response is triggered following the innate immune response which is divided into cellular and humoral responses. Innate and adaptive responses are summarized for influenza as well as cellular responses which link the immune responses. Special emphasis on the interferon response following influenza infection is highlighted.

INNATE IMMUNE RESPONSE

Influenza infection occurs primarily in the respiratory tract. The respiratory tract is divided into the upper respiratory tract (URT) which is comprised of the nasal sinuses, pharynx, and larynx, and the lower respiratory tract (LRT) which is comprised of the trachea, bronchi, and lungs. The human respiratory tract is lined with a pseudo-stratified epithelial cell layer consisting of particle-sweeping columnar ciliated cells, mucus-producing goblet cells, surfactant-secreting Clara cells, sensory neuro-epithelial cells, and basal cells which act as progenitor cells [92]. The cells lining the lung are mainly comprised of type I and type II alveolar epithelial cells (pneumocytes). Influenza primarily infects the ciliated cells and to a lesser extent, goblet cells in the URT and both type I and type II pneumocytes in the alveoli [93, 94]. Mucus secreted by the goblet cells contain mucins and collectins which form the first line of defense to prevent infection of

respiratory epithelial cells with influenza. Initially, influenza becomes trapped non-specifically in the mucus layer and is expelled by mucociliary clearance before infection of the underlying cells [95]. Influenza viral NA can cleave sialic acids, which can prevent trapping of the virus in mucus [96, 97]. Collectins are proteins which contain both collagen and functional lectins. Two collectins, surfactant protein A and surfactant protein D can neutralize influenza by occupying the HA binding site with its own salicylic acid [98] or interacting with high mannose oligosaccharides located near the HA binding site [99] respectively to inhibit HA binding. Once influenza passed these initial defenses and has bound to susceptible respiratory epithelial cells the innate immune response is activated.

The innate immune system forms the first line of defense following influenza infection. Both IAV and IBV have adopted evasion strategies to evade or delay the host innate immune detection/response. During influenza infection several pathogen-associated molecular patterns (PAMPs) are exposed and sensed by different pattern-recognition receptors (PRRs) expressed in respiratory cells. Binding of viral components by PRRs triggers signaling cascades that are responsible for secretion of IFNs, proinflammatory cytokines and chemokines. The most important PRRs involved in recognition of influenza are the Toll-like receptor (TLR)-3 and TLR-7 and the RNA recognition protein RIG-I [100]. TLR-3 and TLR-7 are located on the endosomal membrane and RIG-I is located in the cytosol. However, recently it has been discovered that both TLR-3 and TLR-7 are expressed on the apical surface of human airway epithelial cells [101]. The influenza genome which consists of ssRNA is recognized by TLR7 [102] and RIG-I [103]. TLR-3 recognizes dsRNA that is produced during viral

replication. PAMP-PRR binding leads to activation of several signaling pathways that induce nuclear factor κß (NF-kB) and IFN regulatory factor 3 (IRF3) resulting in the production of type-I and type-III IFNs and inflammatory cytokines [100].

TLR-7, once activated by ssRNA induces MYD88 resulting in the activation of NF-kB and IRF3 depending on the cell type. Activation in respiratory epithelial cells results in the production of IL-6 and type-III IFN [101]. Activation in plasmacytoid DCs produces high levels of type-I IFNs via IRF7 [104]. TLR-3 is predominantly expressed in macrophages, natural killer cells and DCs and involved in the activation of proinflammatory cytokines and chemokines [105]. TLR-3 localizes at the cell surface and in the endosomes of DCs [106]. TLR-3 is a member of the TLR family that mediates the transcriptional induction of type-I IFNs. It is the only RNA sensor that is dependent on the Toll-interleukin-1 receptor (TIR)-domain-containing adaptor-inducing beta interferon (TRIF). Upon activation by binding dsRNA, TLR-3 recruits TRIF to trigger a downstream signaling cascade ultimately activating transcription factors IRF3/7, NF-kB and activator protein 1 (AP-1) thus mediating the production of type-I IFNs, proinflammatory cytokines and chemokines [107].

RIG-I is expressed in epithelial cells, macrophages and DCs [108]. RIG-I recognizes detecting influenza vRNA (ssRNA) in the cytoplasm. RIG-I has also been shown to recognize short dsRNA in the cytoplasm resulting from infection or cell damage [109]. For influenza, RIG-I recognizes 5'-triphosphate -RNA sequence motifs along the RNA containing some dsRNA (panhandle) which is generated by active viral replication within cells [110]. The importance of RIG-I mediated responses in suppressing influenza virus was demonstrated in mouse studies. RIG-I and TLR-7

signaling was required for survival and restriction of virus growth following infection of mice with a lethal dose of influenza [111]. In human PBMC, RIG-I expression was enhanced following influenza infection [112] and patients who exhibited a polymorphism resulting in a nonfunctional RIG-I had resulted in more attenuated antiviral response [113]. Following recognition of vRNA, the RIG-I helicase domain binds to ATP and forms a complex with mitochondrial antiviral signaling protein (MAVS) via caspase recruitment domains. The signaling leads to production of type-I IFNs through IRF and proinflammatory cytokines through NF-kB [114].

CYTOKINES AND CHEMOKINES

Activation of the innate immune response in airway epithelial cells following influenza infection results in the release of several factors to: 1) activate resident immune cells such as innate lymphoid cells (iLCs), macrophages and DCs, 2) recruit neutrophils, macrophages and lymphocytes to the site of infection, 3) stimulate a Th17 (T_{EFF}) response, and 4) stimulate a Th1 response [115]. Airway epithelial cells are the main early sources of cytokines within the first 24-48Hr of infection and this balance shifts to the recruited and resident immune cells thereafter [92, 116, 117]. Timing of cellular activation is critical in generating a protective immune response following influenza infection. Cellular activation results in secretion of cytokines and chemokines which, in turn, enlist aid of other immune cells and send signals to activate other components of the immune response. The inflammatory response; however, is a “double edged sword” since a robust inflammatory response is required following infection to control virus replication, but a sustained response results in lung damage, increased morbidity, and

death. Therefore, a balance between the inflammatory and anti-inflammatory response must be achieved to combat infection and restore immune homeostasis [118]. A list and function of the main cytokine and chemokine groups examined in this work are shown in Table 1.3 and described here.

Interferons

IAV/IBV infection induces the production of interferon(s) which was originally named because of its ability to interfere with influenza virus replication in previously uninfected chick chorio-allantoic membrane and other cells [119-121]. Type-I IFNs (IFNA and IFNB) induce an antiviral state in the cells and signal immune cells. Although plasmacytoid dendritic cells (pDCs) are the primary cell that generates large amounts of type I interferons [122] during IAV infection, IFN signaling and generation also occurs in airway epithelial cells [123]. Once secreted type-I IFNs act in an autocrine or paracrine manner by binding IFN-α/ß receptor present on all cell types, Type-I IFNs result in an inflammatory response in infected cells and is the pivotal innate antiviral response by directly inhibiting virus replication. Type-I IFNs can mediate both innate and adaptive cellular immune functions resulting in in resistance to virus infection and can be used as an immune inducer or prevent persistent virus infection whereas type-III IFNs suppress the inflammatory response and the innate response but it is delayed and prolonged [124]. The response by type-I IFNs induce greater and faster responses than type-III IFNs which emerges later and its induction is more permanent [125, 126]. In addition to induction of an antiviral state in cells, IFNα/ß increases class I MHC expression and regulates antiviral responses by T cells and activates NK cells, B-cells and macrophages [127].

Type-II IFN (IFNγ) is expressed primarily by NK, T-cells, and natural killer T cells. IFNγ affects the local cellular response to influenza in the respiratory tract by regulating leucocyte trafficking to infected lung tissue in mice [128]. Following IAV infection in IFNγ deficient mice, IgG1, IL-4 and IL-5 were increased, suggesting that IFNγ is not necessary for an effective humoral response to influenza, rather its primary function is to modulate disease severity [129]. IFNγ also enhances antigen presentation during T-cell priming and increases MHC-II expression and maturation of DCs [130] and induces IL-12 and co-stimulatory CD80 expression in antigen presenting cells which is critical component of Th1 polarization [131-133].

Type-III IFN (IFNλ) is primarily produced by cells lining mucosal surfaces including the respiratory tract, various DC subsets can also produce IFNλ [134] A major difference between type-III and type-I IFNs is IFNλ's ability to induce a targeted response in the mucosal epithelia without stimulating excessive immune cell recruitment (inflammation) which can lead to immunopathology [135]. IFNλ can recruit DCs, regulate IL-10 production, and enhance type-I helper T cell responses [136]. IFNλ also acts indirectly on DCs through the induction of thymic stromal lymphopoietin (TSLP) in the respiratory tract [137] thus inducing a mucosal immune response. Upon induction TSLP regulates germinal center function and antigen-specific antibody responses [138] thus having an important effect on the magnitude of the adaptive immune response.

T cell helper type 1 (Th1)

T cell helper type 1 (Th1) cytokines produce proinflammatory responses responsible for killing primarily intracellular parasites, and IFNγ is responsible for

initiating this response. Serum IFNγ-induced protein 10 (IP-10) or CXCL10 is induced in airway epithelial cells through viral dsRNA and IFN signaling [139]. Some of its biological effects include monocyte stimulation, NK and activated T-cell migration, modulation of adhesion molecule expression and inhibition of angiogenesis [140]. Antimicrobial effects have been demonstrated at high concentrations [141]. However, these elevated levels of Th1-type cytokines result in tissue destruction. In fact, IP-10 is an important marker of disease severity following IAV infection [142, 143]. Other Th1-type cytokines for studying ferret responses were not available in this work.

T cell helper type 2 (Th2)

Although Interleukin-2 (IL-2) has been characterized as a Th1-like cytokine, increasing evidence indicates that IL-2 and its downstream signaling molecule, STAT5, also are vital for the induction of anti-inflammatory T cell helper type 2 (Th2) cytokines during a primary response [144]. This anti-inflammatory response has also been shown that IL-2 is required to downregulate apoptotic pathways in mice following IAV infection [145]. However, it has also been shown that IL-2 can drive lung inflammation involving NK cells and can synergize with IAV resulting in disease exacerbation [146]. IL-2 can work together with cyclic adenosine 3' ,5'-phosphate in synergy to enhance the antibody production by B-cells [147]. In elderly human subjects, IL-2 treatment enhanced antibody responses to influenza vaccination [148] and may play a role in the adaptive immune response [149].

Chemokines

Chemokines are a specialized group of secreted proteins which function as chemoattractants, attracting cells out of the bloodstream to the site of infection via binding to their receptors. These chemokines attract effector cells, such as macrophages and DCs to the site of infection and activate them to produce signals to other immune cells. Two important chemokines examined in this work are monocyte chemoattractant protein-1 (MCP1) and macrophage inflammatory protein-1 (MIP1ß). MCP1 or CCL2 is an important chemoattractant in influenza pathogenesis. The primary sources of MCP1 are epithelial cells, monocytes/macrophages, pulmonary neutrophils, and fibroblasts and direct the migration and infiltration of monocytes, NK, DC, and T-cells to the site of infection [150]. In mouse studies MCP-1 was important in recruiting macrophages and granulocytes to the lung, increasing pulmonary levels of IgA and reducing inflammatory responses (lower TNFα, IL-6 and MIP1α) compared to MCP-1 knock out mice showing that MCP-1 contributes to protective immune responses against influenza infection in mice [151].

Macrophage inflammatory protein-1ß (MIP1ß) secretion leads to chemotaxis of monocytes, T-cells, eosinophils, NK, and immature DCs [152]. MIP1ß is elevated in the NW and serum during acute influenza infection in both immunocompromised and immune competent individuals [153]. Human studies on H1N1 influenza infection showed that increased levels of MIP1ß correlated with severity of disease in NW samples [154]. Mouse studies have shown that MIP-1α secreted by monocytes was important to development of an inflammatory response following influenza infection and increased pulmonary clearance [155]. Data show that inflammatory responses and recruitment of macrophages is important in clearance of influenza viruses following infection.

T-effector cells (Teff)

T-effector cells (Teff) are T-cells steering the immune responses to execute specific immune functions such as inflammatory responses and B-cell help. Effector T-cells are divided into T-helper (Th) and cytotoxic lymphocytes (CTLs). Th cells are further divided into Th1, Th2, Tfh and Th17 subsets with Th1 cells characterized by the production of IFNγ, Th2 characterized by the production of IL-4, IL-5 and IL-13, Tfh cells characterized by the production of IL-4 [156] and IL-21 and Th17 characterized by the production of IL-17 and IL-22 [157]. IL-4 has also been secreted by Tfh in mice infected with IAV H1N1 has been shown to be essential to facilitate B-cell proliferation and controls germinal center expansion [156]. IL-4 also promotes Th2 differentiation by inhibiting Th1 function and was demonstrated for IAV in mice in an adoptive transfer with Th1 or Th2 clones [158].

Th17 cells are recognized in inducing protective immunity against bacteria and fungi by neutrophil recruitment and promoting integrity of mucosal epithelial barriers; however, they play a critical role in in the production of pro-inflammatory cytokines and recruiting and activating immune cells. IL-17 promotes protective immunity against many pathogens and also drives inflammatory pathology during infection. IL-17 is produced by Th17 cells, CD4+ and CD8+ T-cells, γδT-cells and other innate cell populations in response to IL-1ß and IL-23. IL-17 driven inflammation is normally controlled by regulatory T-cells (Treg) and the anti-inflammatory cytokines IL-10 and TGFß; however, if dysregulated in can result in immunopathology [159]. The role of IL-17 was assessed following influenza IAV H5N1 infection in mice. In this study, influenza

infected *il17*$^{-/-}$ mice showed greater susceptibility to infection and lower survival than wild-type mice. The *il17*$^{-/-}$ mice also showed lower numbers of B -cell in the lungs, suggesting that IL-17 played a crucial role in B-cell recruitment into the lungs following H5N1 infection [160].

IL-12 is produced by macrophages and DC and activates NK and Th1 cells. Activated Th1 cells produce IFNγ and IL-2 which help B-cells generate antibodies, especially neutralizing antibodies [161]. IL-12p70 is a heterodimer, composed of p35 and p40 subunits. The IL-12p40 is secreted predominantly by activated monocytes, macrophages and DC and functions as a chemoattractant for macrophages and promotes DC migration and T-cell priming [162]. IL-12 is regulated by positive and negative feedback mechanisms involving Th1 cytokines (IFNγ) and Th2 cytokines (IL-10) [163]. The free p40 monomer does not mediate IL-12 activity but acts as an IL-12 antagonist (IL-12p70). Following influenza infection in mice, IL-12 attracts and activates NK cells which secrete IFNγ inhibiting virus replication and enhancing CD8+ T-cell responses [164].

Pro-inflammatory

The primary innate immune response in cells following influenza infection result in the production of IFNs and pro-inflammatory cytokines. Primary pro-inflammatory cytokines investigated in this work, and where ferret reagents are available include: TNFα, IL-6, IL-8, IL-1ß and IL-23. A brief review of each in relation to IAV infection is presented below.

Tumor necrosis factor α (TNFα) is considered to be the prototypical cytokine of the influenza "cytokine storm" which can exacerbate host pathological damage [165]. TNFα is an inflammatory cytokine which recruits monocytes, T-cells, and B-cells to the site of infection and plays a key role in clearing virus infection in the respiratory tract before the activation of the secondary immune response. Macrophages are the primary producers of TNFα which functions to activate the vascular endothelium thereby increasing vascular permeability leading to entry of IgG, complement and cells to the tissues and increased fluid drainage to the lymph nodes [166].

Interleukin 6 (IL-6) along with IL-1 are the main pro-inflammatory cytokines released by hosts during viral infections. IL-6 has been primarily considered a proinflammatory marker for inflammation in arthritis and inflammatory bowel diseases [167]. IL-6 was originally identified as a T-cell derived lymphokine that induces final maturation of B-cells into antibody producing cells. IL-6 was initially identified as a marker of inflammation to a target to control inflammation [168]. During the initial inflammatory response, IL-6 recruits neutrophils initially which are then cleared and followed by mononuclear cells through IL-6 *trans*-signaling [169]. To control inflammation, IL-6 blocks the TNFα or IL-1ß induced control of neutrophil chemokines (CXCL1, CXCL8 and CXCL3) and directly enhances CXCL5, CXCL6, CCL2 and CCL8 secretion to activate macrophages, DC, and T-cells and B-cells [170-173]. IL-6 affects acquired immunity by influencing T-cell polarization to Treg cells, DC maturation and activity [174]. Following influenza infection in mice, IL-6 has been shown to limit inflammation in lungs and activate influenza-specific T-cell responses [175]. IL-6 has also been shown to play an important role following influenza infection and Tfh cell

development and critical communication with B cells in germinal centers [176]. IL-6 is important in initial inflammatory responses to influenza as well as Treg response and downstream acquired immune responses.

Interleukin-8 (IL-8) is a proinflammatory chemokine that is produced in epithelial cells in response to influenza infection [177, 178]. Its primary chemotactic role is towards neutrophils and angiogenesis [179]. Interestingly, IL-8 has also been shown to inhibit the antiviral action of type-I IFN inhibition of virus replication of picornaviruses and polioviruses in vitro [180]; however, a correlation between IL-8 and influenza virus replication or disease severity was not observed in humans experimentally infected with IAV [181]. IL-8 levels were increased very late following influenza infection and observations suggest that it may be part of a second wave of proinflammatory cytokines that may be involved in in more severe influenza infection of the LRT [181]. In a separate human IAV study IL-6 levels correlated with symptom severity, whereas IL-8 levels did not [182].

Interleukin-1 (IL-1) is a key mediator of the inflammatory response following infection of the cell. It is crucial for the host defense following infection and injury [183]. Following PAM-PRR binding, Pro-IL-1ß is cleaved by pro-inflammatory protease caspase-1. Caspase-1 activation occurs in the inflammasome and following interaction with CARD domains results in mature IL-1ß production and secretion by the cell. IL-1ß is essential for the host response and resistance to pathogens, but it also exacerbates tissue damage during acute infection [184]. In addition to inducing neutrophil and macrophages and production of IL-2, IL-3, IL-4, IL-5 and IL-6 [185] which have downstream effects on immune activation. IL-1ß activation and release attracts and

activates neutrophils as a first responder following respiratory cell infection. Neutrophils, in turn expand the release of IL-1ß and other factors to recruit and activate alveolar macrophages to the infection site and thus amplifying the inflammatory response [117]. IL-1ß secreted by neutrophils also acts on DC to induce differentiation of Th17 cells and secretion of IL-17 and IFNγ [186]. This hyperinflammatory response by IL-1ß exacerbates influenza disease and plays a crucial role in influenza pathogenesis [187].

Interleukin-23 (IL-23) is a member of the IL-12 family of cytokines consisting of proinflammatory properties. It is a central regulator of inflammation and enhances the expansion of Th17 cells which are associated with immune activation, increased viral pathology, and chronic inflammation [188]. IL-23 is mainly secreted by activated macrophages and DCs located in the skin and mucosal tissues including the lung [189]. Therefore, IL-23 secretion by DCs likely drives Th17 polarization in T-cells. Influenza studies performed in mice demonstrating the effects of IL-23 on Th17 polarization were conducted in an IAV-bacterial challenge model [190]. A Th17 response for *S. aureus* is critical in bacterial clearance. IAV challenge followed by bacterial challenge showed increased inflammation with decreased viral and bacterial clearance. Virus-bacterial challenge also showed greater type-I IFN in lungs compared to virus alone, and suppressed IL-23 production induced by *S. aureus*. The study demonstrated that type-I IFN induced by IAV inhibits IL-23, which is required for Th17 pathway activation. IL-23 may play a role as an important modulator of adaptive immunity. In another study, mice mucosally vaccinated with inactivated influenza vaccine containing IL-23 as an adjuvant, significantly boosted robust IgA responses and reduced viral lung burden following

challenge [191]. These studies show that IL-23 stimulates a Th17 response and that IAV suppresses this response through type-I IFN.

B-Cell Development

Several cytokines have an effect on B-cell development and activation resulting in antibody production and clearance from viral infection. Since several cytokines have effects on other processes (IL-4, IL-6, and IFN) in addition to B-cell development, they have been previously described but listed in this group. Thymic stromal lymphopoietin (TSLP) is a cytokine which has stimulatory effects on B cells and plays a role in B cell development [192]. IFNλ secreted by infected respiratory epithelial cells can induce M cells to release TSLP which acts on migrating CD103+ DCs to stimulate the adaptive immune responses by enhancing CD8+ T-cell maturation and promoting germinal center reactions in the lymph node through T-follicular/helper (Tfh) cells [124]. Tfh cells aid in B-cell survival and proliferation in germinal centers [124, 137, 193] resulting in an increase of IgG1 and IgA antibody [137]. IFNλ was shown to induce TSLP expression following influenza infection leading to an increase in adaptive mucosal immunity [137]. The importance of TSLP and IFNλ in generation of a robust adaptive immune response cannot be understated. Studies in mice confirming that the mucosal administration of influenza subunit vaccine containing TSLP effectively generated serum IgG1 levels to similar extent as was triggered by IFNλ alone. This response was inhibited in *Tslpr*$^{-/-}$ mice vaccinated with IAV and IFNλ indicating that the positive effects of IFNλ depend on TSLP [137].

Table 1.3: Cytokine and chemokine properties.

FAMILY	*NAME*	*PRODUCER CELLS*	*ACTIONS*
INTERFERONS	IFNα/ß(Type-I)	Leukocytes DC Epithelial cells (Fibroblasts, IFNß)	Antiviral, Increases MHC-I expression
	IFNγ(Type-II)	T cells NK Neutrophils ILC1s	Mph activation, Increases MHC-I expression Ig class switching, Suppress Th17/Th2
	IFNλ(Type-III)	Epithelial cells, DC Macrophages	Antiviral, Suppress inflammatory response
Th1	IP-10	Monocytes Lymphocytes Epithelial cells	Recruits activated T-cells to site of inflammation
Th2	IL-2	T cells Airway epithelial cells	T_{REG} maintenance and function B-cell growth factor and stimulus of antibody synthesis T cell proliferation and differentiation
CHEMOKINES	MCP1 (CCL2)	Macrophages Neutrophils Epithelial cells	Attracts (monocytes,NK,T-cells, DC) Activates macrophages Promotes Th2 response
	MIP1ß (CCL4)	Macrophages monocytes	Attracts (monocytes,NK,T-cells, DC) Activates macrophages Promotes Th1 response
Teff	IL-4	Mast cells Tfh cells Th2 cells	B-cell activation Increases MHC-II T/B cell survival factor Tissue adhesion and inflammation IgE switch Th2 differentiation
	IL-17	Th17 cells γδT cells NK T cells ILC3s CD8+ Th17 cells	Induces proinflammatory cytokines/chemokines Activates neutrophils
	IL-12p40	Macrophages DC	Th1 driving cytokine; Promotes cell-mediated immunity DC maturation

FAMILY	*NAME*	*PRODUCER CELLS*	*ACTIONS*
			NK activity
	IL-12p70	Macrophages DC	IL-12 antagonist (p35 monomer bound)
PRO-INFLAMMATORY	TNFα	Macrophages Alveolar macrophages	Promotes inflammation; endothelial cell activation
	IL-6	T cells Monocytes Macrophages DC Airway epithelial	T- and B-cell growth, differentiation, cytokine production, fever B-cell differentiation and production of IgG/A/M
	IL-8	Monocytes DC Neutrophils Epithelial cells	Attracts/activates neutrophils, NK, and T cells Angiogenesis
	IL-1ß	Macrophages DC Epithelial cells	Proinflammatory (Fever) Th17 differentiation T-cell activation Macrophage activation
	IL-23	Macrophages DC	Activates macrophages Maintains & expands Th17 cells
B-CELL DEVELOPMENT	TSLP	Epithelial cells DC	Ig rearrangement Acts on DC to: -Enhance T-cell maturation, -GC reactions through T_{FH} DC→T_{REG} development
	IL-4	Mast cells Th2 cells	B-cell differentiation IgG1 selection Drive Th2 response Increase MHC-II expression
	IL-6	T cells & B cells Monocytes Macrophages DC Airway epithelial	Increase IgM/IgG secretion
	IFNs	Leukocytes DC Epithelial cells (Fibroblasts, IFNß)	Promote B-cell proliferation & differentiation to ASC

DENDRITIC CELL – LINK BETWEEN INNATE AND ADAPTIVE IMMUNE RESPONSE

Dendritic cells (DC) are the major players in both the innate and adaptive immune responses to influenza. DC are separated into two primary subsets: classical or conventional dendritic cells (cDC) and plasmacytoid dendritic cells (pDC). cDC are a small subset of cells that populate lymphoid and nonlymphoid tissues. They have an enhanced ability to sense tissue injuries, capture environmental- and cell-associated antigens and present them to T lymphocytes. cDC induces immunity to foreign antigens that invade tissues as well as enforcing tolerance to self-antigens. pDC are a small subset of DC and accumulates mainly in the blood and lymphoid tissues and enter the lymph nodes via the circulation. Upon recognition of foreign antigens, they produce massive amounts of IFNs and present foreign antigens [194]. Although DC present antigen primarily through MHC-I [195], since they express both MHC-I and MHC-II, they can activate both CD8+ and CD4+ T-cells [196] . In addition to classical antigen presentation, DC are unique in that they are able to also acquire MHC-I and MHC-II peptide complexes from dead cells by cell-contact-mediated mechanism and present to CD8+ and CD4+ T-cells respectively by a mechanism termed “cross-dressing” [197-199]. Adaptive immunity relies on the activation of T lymphocytes by DCs which can present to CD4 Th and CD8 Tc lymphocytes [200]. Following IAV infection, DCs can rapidly migrate to draining mediastinal lymph nodes, where antigen presentation and induction of adaptive immune responses occurs [91].

DC can also promote plasma cell differentiation to produce antibodies following IAV infection. A study using pDC depleted human PBMCs followed by IAV infection demonstrated a 90% decrease IFNα secretion and no detection of influenza specific antibodies. It was proposed that when pDCs are exposed to virus they secrete type-I IFNs

and become mature antigen-presenting DCs. T-cells respond by secreting IL-2 and CD40L expression, which stimulates pDCs to secrete IL-6 and activates B-cells. Type-I IFNs from the pDCs induce B cells to become plasmablasts [201]. This role for pDC was confirmed IAV infection in a MyD88- and TLR7-knockout mouse model. Mice lacking these molecules, which are essential for signaling for pDC activation and IFNα release, also showed defective isotype switching [202].

Migratory DCs can strongly enhance mucosal immunity and influenza virus resistance through IFNλ-TSLP axis. IFNλ can stimulate IgG synthesis in B-cells [203]. However, the regulatory effects of IFNλ on adaptive immunity are not a result of IFNλ acting directly on immune cells, rather it acts indirectly and involves TSLP, which is produced by upper airway M cells in response to exposure to IFNλ [137]. TSLP in turn acts on migratory DC to stimulate adaptive immune responses by enhancing CD8+ T-cell maturation, promotion of GC reactions through Tfh which then promotes the production of IgA [204]. These examples indicate that DCs constitute an important bridge between the innate and adaptive immune response.

ADAPTIVE IMMUNE RESPONSE

T cells and B cells play key roles in the adaptive immune response following influenza virus infections. The adaptive responses described for influenza are divided into the humoral response and the cellular response [205]. The humoral response to influenza produces antibodies against primarily to HA and NA. Antibodies to virus HA, primarily the head domain, are the most important for virus neutralization by inhibiting attachment to host cells. Other HA-specific antibodies bind to FC receptor-expressing infected cells

and target for phagocytosis by antigen presenting cells. Antibodies generated to viral NA limit virus spread by blocking NA activity. Antibodies to NA can also facilitate antibody-dependent cell-mediated cytotoxicity (ADCC).

The cellular response is further divided into the cytotoxic response, primarily CD8+ T cells, and the helper response, primarily by CD4+ T cells. The cytotoxic response driven by cytotoxic T cells (CTLs) involves lysis of influenza-infected cells. CTLs migrate to the site of infection and lyse infected cells via the action of perforin and granzymes. CTLs also can induce apoptosis via Fas/FasL interactions. Additionally, CTLs generate cytokines with upregulates MHC-I expression further targeting cells for lysis. CTLs are primarily directed against cells expressing viral NP, M1 or PA antigens on their surface in association with MHC-I. T-helper cells (Th0) are activated by cytokines by DCs and other antigen presenting cells or secreted by virally infected cells to differentiate into Th1, Th2, Th17 or Treg effector cells. Th cells interact with viral epitopes associated with MHC-II. Th subsets aid in cellular responses by secreting cytokine to activate B cells, increase the inflammatory response, or down regulate the inflammatory response. In this work the disparity between antibody responses to influenza A and B viruses is explored and impact of T and B cells are reviewed. A simplified overview of the immune responses to influenza are illustrated in Figure 1.1. Adaptive immune responses will focus primarily on the role of T cell (T helper cells: Th1 and Th2; cytotoxic T cells: CTL) and B cell responses to influenza virus infection.

B cell responses

The primary function of B cells in response to influenza infection is to produce antibodies to prevent infection as well as to bind to infected cells and mark for destruction by other immune cells. Antibodies to influenza been the primary correlate of protection for influenza. Reduction in disease and severity in mouse models following parenteral or intranasal administration of antibodies has been confirmed [206, 207], as well as in neonatal animals following transfer of maternal IgG [208]. Human vaccine studies in pregnant women have confirmed a significant reduction of 63% in laboratory-confirmed infection among infants [209].

There are two primary B cell lineages that have been defined in mice: B-1 and conventional B-2 cells, and can be distinguished based on their phenotype, ontogeny, anatomical location and function [210]. B-1 cells spontaneously secrete natural antibodies against antigens, including influenza in the absence of exogenous immunization allowing B-1 cells to provide immediate defense to counteract infection [211]. These B-1 cells, particularly IgM-secreting B-1 cells are present at birth and may be the principal B cells responsible for establishing natural immunity at birth. Conventional B-2 cells, on the other hand, cooperate with T cell in the germinal center of lymph nodes and provide high-affinity, long lasting antibody responses [212]. Since B-1 cells only represent ~5-10% of B cells in blood and primarily generate innate responses [213], only B cell responses derived from B-2 cells will be described. B-2 cells precursors continually are generated in the bone marrow and circulate in the blood and secondary lymphoid organs where they undergo class switching, somatic hypermutation and generate memory cells.

The primary antibody response studied in this work are anti-HA antibodies and the differences between antibodies generated following IAV and IBV infection. Priming of naïve B cells occurs when they migrate through regional lymphoid tissue and are presented with viral antigens by activated DCs migrating from the respiratory tract. B cell responses occur in lymph nodes and spleen. In mice infected intranasally with IAV, B cell responses are detected in both the mediastinal lymph nodes and spleen; however, responses in the spleen were minimal and of shorter duration [214]. Severe influenza infections in humans proceeds from the URT to the LRT and involve draining cervical lymph nodes indicating these as sites of B cell activity. The critical outcome of B cell activation is the induction of antibody secreting cells (ASCs) producing class-switched protective antibodies primarily to influenza glycoproteins (i.e. HA) and not internal genes [215].

B cells are activated following encounters with professional antigen presenting cells displaying viral antigens. Interactions with Tfh promote the formation of germinal centers in lymph nodes where somatic hypermutation, affinity maturation and generation of antigen-secreting cells (ASC) and memory B cells to influenza occur [216]. Adaptive responses of T and B cells in the LN and the generation of antibody responses are reviewed [217] and described following T cell responses.

T cell responses

T cells are mainly divided into two groups according to their surface receptors. CD8+ T cells and CD4+ T cells. Both types of T cells play a role in the adaptive immune

response to influenza by killing virally infected cells, promoting B cell responses, and activating or suppressing inflammatory immune responses.

CD8+ T cells differentiate into cytotoxic T lymphocytes (CTLs) which produce cytokines and effector molecules (perforin, granzyme) to restrict virus replication and kill virus-infected cells. Upon influenza infection, naïve CD8+ T cells are activated by DC migrating from respiratory tissue to the T-cell zone of lymph nodes (LNs) leading to T-cell proliferation and differentiation into CTLs [218]. Type-I and type-II IFNs, IL-2 and IL-12 help CD8+ T cells differentiate into CTLs [219, 220]. Interestingly, type-III IFN (IFNλ) has also been demonstrated to enhance T cell proliferation and antibody responses following influenza vaccination in humans [221]. Virus infected cells are identified by CD8+ T cells via MHC-I restricted binding to cells expressing viral antigens. Upon binding, CTLs produce and release cytotoxic granules containing perforin and granzyme (granzyme A and granzyme B). Perforin creates pores in the infected cell followed by the delivery of granzyme, a serine protease, into the cell resulting in lysis [222]. In addition to perforin-mediated cell lysis, CTLs can induce apoptosis by expressing cytokines such as TNF, Fas/FasL, and TNF-related apoptosis-inducing ligand (TRAIL), which recruit death receptors in influenza-infected cells [223-225]. Although neutralizing antibodies protect from viruses from the same serotype, CTLs are specific for their epitopes in conserved IAV proteins such as NP, M1 and PA and are therefore heterosubtypic in their protection [226] and can prevent from viral transmission influenza from the URT to the lung [227].

Another key component involved in adaptive immunity against IAV infection are CD4+ T cells. CD4+ T cells target IAV-infected epithelial cells through MHC-II and

can induce MHC-II expression in these cells in mice [146, 228] as well. As for CD8+ T cells, CD4+ T cells are activated by DCs that migrate from the lung to LNs following IAV infection [229]. CD4+ T cells Th0 differentiate into Th1 cells according to their stimulators (shown in Table 1.4) plus antigen, co-stimulatory molecules and cytokines secreted by DCs, epithelial cells and other inflammatory cells [230]. Th1 cells express antiviral cytokines including IL-2, IFNγ, and TNFα and activate alveolar macrophages [231]. CD4+ T cells are also able to differentiate into Th2, Th17 effector T cells (Teff), regulatory T cells (Treg), and T follicular/helper T cells (Tfh) [232]. Th2 cells bind to influenza antigens associated with MHC-II on APCs and produce IL-4 and IL-13 to promote B cell responses [233]. Teff and Treg cells are involved in regulating cellular immunity to IAV by enhancing or suppressing inflammatory responses respectively [234, 235]. Tfh cells are specialized providers of T cell help to B cells and are essential for germinal center formation in the lymph node, affinity maturation and development of most high affinity antibodies and memory B cells [193]. Tfh cells facilitate production of high affinity antibodies through secretion of IL-21, IL-4, and IFNγ and through cell-to-cell interactions [236]. Th subsets are shown in Table 1.4 which indicates factors that stimulate their development, as well as cytokines released. Explanation of functions of cytokines driving immune responses [237], including influenza, are shown in Table 1.3.

Table 1.4: Differentiation factors of naïve CD4+ T-cell (Th0) following antigen presentation by DC.

STIMULATING CYTOKINES	***TRANSCRIPTION FACTOR***	***DIFFERENTIATED CELL TYPE***	***DIFFERENTIATED CELL FACTOR SECRETION***
IL-12 IFNγ	STAT1 STAT4 T-bet	**Th1**	IL-2 IFNγ TNFα
IL-4	STAT6	**Th2**	IL-4

STIMULATING CYTOKINES	*TRANSCRIPTION FACTOR*	*DIFFERENTIATED CELL TYPE*	*DIFFERENTIATED CELL FACTOR SECRETION*
IL-2	GATA3 IRF4		IL-5 IL-6 IL-10 IL-13
IL-21 IL-12 IL-23 TGFß	Bcl6	**Tfh**	IL-21 IL-4 IFNγ
TGFß IL-6	RORγt RORα STAT3 IRF4	**Th17(Teff)** **Pro-Inflammatory**	IL-17 IL-21 IL-22 IL-6
TGFß IL-12	SMAD FoxP3	**Treg**	TGFß IL-35 IL-10

Germinal center (GC) reactions in the lymph node and antibody generation

Once a B cell matures and leaves the bone marrow, it is a naïve mature B cell and expresses a functional B cell receptor and IgD and IgM on its surface. It then migrates to secondary lymphoid organs, such as the lymph node where it undergoes activation, class switching, division and proliferation. Class switching from IgM/IgD to other isotypes such as IgA and IgG are determined by the type of cytokine signal received from Th cells after antigen presentation [238]. Cytokines IL-4→IgG1 [239], IL-5→IgG1/IgE [240], TGFß→IgA [241], and IFNγ→IgG2a [242] are all known to induce isotype switching after activation in mice and humans.

The GC of lymphoid organs is the main structure of intense cell proliferation and death, where antigen-activated B cells diversify their immunoglobulin genes by somatic hypermutation to generate high affinity antibodies. Most of these cells also undergo class-switching to generate antibodies with specialized effector functions [243]. Naïve

circulating B cells enter lymph nodes from the blood through high endothelial venules and are attracted by chemokines into the primary lymphoid follicle. If the B cells do not encounter viral antigen in the follicle, they leave through the efferent lymphatic vessel.

Following primary activation of DCs by virus or antigen and activation of the innate immune responses, DCs traffic to the draining LN where processing and presentation of peptide antigens occurs on MHC-I or MHC-II to naïve lymphocytes allowing clonal expansion of CD8+ cytotoxic or CD4+ helper T cells respectively [244, 245]. Effector T cells traffic back to the airways and Th2 cells train short-lived plasma B cells resulting in low levels of IgG and IgA production [246]. In GC reactions involving T cell responses and antibody production, Teff cells amplify innate responses or CTLs engage in antigen-specific cell killing. Antigen experienced B cells engage with Tfh cells leading to class switch recombination, affinity maturation (somatic hypermutation) and differentiation into long-lived plasma or memB secreting high-affinity antibodies [247, 248].

Immunoglobulin isotypes and function

For ferrets five immunoglobulin isotypes have been identified (IgM, IgG, IgE, IgA and IgD). All but IgD were found to be homologous in sequence to human isotypes [249]. So far, only one subclass of IgG has been identified in ferrets [250]. For purposes of type and function, human and mouse immunoglobulins are compared. For humans there are five different classes of immunoglobulins (Ig) that are distinguished in their different structures of their constant regions; these are known as immunoglobulin M (IgM), immunoglobulin D (IgD), immunoglobulin G (IgG), immunoglobulin A (IgA),

and immunoglobulin E (IgE). All antibodies are constructed in the same way consisting of paired heavy and light polypeptide chains. Subtle differences in the variable region account for the specificity of antigen binding. The IgG molecule will be used to describe the general structural features of immunoglobulins [251].

IgG antibodies are composed of two different kinds of polypeptide chains; one of approximately 50 kDa is called the heavy chain and the other of 25 kDa is called the light chain. Each IgG molecule consists of two heavy chains and two light chains with the two heavy chains linked to each other by disulfide bonds, and each heavy chain is linked to a light chain by a disulfide bond. In any given Ig molecule, the two heavy chains and two light chains are identical allowing for the antibody molecule to bind to two identical antigens on a surface thereby increasing the total strength of the reaction (avidity). The strength of an interaction between a single antigen-binding site and its antigen is known as affinity. Two types of light chains lambda (λ) and kappa (κ) are found in antibodies. Functional differences have not been determined; however, different binding preferences for influenza have been found for ferret κ and λ light chains [252, 253]. Ig heavy and light chains are composed of constant and variable regions which recombine in various combinations which account for their antibody diversity.

IgM – Immunoglobulin mu (IgM) is the first immunoglobulin produced after activation of a B cell. It is secreted as a pentamer and therefore has high avidity but low affinity and represents ~10% of total serum antibody. IgM plays a key role in early response to influenza virus since it can be secreted to mucosal surfaces and interacts strongly with complement which is its primary effector function[254]. IgM is one of the antigen receptors on naïve B cells.

IgG – Immunoglobulin gamma (IgG) is one of the most abundant proteins in human serum, accounting for about 10-20% of plasma protein and 75% of antibody found in serum [255]. IgG has higher affinity than IgM and primarily function to neutralize toxins, viruses and bacteria, opsonize them for phagocytosis and activate the complement system. They can also activate ADCC by NK cells and transfer across the placenta or gut. There are four subclasses of IgG: IgG1, IgG2, IgG3, and IgG4 named for their decreasing order of abundance in the serum. Each subclass differs in their hinge region and upper constant region 2 resulting in different effector functions [254]. The relative half-life ($T_{1/2}$) is relatively short $T_{1/2}$=7 days compared to the other isotypes ($T_{1/2}$ = 21 days). The majority of the IgG antibodies targeting influenza are IgG1, followed by IgG3 [256-258]. IgG1 has a long $T_{1/2}$ and reacts strongly with Fcγ receptors (FcγRs) making it highly effective ad direct virus inhibition and FcR-mediated effector functions [254]. IgG2 and IgG4 antibodies to influenza are negligible and IgG2 is mostly involved in responses to bacterial capsular polysaccharide antigens [259].

IgA – Immunoglobulin alpha (IgA). IgA represents ~15% of total serum antibody and exists as IgA1 and IgA2 subtypes. IgA1 mostly forms the monomeric IgA fraction in the serum and is also secreted as a dimer on mucosal surfaces. IgA2 is mostly found as a dimer in the URT [260]. It has been proposed that the large number of glycosylation sites on IgA compared to the other antibody isotypes might increase its affinity for influenza HA through interactions between HA and sialic acid [261]. It has been reported that the LRT is mainly protected by IgG, with a ratio of IgG:IgA of 2.5:1, whereas the antibody response in the URT is mainly IgA, with a ration of IgG:IgA of 1:3 [262]. IgA does not activate complement.

IgD and IgE – Immunoglobulin delta (IgD) and Immunoglobulin epsilon (IgE). IgD is membrane bound and found on the surface of mature B cells and co-expressed with IgM prior to class switching. IgE response is generated primarily towards intracellular parasites.

While antibodies to HA and NA are clearly protective antiviral activity towards influenza internal proteins has been studied less frequently. Due to the inaccessibility of their targets on live infected cells, theses antibodies show no direct antiviral activity; however, antibodies to NP have been shown to provide weak protection against influenza in a mouse model [263, 264]. The importance of antibodies, especially neutralizing antibodies to HA, cannot be overstated. Additional ferret immune reagents, including reagents to differentiate antibody isotypes and subclasses are critical in understanding differences following IAV and IBV infection. A general overview of the immune response following influenza infection is illustrated in Figure 1.1 (Used with author and journal permission [265]).

Figure 1.1 : General overview of the immune response following influenza infection.

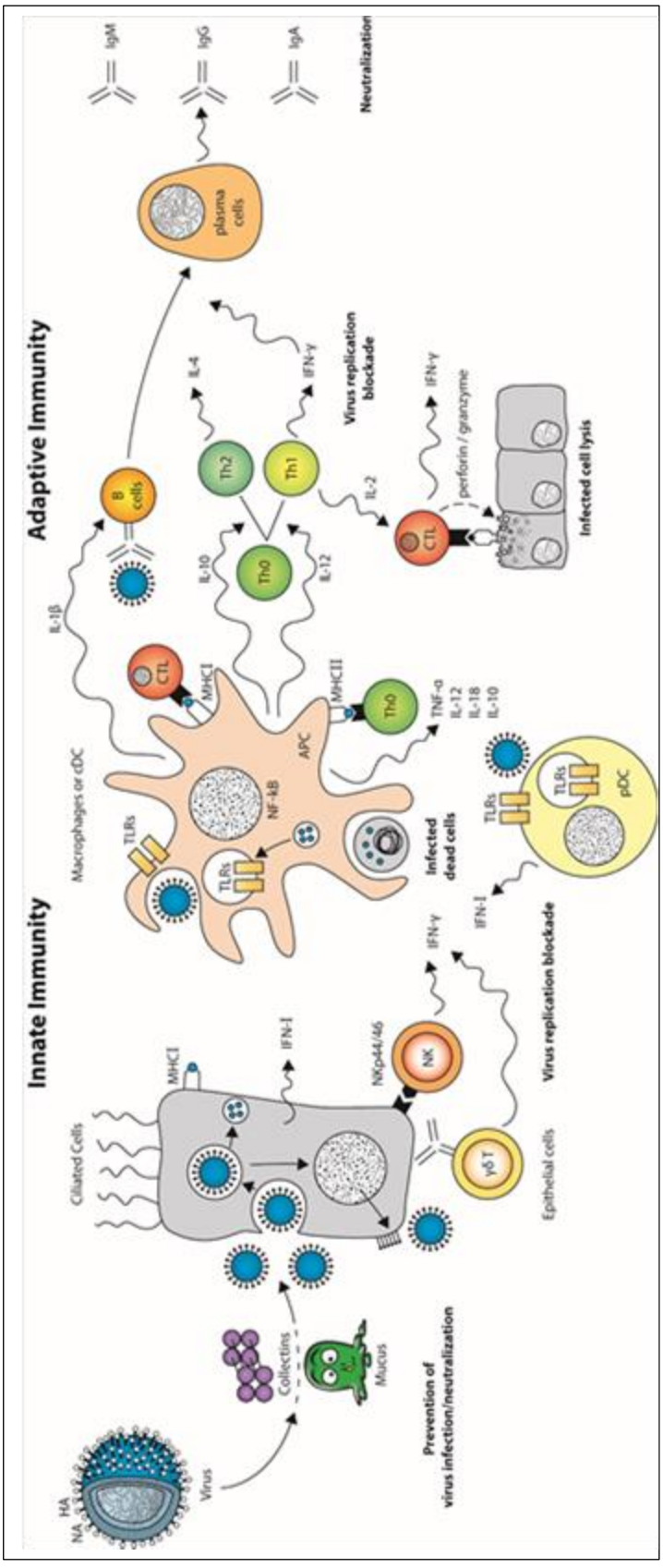

ANIMAL MODELS FOR INFLUENZA RESEARCH

It is important to choose the correct animal for research. To be accepted and widely used, the animal model must accurately mimic the desired function or disease, be available to multiple investigators, have defined genetic information available, and demonstrate a thorough understanding of the similarities and differences in responses between humans and the model [266]. In order for an animal model to be used for developing and testing of new vaccines and interventions, such as for influenza viruses, the Animal Model Qualification Program of the Food and Drug Administration has concluded:

> *"The animal model (i.e., the specific combination of an animal species, challenge agent, route of exposure) can reliably produce a disease process or pathological condition that in multiple important aspects corresponds to key elements the human disease or condition of interest." [267]*

Comparisons of animal models commonly used in influenza research are important in understanding the pros and cons for each and why the ferret was selected for this body of work. Comparisons of the most common animal models used in influenza research are described below and summarized in Table 1.3.

Mouse

The mouse (*Mus musculus*) is the most widely used animal model for influenza research. In the URT of mice α2,3-linked sialic acid and α2,6-linked sialic receptors are evenly distributed but more α2,3-linked receptors in the lungs [268]. This allows for its

use as a more suitable model for avian influenza viruses [269]. Mice infected with non-adapted human influenza viruses generally do not exhibit symptoms typically seen in humans; however, some highly pathogenic avian influenza viruses can infect mice directly with high mortality [269-271]. Most human IAV and IBV require adaptation through serial passage in mouse lungs. Although mouse-adapted influenza viruses can be used for experiments with reproducible results, serial passage introduces several mutations in order to efficiently replicate in mice [272-274]. Since most strains of mice lack a functional *Mx* gene [275], innate immune studies involving effects of IFN, such as in this work, are not possible. Different strains of inbred mice show varying susceptibilities to IAV infection. DBA/2 mice are relatively susceptible to various IAV whereas BALB/c and C57/Bl6 strains being relatively resistant to these same viruses [276]. Hyper-immune inflammatory response was only partially due to viral loads, indicating that gene regulation by the host innate response played an important role [277]. However, the availability of a variety of genetic backgrounds including knock-out stains of specific immune components make them a valuable model for exploring immunological pathways.

Unlike ferrets, mice do not develop fever following infection with influenza viruses, instead they may become hypothermic [278, 279]. In typical mouse influenza experiments two clinical outcomes are generally evaluated: weight loss and survival [280]. Although these endpoints are valuable, they do not fully measure respiratory distress which has been associated with pneumonia [281]. Respiratory distress is not easily observed and has primarily been detected post-mortem by comparison of lung weight or histological evidence of tissue injury [282, 283]. Evidence of respiratory

distress have been measured in arterial O_2 and CO_2 levels; however, this is also post-mortem and involves ligation of the carotid artery, collection of arterial blood, and testing on a blood gas analyzer [284]. Another limitation of this model is the inability to transmit influenza from one animal to another by aerosol. Mice do not sneeze, so mouse-to-mouse transmission can only occur via contact. Influenza transmission in mice by contact has been reported [285]. Transmission was subtype dependent as well and an association between viral loads in saliva and increased likelihood of transmission was found.

Mice are frequently used in the initial stages of vaccine testing in animals. Vaccine safety, efficacy, and immunogenicity are tested in this model [286]. Mice are commonly vaccinated usually with a prime dose followed by 1 – 2 booster doses several weeks apart in order to develop a sufficient antibody response. Animals are then usually challenged with either a mouse-adapted influenza strain or dose which results in at least weight loss following challenge. Vaccine effectiveness in mice can be challenging since intertypic effectiveness of the immune response is different from humans. Mice recovering from infection may be protected not only from drift viruses within the same subtype (subtype specific immunity) but also by another subtype (heterosubtypic immunity); whereas, heterosubtypic immunity is not generally observed in humans [287]. Therefore, experiments using a second animal species is required for vaccine regulatory approval. The selection of animal models must be appropriate and closely resemble immune responses in the target host [288]. Key benefits of the mouse model include cost and housing requirements, inbred strain availability for mechanism studies, and availability of immune reagents. Use of mice for future experiments from this work may

prove invaluable in understanding key regulators of the immune response following influenza infection or vaccination.

Guinea pig

The guinea pig (*Cavia porcellus*) is naturally susceptible to infection with human influenza strains and is primarily used for transmission studies [289]. The outbred Hartley strain is most commonly used for influenza research and has first been described as a transmission model for influenza by Lowen *et al.* in 2006 [290]. In the study using IAV (H3N2 subtype), efficiently transmitted via aerosol to adjacently housed animals indicated by high titers for virus in nasal washes. Unfortunately, no clinical signs (weight loss or temperature differences) were evident in infected animals. IBV show high levels of transmission in a contact model and intermediate transmission (1/2 of animals) via aerosol in guinea pigs. Interestingly, housing inoculated animals at lower temperatures (5°C) resulted in increased and prolonged virus shedding in the URT compared to animals housed at higher (20°C) temperatures [291]. Although histological changes were observed in some lung tissue, no virus was detected. This model may also be used in studies on the effects of the use of IFNs on infection or spread. Guinea pigs treated intranasally with human recombinant IFNA prior to IAV(H1N1) infection and daily thereafter showed reduced virus replication 1,000-fold and was able to block transmission to exposed animals [292]. Although neutralizing antibodies to influenza examined, other studies have shown that guinea pigs generate high levels of mucosal and serum antibodies to influenza following infection or vaccination [293, 294]. Therefore, the guinea pig can be used as a potential model to address transmission of influenza as well

as vaccine efficacy; however, the absence of clinical signs and limited immune reagents preclude this model for further exploration in this work.

Non-human primates

Because non-human primates (NHP) are closely related to humans due to their phylogenetic relatedness, physiology, and immune system they could be used as an animal model for studying respiratory viruses [295] . Thus, in theory, they should be good models for human disease. Seroprevalence studies in NHP (from pets, performing animals, temple animals, and in reserves) in southeast Asia have found between 13 – 29% seropositivity to IAV [296] indicating that may play a role in the ecology of influenza. Transmission to NHP may be the result of human contact, thus demonstrating they are naturally susceptible to infection by influenza viruses. In fact, NHP sialic acid receptor linkage is primarily α2,6- in the URT and both α2,3- and α2,6- in the LRT [297]. Several macaques subspecies have been developed as an NHP model for influenza viruses. These include: cynomologous macaques (*Macaca fascicularis*), rhesus macaques (*Macaca mulatta*) and pigtailed macaques (*Macaca nemestrina*) [298].

NHP susceptibility to IAV isolates, including H1N1 [299], H3N2 [300], H1N1pdm09 [301] and H5N1 [302, 303] subtypes has been demonstrated; however, clinical signs were not always consistent to humans. Even though the viruses replicated well in the respiratory tract, most seasonal viruses to not generally show symptoms in NHP [304], but highly pathogenic strains induce clinical signs similar to those in humans [305]. Inflammatory responses, including IFN following challenge with H1N1pdm09 viruses were upregulated in NHP [301] which was similar to responses observed in

ferrets [306]. Limitations to widespread use are ethical, housing and husbandry costs, animal handling expertise, and study size. The main advantage of the NHP animal model is for vaccine and therapeutic studies since it allows for analyses of immune responses due to the closeness to human responses.

Ferret

Ferret (*Mustela putorius furo*) susceptibility to influenza was first demonstrated in 1933 when virus was isolated in animals following infection with throat washes from infected humans [307]. The ferret remains one of the best small animal models for influenza research. Sequencing of the complete ferret genome has allowed functional genomic analysis and expanded use of this model [308, 309]. In fact, the ferret has been used as an animal model for a number of respiratory pathogens including respiratory syncytial virus [310, 311], measles virus [312], parainfluenza virus [313], metapneumovirus [314]. Ferrets have also been used as a model for coronaviruses from the initial viruses which caused Severe Acute Respiratory Syndrome (SARS) [315] in humans as well as the more recent SARS-CoV2 virus resulting in the COVID19 pandemic [316]. The ferret model has been used extensively for influenza research and remains the primary animal model due to the wide array of research uses [317].

Human clinical IAV and IBV can readily infect and transmit in ferrets without adaptation as required in mice. Several clinical signs in ferrets following infection mimic those in humans including development of fever, weight loss, sneezing, nasal discharge, and fever [318]. Additionally, ferrets display similar distribution of α2,3-linked and α2,6-linked sialic acid receptors as humans on cells lining their respiratory tracts [54, 319,

320] allowing for efficient infection by human influenza isolates. This allows the ferret to be an effective model for studies of pathogenicity, transmission and tropism of influenza viruses [318, 321-325]. The ferret transmission model for influenza was key in confirming lack of human-to-human transmission of highly pathogenic avian influenza viruses (H5N1) [321] and demonstration of a two amino acid change in the HA altered the transmissibility of 1918 influenza virus [326] allowing for the confirmation of the role of HA receptor specificity in influenza transmission in mammals.

Only outbred ferrets are currently available thus limiting their use in dissecting specific immune responses or disease conditions. To date, the only knock-out ferret developed has been in an anion channel, cystic fibrosis transmembrane conductance regulator, which was disrupted in neonatal ferrets resulting in a cystic fibrosis phenotype and use for research [327, 328]. However, advances in using the ferret for evaluating the effects of influenza infection and vaccination in high-risk populations have been possible. Aged ferrets have been used in understanding challenges of influenza vaccination in the elderly [329]. Higher susceptibility to infection including increased clinical signs and mortality than adult ferrets for H1N1pdm09, mimicked responses observed in elderly human populations [330]. Research into other populations at high risk for influenza include an diet-induced obesity model where increased disease severity and reduced vaccine efficacy has been recently reported in an obese ferret influenza model [331], and pregnancy model for vaccine efficacy and maternal antibody transmission [332, 333].

A key component in the immune response following influenza infection or vaccination is the understanding of the initial innate response in the host. For the ferret model, due to a limitation in the availability of immune markers, only a few areas have

been explored and these are primarily by differential gene expression for IAV studies [5, 306, 334-336]. Due to the susceptibility to influenza infection, transmission, and similarities to human responses the ferret model has great versatility for influenza virus research. Availability of additional immune reagents will allow for increased use in understanding immune responses to influenza and development of better countermeasures.

Other animal models

Other animal models are not as widely used and are mentioned briefly. The cotton rat (*Sigmodon hispidus*) has been reported to be primarily used as an animal model for respiratory syncytial virus [337, 338]; however, it has also been shown to be susceptible to influenza [339-341]. IAV are able to replicate and induce symptoms in the cotton rat without virus adaptation as in the mouse model [340, 342]. Unlike mice [275, 343, 344], cotton rats have a functional *Mx1* gene which is a an IFN-inducible gene involved in the innate response to influenza infection [345-347]. Difficulty in handling [348], minimal clinical signs comparable to humans [349, 350], and immune reagent availability [351, 352] limit the use of this animal model for influenza studies.

The Syrian hamster (*Mesocricetus auratus*) is mainly used for influenza transmission studies, but only observed by contact and not aerosol [353]. Hamster have also been used for influenza vaccine studies, primarily LAIV since their core temperature is similar to humans. Virus growth was reduced in the lungs but replicated in the URT, showing similar phenotypes to these viruses in humans [354, 355]. Hamsters show evidence of infection by detection of virus in the URT and LRT and generation of

antibodies to influenza. Unfortunately, hamsters do not show clinical signs of infection [356-358] thus limiting in their use detecting morbidity and mortality in challenge studies following vaccination or treatment with antivirals.

Table 1.3: Comparison of animal models for influenza research

	Mouse	**GP**	**NHP**	**Ferret**
Human Seasonal IAV/IBV replication	No (Adaptation Required)	Yes	Yes	Yes
Sialic Acid Receptor linkage	URT(α2,3 & α2,6) LRT(α2,3)	URT(α2,6) LRT(α2,3 & α2,6)	URT(α2,6) LRT(α2,3 & α2,6)	URT(α2,6) LRT(α2,3 & α2,6)
Fever	No	No	+/-	Yes
Clinical signs (Similar to Human)	No	No	No	Yes
Clinical signs	Weight loss Ruffled fur Respiratory distress death	Limited sneezing	+/-Fever +/-Sneezing +/-Nasal discharge +/-Lethargy +/-Weight loss	Fever Sneezing Nasal discharge Lethargy Weight loss
Transmission model	No	Yes	+/- (cost prohibited)	Yes
Immune reagents	Yes	+/- (limited)	Yes	+/- (limited)

	Mouse	GP	NHP	Ferret
Limitations	Requires virus adaptation Limited clinical signs No transmission	No clinical signs Limited immune reagents	Inconsistent clinical signs High costs	Limited immune reagents Medium costs

HYPOTHESIS AND SPECIFIC AIMS

The studies in this dissertation will determine if infection with IBV induces altered innate immune responses, compared to IAV, which could suppress the development of robust adaptive immune responses. The studies will also address overcoming innate immune deficiencies through vaccination with immunomodulators and determination whether a robust adaptive immune response to IBV can be induced in these animals. An understanding of factors that result in reduced antibody responses in ferrets may lead to the development of improved IBV vaccines in humans. These hypotheses will be addressed in the following Specific Aims:

SPECIFIC AIM 1: To determine the differences in cellular responses to infection with IAV and IBV in vitro.

The working hypothesis is that IBV infection results in an alteration of the innate immune response in respiratory epithelial cells and their immunological crosstalk with peripheral blood mononuclear cells. For the first part of this aim, human IBV from both Yamagata and Victoria lineages were used for infection in primary ferret upper respiratory tract cells [359]. Samples were collected at various time points (1h, 6h, and days 1-3) post-inoculation. Cytopathic effects, viral titers, and gene expression levels were measured In vitro. Gene expression profiles were examined for multiple pro-inflammatory cytokines involved in innate responses to IBV and compared to seasonal and pandemic IAV [306, 360].

For the second part of this aim, factors released by IBV-infected respiratory epithelial cells fail to activate innate immune responses in peripheral blood mononuclear cells. Differentiated ferret primary upper and lower respiratory tract cells were apically infected with IBV and IAV in Transwell™ chambers followed by the addition of peripheral blood mononuclear cells (PBMC) to the basolateral side of the cultures one day post infection. Innate gene expression profiles were examined in both the respiratory cells and PBMC following infection. Co-cultured PBMC were assessed for innate gene expression. Secreted factors were measured in the supernatant from the basolateral side of the epithelial cell cultures following infection with IBV and compared to those secreted following IAV infection.

SPECIFIC AIM 2: To determine the differences in adaptive responses to infection with IAV and IBV in vivo.

The working hypothesis is that delay of the innate immune response following IBV infection affects the development of a robust antibody response in ferrets. Ferrets were infected intranasally with IAV (H1N1PDM09 and H3N2 subtypes) or IBV (Victoria and Yamagata lineages) and samples from the respiratory tract and blood were collected at various times post infection. Viral titers were assessed in respiratory samples and gene expression profiling was performed in respiratory and systemic (blood) samples to measure innate gene expression levels, cytokine/chemokine expression levels and these data compared to human clinical, pathological, immune, and viral outcomes of IAV and IBV. Antibody levels were measured in blood samples from 1 to 4 weeks post infection. Statistical analysis of gene expression, cytokine/chemokine, and antibody levels were

compared to observed differences between weak and strong responders to determine the effect of innate immunity on adaptive immunity.

SPECIFIC AIM 3: To determine the effects of immune adjuvants on enhancing adaptive responses following infection or vaccination with IBV in vivo.

The working hypothesis is that delay of the innate immune response following IBV infection or vaccination affects the development of a robust antibody response in ferrets which can be overcome by specific immune adjuvants. Ferrets were challenged with IBV or mock challenged followed by intranasal administration of innate immunomodulators (IFNα and IFNλ), which should enhance innate and adaptive immune responses. Assessment of innate and adaptive immunological responses occurred over a three-month period following challenge. Animals were either re-challenged or challenged (mock challenge group) with homologous IBV and protection was compared to non-adjuvanted animals. Innate and adaptive immune responses from blood and nasal washes were assessed by transcription status, cytokine/chemokine levels, and antibody responses. Assessment of protection following viral challenge was measured by a reduction in clinical signs and viral loads in nasal washes and compared to non-adjuvanted and previously infected animals. For the second part of this aim, the effects of innate immune modulators on the protection of ferrets were compared to naïve and non-adjuvanted vaccinated animals demonstrating that overcoming innate immune dysregulation reduced ferret morbidity. I anticipate that this work will reveal a potential mechanism that IBV have evolved to allow persistence of circulating virus in humans through a suppression in

innate immune and antibody responses. I predict that IBV-mediated immune delays can be overcome by addition of innate immunomodulators.

CHAPTER 2

DIFFERENTIAL INTERFERON RESPONSES TO INFLUENZA A AND B VIRUSES IN PRIMARY FERRET RESPIRATORY EPITHELIAL CELLS[1]

[1] Rowe, Thomas, Davis, William G., Wentworth, David E. and Ross, Ted M. Differential interferon responses to influenza A and B viruses in primary ferret respiratory epithelial cells. Journal of Virology vol. 98,2 (2024): e0149423. doi:10.1128/jvi.01494-23. Reprinted here with permission of the publisher.

ABSTRACT

Influenza B viruses (IBV) co-circulate with influenza A viruses (IAV) and cause periodic epidemics of disease, yet antibody and cellular responses following IBV infection are less well understood. Using the ferret model for antisera generation for influenza surveillance purposes, IAV resulted in robust antibody responses following infection, whereas IBV required an additional booster dose, over 85% of the time, to generate equivalent antibody titers. Methods: In this study we utilized primary differentiated ferret nasal epithelial cells (FNEC) which were inoculated with IAV and IBV to study differences in innate immune responses which may result in differences in adaptive immune responses in the host. FNEC were inoculated with IAV (H1N1pdm09 and H3N2 subtypes) or IBV (B/Victoria and B/Yamagata lineages) and assessed for 72 hours. Cells were analyzed for gene expression by qRT-PCR and apical and basolateral supernatants were assessed for virus kinetics and interferon (IFN), respectively. Results: Similar virus kinetics were observed with IAV and IBV in FNEC. Comparison of gene expression and protein secretion profiles demonstrated that IBV-inoculated FNEC expressed delayed type-I/II IFN responses and reduced type-III IFN secretion compared to IAV-inoculated cells. Concurrently, gene expression of Thymic Stromal Lymphopoietin (*TSLP*), a type-III IFN-induced gene which enhances adaptive immune responses, was significantly down-regulated in IBV-inoculated FNEC. Significant differences in other pro-inflammatory and adaptive genes were suppressed and delayed following IBV-inoculation. Conclusions: Following IBV infection, *Ex vivo* cell cultures derived from the ferret upper respiratory tract exhibited reduced and delayed innate responses which may contribute to reduced antibody responses in vivo.

INTRODUCTION

Most influenza studies focus on influenza A viruses (IAV); however, influenza B viruses (IBV) represent nearly one quarter of all influenza cases and are generally responsible for most cases that occur late in influenza annual epidemics [1]. Even though IBV co-circulates with IAV, little is known about the antibody and cellular responses following IBV infection [2, 47]. Additionally, the influenza B lineages selected for annual influenza vaccines have only matched the dominating circulating influenza B strains in 5 of the 10 seasons between 2001 – 2011 [361]. During the 2014-2015 influenza season, the vaccine effectiveness against influenza B (Yamagata lineage) was ~57% and fewer than 20% of older children and adults had a ≥4-fold rise in HAI titer following vaccination[362]. More recently, during the 2019-2020 influenza season which was characterized by two consecutive waves of activity, beginning with influenza B (Victoria lineage) and followed by influenza A (H1N1pdm09), the vaccine efficacy (VE) to influenza B in adults was 30% [363]. In northern India where Influenza B dominated during the same season, the genomic mismatch between circulating influenza B strain and the WHO-recommended vaccine strain resulted in a VE of 0% [364].

The domestic ferret (*Mustela putorius furo*) is an important model for influenza since human clinical IAV and IBV can infect ferrets, produce clinical symptoms like those seen in humans, and readily transmit between animals. Furthermore, human clinical isolates can readily infect ferrets without adaptation [365], as required for mice [272, 274, 366, 367]. Since there exists significant similarity in the infection and disease course of IAV and IBV in both humans and ferrets, understanding the mechanism of immune

responses in the IBV-infected ferret may aid in better understanding human IBV infections and vaccine development. This model has limitations in the reagents available for studying the innate and adaptive immune responses; however, recent advances in reagent development [368, 369], including sequencing the ferret genome [308], have allowed for exploration into innate and adaptive immune responses in ferrets following influenza infection. Ferrets infected with influenza viruses have been used to generate reference antisera for human and animal influenza virus surveillance activities, including use of antisera in hemagglutination inhibition (HI) and virus neutralization assays [370]. Previous studies involving generation of immune sera from ferrets intranasally infected with influenza have shown dampened antibody responses in ferrets following influenza B inoculation compared to influenza A. IBV infection required two doses of IBV, intranasal prime and intramuscular boost, to obtain the same immune response and antibody titer as observed following one dose of influenza A.

Innate immune responses in ferrets have primarily focused on IAVs where an association between innate immune responses and transmission and virulence has been found [5]. In this study we wished to determine whether infection with IBVs induce altered innate immune responses which could suppress the development of robust adaptive immune responses. To fully understand the differences in the innate responses to IAV or IBV infections, we utilized differentiated primary ferret nasal epithelial cells (FNEC) for this study.

Initial innate immune responses following influenza infection include activation of the interferon (IFN) response. IFN not only limits viral load, but also has immunostimulatory functions by inducing high levels of proinflammatory cytokines such

as TNF, IL-1B, IL-6 and other chemokines, which result in pathological lung effects [371]. IFNs have roles in determining the rate of virus replication initially, shaping downstream inflammatory responses and adaptive immune responses. IFNs can have both positive and negative effects on adaptive immune responses. For example, during acute lymphocytic choriomeningitis virus (LCMV) infection an upregulation of type-I IFN is beneficial in activating dendritic cells (DCs) and T-cell adaptive functions; however, chronic infection with sustained IFN production has been shown to suppress DC expansion and induce an immunosuppressive phenotype [372]. Type-III IFN (IFNL3) has been shown to induce thymic stromal lymphopoietin (TSLP) following influenza infection, leading to increased adaptive mucosal immunity [137]. TSLP was first identified in a mouse thymic stromal cell line and found to affect B-cell proliferation and development [373, 374]. TSLP has also shown a direct effect on CD8+ T-cells and an indirect effect through dendritic cells (DCs) following influenza A infection in mice [375].

Immune responses following infection of ferrets with pre-2009 seasonal H1N1 or 2009 pandemic H1N1 (H1N1pdm09) influenza A viruses demonstrated an immune switching from an innate immune response to an adaptive immune response. A correlation of the innate immune gene signatures between a ferret-pathogenic H1N1pdm09 virus (A/California/07/2009) to a mildly pathogenic pre-2009 seasonal H1N1 (A/Brisbane/59/2007) in ferrets indicated that robust expression of chemokines and interferon-stimulating genes (ISGs) were expressed early in the pathogenic strain and correlated to lung pathology. Comparisons of the two viruses in ferrets indicated that a more robust innate response resulted in development of an early, high adaptive immune

response[306]. When producing reference antisera for influenza surveillance studies from 1998-2019, 97% (1064/1094) of ferrets infected with influenza A viruses resulted in reproducible, high-titered ferret antisera within 14 days post infection, whereas following infection with influenza B viruses, only 13% (61/448) generated sufficient titers during the same timeframe and required boosting animals with concentrated virus plus adjuvant (TiterMax^{TM}) to generate comparable serum titers.

Epithelial cells lining the respiratory tract are important regulators of innate and adaptive immunity to influenza viruses [376]. To determine if these specific innate responses could be recapitulated in vitro, we isolated and differentiated ferret respiratory epithelial cells from the upper respiratory tract and compared differences in gene expression, interferon secretion and viral kinetics following infection with IAV or IBV.

MATERIALS AND METHODS

Viruses

Viruses used were passaged in Madin Darby Canine Kidney (MDCK) cells to retain antigenic similarity to the original human isolates and to avoid structural changes in the hemagglutinin which could occur from passage in eggs [377-379]. All influenza viruses were passaged in MDCK "C#" or MDCK-SIAT1 [380] "S#" cells according to established procedures[381, 382]. Representative IAV used in this study were: A/California/07/2009 "CA" (H1N1pdm09 subtype, Passage: C3) and A/Kansas/14/2017 "KS" (H3N2 subtype, Passage: S3). Representative IBV used in this study were: B/Brisbane/60/2008 "BR" (B-Victoria lineage, Passage: CX/C6) and B/Phuket/3073/2013 "PH" (B-Yamagata lineage; Passage: C4).

Isolation and culture of ferret primary respiratory epithelial cells

All animal procedures were approved by the Institutional Animal Care and Use Committee (IACUC) of the Centers for Disease Control and Prevention in an Association for Assessment and Accreditation of Laboratory Animal Care (AAALAC) International accredited facility. Influenza naïve male fitch ferrets (Triple F Farms, Sayre, PA), between 10 to 18 months of age and seronegative for currently circulating influenza viruses, were anesthetized with an intramuscular cocktail of ketamine (25-30mg/kg) and xylazine (1.5-2mg/kg), exsanguinated and euthanized with intracardiac injection of Euthasol™ (1ml/kg) prior to collection of respiratory tissues. Nasal turbinates, representing the upper respiratory tract (URT) were collected and processed in the following manner:

Nasal turbinates were digested in 25mL digestion medium (MEM, 1.4mg/ml pronase, 0.1mg/ml DNase I) for 48Hr at 4°C and neutralized with 10% final concentration of characterized fetal bovine serum. The cell suspensions were passed through a 70uM mesh cell strainer and erythrocytes were lysed with ammonium chloride. Contaminating fibroblasts were removed by adherence followed by culturing the suspension cells in selective media. Following a two hour adherence of the cells in Petri dishes, the suspension cells were cultured in medium replacing L-Valine with D-valine (D-Val EC basic media) due to the lack of D-amino oxidase enzyme in fibroblasts [383]. D-Val EC basic medium consisted of D-Val MEM (MyBiosource, San Diego, CA USA), HEPES, sodium pyruvate, non-essential amino acids, penicillin/streptomycin, 0.05% BSA. The ferret nasal epithelial cells (FNEC) were cultured in D-Val EC basic medium

on collagen-coated flasks for 7-10 days at 37°C, 5% CO_2 until confluency, detached with 0.05% Trypsin-EDTA, and either cryopreserved or cultured on collagen-coated 1.12cm^2 Transwell® inserts (Corning Life Sciences, Tewksbury, MA USA) at 5x10^4 cells/cm^2. 0.5mL cell suspensions were added to the apical side of Transwell® plates and 1mL D-Val EC basic media added to the basolateral side of the well. Cells were cultured in D-Val EC basic media for seven to ten days and then changed to culturing in EC+ medium [(F12/MEM, HEPES, NEAA, sodium pyruvate, 0.05% BSA, antibiotics) supplemented with growth factors in SingleQuots (Lonza, Walkersville, MD) and retinoic acid (15ng/ml)]. Medium exchanges every 2 – 3 days to the apical and basolateral sides of the cultures continued until the cells formed a confluent monolayer and the transmembrane resistance of >800Ω/cm^2, as measured using a Millicell ERS-2 volt/ohm meter (Millipore Sigma, Burlington, MA), was achieved. The apical medium was removed at this point to create an air-liquid interface (ALI), and the basolateral medium was exchanged three times/week for an additional 3 to 4 weeks. After this time, evidence of ciliary action was observed in the cultures and mucous production by goblet cells. Following ALI culture, the monolayers were rinsed weekly with PBS to remove any residual mucous accumulation. Cell cultures isolated from the URT consisted of primary ferret nasal epithelial cells (FNEC) and have previously been shown to be structurally similar to nasal epithelium [359]. Three to four weeks post ALI culture, cells were inoculated with influenza viruses.

Infection of FNEC with influenza A and B viruses

The apical side of differentiated FNEC was rinsed three times with F12/MEM to remove any dead cells and mucus. Cells were counted from a representative well following trypsinization with 0.05% Trypsin-EDTA solution (Life Technologies, Carlsbad, CA USA) to determine average cell number per well followed by infection with IAV and IBV viruses at a 0.3 multiplicity of infection. Cells were inoculated apically with 0.3ml/well diluted virus in F12/MEM and incubated at 33°C. The virus inoculum was removed after one hour and the apical side of the cells was rinsed three times with F12/MEM. The basolateral media was removed and replaced with fresh 1ml/well EC+ media and plates were incubated at 33°C throughout the infection.

Virus titration by focus forming assay (FFA)

At various timepoints post infection, 0.3ml of EC+ media was added to the apical surface of inoculated or control wells and incubated for 10 minutes at 33°C. The supernatant was removed from the apical surface and stored at -80°C until evaluated for virus. Influenza virus titers were determined using a Focus Forming Assay (FFA) [384], using MDCK-SIAT1(SIAT) cells, which constitutively express human 2,6-sialtransferase-1 and have shown improved isolation rates for recent A(H3N2) influenza viruses [385] . The FFA was modified and optimized for detection of influenza A and influenza B viruses with increased sensitivity and reproducibility as follows: SIAT cells were seeded in 96-well flat-bottom tissue culture plates overnight to form a confluent monolayer in Dulbecco's Modified Eagle Medium (DMEM) containing 5% heat-inactivated fetal bovine serum (FBS) and antibiotics. The following day, the cell monolayers were rinsed with 0.01M phosphate-buffered saline pH 7.2 (PBS), (Gibco

BRL, ThermoFisher Scientific Inc., Waltham, MA, USA) followed by the addition of fifty microliters per well of virus growth medium plus TPCK-treated trypsin, "VGM-T" [DMEM, 0.1% fraction-V bovine serum albumin (BSA), antibiotics (penicillin/streptomycin) and 1µg/ml TPCK-treated trypsin (Sigma, St. Louis, MO, USA)]. Afterwards, 50µl ½-log serially diluted (10^{-1} to 10^{-6}) sample in VGM-T was added in quadruplicate or VGM-T to cell control wells. A control virus influenza A or B virus standard was also titrated and included as a positive control in each assay. Following a 2 Hr incubation period at 37°C, 100 µl media overlay [equal volumes of 1.2% Avicel RC/CL [386] (Type: RC581 NF; FMC Health and Nutrition, Philadelphia, PA, USA) in 2X MEM containing 1µg/ml TPCK-treated trypsin, 0.1% BSA, and antibiotics] was added. After an incubation of 18-22 hours at 37°C, 5% CO_2, the overlay was removed, and the monolayers were washed once with PBS to remove any residual Avicel. The plates were fixed with ice-cold 4% (w/v) paraformaldehyde in PBS (10% formalin) for 30 minutes at 4°C, followed by a PBS wash and cell permeabilization using 0.5% Triton-X-100 in PBS/glycine at room temperature for 20 minutes. Plates were washed three times with PSBT (PBS, 0.1% Tween-20), incubated for 1 hour with a monoclonal antibody pool to influenza A or B nucleoproteins (International Reagent Resource; www.internationalreagentresource.org) in ELISA buffer (PBS,10% horse serum, 0.1% Tween-80). Following three washes with PBST, the cells were incubated with goat anti-mouse peroxidase-labelled IgG (Sera Care, Inc., Milford, MA) in ELISA buffer for one hour at room temperature. Plates were washed three times with PBST, and infectious foci (spots) were visualized using TrueBlue substrate (Sera Care, Inc., Milford, MA USA) containing 0.03% H_2O_2 incubated at room temperature for 10-15 minutes. The

reaction was stopped by washing five times with deionized water. Plates were dried and foci enumerated using a CTL Bio Spot Analyzer with ImmunoCapture 6.4.87 software (CTL, Shaker Heights, OH). The FFA titer was determined by multiplying sample dilution which gave between one hundred to three hundred spots by the spot number at that dilution, to obtain the FFU/well. The foci in the cell control were subtracted and the number of foci remaining was multiplied by twenty to give FFU/ml. All samples were expressed in log Focus Forming Units per milliliter (FFU/ml). The limit of detection was $10^{3.3}$ FFU/ml.

Gene expression in FNEC

One hundred microliters PBS was added to inoculated or control FNEC monolayers on Transwell® inserts followed by 280 microliters AVL lysis buffer (Qiagen, Germantown, MD USA). Samples were mixed 3-4 times and lysate was frozen at -80°C until RNA extraction. Carrier RNA was added to each sample and RNA was extracted using EZ1 DSP kit on a Qiagen EZ1 Advanced XL extractor according to the manufacturer's instructions (Qiagen, Germantown, MD USA). RNA was eluted in 120 microliters RNAse-free water and stored at -80°C until evaluated for gene expression.

For unpublished primer/probe sets, five sets of primers and probes were designed for each gene using Integrated DNA Technologies PrimerQuest tool (www.idtdna.com/Primerquest/) for ferret sequences found using NIH basic local alignment search tool (BLAST) sequence search (https://blast.ncbi.nlm.nih.gov/Blast.cgi). All unpublished primer/probe sets were chosen following testing using mitogen-stimulated ferret PBMC or LPS-stimulated ferret

respiratory epithelial cells. Designed ferret primer sequences used with TaqMan amplification were as follows: for interferon lambda3 "***IFN-L3***", 5'-ACTCCACACTGCTGCTGCTTAG-3' (forward), 5'-CCTTCCTGTTTACTTGTGCATATTG-3' (reverse), and probe 5'-ATGAAACCAG<LNA A>GTGCTGACCCAAA-3' (probe); transforming growth factor beta1 "***TGFB1***", 5'-CGTGCGGCAGCTCTATATT-3' (forward), 5'-GCAGAAATTGGCGTGGTAAC-3' (reverse), 5'-AAGGATCTGGGCTGGAAGTGG<LNA A>ATC-3' (probe); tyrosine kinase 2 "***TYK2***", 5'-CTCGCATAGAGATCAACCAAGAA-3' (forward), 5'-GAAGTCACACAGGGAGGAAAG-3' (reverse), 5'-AAGCTTATCTACCTGGTGCAGGGC-3' (probe); ubiquitin specific peptidase 18 "***USP18***", 5'-TGCTGTCTTAACTCCCTGATTC-3' (forward), 5'-CTTCTCCTCTGCTCTTCTGTTC-3' (reverse), 5'-TGT GGGCTTCACCAAGATATTGAAGAGG-3' (probe); thymic stromal lymphopoietin "***TSLP***", 5'-GTCTGGGCACATAACTCTAAGG-3' (forward), 5'-CACCCTGGTGTCTCACTAAAC-3' (reverse), 5'-CAGGCCTTGC<LNA A>GATATAGAGCCGATT-3' (probe). All probes were modified with 6-FAM, fluorescein amidites (FAM) fluorophore on the 5' end and a non-fluorescent Black Hole Quencher®-1 (BHQ-1) on the 3' end. Additionally, a locked nucleic acid at adenine <LNA A> was incorporated in most probes in order to increase template binding strength for real-time PCR [387]. Primers and probes for all other ferret genes were generated from published ferret sequences [5, 306, 388-391]. All primer/probe sets used are shown in Table 2.1.

Quantitative real time PCR (qRT-PCR) was performed on triplicate samples using an ABI 7500 Fast Dx Real-Time PCR instrument (Applied Biosystems, Waltham, MA USA). PCR reactions were performed in a 5 microliter RNA reaction volume using SYBR™GreenER™ qPCR SuperMix (Applied Biosystems) or SuperScript™ III Platinum™ One-Step qRT-PCR Kit for TaqMan reactions (InvivoGen, San Diego, CA USA). An RT reaction for 30 minutes at 50°C, was followed by inactivation for 2 minutes at 95°C, then followed by 40 amplification cycles at an annealing temperature of 50°C. Reactions were performed on triplicate samples for each experiment and the values were normalized by subtracting the mean value of the cycle threshold (C_T) from that of the C_T for glyceraldehyde-3-phosphate dehydrogenase (*GAPDH*) housekeeping gene (ΔC_T). The relative levels of gene expression for inoculated cells were determined by subtracting the individual ΔC_T values from that of average ΔC_T values of mock inoculated cells ($\Delta\Delta C_T$) and expressing the final quantification values ($2^{-\Delta\Delta CT}$) as relative fold changes.

Type-III interferon bioassay

Basolateral secretion of interferon lambda (IFN-L) from inoculated FNEC was detected using HEK-L reporter cells (HEK-Blue™ IFN-L cells: InvivoGen, San Diego, CA USA) designed to monitor the activation of the JAK/STAT/ISGF3 pathway induced by type III IFNs. The HEK-L cells were generated by stable transfection of HEK-293 cells with the human IFNLR and IL10R receptor genes as well as the human signal transducers and activators of STAT2 and IRF9 resulting in a fully active IFN-L signaling pathway. Activation of the pathway was detected since these cells harbored the secreted

embryonic alkaline phosphatase (SEAP) under the control of the ISG54 promoter, which is activated by IFN-L. Stimulation of the IFN-L triggered the JAK/STAT/ISGF3 pathway and induced SEAP production which was measured by a colorimetric assay at 650nm using Quanti-Blue^{TM} solution according to the manufacturer's instructions (InvivoGen, San Diego, CA USA).

Twenty microliters of supernatants collected from mock (PBS), IAV and IBV infected FNEC, or media control were added in triplicate wells of 96-well tissue culture plate. A tissue culture flask containing HEK-L cell monolayers was gently rinsed once with PBS and cells were dislodged and suspended in HEK medium (DMEM, 10% FBS, antibiotics) to a concentration of $2.8x10^5$ cells/ml. 180 microliters of HEK-L cells were added to each well containing twenty microliters of sample and to serially 1/2-log diluted (0.1 – 1000ng/ml) recombinant ferret IFN-L3 (Kingfisher Biotech, St. Paul, MN USA). The plates were incubated for 20Hr at 37°C, 5%CO_2. After incubation, twenty microliters of supernatant from the wells were transferred to a new 96-well plate and 180 microliters of Quanti-Blue^{TM} substrate was added and incubated for 2Hr at 37°C, 5%CO_2. Absorbance was read at 655nm. A sigmoidal 4-point standard curve from 0.1 to 1000 ng/ml was generated using recombinant ferret IFNL3 protein and unknown samples were extrapolated from the standard curve. The assay was specific for type-III IFN since type-I ferret and human type-I/II IFNs did not result in an absorbance signal (supplemental figure 2.S1). Detection of type-I IFN was not possible since HEK-A/B cell (type-I IFN bioassay) could not distinguish between human or ferret type-I and type-III IFNs (supplemental figure 2.S1).

Statistical analysis

GraphPad Prism 9 was used for all statistical analyses (GraphPad Software, La Jolla, CA USA). One-way ANOVA was used to determine total IFN-L3 protein concentrations over time between infection groups and significance between groups was determined by 2-way ANOVA analysis. Gene expression analysis was performed by triplicate independent samples per experiment, and outliers were identified by the Grubbs' test (α=0.05) by Extreme Studentized Deviate method for removal of a single outlier plus one iteration from all assays (N=12 total replicates) if found. Spearman (1-tailed, 95% confidence) correlation method used for comparison of virus replication and gene expression. The Student's *t* test was used to assess the statistical differences in the gene expression levels in respect to the mock controls and for comparing influenza A to influenza B viruses. A *p*-value of <0.05 was considered statistically significant: * $p<0.05$, ** $p<0.01$, *** $p<0.001$, **** $p<0.0001$.

RESULTS

Influenza A and B viruses replicate equally in ferret nasal epithelial cells (FNEC).

Following inoculation of differentiated ferret nasal epithelial cells (FNEC) at temperatures consistent with the upper respiratory tract (33°C), similar viral replication kinetics were observed for IAV and IBV (Figure 2.1). When comparing average virus replication for each experiment at each timepoint (Figure 2.1A), no significant differences were observed between any of the viruses (Sidak's multiple comparison test). Additionally, when comparing all experimental samples for viruses from IAV (CA and KS) to IBV (BR and PH) in FNEC, no statistical differences were seen (Figure 2.1B) between groups. Although no differences in the overall virus kinetics were observed, IAV

viruses replicated earlier than IBV in FNEC; however, equivalent virus replication was attained by 72Hr.

Differential gene expressions observed in FNEC following influenza A and B infections.

To determine the temporal relationship between host immune responses and the progression of influenza infection in the upper respiratory tracts of ferrets, FNEC were inoculated with IAV and IBV viruses and examined for gene expression at various time points. The ferret genes (Table 2.1) were assessed by qRT-PCR and fold changes over mock-inoculated FNEC were shown for 72Hr following challenge. When comparing IAV (H1N1pdm09 and H3N2 subtypes) inoculated FNEC to IBV (B-Victoria and B-Yamagata lineages) inoculated FNEC, proinflammatory genes were upregulated and sustained only in IAV (CA and KS) samples (Figure 2.2A). Only proinflammatory genes *IL-6* and *IL-8* were upregulated late (72Hr) following IBV (BR and PH) infection. For comparisons of differences in gene expression following IAV and IBV inoculation of FNEC, an overall upregulation with IAV can be observed compared to IBV (Figure 2.2B). Significant upregulation of all gene categories by IAV compared to IBV-inoculated FNEC was observed by 24Hr (Figure 2.3). Inflammatory response gene functional group (comprised of *CCL2, MCP1, CCL5, IL-1A/1B, IL-6, IL-8* and *TNFA* genes) was significantly upregulated by IAV at 24Hr ($p=0.00007$) and 48Hr ($p=0.0016$) post infection. Early significant differences between IAV and IBV was also observed in interferon (comprised of type-I, -II, and -III interferons) at 24Hr ($p=0.0019$) and 48Hr

(p=0.0046), and T-effector (comprised of *IL-4*, *IL-12*, and *IL-17* genes) functional categories, p=0.0011 and p=0.019 at 24Hr and 48Hr respectively.

For gene categories affecting adaptive responses as well, IAV caused significant upregulation in genes from 12Hr – 48Hr (p=0.0018 @12Hr, p=0.0009 @24Hr and p=0.005 @48Hr) for Th1 (comprised of *CXCL10, CXCL11* and *CXCL*) and 24 – 48Hr (p=0.02 for 24Hr and p=0.021 for 48Hr) for Th2 (*IL-2* gene) functional categories. For all gene categories evaluated, IAV resulted in significant early and sustained upregulation compared to IBV in FNEC.

Temporal differences between gene expression from IAV and IBV inoculated FNEC as shown in Table 2.2. Significant differences are indicated by p values and average fold upregulation shown in pink (>2-fold over mock) and down regulated genes are shown in blue (<1-fold over mock). In all cases IAV showed significantly higher upregulation of genes (>2-fold over mock) to IBV, except for at 72Hr for expression of *CXCL11*. For inflammatory responses, *CCL5* "RANTES show significant differences between IAV and IBV at 12Hr and has been shown to be upregulated following H3N2 inoculation of human airway epithelial cells [392]. Other early (24 – 48Hr) pro-inflammatory and inflammatory genes show significant differences between IAV and IBV and include *CCL2, MCP1, IL-12, IL-1A/B* and *TNFA*. Conversely, significant differences between IAV and IBV for type – I/III IFN genes (*IFNA, IFNB, IFNL3*) are seen late (72Hr), except for type – II IFN (*IFNG* gene), which is upregulated earlier (48Hr). T-effector responses were generally upregulated earlier than T-regulatory responses. Th1 responses were significantly earlier in IAV than IBV, except for *CXCL11* which was significantly higher in IBV very late (72Hr). Early inflammatory responses seen following IAV

inoculation of FNEC are consistent with findings in human airway epithelial cells inoculated with IAV [393-395]. Differences between IAV or IBV compared to mock-infected are shown supplemental Table 2.S2.

Interferons are delayed in FNEC by influenza B viruses.

Since the focus of this study was to discern whether differences in interferon responses following inoculation of FNEC with IAV and IBV may influence adaptive responses, type I/II/III IFN responses were analyzed (Figure 2.4). The average fold gene expressions of Type-I IFNs (Figure 2.4A and 3.4B), type-II IFN (Figure 2.4C) and type-III IFN (Figure 2.4D) were compared following IAV (CA and KS) and IBV (BR and PH) inoculation of FNEC. IAV induced early IFN expression compared to delayed expression by IBV for all IFN types. Significant differences were observed at 48Hr for type-II IFN (*IFNG*, p=0.014) and at 72Hr for type-I IFN (*IFNA* and *IFNB*, p=0.002) and type-III IFN (*IFNL3*, p=0.0154). To determine whether an upregulation in IFN resulted in secretion of IFN protein, we collected basolateral supernatants from IAV and IBV-inoculated FNEC and evaluated using an HEK-IFN reporter assay. Type-III IFN expression system was able to detect recombinant ferret IFNL3 while not detecting type-I/II recombinant ferret IFNs (Supplemental Figure 2.S1). IAV inoculation of FNEC was able to upregulate not only *IFNL3* gene expression but was also able to induce basolateral IFNL3 protein secretion either directly from infected cells or indirectly from bystander cells, were as, IBV-inoculated cultures did not secrete detectable levels of IFNL3 over 72Hr post inoculation (Figure 2.5).

Thymic stromal lymphopoietin (TSLP) is downregulated in FNEC by influenza B viruses.

Since it has been reported that IFNL3 can stimulate adaptive immune responses by triggering TSLP [124], we tested for *TSLP* gene expression following IAV and IBV inoculation in FNEC (Figure 2.6). *TSLP* gene is highly upregulated in FNEC by IAV by 24Hr to 48Hr and remains upregulated through 72Hr. In IBV inoculated FNEC, *TSLP* is downregulated. Significant differences (p=0.037) were observed at 48Hr. *IFNL3* was upregulated (Figure 2.4) following IAV inoculation by 24Hr and remained elevated and was concurrent to *TSLP* upregulation.

Direct correlation between virus replication and IFNB/IFNL3 gene expression, but not IFNA/IFNG, in ferret respiratory epithelial cells.

We have shown the IAV replicated to higher levels earlier (12Hr and 24Hr); however, IAV and IBV reach equivalent titers by 48 – 72Hr in FNEC. Since IFN expression was delayed and lower in IBV-inoculated FNEC, we wanted to determine whether there was a correlation to IFN expression and other genes (Table 2.2). Using nonparametric Spearman correlation, we showed that type-I (*IFNA*) expression did not correlate with viral titer in IAV or IBV, whereas type-III IFN (*IFNL3*) showed a direct correlation for IAV and IBV. However, type-I IFN (*IFNB*) showed a direct correlation to viral load with IAV and IBV. A direct correlation with all proinflammatory genes evaluated to viral load is seen for IAVs. Only *IL-1A, IL-6* and *IL-8* correlate to viral load for both IAV and IBV. Th1 gene (*CXCL11*) showed an inverse correlation for IAV and a direct correlation for IBV. Interferon stimulating genes *STAT1* and *STAT2* showed

correlations for both IAV and IBV; however, only *STAT2* showed a direct correlation for both IAV and IBV. As expected, cell death marker (*GRANA*) showed direct correlation to viral load for both IAV and IBV.

DISCUSSION

Even though the interferon system has potent antiviral activity, it is unable to completely prevent influenza virus infection. Influenza viruses have evolved strategies to attenuate the IFN response to allow for replication and transmission in the host. The interferon response, however, is important in downstream adaptive immune responses and development of antibodies as well as responses to protect the host from tissue damage and clear the infection. Influenza IFN antagonism has been demonstrated for IAV, primarily by the NS1 gene [396]; however, only recently have other influenza viruses (B, C and D) NS1 genes been shown to possess similar functions [397, 398]. In this study we show that IBV inoculation of respiratory epithelial cells results in reduced IFN, and inflammatory responses compared to IAV inoculation which may explain differences in downstream adaptive immune responses. The role of RIG-I in inducing a rapid IFN response following IBV infection over IAV has been demonstrated in human macrophages and dendritic cells [399] and human alveolar epithelial cells [400]. FNEC in this study may show reduced responses compared to other immune cells as well as those in the lower respiratory tract. Macrophages play a vital role in eliminating viruses and triggering innate immune responses. While they are abundant in the LRT, they are less likely to be involved in influenza infections, such as IBV, restricted to the URT [401]. FNEC represent the initial site of infection in the upper respiratory tract and therefore be

unable to initiate an early IFN response to IBV as compared to IAV which is contradictory to responses in other immune cells or viruses which are able to effectively spread to the lower respiratory tract. Differences in the responses seen in this study in cells representing the URT may be more representative in milder influenza infections in viruses restricted to this respiratory compartment Recently, a study using human nasal epithelial cells (hNEC) infected with B-Victoria or B-Yamagata viruses have shown strong upregulation of type-I/III IFNs compared to mock as well as differences between the lineages [402]; however, these studies were only compared to mock-infected and observations were conducted at later timepoints (48Hr and 96Hr post inoculation). This study shows a direct comparison of IAV versus IBV inoculated FNEC from 12Hr to 72Hr. Another recent study using human alveolar epithelial cells (A549) demonstrated a robust ISG and IFN response following B-Yamagata infection [403]. The study utilized a cell line derived from a lung carcinoma and represents a human alveolar cell from the lower respiratory tract. Depending on which respiratory compartment is tested, there are differences in innate immune responses [404, 405]. For example, reduced IFN in the upper respiratory tract compared to the lower respiratory tract have been shown SARS-CoV2-infected patients [406]. This study utilized primary respiratory cells from the upper respiratory tract. Comparison of IFN responses in primary cells from the trachea of ferrets may be important in further elucidating differences between upper and lower respiratory tracts.

In this study IAV-inoculated FNEC activated both inflammatory responses as well as IFN responses, but IBV-inoculated FNEC suppressed and delayed inflammatory and IFN responses. IAV inoculation triggered apoptosis, as evidenced by granzyme A

upregulation (significant 24→72Hr post-infection); whereas granzyme A was not upregulated following IBV inoculation. IAV granzyme upregulation was consistent with studies using human nasal epithelial cell cultures infected with IAV which show upregulation of caspases, *bax* and *BCL-2* [407]. In this study we have also shown upregulation of granzyme pathway genes by IAV. TSLP was also upregulated early (24Hr) in IAV and could result in recruitment and activation of DCs in contrast to IBV where TSLP was not upregulated and may result in a delay in DC activation and downstream immune responses. This delay or suppression of inflammatory and IFN gene activation may be one component leading to lower adaptive immune responses following IBV infection and/or vaccination. Even though differences in virus replication were observed at some individual timepoint between IAV and IBV; overall replication kinetics over 72Hr was not different. Viral replication kinetics was determined from supernatants from infected cell cultures; however, there may be differences in cellular accumulation of viral RNA between IAV and IBV which could affect innate gene activation. Genomic RNA levels to influenza M1 were measured by Zeng et al. and no significant differences were observed in cells following A/H1N1 compared to A/H5N1 in FNEC [359]. Further experiments are warranted to determine if this is similar for IAV and IBV.

Influenza B may show greater IFN antagonism than influenza A as demonstrated a greater suppression and delay of the IFN response in this study. The interferon response was suppressed, as well as other inflammatory responses, in IBV inoculated FNEC. Gene expression responses between IAV and IBV inoculated FNEC showed significantly higher expression levels of Type-I and Type-II IFNs at 24 and 48Hr ($p<0.05$). Interferon antagonism has been shown for influenza A viruses, primarily by the NS1 gene [408].

For IBV, in addition to NS1 [409, 410], polymerase proteins (PB1 and PA) have shown type-1 IFN antagonistic properties [45, 411, 412]. Studies using human cells isolated from the respiratory tract have shown that IFN signaling is primarily disrupted by NS1 protein [413, 414].

Similar responses seen in inflammatory gene expression were observed in human bronchial epithelial cells following IAV H1N1pdm09 (CA) inoculation [52]. FNEC showed early significant upregulation of Th1 gene expression from 12Hr – 48Hr following IAV inoculation, whereas IBV inoculation showed a significant delay in Th1 gene expression. A concurrent reduction and delay in IFN gene expression and protein secretion as well as significant delay in Th1 gene expression following IBV inoculation of FNEC may influence DC activation and MHC-I presentation. Type-I interferons have been shown to activate DCs resulting in an MHC-I dressing [199] and presentation to CD8+ T-cells [415]. Both IAV and IBV have been shown to reduce surface expression of MHC-I in A549 cells by different mechanisms [45]. IAV downregulated both surface and intracellular MHC-I; however, with IBV only surface levels of MHC-I were significantly reduced. This reduction was due to a delay in trafficking of MHC-I to the cell surface and not an increase in the rate of MHC-I internalization and degradation. Trafficking of viral proteins to the cell surface was not affected; however, CD71 (TfR) and HLA-DR (MHC-II) were also downregulated at the cell surface of IBV-infected cells. We have shown that IFN responses and both Th1 and Th2 responses are downregulated and delayed in IBV-inoculated FNEC. The downregulation of MHC-I as well as MHC-II by IBV may play a crucial role in reducing a robust adaptive immune response in vivo. Further comparisons of IAV and IBV in the ferret will be critical to confirming whether the results from FNEC

studies are reproducible and if downstream adaptive immune responses are affected as hypothesized. Since IAV replicated earlier than IBV, and this correlated to IFN gene expression, addition of IFN following IBV infections may result in shifting the virus kinetics similar to IAV. Confirmation of IFN lambda secretion in human nasal epithelial cells would be of great interest to determine whether these responses are similar observations in FNEC following IAV and IBV inoculation. This may allow for increased inflammatory responses and downstream antibody increases. In vivo studies are currently underway to determine the impact of IFN-adjuvants on adaptive immune responses in IBV inoculated and vaccinated animals.

Table 2.1: qRT-PCR primers and probes.

GENE TARGET	FORWARD PRIMER 5'→3'	REVERSE PRIMER 5'→3'	PROBE: (5' CHEMISTRY), <MODIFIED BASE>, (3' CHEMISTRY)	USE	REFERENCE	FUNCTION
GAPDH	TGCGGCCAAGGCAGTAG	AGGCCATGCCAGTGAGCTT		SYBR green	Carolan et al.	Housekeeping gene
MCP1	GCAGCAAGTGTCCCAAAGAAG	GACTGGGGTCAGCGCAGAT	FAM-ATCCTCAAGAC<LNA A>TTCCT-BHQ1	TaqMan	Carolan et al.	Inflammatory
CXCL10	CCTGGCTTCACCGAGTTCT	AGTAGCAGCCCATGGAGTAAAA		SYBR green	Maines et al.	Th1
IL-2	GTTAAAAATTATGAGAGCCCCAGGA	TTGAGTTCTTCTGCTAGACATTGAAGA	FAM-CTAC<LNA A>TGCCCAAGAAG-BHQ1	TaqMan	Carolan et al.	Th2
TGFB1	CGTGCGGCAGCTCTATATT	GCAGAAATTGGCGTGGTAAC	FAM-AAGGATCTGGGCTGGAAGTGG<LNA A>ATC-BHQ1	TaqMan	Rowe et al. (2024)	Treg
IL-4	CCAACAGATTGCTCAGAGGACTT	CACCGAACAGGTCATGTTTGC	FAM-CAGGAACCTC<LNA A>GGAACAT-BHQ1	TaqMan	Carolan et al.	Teff
IL-12p40	GGTGCTATTCACAAGCTCAAGTATG	GGTTTGATGATGTCCCTGATGA	FAM- TACACCAGC<LNA A>GCTTC-BHQ1	TaqMan	Carolan et al.	Teff
IL-17	GGACGGTAAACTACCACATGAACTC	AGACTCCCTTCGCAGAACCA	FAM-TCCCC<LNA A>TCCAGCAAGA-BHQ1	TaqMan	Carolan et al.	Teff
IL-1B	CCTGGTGCTGTATAACTCGTATGAG	TTGGTTCACACTAGTTCCGTTGA	FAM-TCGGGCGCTCC<LNA A>C- BHQ1	TaqMan	Carolan et al.	Pro-inflammatory
IL-6	GCAGAGAACAACCTAAATCTTCCAA	TGATTGAATTGAGACTGGAAGCA	FAM-CTGGC<LNA A>GAAGAGGAC-BHQ1	TaqMan	Carolan et al.	Pro-inflammatory
Granzyme A	GGATCCTCCCTCTCCCTAAGAA	CCCAGCCTGCAACTTGACA	FAM-ATG<LNA A>TGTCAAACCCGAAAC-BHQ1	TaqMan	Carolan et al.	Apoptosis
IFNA	TCCATCCTGAGGAACTACTTCCAG	AGGCACAAGGGCTGTATTGC	FAM-GAATCTCCCTCT<LNA A>TCTGC-BHQ1	TaqMan	Carolan et al.	IFN (Type I)
IFNB	ATATTTCTCCACCACGGTTCTTG	ACTCCACACTGCTGCTGCTTAG	FAM-AACTATAACTT<LNA A>CTTCGATTCCA-BHQ1	TaqMan	Carolan et al.	IFN (Type I)
IFNG	AACTGGAGAGAGGAGAGTGACAAAA	GTCTTCCTTGATGGTATCCATGC	FAM-TCTCCTTCT<LNA A>CTTGAAACTGT-BHQ1	TaqMan	Carolan et al.	IFN (Type II)
IFNL3	CCAGCCCTGCCTTAAGTTATT	CCTTCCTGTTTACTTGTGCATATTG	FAM-ATGAAACCAG<LNA A>GTGCTGACCCAAA-BHQ1	TaqMan	Rowe et al. (2024)	IFN (Type III)
STAT1	AGCCTTGCATGCCAACTCA	ACAGTCCAGCTTCACCGTGAA		SYBR green	Fang et al.	IFN response
STAT2	AGCTGCTGAAGGAGCTGAAG	TGCCTTCCTGGAGTCTCACT		SYBR green	Fang et al.	IFN response
STAT3	CAACCCCAAGAACGTGAACT	AGCCCACGTAATCTGACACC		SYBR green	Fang et al.	IFN response
RIG-I	AGAGCACTTGTGGACGCTTT	TGCAATGTCAATGCCTTCAT		SYBR green	Fang et al.	IFN response
SOCS3	GCTGGTGCATCACTACATGC	GACCGTCTTCCGACAGAGAT		SYBR green	Fang et al.	IFN response
TSLP	GTCTGGGCACATAACTCTAAGG	CACCCTGGTGTCTCACTAAAC	FAM-CAGGCCTTGC<LNA A>GATATAGAGCCGATT-BHQ1	TaqMan	Rowe et al.(2024)	IFN response

List of PCR primers. Ferret primers designed for this study are: TGFB1 (T-reg group), IFNL3 (Type-III interferon), and TYK2, USP18, TSLP (Interferon response genes). All other primers used in this study are referenced. Forward (5' to 3'), reverse (3' to 5') and probes are listed. Probes using TaqMan enzyme include special chemistry at the 5'-end (FAM) 3'-end (BHQ1) and internally modified bases (LNA A) that were specifically designed for this study to enhance binding and specificity for ferret genes.

Figure 2.1: Replication kinetics of IAV/IBV in FNEC.

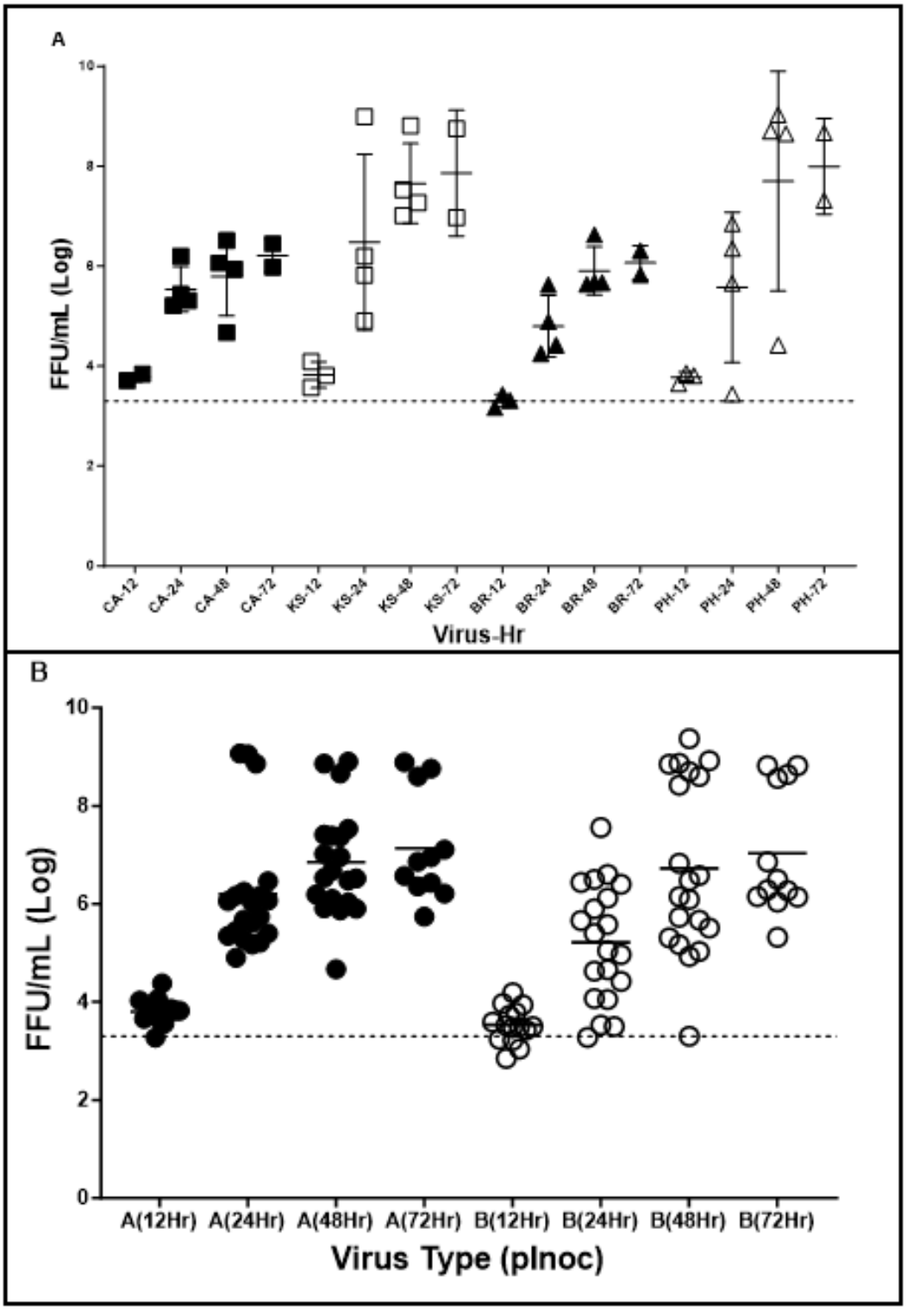

Replication kinetics of IAV [H1N1pdm09 "CA" (A/California/07/2009), H3N2 "KS" (A/Kansas/14/2017)] and IBV [B-Victoria lineage "BR" (B/Brisbane/60/2008), B-Yamagata lineage "PH" (B/Phuket/3073/2013)] inoculation of FNEC at 33°C (MOI=0.3) over 72Hr. A) H1N1pdm09 = red, H3N2= orange, B-Victoria = green, B-Yamagata= yellow. B) Comparison of IAV (CA/KS) and IBV (BR/PH) in black and white circles, respectively. All points are from four independent assays in FNEC conducted in triplicate. Limit of detection, indicated by a dotted line, was $10^{3.3}$ FFU/mL. Significance between groups was determined using 1-way ANOVA (Sidak's multiple comparison test).

Figure 2.2: Heatmap of early/late gene expression in IAV/B-inoculated FNEC.

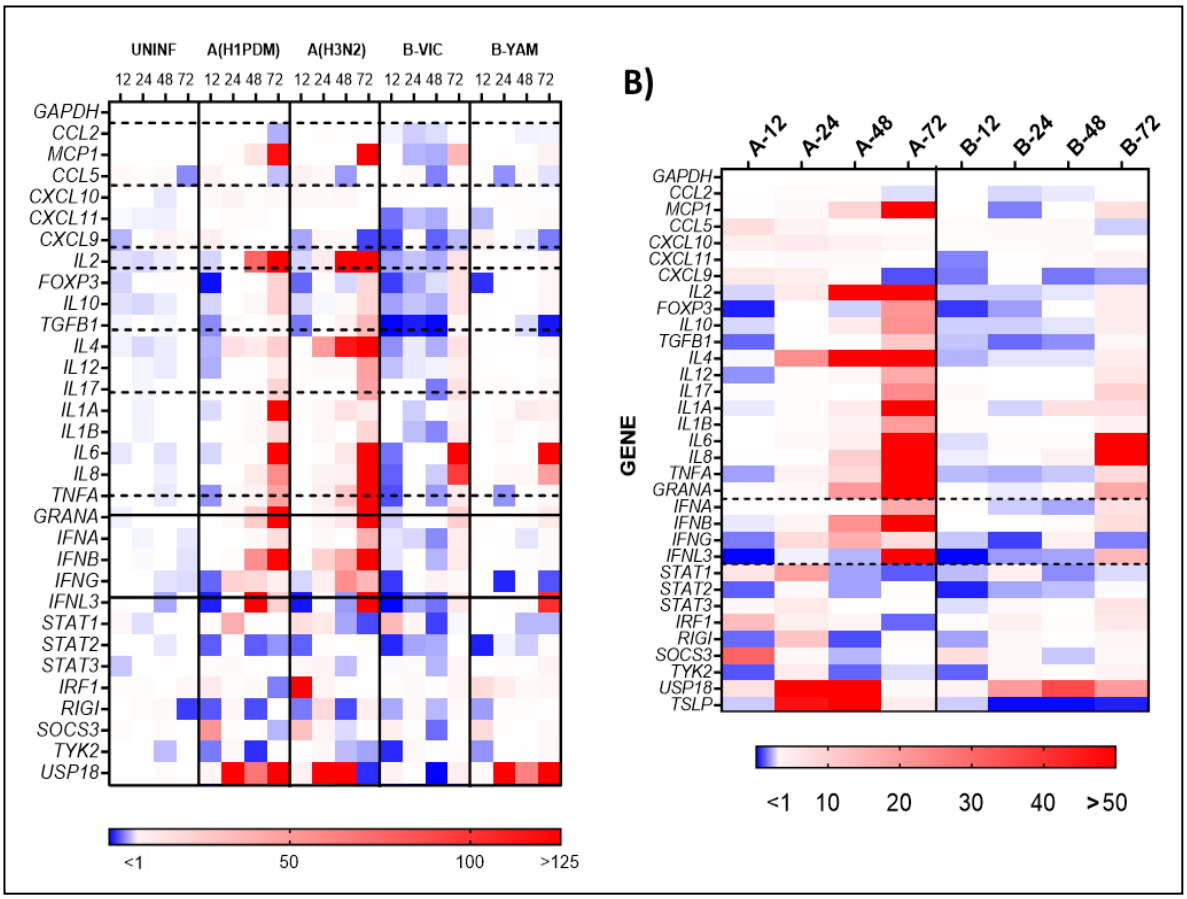

Influenza A and B inoculated (33°C, MOI=0.3) FNEC from four independent experiments performed in triplicate. Average fold gene expression, compared to mock inoculated FNEC, blue = downregulated and red = upregulated. A) Comparison of IAV: CA and KS, H1N1PDM09 and H3N2 respectively; IBV: BR and PH, B-Victoria, and B-Yamagata lineages, respectively. Temporal RNA expression from 12Hr to 72Hr post inoculation. All gene groups (Table 2.1) are separated by dotted lines or solid lines for interferons. B) Average gene expression comparison of all IAV "A" to all IBV "B" inoculated FNEC by type followed by Hr post inoculation. Interferon gene regulation

demarcated between dotted lines. Up to two outliers removed using statistical analysis (Grubb's test) from 12 replicates/gene from 4 independent experiments if necessary.

Figure 2.3: Regulation of genetic functional categories by IAV and IBV in FNEC

Comparison of temporal changes in gene expression following IAV and IBV inoculation of FNEC. Individual points for each gene/category shown for each timepoint 12Hr (white circles), 24Hr (light grey circles). 48hr (dark grey circles) and 72Hr (black circles) from individual samples used in figure 2.2 are presented. Panels comparing specific functional categories: A) *Inflammatory response* genes (CCL2, MCP1, CCL5, IL-1α, IL-1ß, IL-6,

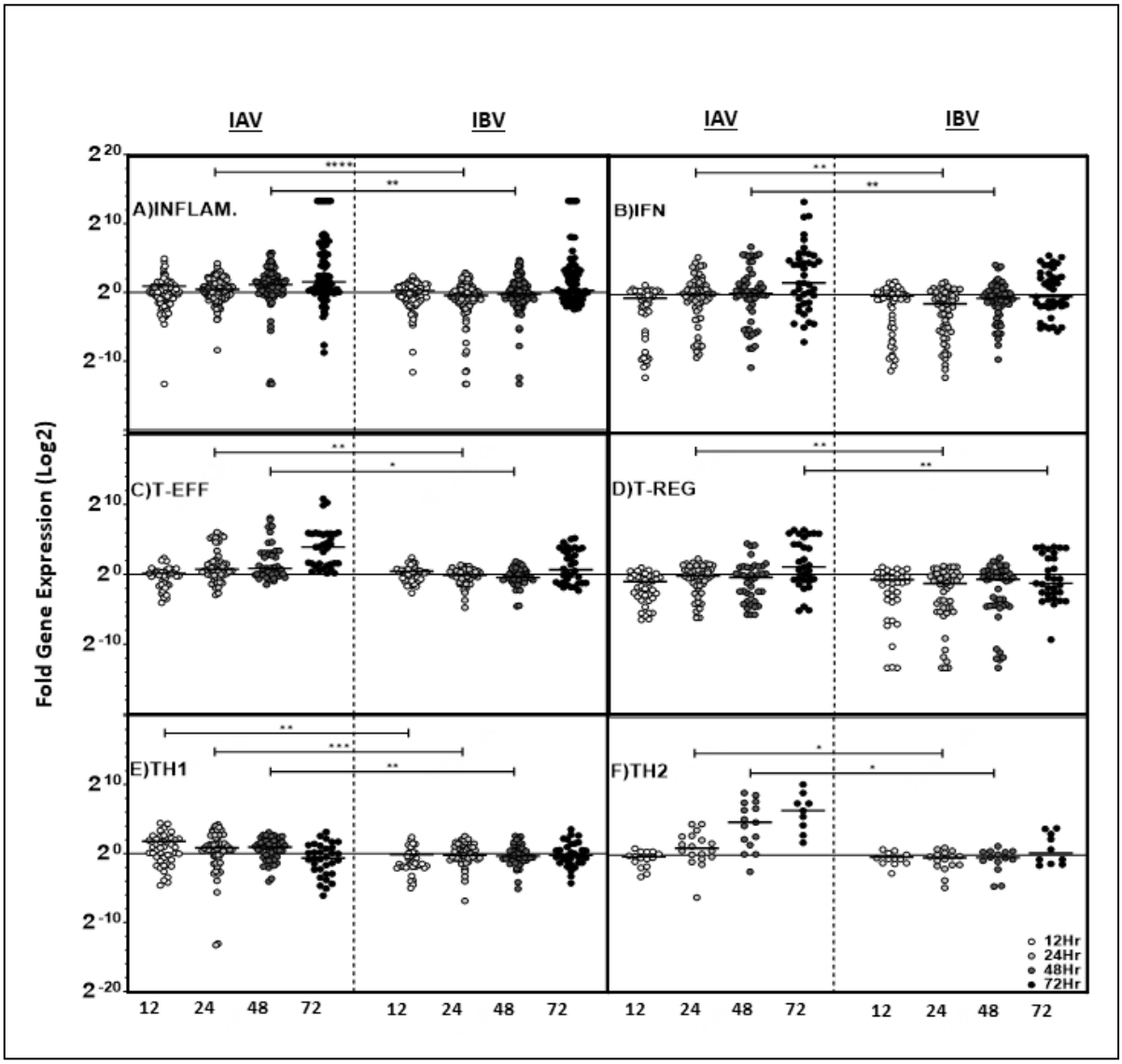

IL-8, and TNFα). Significant differences between IAV and IBV at 24Hr (p=0.00007) and 48Hr (p=0.0016). B) *Interferon response* genes (IFNα, IFNß, IFNγ and IFNλ). Significant differences between IAV and IBV at 24Hr (p=0.0019) and 48Hr (p=0.0046). C) *T-effector response* genes (IL-4, IL-12, and IL-17). Significant differences between IAV and IBV at 24Hr (p=0.0011) and 48Hr (p=0.019). D) *T-regulatory response* genes (FOXP3, IL-10 and TGFß1). Significant differences between IAV and IBV at 24Hr (p=0.002) and 72Hr (p=0.005). E) *Th1 response* genes (CXCL10, CXCL11and CXCL9). Significant differences between IAV and IBV at 12Hr (p=0.0018), 24Hr (p=0.0009) and 48Hr (p=0.005). F) *Th2 response* gene (IL-2). Significant differences between IAV and IBV at 24Hr (p=0.02) and 48Hr (p=0.021). Significance at each timepoint was determined using multiple unpaired t-tests.

Figure 2.4: Interferon gene expression following IAV/B-inoculation of FNEC

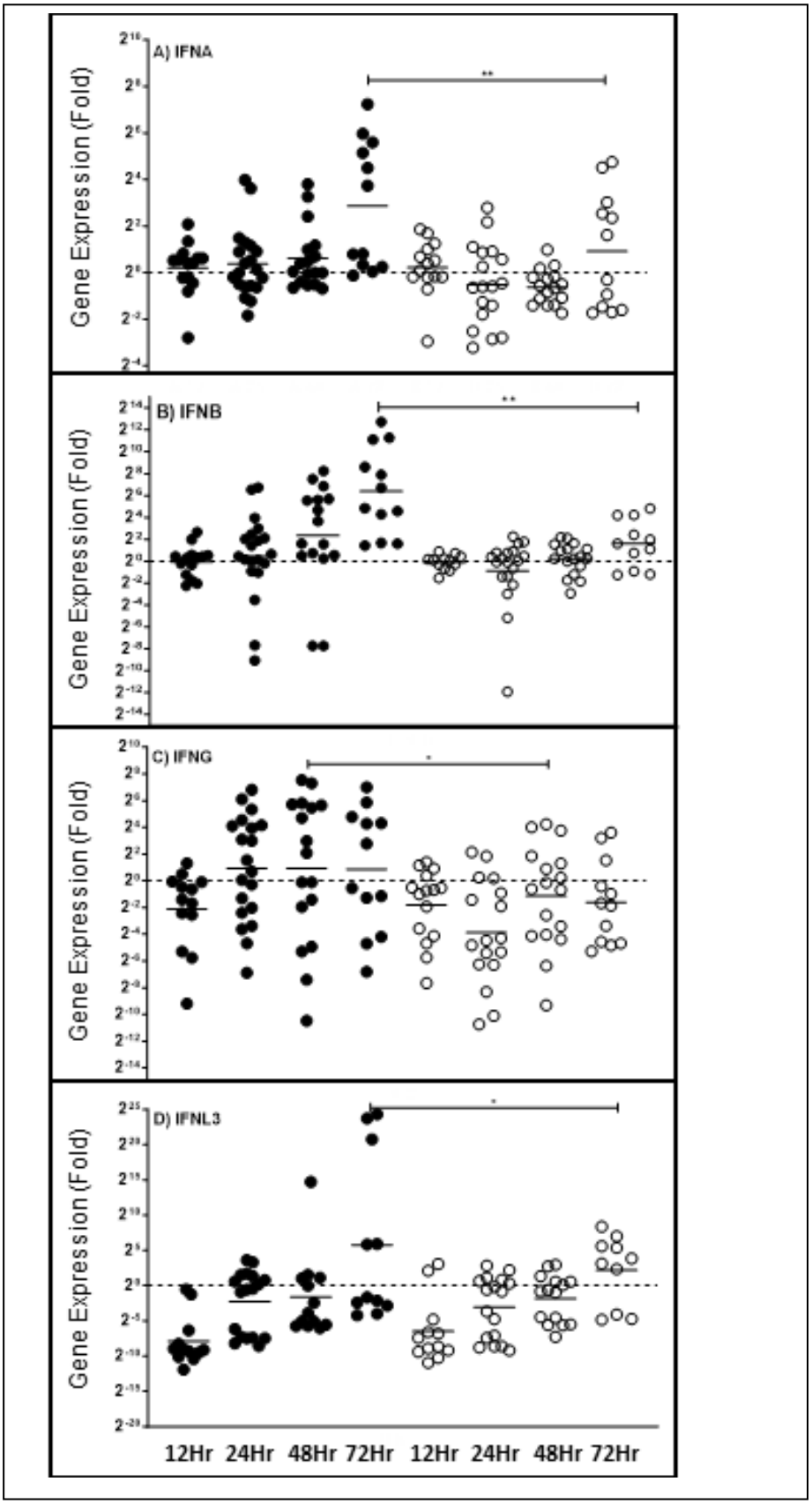

Influenza A and B inoculated (33°C, MOI=0.3) FNEC from four independent experiments performed in triplicate. Average fold interferon (IFN) gene expression, compared to mock inoculated FNEC, over 72 hours. Black circles (IAV; CA and KS) and white circles (IBV; BR and PH). A) Type-I, IFN-α. Significant differences between IAV and IBV at 72Hr ($p=0.002$). B) Type-I, IFN-ß. Significant differences between IAV and IBV at 72Hr ($p=0.002$). C) Type-II, IFN-γ. Significant differences between IAV and IBV at 48Hr ($p=0.014$). D) Type-III, IFN-λ. Significant differences between IAV and IBV at 72Hr ($p=0.0154$). Data from 4 independent experiments using one-way ANOVA for determination of significance between IAV and IBV.

Figure 2.5: TSLP gene expression following IAV/B-inoculation of FNEC

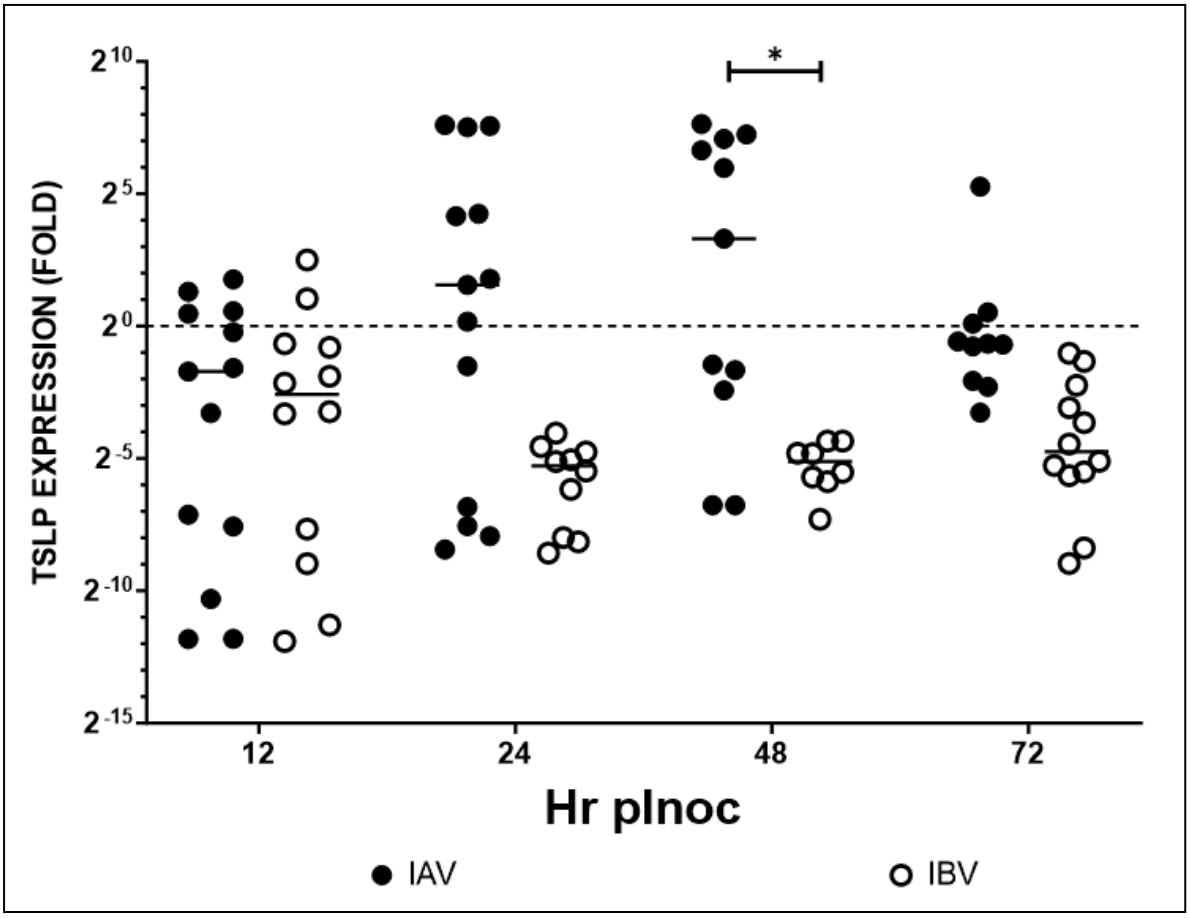

Influenza A (IAV) and B (IBV) inoculated (33°C, MOI=0.3) FNEC from four independent experiments performed in triplicate. Average fold Thymic Stromal Lymphopoietin (TSLP) gene expression over 72 hours is shown. Black circles (IAV; CA and KS) and white circles (IBV; BR and PH). Significant differences between IAV and IBV at 48Hr ($p=0.037$). Data from 4 independent experiments were analyzed to determine significance between IAV and IBV.

Figure 2.6: Type-III IFN protein levels following IAV/B-inoculation in FNEC.

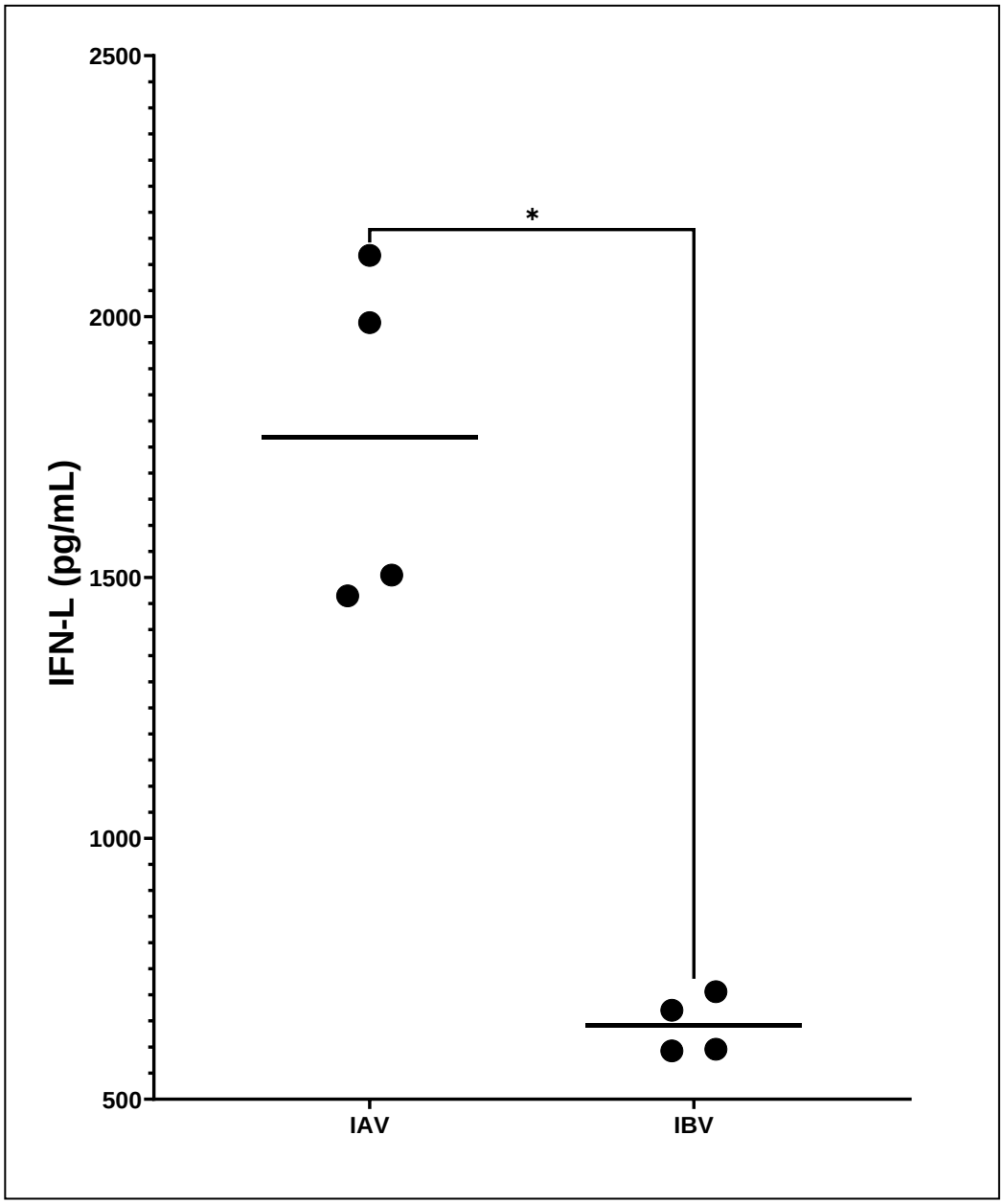

Average IFNL levels (pg/mL) secreted from the basolateral side of inoculated FNEC from 12Hr to 72Hr post inoculation. IAV vs IBV p=0.0238 (one-way ANOVA). Significant differences for timepoints: IAV vs IBV (24Hr p=0.0165, 48Hr p=0.049).

Table 2.2: Significance of gene expression between IAV/IBV-inoculated FNEC.

	12HR			24HR			48HR			72HR			
GENE	A	B	p	A	B	p	A	B	p	A	B	p	FUNCTION
GAPDH	1.0	1.0		1.0	1.0		1.0	1.0		1.0	1.0		Housekeeping
CCL2	1.4	1.1		1.7	0.8	**0.0046**	1.4	0.9	**0.037**	0.9	1.2		Inflammatory chemokine
MCP1	1.3	1.3		1.9	0.5	**0.0357**	9.0	1.0		89.5	7.3		Inflammatory chemokine
CCL5	7.2	1.7	**0.045**	3.2	2.1		1.5	2.1		1.4	0.8		Chemokine (RANTES)
CXCL10	3.8	1.6		4.7	1.6	**0.0188**	3.6	1.9	**0.033**	2.4	1.1		Th1 (IP-10)
CXCL11	1.6	0.5	**0.006**	2.1	1.2		1.9	1.6		1.3	3.4	**0.05**	Th1 (IP-9)
CXCL9	5.1	0.5	**0.041**	3.8	1.5		1.6	0.5	**0.004**	0.3	0.6		Th1 (MIG)
IL2	0.8	0.8		5.0	0.8	**0.0201**	108.0	0.9	**0.021**	248.7	4.6		Th2
FOXP3	0.1	0.2		1.2	0.6		0.8	1.2		21.3	4.3		Treg
IL10	0.8	0.8		1.2	0.8		4.7	0.9		22.0	4.6		Treg
TGFB1	0.4	0.8		1.1	0.4	**0.0237**	1.0	0.6		11.4	2.5		Treg
IL4	1.0	0.7		22.7	0.9	**0.0005**	56.0	0.9	**0.018**	356.9	4.6		Teff
IL12	0.6	1.3	**0.017**	1.4	1.1		2.4	1.1	**0.049**	17.1	5.6		Teff
IL17	1.7	2.0		1.5	1.1		1.1	1.1		23.3	9.7		Teff
IL1A	0.9	1.5		1.7	0.8	**0.0157**	4.7	6.8		>500	7.1		Pro-inflammatory cytokine
IL1B	1.2	1.5		1.6	1.2		3.3	1.1	**0.049**	19.9	3.5	**0.04**	Pro-inflammatory cytokine
IL6	1.1	0.9		2.2	1.8		3.7	1.5	**0.041**	>500	>500		Pro-inflammatory cytokine
IL8	1.2	0.9		1.2	1.3		10.0	3.4		62.4	72.4		Pro-inflammatory cytokine
TNFA	0.6	0.7		3.3	0.7	**0.0185**	8.4	0.8	**0.001**	87.2	7.9		Pro-inflammatory cytokine
GRANA	1.3	1.5		2.5	0.9	**0.0306**	20.5	2.0	**0.011**	331.6	17.6	**0.03**	Apoptosis
IFNA	1.4	1.5		2.5	1.3		2.6	0.7		28.4	6.2	**0.002**	Interferon (Type-I)
IFNB	1.5	1.0		12.6	1.3		50.0	1.7		>500	7.5	**0.002**	Interferon (Type-I)
IFNG	0.6	0.8		16.0	0.7		34.6	3.5	**0.014**	21.8	2.2		Interferon (Type-II)
IFNL3	0.1	1.1		2.1	1.2		>500	1.5		>500	57.7	**0.015**	Interferon (Type-III)
STAT1	5.8	0.7		19.1	3.9		0.6	0.5		0.4	0.9	**0.01**	ISG (IFNγ, IFNα, IFNß)
STAT2	0.4	0.1	**0.006**	2.0	0.7		0.6	0.7		1.5	1.0		ISG (IFNα, IFNß)

Gene expression comparison between IAV (CA/KS) "A" and IBV (BR/PH) "B" inoculated FNEC over 72Hr post inoculation at 33°C. Average fold changes for ferret gene expression indicated comparing IAV/IBV infected FNEC. Upregulated genes >2-

fold (pink shade) and downregulated genes <1 (blue shade). Significant gene expression differences between IAV and IBV, using multiple unpaired t test, is in bold with p-value listed.

Table 2.3: Correlation of virus replication to gene expression in FNEC.

	IAV			IBV				
GENE	r	p	Signif.	r	p	Signif.	FUNCTION	A & B
CCL2	-0.0238	0.4884	ns	0.1905	0.3323	ns	Inflammatory chemokine	
MCP1	0.619	0.0575	ns	0.381	0.1799	ns	Inflammatory chemokine	
CCL5	-0.5952	0.0661	ns	-0.1429	0.376	ns	Chemokine (RANTES)	
CXCL10	-0.4048	0.1634	ns	0.0238	0.4884	ns	Th1 (IP-10)	
CXCL11	-0.8095	0.0109	*	0.7857	0.014	*	Th1 (IP-9)	Y
CXCL9	-0.2619	0.2682	ns	-0.1667	0.3517	ns	Th1 (MIG)	
IL2	0.881	0.0036	**	0.5714	0.0756	ns	Th2	
FOXP3	0.6667	0.0415	*	0.8095	0.0109	*	Treg	Y
IL-10	0.6667	0.0415	*	0.5714	0.0756	ns	Treg	
TGFB	0.8095	0.0109	*	0.1429	0.376	ns	Treg	
IL4	0.9762	0.0002	***	0.5714	0.0756	ns	Teff	
IL12	0.8333	0.0077	**	0.5714	0.0756	ns	Teff	
IL17	0.3333	0.2139	ns	0.2857	0.2504	ns	Teff	
IL1A	0.8095	0.0109	*	0.8095	0.0109	*	Pro-inflammatory cytokine	Y
IL1B	0.8333	0.0077	**	0.3333	0.2139	ns	Pro-inflammatory cytokine	
IL6	0.881	0.0036	**	0.7143	0.0288	*	Pro-inflammatory cytokine	Y
IL8	0.7857	0.014	*	0.7619	0.0184	*	Pro-inflammatory cytokine	Y
TNFA	0.9286	0.0011	**	0.5952	0.0661	ns	Pro-inflammatory cytokine	
GRANA	0.7857	0.014	*	0.7143	0.0288	*	Apoptosis	Y
IFNA	0.5952	0.0661	ns	0.381	0.1799	ns	Interferon (Type-I)	
IFNB	0.8095	0.0109	*	0.6667	0.0415	*	Interferon (Type-I)	Y
IFNG	0.7619	0.0184	*	0.1429	0.376	ns	Interferon (Type-II)	
IFNL3	0.6429	0.0481	*	0.7619	0.0184	*	Interferon (Type-III)	Y
STAT1	-0.7143	0.0288	*	-0.7619	0.0184	*	ISG (IFNγ, IFNα, IFNß)	Y
STAT2	0.6905	0.0347	*	0.8571	0.0054	**	ISG (IFNα, IFNß)	Y
STAT3	-0.5476	0.0855	ns	0.5476	0.0855	ns	ISG (Teff)	
IRF1	-0.6905	0.0347	*	0.0476	0.4674	ns	Type I (ISG)	
RIGI	0.2619	0.2682	ns	0.4048	0.1634	ns	Type I Resp	
SOCS3	-0.619	0.0575	ns	-0.5476	0.0855	ns	IFN (↓Reg)	
TYK2	0.04762	0.4674	ns	0.5952	0.0661	ns	Type I (Reg)	
USP18	0.09524	0.4201	ns	0.4524	0.1337	ns	Type I (Reg) Type III (↑Reg)	

Pearson correlation coefficients were estimated to determine the relationship between virus replication (FFU/mL) and gene expression (fold change) following IAV or IBV inoculation of FNEC. Significance ($p<0.05$) highlighted in pink. Significant correlation of gene expression and virus replication by both IAV and IBV are indicated by a "Y" in the right column. A Pearson correlation coefficient of $r<0$ indicates an inverse correlation of virus replication to gene expression and an $r>0$ indicates a direct correlation.

Figure 2.S1: Type-I/III IFN bioassay standard curves.

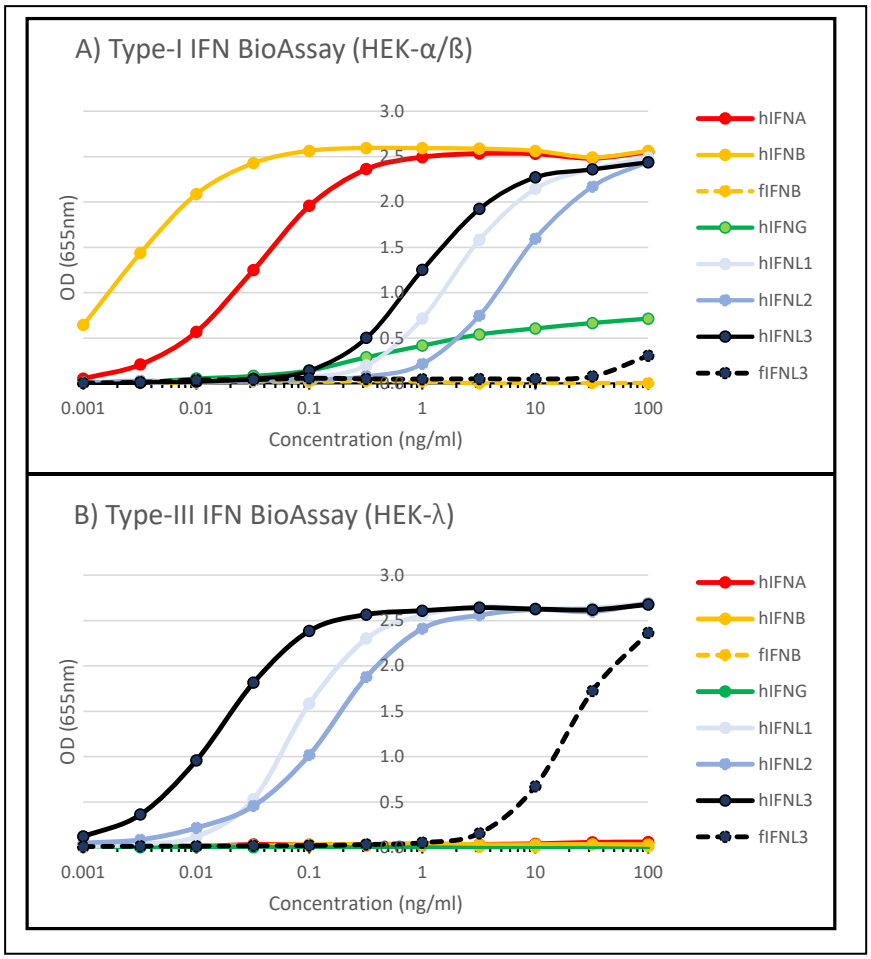

Recombinant interferon concentrations (ng/mL) versus absorbance (655nm) values. Human interferons (hIFNx): type-I IFN = hIFNA (red solid line) and hIFNB (orange

solid line); type-II IFN = hIFNG (green solid line); type-III IFN = hIFNL1 (light blue solid line), hIFNL2 (blue solid line) and hIFNL3 (black solid line). Ferret interferons (fIFNx): type-I IFN = fIFNB (orange dashed line); type-III IFN = fIFNL3 (black dashed line). A) Type-I IFN bioassay results and B) Type-III IFN bioassay results.

Table 2.S2: Significance of gene expression of IAV/IBV-inoculated FNEC compared to mock FNEC.

	12Hr								24Hr							
GENE	UN	CA	p	KS	p	BR	p	PH	p	UN	CA	p	KS	p	BR	p	PH	p
GAPDH	1.00	1.00		1.00		1.00		1.00		1.00	1.00		1.00		1.00		1.00	
CCL2	1.07	1.26		1.45		0.95		1.31		1.13	1.33		2.07	0.039	0.81		1.23	
MCP1	1.21	1.32		1.38		1.89		1.24		1.02	2.20		1.46		0.71		1.90	
CCL5	3.07	7.11		7.37		1.22		2.86		2.28	1.90		4.29		3.31		0.56	
CXCL10	1.26	3.53	0.030	3.96		2.03		1.17		1.03	5.88	0.039	3.50		1.65		2.08	
CXCL11	0.97	1.64		1.51		0.45	0.025	0.72		0.95	2.82		1.48		0.75		1.59	
CXCL9	0.70	8.92	0.039	0.65		0.28		8.33		1.31	2.29		5.16		1.63		1.33	
IL2	0.88	0.83		0.83		0.62		1.88		0.84	1.38		9.50	0.024	0.76		1.91	
FOXP3	0.83	0.05		0.40		0.24		0.18		1.08	1.58		2.66		0.66		1.67	
IL10	0.88	0.83		0.85		0.62		1.88		0.84	1.38		0.97		0.76		1.91	
TGFB1	0.96	0.54		0.47	0.048	0.00	0.0004	1.52	0.038	1.06	3.51		1.13		0.11	0.002	1.18	
IL4	0.94	0.70		1.24		0.56		1.76		0.84	16.50		49.06	0.032	0.92		1.91	
IL12	1.12	0.68		2.20		0.75		1.69		0.96	1.50		3.27		0.91		1.47	
IL17	1.02	1.08		2.23		1.83		2.08	0.007	0.96	1.65		1.37	0.049	1.02		2.77	
IL1A	1.05	0.86		2.06		1.18		1.72		0.95	1.78		5.18		0.81		2.50	
IL1B	1.04	1.05		1.67		1.24		1.74	0.020	0.94	1.77		4.86		0.74		5.37	
IL6	0.91	0.84		1.32		0.45	0.023	1.23		1.00	2.22		2.27	0.023	1.48		2.07	
IL8	1.06	1.14		1.30		0.37	0.002	1.42		1.20	1.25		6.03		1.24		3.82	
TNFA	1.14	0.57		0.99		0.30	0.005	2.63		1.00	2.69		8.19		1.03		0.57	
GRANA	0.94	1.34		1.31		0.80		2.11	0.020	1.08	3.60	0.035	5.60		1.87		1.06	
IFNA	1.20	1.15		1.67		0.90		1.94		0.96	1.26		3.72		0.84		1.86	
IFNB	1.03	1.00		1.91		0.89		1.18		0.98	2.65		22.55		1.11		1.56	
IFNG	1.24	0.39	0.016	0.84		0.22	0.003	1.26		1.11	22.76		9.14	0.018	1.30		0.14	0.007
IFNL3	1.53	0.12	0.017	0.07	0.015	0.00	0.012	1.83		1.04	1.23		2.74		0.65		1.72	
STAT1	5.03	2.57		16.32		34.74		1.28		0.87	40.18		11.25	0.038	5.51	0.023	1.82	
STAT2	1.30	0.36	0.031	0.38	0.034	0.14	0.012	0.11	0.010	1.12	1.80		2.18		0.64		0.95	
STAT3	0.77	2.89		5.13		0.98		1.39		1.39	3.23	0.022	6.69	0.030	2.51		2.25	
IRF1	2.13	10.70		483.05		2.24		17.78		2.68	2.30		5.61		2.95		9.81	
RIGI	1.05	0.34		0.47		0.66		0.61		2.62	4.71		19.14	0.019	4.39		1.99	
SOCS3	2.79	53.01		31.29		7.92		18.38		1.43	2.16		5.74		2.29		2.21	
TYK2	1.16	0.48	0.040	1.03		0.15	0.001	0.58		1.44	4.82		4.68		3.99		1.30	
USP18	1.43	5.74		7.48		6.50		3.64	0.024	1.14	1.90E+04		1083		1.94		4617	
TSLP	1.16	0.00	0.011	1.29		0.15	0.020	3.96		1.05	80.67		7.42		0.01	0.005	0.04	0.006

	48Hr								72Hr							
GENE	UN	CA	p	KS	p	BR	p	PH	p	UN	CA	p	KS	p	BR	p	PH	p
GAPDH	1.00	1.00		1.00		1.00		1.00		1.00	1.00		1.00		1.00		1.00	
CCL2	1.12	1.13		1.81		0.87		0.95		1.04	0.69		1.05		1.45		0.95	
MCP1	1.07	14.25		1.41		0.67		1.30		1.02	119.38		375.39		35.66		6.38	
CCL5	4.26	1.95		0.60		0.51		3.00		0.54	0.75		1.94		2.76		0.88	
CXCL10	0.91	2.68		4.87	0.0001	1.07		2.51		1.09	3.11		1.78		2.12		0.99	
CXCL11	0.94	2.46		1.06		0.67		2.14	0.032	1.54	1.48		0.99		3.68		3.15	
CXCL9	7.00	1.02		3.23		0.37		0.93		3.42	1.17		0.26		0.72		0.48	
IL2	0.92	75.74		144.80	0.036	0.67		1.74		1.04	305.88		1627		15.25		5.09	
FOXP3	2.42	1.76		0.84		0.87		1.41		2.02	22.24		19.97		15.11		4.83	
IL10	0.92	4.95		4.38		0.68		1.74		1.04	22.78		20.74		15.25		5.09	
TGFB1	0.97	1.44		7.81		0.02	0.006	0.85		1.01	5.48		36.49		4.56		0.08	0.010
IL4	0.92	10.57	0.008	114.40	0.025	0.68		1.74		1.04	25.13		688.76		15.25		5.22	
IL12	0.92	1.50		3.50	0.045	0.95		1.42		1.01	9.84		47.66		8.85		2.30	
IL17	1.02	1.88		1.16		0.48	0.0003	1.59		1.01	22.32		44.78		14.15		5.20	
IL1A	1.05	3.21	0.001	15.25		1.19		10.78	0.009	1.02	7.65E+08		9.99		6.09		8.60	
IL1B	1.01	4.32		1.86		0.53	0.0001	1.46		1.01	18.70		21.29		10.59		4.20	
IL6	0.89	2.69	0.003	12.19		1.03		1.79		1.02	4.95E+08		6.00E+08		3.20E+08		1.08E+08	
IL8	0.93	11.50		7.60		0.80		4.94	0.049	1.02	57.07		138.96		96.67		48.07	
TNFA	0.91	6.90	0.005	27.71		0.61		1.92		1.04	46.11		136.43		11.30		4.47	
GRANA	1.03	26.05	0.042	12.63	0.015	1.49		2.97	0.023	1.01	310.29		667.73		24.02		11.09	0.035
IFNA	1.01	3.60		1.26		0.54	0.001	0.90		0.91	16.75		40.12		9.30		3.10	
IFNB	1.04	55.61		42.77	0.025	0.71		2.40	0.012	0.89	123.44		1923		11.06		3.22	0.022
IFNG	0.89	19.86	0.035	55.59		6.94		1.15		0.86	7.91		35.59		4.07		0.32	0.005
IFNL3	0.66	3395		0.60		0.45		2.46		1.53	24		6.07E+06		12.54		102.85	
STAT1	1.18	2.39		0.65		0.24		0.72		1.29	1.06		0.28		0.97		0.72	
STAT2	0.91	0.36	0.009	1.04		0.67		0.80		1.16	0.58		2.33		1.11		2.41	
STAT3	1.61	1.81		0.75		0.71		1.54		1.14	1.14		1.02		5.55		6.76	
IRF1	1.16	3.40		2.18		1.78		3.42		4.54	0.49		1.47		5.38		5.10	
RIGI	3.14	0.30		0.29		0.72		2.15		0.22	1.38		9.22		3.33	0.010	1.85	0.042
SOCS3	2.91	1.55		0.86		0.42		1.06		1.02	0.71		1.82		1.41		3.79	
TYK2	0.74	0.18	0.015	0.74		1.25		1.75		1.02	1.79		0.63		2.44		3.98	
USP18	2.80	68.44		1617		0.00		62.39		1.03	181.30		0.17	0.018	8.93		249.36	
TSLP	2.44	72.29		223.22		0.19		0.05		1.05	31.08		0.54		0.20	0.040	0.04	0.040

Gene expression comparisons between IAV (CA and KS) and IBV (BR and PH) to mock-inoculated (UN) FNEC, normalized to GAPDH, over 72Hr post inoculation at 33°C. Average fold changes for ferret gene expression indicated comparing each virus to mock (UN). Significant gene expression differences between each virus and mock, using multiple unpaired t test, is shown with p-value listed.

CHAPTER 3

IMMUNOLOGICAL "CROSS TALK" BETWEEN INFLUENZA A AND B INFECTED RESPIRATORY EPITHELIAL CELLS AND PERIPHERAL BLOOD MONONUCLEAR CELLS[2]

[2]Rowe, Thomas, Davis, William G., Wentworth, David E. and Ross, Ted M. To be submitted to Journal of Virology.

ABSTRACT

The link between innate and adaptive immune responses following influenza virus infection may be induced by direct or indirect communication between cells at the site of infection and circulating immune cells in the blood. In order to assess whether indirect communication can activate innate immune responses in circulating peripheral blood mononuclear cells (PBMC), primary differentiated ferret nasal epithelial cells (FNEC) on Transwell™ inserts were apically inoculated with influenza A and B viruses. Twenty-four hours post inoculation, FNEC were added to PBMC in wells on the basolateral side. The physical separation of the FNEC and PBMC along with the tight junctions formed between the FNEC prevented any virus from directly infecting the PBMC. Differential gene expression in co-cultured PBMC and type-III interferon secretion in the basolateral compartments of FNEC-PBMC co-cultures show that IAV inoculated FNEC released factors which resulted in inflammatory responses and interferon secretion in PBMC that is reduced or delayed in IBV inoculated FNEC.

INTRODUCTION

While both innate and adaptive immune responses play important roles in viral clearance and mediating protective immunity, the innate immune response can influence the outcome of the adaptive immune response [105]. Initially, respiratory epithelial cells are infected by influenza viruses and send signals to attract and activate circulating immune cells to mount an innate response resulting in an affective adaptive response to clear the infection and protect the host.

In this experiment IAV [H1PDM09 (A/California/07/2009) and H3N2 (A/Kansas/14/2017)] and IBV [B-Victoria (B/Brisbane/60/2008) and B-Yamagata (B/Phuket/3073/2013)] virus-infected primary ferret nasal epithelial cells (FNEC) were co-cultured with heterologous ferret peripheral blood mononuclear cells (PBMC) to determine whether soluble factors released basolaterally from FNEC could activate innate immune responses in PBMC. Cultured confluent and differentiated FNEC were infected at 33°C and co-cultured with PBMC on D1 post infection.

FNEC were apically inoculated with a multiplicity of infection (MOI=0.3) with H1N1PDM09, H3N2, B-Victoria or B-Yamagata virus on D0 and heterologous PBMC were added to the basolateral side on D1 post inoculation. One set of experiments was conducted at 33°C and another set was conducted at 37°C. Supernatants collected from infected FNEC were collected from the apical side to assess viral replication and from the basolateral compartment to assess viral replication and interferon lambda (IFN-λ). Daily resistivity was measured to ensure that the FNEC tight junctions were intact and virus did not pass to the basolateral side of the cultures. RNA from FNEC and PBMC was purified and analyzed for innate immune responses by qRT-PCR. Samples were collected at the following timepoints post co-cultivation: 24Hr and 48Hr, 48Hr and 72Hr post FNEC infection, respectively. The supernatant samples collected were assessed for virus load (FFA) and IFNλ (bioassay). The cells were placed in AVL buffer and RNA was isolated for gene expression by qRT-PCR.

MATERIALS AND METHODS

Viruses

Viruses used were passaged in Madin Darby Canine Kidney (MDCK) cells, to retain antigenic similarity to the original human isolates and to avoid structural changes in the hemagglutinin which could occur from passage in eggs [377-379]. All influenza viruses were passaged in MDCK or MDCK-SIAT1 [380] cells according to established procedures [381, 382]. Representative influenza A viruses used in this study were: A/California/07/2009 "CA" (H1N1PDM09 subtype) and A/Kansas/14/2017 "KS" (H3N2 subtype). Representative influenza B viruses used in this study were: B/Brisbane/60/2008 "BR" (B-Victoria lineage) and B/Phuket/3073/2013 "PH" (B-Yamagata lineage).

Ferret cell isolation and culture

All animal procedures were approved by the Institutional Animal Care and Use Committee (IACUC) of the Centers for Disease Control and Prevention in an Association for Assessment and Accreditation of Laboratory Animal Care (AAALAC) International accredited facility. Uninfected male fitch ferrets (Triple F Farms, Sayre, PA), between 10 to 18 months of age and seronegative for currently circulating influenza viruses, were anesthetized with an intramuscular cocktail of ketamine (25-30mg/kg) and xylazine (1.5-2mg/kg), exsanguinated and euthanized with intracardiac injection of Euthasol™ (1ml/kg) prior to collection of respiratory tissues.

Nasal turbinates, representing the upper respiratory tract (URT) were collected and processed in the following manner:

Nasal turbinates were digested in 25mL digestion medium (MEM, 1.4mg/ml pronase, 0.1mg/ml DNase I) for 48Hr at 4°C and neutralized with 10% final concentration of characterized fetal bovine serum. The cell suspensions were passed through a 70uM mesh cell strainer and erythrocytes were lysed with ammonium chloride.

Contaminating fibroblasts were removed by adherence followed by culturing the suspension cells in selective media. Following a two-hour adherence of the cells in Petri dishes, the suspension cells were cultured in medium replacing L-Valine with D-valine (D-Val EC basic media) to prevent outgrowth of any remaining fibroblasts. Fibroblasts would not continue to expand due to the lack of D-amino oxidase enzyme in these cells[383]. D-Val EC basic medium consisted of D-Val MEM (MyBiosource, San Diego, CA USA), HEPES, sodium pyruvate, non-essential amino acids, penicillin/streptomycin, 0.05% BSA. The ferret nasal epithelial cells (FNEC) were cultured in D-Val EC basic medium on collagen-coated flasks for 7-10 days at 37°C, 5% CO_2 until confluency, detached with 0.05% Trypsin-EDTA, and either cryopreserved or cultured on collagen-coated 1.12cm^2 Transwell® inserts (Corning Life Sciences, Tewksbury, MA USA) at $5x10^4$ cells/cm^2. 0.5mL cell suspensions were added to the apical side of Transwell® plates and 1mL D-Val EC basic media to the basolateral side of the well. Cells were cultured in D-Val EC basic media for seven to ten days and then changed to culturing in EC+ medium [(F12/MEM, HEPES, NEAA, sodium pyruvate, 0.05% BSA, antibiotics) supplemented with growth factors in SingleQuots (Lonza, Walkersville, MD) and retinoic acid (15ng/ml)]. Medium exchanges every 2 – 3 days to the apical and basolateral sides of the cultures continued until the cells formed a confluent monolayer and the transmembrane resistance of >800Ω/cm^2, as measured using a Millicell ERS-2 voltohmeter (MilliporeSigma, Burlington, MA), was achieved. The apical medium was removed at this point to create an air-liquid interface (ALI), and the basolateral medium was exchanged three times/week for an additional 3 to 4 weeks. After this time, evidence of ciliary action was observed in the cultures and mucous production by goblet cells.

Following ALI culture, the monolayers were rinsed weekly with PBS to remove any residual mucous accumulation. Cell cultures isolated from the URT consisted of primary ferret nasal epithelial cells (FNEC) and have previously been shown to be structurally like nasal epithelium [359]. Three to four weeks post ALI culture, cells were infected with influenza viruses. An overview of the ferret FNEC isolation procedure is depicted in Table 3.1.

For peripheral blood mononuclear cells (PBMC) used for co-culture experiments, a 13-month-old male ferret was anesthetized followed by collection of blood in K-ETDA and SST tubes for cell and serum processing, respectively. To retain all cells, present in the peripheral blood, cells were not layered over a density gradient, ficoll-hypaque. Only erythrocytes were removed from the samples. For cell processing, erythrocytes were lysed by six-minute incubation of one-part whole blood in K-EDTA plus twenty parts 0.15M chloride solution. Cells were pelleted at 600 x G for ten minutes at 4°C and washed once with phosphate buffered saline. PBMC were cryopreserved at $2x10^7$ cells/vial in freezing medium (RPMI, 50% autologous serum and 10% DMSO) and stored in the vapor phase of a liquid nitrogen freezer until used in co-culture experiments.

Inoculation of FNEC with influenza A and B viruses and coculturing with PBMC

The apical side of differentiated FNEC was rinsed three times with F12/MEM to remove any dead cells and mucus. Cells were counted from a representative well following trypsinization with 0.05% Trypsin-EDTA solution (Life Technologies, Carlsbad, CA USA) to determine the average cell number per well followed by infection with IAV and IBV viruses at a 0.3 multiplicity of infection. Cells were inoculated

apically with 0.3ml/well diluted virus in F12/MEM and incubated at 33°C or 37°C. The virus inoculum was removed after one hour and the apical side of the cells was rinsed three times with F12/MEM. The basolateral media was removed and replaced with fresh 1ml/well EC+ media and plates were incubated at 33°C or 37°C throughout the infection.

Frozen heterologous ferret PBMC were thawed and plated at one million cells per well in RPMI medium supplemented with 10% heat-inactivated fetal bovine serum in a 12-well plate and incubated overnight at 37°C, 5% CO_2. At one day post inoculation, Transwell™ inserts containing FNEC monolayers were placed in wells containing PBMC, in triplicate and incubated at 33°C, 5%CO_2. At 24Hr and 48Hr (48Hr and 72Hr post FNEC inoculation). At timepoints indicated, supernatants were collected (basolateral and apical) and cells (FNEC and PBMC) for analyses. For supernatant collection, 0.3mL EC+ medium was added to the apical surface of the FNEC and incubated for 10-15min at 33°C or 37°C. The medium was removed and stored at -80°C until analyzed. At each timepoint the Transwell™ insert containing FNEC was removed from the well and FNEC were lysed with AVL extraction buffer, and lysate stored at -80°C for RNA extraction and subsequent qRT-PCR. The basolateral compartment was collected and PBMC were pelleted. The supernatant was stored at -80°C for FFA/cytokine testing. The PBMC cell pellet was resuspended in 0.2mL RPMI, 10% FBS. AVL extraction buffer was added to ½ of the sample and stored at -80°C for RNA extraction. Freezing medium (90% FBS, 10% DMSO) was added to the remaining sample, rate cooled to -80°C, and stored in vapor phase of LN_2 for further processing. A general overview of the isolation, differentiation, and processing FNEC is illustrated in Figure 3.1.

Virus titration by focus forming assay (FFA)

At various timepoints post infection, 0.3ml of EC+ media was added to the apical surface of infected or control wells and incubated for 10 minutes at 33°C or 37°C. The supernatant was removed from the apical surface and stored at -80°C until evaluated for virus. Influenza virus titers were determined using a Focus Forming Assay (FFA) [384], using MDCK-SIAT1(SIAT) cells, which constitutively express human 2,6-sialtransferase-1 and have shown improved isolation rates for recent A(H3N2) influenza viruses [385]. The FFA was modified and optimized for detection of IAV and IBV with increased sensitivity and reproducibility [416] as follows: SIAT cells were seeded in 96-well flat-bottom tissue culture plates overnight to form a confluent monolayer in Dulbecco 's Modified Eagle Medium (DMEM) containing 5% heat-inactivated fetal bovine serum (FBS) and antibiotics. The following day, the cell monolayers were rinsed with 0.01M phosphate-buffered saline pH 7.2 (PBS), (Gibco BRL, ThermoFisher Scientific Inc., Waltham, MA, USA) followed by the addition of fifty microliters per well of virus growth medium plus TPCK-treated trypsin, VGM-T [DMEM, 0.1% fraction-V bovine serum albumin (BSA), antibiotics (penicillin/streptomycin) and 1µg/ml TPCK-treated trypsin (Sigma, St. Louis, MO, USA)]. Afterwards, 50µl ½-log serially diluted (10^{-1} to 10^{-6}) sample in VGM-T was added in quadruplicate or VGM-T to cell control wells. A control virus influenza A or B virus standard was also titrated and included as a positive control in each assay. Following a 2 Hr incubation period at 37°C, 100 microliters overlay [equal volumes of 1.2% Avicel RC/CL [386] (Type: RC581 NF; FMC Health and Nutrition, Philadelphia, PA, USA) in 2X MEM containing 1µg/ml TPCK-treated trypsin, 0.1% BSA, and antibiotics] was added. After an incubation of 18-22 hours at 37°C, 5% CO_2, the overlay was removed, and the monolayers were washed

once with PBS to remove any residual Avicel. The plates were fixed with ice-cold 10% formalin in PBS (4% w/v paraformaldehyde) for 30 minutes at 4ºC, followed by a PBS wash and cell permeabilization using 0.5% Triton-X-100 in PBS/glycine at room temperature for 20 minutes. Plates were washed three times with PSBT (PBS, 0.1% Tween-20), incubated for 1 hour with a monoclonal antibody pool to influenza A or B nucleoproteins (International Reagent Resource; www.internationalreagentresource.org) in ELISA buffer (PBS,10% horse serum, 0.1% Tween-80(PBST)). Following three washes with PBST, the cells were incubated with goat anti-mouse peroxidase-labelled IgG (Sera Care, Inc., Milford, MA) in ELISA buffer for one hour at room temperature. Plates were washed three times with PBST, and infectious foci (spots) were visualized using TrueBlue substrate (Sera Care, Inc., Milford, MA USA) containing 0.03% H_2O_2 incubated at room temperature for 10-15 minutes. The reaction was stopped by washing five times with deionized water. Plates were dried and foci enumerated using a CTL Bio Spot Analyzer with ImmunoCapture 6.4.87 software (CTL, Shaker Heights, OH). The FFA titer was determined by multiplying sample dilution which gave between one hundred to three hundred spots by the spot number at that dilution, to obtain the FFU/well. The foci in the cell control were subtracted and the number of foci remaining was multiplied by twenty to give FFU/ml. All samples were expressed in log Focus Forming Units per milliliter (FFU/ml). The limit of detection was $10^{3.3}$ FFU/ml.

Gene expression in FNEC/PBMC

One hundred microliters PBS was added to virus-inoculated or control FNEC monolayers on Transwell® inserts followed by 280 microliters AVL lysis buffer (Qiagen, Germantown, MD USA). Samples were mixed 3-4 times and lysate was frozen at -80°C

until RNA extraction. Carrier RNA was added to each sample and RNA was extracted using EZ1 DSP kit on a Qiagen EZ1 Advanced XL extractor according to the manufacturer's instructions (Qiagen, Germantown, MD USA). RNA was eluted in 120 microliters RNAse-free water and stored at -80°C until evaluated for gene expression. For PBMC, supernatants and cells, were removed from basolateral side of the Transwell™ chambers and centrifuged to pellet the cells. Supernatants were stored at -80°C for virus titration and cytokine/chemokine analysis. The cell pellets were resuspended in 100 microliters PBS followed by 280 microliters AVL lysis buffer and processed as FNEC samples.

Primers and probes for all ferret genes were generated from published ferret sequences [5, 306, 388-391] or developed and tested previously [416]. All primer/probe sets used are shown in Table 2.1. Quantitative real time PCR (qRT-PCR) was performed on triplicate samples using an ABI 7500 Fast Dx Real-Time PCR instrument (Applied Biosystems, Waltham, MA USA). PCR reactions were performed using SYBR™GreenER™ qPCR SuperMix (Applied Biosystems) or SuperScript™ III Platinum™ One-Step qRT-PCR Kit for TaqMan reactions (Invitrogen, San Diego, CA USA). An RT reaction for 30 minutes at 50°C, inactivation for 2 minutes at 95°C, followed by 40 amplification cycles at an annealing temperature of 50°C. Reactions were performed on triplicate samples for each experiment and the values were normalized by subtracting the mean value of the cycle threshold (C_T) from that of the C_T for glyceraldehyde-3-phosphate dehydrogenase (GAPDH) housekeeping gene (ΔC_T). The relative levels of gene expression for infected cells were determined by subtracting the individual ΔC_T values from that of average ΔC_T values of uninfected cells ($\Delta\Delta C_T$) and

expressing the final quantification values ($2^{-\Delta\Delta CT}$) as relative fold changes. Gene expression $>10^4$-fold increase over control were given an expression value of 10,000 and gene expression $>10^{-4}$-fold were given an expression value of 0.0001.

Type-III IFN bioassay

Basolateral secretion of interferon lambda (IFN-λ) from basolateral supernatants was detected using HEK-λ reporter cells (HEK-Blue™ IFN-λ cells: InvivoGen, San Diego, CA USA) designed to monitor the activation of the JAK/STAT/ISGF3 pathway induced by type III IFNs. The HEK-λ cells were generated by stable transfection of HEK-293 cells with the human IFNLR and IL10R receptor genes as well as the human signal transducers and activators of STAT2 and IRF9 resulting in a fully active IFN-λ signaling pathway. Activation of the pathway was detected since these cells harbored the secreted embryonic alkaline phosphatase (SEAP) under the control of the ISG54 promoter, which is activated by IFN-λ. Stimulation of the IFN-λ triggered the JAK/STAT/ISGF3 pathway and induced SEAP production which was measured by a colorimetric assay at 650nm using Quanti-Blue™ solution according to the manufacturer's instructions (InvivoGen, San Diego, CA USA).

Twenty microliters of basolateral supernatants collected from uninfected, IAV and IBV infected FNEC with and without cocultured PBMC, or media control was added in triplicate wells of 96-well tissue culture plate. A tissue culture flask containing HEK-λ cell monolayers was gently rinsed once with PBS and cells were dislodged and suspended in HEK medium (DMEM, 10% FBS, antibiotics) to a concentration of $2.8x10^5$ cells/ml. 180 microliters of HEK-λ cells were added to each well containing twenty microliters of sample and to serially 1/2-log diluted (0.1 – 1000ng/ml) recombinant ferret

IFN-λ3 (Kingfisher Biotech, St. Paul, MN USA). The plates were incubated for 20Hr at 37°C, 5%CO_2. After 20hr, twenty microliters of supernatant from the wells were transferred to a new 96-well plate and 180 microliters of Quanti-Blue™ substrate was added and incubated for 2Hr at 37°C, 5%CO_2. Absorbance was read at 655nm. A sigmoidal 4-point standard curve from 0.1 to 1000 ng/ml was generated using recombinant ferret IFNλ3 protein and unknown samples were extrapolated from the standard curve. The limit of detection was determined to be 100 pg/mL. The assay was specific for Type-III IFN since type-I/II ferret and human IFNs did not result in an absorbance signal (Figure 2.S1).

Statistical analysis

GraphPad Prism 10 was used for all statistical analyses (GraphPad Software, La Jolla, CA USA). One-way ANOVA was used to determine total IFN-λ protein concentrations over time between infection groups and significance between groups was determined by 2-way ANOVA analysis. Gene expression analysis was performed by triplicate independent samples per experiment, and outliers were identified using the Grubbs' test (α=0.05) of Extreme Studentized Deviate method for removal of a single outlier plus one iteration from all assays (N=12 total replicates) if found. Spearman (1-tailed, 95% confidence) correlation method used for comparison of virus replication and gene expression. The Student's *t* test was used to assess the statistical differences in the gene expression levels in respect to the uninfected controls and for comparing influenza A to influenza B viruses. A *p*-value of <0.05 was considered statistically significant: * $p<0.05$, ** $p<0.01$, *** $p<0.001$, **** $p<0.0001$.

RESULTS

PBMC co-cultivation did not have an overall effect on IAV or IBV Replication in FNEC.

Replication kinetics were compared for IAV and IBV at both 33°C and 37°C with and without the addition of PBMC. For experiments conducted at 37°C, FNEC were only inoculated with one IAV (CA) and one IBV (BR) virus prior to PBMC co-cultivation; whereas, at 33°C, two IAV (CA and KS) and two IBV (BR and PH) were used in experiments. At 33°C, no differences in virus replication were observed with or without PBMC co-cultivation (Figure 3.2); however, significant differences were observed within groups since at 48Hr and 72Hr post challenge. PH ($10^{8.65}$ FFU/mL) replicated to higher levels than CA ($10^{6.06}$ FFU/mL; p=0.0013), KS ($10^{7.01}$ FFU/mL; p=0.0137), or BR ($10^{5.68}$ FFU/mL; p=0.0081) at 48Hr and post inoculation in FNEC. At 72Hr post inoculation PH ($10^{8.67}$ FFU/mL) replicated higher than KS ($10^{6.97}$ FFU/mL; p=0.0003) and BR ($10^{5.83}$ FFU/mL; p=0.0134) in FNEC. In previous experiments, IBV viruses tended to reach higher titers in FNEC than IAV. This effect would be expected since virus supernatants were analyzed starting at 48Hr post challenge. When comparing the effects of temperature on virus replication kinetics with or without PBMC cocultivation (Figure 3.3), no statistical differences were observed with IAV (CA) and IBV (BR). Only CA inoculated FNEC co-cultivated with PBMC ($10^{6.58}$ FFU/mL) at 37°C showed statistically significant differences from FNEC alone ($10^{6.38}$ FFU/mL; p=0.0245). No other viral titers with or without PBMC cocultivation between groups or between temperatures was seen. This indicates, at 33°C no statistical differences were observed in this experiment when comparing IAV from IBV with and without cocultivation of PBMC.

Soluble factors released from FNEC challenged with IAV not IBV differentially upregulate genes in PBMC.

Since FNEC represent the URT, gene regulation and IFN-λ responses were only compared for experiments at 33°C. The link between innate and adaptive immune responses following influenza infection may be induced by communication between cells at the site of infection and circulating immune cells in the blood. Since there was no physical contact between FNEC and underlying PBMC and tight junctions prevented virus transfer (data not shown), only secreted factors could have an effect on the activation of PBMC following IAV and IBV challenge of FNEC. Since, at the time of these experiments, ferret cytokine detection by multiplexing was not available, only IFN-λ levels could be assessed.

Gene expression profiles in PBMC following cocultivation with FNEC after IAV and IBV were quantified by qRT-PCR at 48Hr (24Hr post cocultivation) and 72Hr (48hr post cocultivation) Figure 3.4. Genes were normalized to mock-challenged cultures and fold expression levels $>2^0$ was considered upregulated and expression levels $<2^0$ were considered downregulated. At 48Hr post IAV inoculation (24Hr post cocultivation) PBMC (Figure 3.4A) show a high upregulation of T-regulatory response genes (*Foxp3* and *IL-10*) to control lung inflammation following IAV infection to induce a T-regulatory response in mice [417, 418]. Inflammatory response genes (*CCL5*, *CXCL10*, and *IL-6)* were also preferentially upregulated in PBMC co-cultivated cells following IAV inoculation of FNEC. Interestingly, as seen in previous experiments with FNEC, type-III IFN (*IFNL3*) gene was highly upregulated only by IAV. Concurrently *TSLP* gene was upregulated higher in IAV PBMC co-cultivated samples but not in FNEC at 48Hr.

Average fold expression for by IAV and IBV for each gene from PBMC and FNEC of co-cultivated wells and significance is shown in Table 3.1. A clear difference in expression of pro-inflammatory and type-III IFN genes can be seen by 24hr post cocultivation (48Hr post inoculation). By 48Hr post cocultivation (72Hr post inoculation) this difference has been resolved.

Since only type-III IFN levels in the basolateral compartment of FNEC-PBMC could be determined other soluble factors could only be inferred. For type-III IFN (Figure 3.5) significant increases in IFN-λ over mock-infected FNEC and FNEC-PBMC cultures following IAV and IBV can be seen. Significantly higher levels of IFN-λ were found early (48hr post inoculation) in all FNEC only cultures compared to FNEC-PBMC co-cultivated samples ($p<0.01$); however, this significance was not seen later (72Hr post inoculation) between these groups. For FNEC-PBMC cultures only IAV (KS) inoculated samples showed significantly higher ($p<0.05$) levels of IFN-λ early (24Hr post cocultivation) to mock (UN) and IBV (PH) samples.

Pro-inflammatory and type-I IFN gene expression strongly correlate with virus replication in PBMC co-cultures.

Table 3.2 shows correlations between virus replication in FNEC and gene expression in FNEC±PBMC cultures. Generally (Table 3.2, panel A), pro-inflammatory gene responses show a strong positive correlation with virus replication in FNEC only and PBMC co-cultivated samples for influenza. Type-I and Type-III IFNs are also strongly correlated with increased virus replication. When comparing IAV (Table 3.2B) only IFN (*IFNA)* gene shows a strong correlation ($r=1;p=0.04$) to virus replication in PBMCs. In FNEC, inflammatory response (*CCL2*) and T-effector (*IL-4*) genes show a

strong direct correlation between virus replication and gene expression. For FNEC and inverse correlation can be seen for most genes compared to what was seen in PBMC when cocultured. For IBV (Table 3.2C) direct correlations between inflammatory response (*MCP1* and *IL-6*), T-effector (*IL-4* and *IL-17)*, apoptosis (*GranzymeA*), and type-I IFN (*IFNA* and *IFNB*) are observed. For IBV, a clear correlation for proinflammatory and IFN responses can be seen in PBMC following infection of FNEC indicating a potential process of communication between cells at the site of infection and cells in the peripheral blood.

DISCUSSION

Since the respiratory tract represents the initial site of infection for influenza viruses communication, or "cross talk", between respiratory epithelial cells and PBMC is important to mount a protective immune response. A key component to understanding the disparity between IAV and IBV in generation of a robust immune response in the host, is communication between the cells at the site of infection and immune cells in the peripheral blood. A demonstration of communication between pulmonary epithelial cells (A549) and PBMC in response to various bacterial stimuli showed that cocultivation of A549 and PBMC resulted in a significant increase in inflammatory cytokines [419] compared to PBMC only cultures. A549 cells alone did not show any cytokine release following bacterial stimulation [420]. Studies with IAV-infected human nasal epithelial cells (hNEC) co-cultivated with PBMC confirmed communication between epithelial cells and PBMC in response to infection. IAV-infected hNEC released type-I/II/III IFNs and pro-inflammatory cytokines which activated various cells in cocultured PBMC [421].

Unfortunately, immune reagents are currently not available for ferret cells in order to fully assess the effects of FNEC-PBMC communication on specific cell type activation markers. Studies for influenza only investigated effects of IAV infection on communication between respiratory epithelial cells and PBMC; however, this study was conducted to confirm responses seen with IAV as well as to ascertain differences between IAV and IBV on FNEC and the effects on co-cultivated PBMC.

To determine the communication between virus-infection of FNEC and underlying PBMC, addition of PBMC to the basal compartment following IAV/IBV infection of FNEC were evaluated. Effects on virus replication at both 33°C and 37°C following cocultivation were initially conducted. Subsequent studies to determine gene expression and type-III IFN production in both FNEC and co-cultivated PBMC as well as the correlation between virus replication and gene expression were performed. The initial effects on the contribution of FNEC-PBMC cross talk on virus replication showed that there was no significant difference in virus replication at the apical surface of infected FNEC over the first 72Hr post inoculation. There were differences between IAV and IBV, with IBV (PH) replicating to the highest levels in FNEC over the time period assessed. This confirmed previous findings in IAV/IBV infected FNEC cultures (Figure 3.1). Studies were conducted comparing IAV (CA) and IBV (BR) replication in FNEC±PBMC cultures at temperatures representing the upper (33°C) and lower (37°C) respiratory tract in humans. Both IAV and IBV replicated slightly higher at 37°C in FNEC. However, this was not significant. The increased replication for CA in FNEC cocultured with PBMC at 24Hr post coculture ($p=0.025$) may be due to factors secreted

by PBMC; however, since only two viruses were compared, additional viruses need to be studied to confirm this response.

Due to the availability of ferret cytokine detection, only gene expression differences in FNEC-PBMC co-cultivated samples could be tested. This study showed an early upregulation of pro-inflammatory (*MCP-1, CXCL10, IL-6, IL-8* and *TNFA*), T-effector (*IL-4)* and IFN (*IFNG* and *IFNL3*) gene expression in PBMC following cocultivation with IAV-infected FNEC (48hr post infection; 24Hr post cocultivation); whereas this response was delayed in PBMC following cocultivation with IBV-infected FNEC (72Hr post infection; 48Hr post cocultivation). PBMC isolated from transplant patients who seroconverted to seasonal influenza vaccine, demonstrated significantly elevated levels of type I/II IFNs, and proinflammatory cytokines in supernatants following H1N1pdm09 stimulation in vitro [422]. Thus, demonstrating that a strong IFN and pro-inflammatory response in PBMC was essential for development of a robust antibody response to influenza virus infection. These responses, at least for gene expression, were observed early in PBMC following cocultivation with IAV-infected FNEC.

The timing and magnitude of innate immune responses is critical in activating downstream immune cells to develop a robust immune response to influenza infection. Correlations of innate gene expression to viral replication are a critical component in understanding the initiation of downstream immune responses. All influenza viruses assessed showed a strong correlation between pro-inflammatory (*IL-1A/B, IL-6, IL-8*, and *TNFA*) and type-I/III IFN (*IFNB* and *IFNL3*) gene expression and virus replication in FNEC. Interestingly, co-cultivated PBMC showed an inverse correlation of

proinflammatory (*IL-A, IL-8,* and *TNFA*) gene expression in PBMC and virus replication in FNEC. Co-cultivated PBMC did show a strong correlation in type-I IFN (*IFNA*) gene expression in PBMC and virus replication in FNEC. Since type-I IFN showed a strong correlation in PBMC with virus replication in FNEC and type-III IFN showed a strong correlation in FNEC with replication in FNEC, IFN remains a key component of the innate immune response in developing a robust adaptive response. A strong Type-III IFN response is a key component the respiratory tract while strong type-I/II IFN responses remain an important component in PBMC to trigger adaptive immunity to influenza viruses.

Future analysis of ferret cytokine/chemokine levels in the basolateral compartment of FNEC-PBMC cocultures as well as activation of ferret PBMC cell subsets will validate findings observed in humans and allow for a greater understanding of disparities between the immune responses of IAV and IBV.

Figure 3.1: Isolation/Differentiation of FNEC.

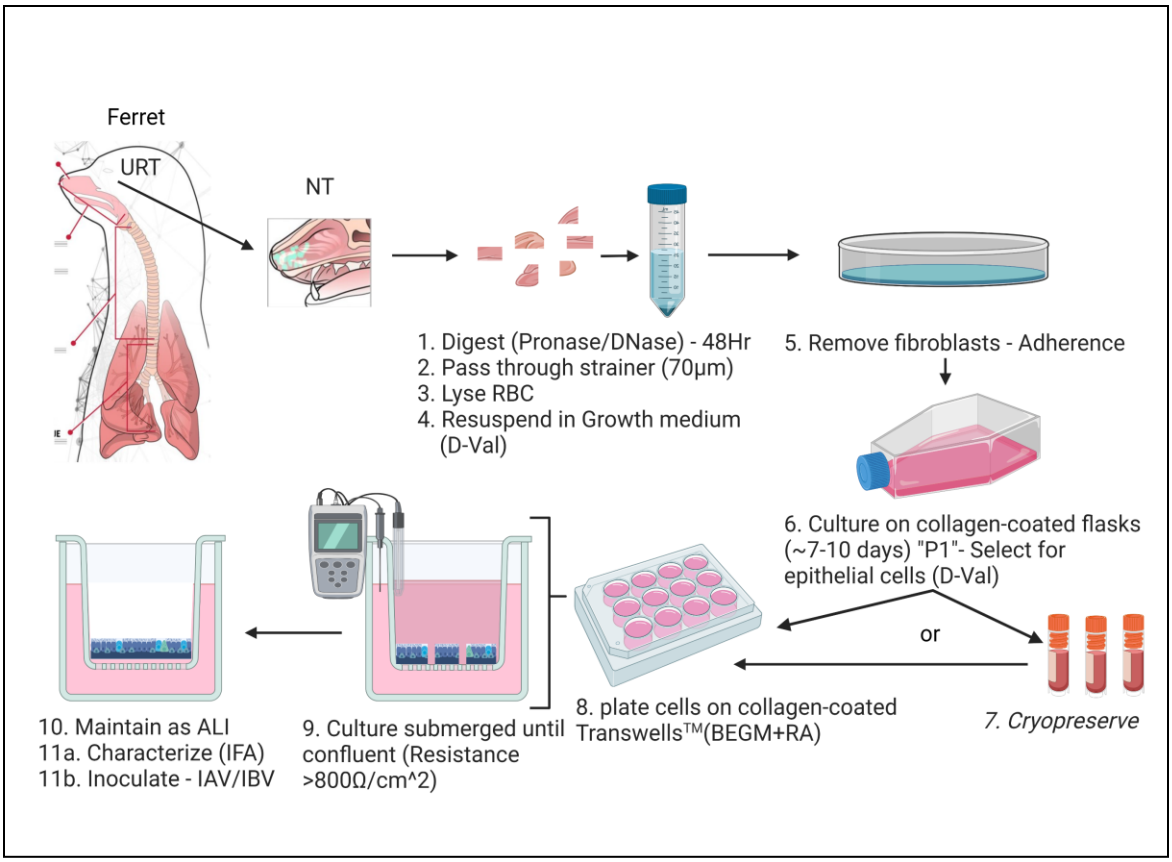

Isolation and differentiation of FNEC from ferret upper respiratory tract (URT). Nasal turbinates (NT) collected and processed. Steps 1 – 4: Pronase digestion, single cell suspension, red blood cell lysis (RBC) and resuspension in D-valine selection medium. Steps 5 – 7: Removal of contaminating fibroblasts by adherence, cell culture in D-valine selection media until confluence, cryopreservation, or culture initiation. Steps 8 – 11: Culture of cells on Transwells™ in differentiation medium, culture until tight junctions form (resistance >800Ω/cm^2), culture in air-liquid interface (ALI), characterize surface receptors and inoculate. Figure created with Biorender.com.

Figure 3.2: Effect of PBMC co-cultivation on virus replication in FNEC.

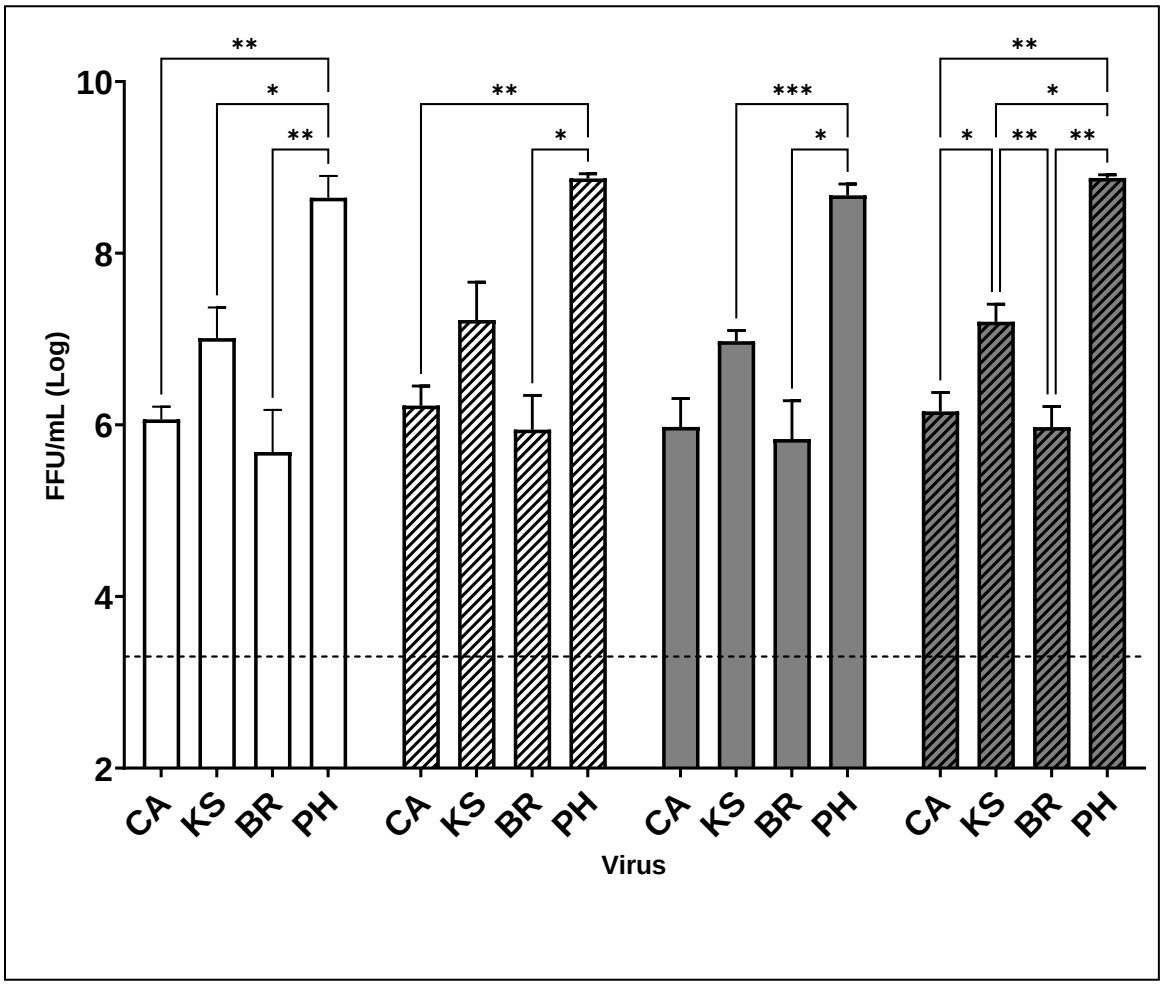

Replication kinetics of IAV [H1N1pdm09 "CA" (A/California/07/2009), H3N2 "KS" (A/Kansas/14/2017)] and IBV [B-Victoria lineage "BR" (B/Brisbane/60/2008), B-Yamagata lineage "PH" (B/Phuket/3073/2013)] inoculation of FNEC at 33°C (MOI=0.3) with or without PBMC co-cultivation over 72Hr. PBMC were added to the basolateral compartment at 24Hr post challenge. White bars and white/hashed bars indicate 48Hr post challenge without PBMC or with PBMC co-cultivation (24hr cocultivation) respectively. grey bars and grey/hashed bars indicate 72Hr post challenge without PBMC or with PBMC co-cultivation (48Hr cocultivation) respectively. No significant differences between groups seen (1-way ANOVA); however, within groups, significant

differences between PH and other groups are seen (mixed-effects analysis). Limit of detection, indicated by a dotted line, was $10^{3.3}$ FFU/mL.

Figure 3.3: Effects of temperature on virus replication in FNEC co-cultivated with

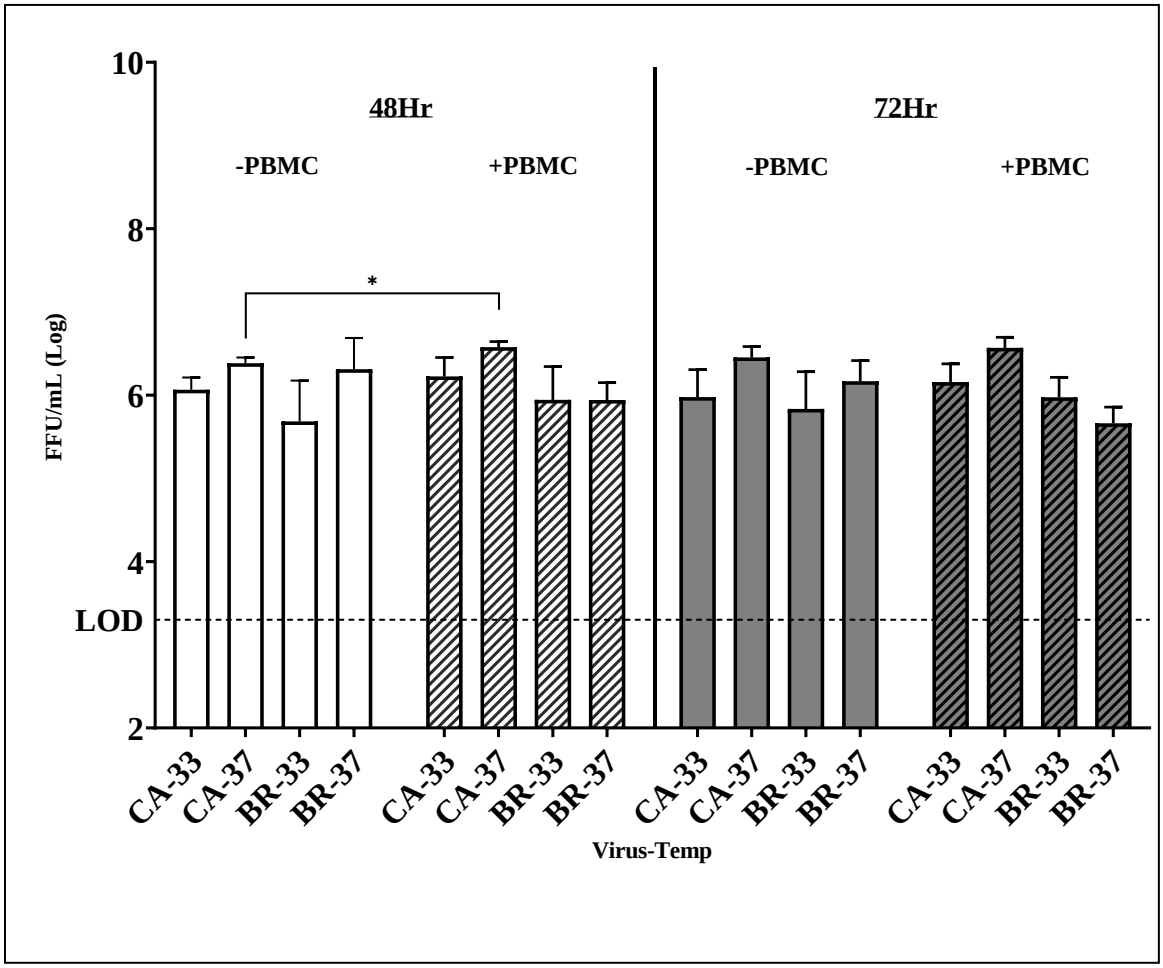

PBMC.

Replication kinetics of IAV, "A" (H1N1pdm09; A/California/07/2009) or IBV, "B" (B-Victoria lineage; B/Brisbane/60/2008) in FNEC at 33°C and 37°C (MOI=0.3) with or without addition of PBMC (co-cultivated with FNEC at 24Hr post challenge). Forty-eight Hr post challenge (24Hr post PBMC co-cultivation) are indicated in white bars (no PBMC co-cultivation) or white/hashed bars (plus PBMC co-cultivation. Seventy-two Hr

post challenge (48Hr post PBMC co-cultivation) are indicated in grey bars (no PBMC co-cultivation) or grey/hashed bars (plus PBMC co-cultivation). There were no significant differences between temperatures or ±PBMC cultivation except for IAV at 37°C ±PBMC ($p=0.025$). The limit of detection (LOD), indicated by a dotted line, was $10^{3.3}$ FFU/mL. Significance between groups was determined using multiple unpaired t tests.

Figure 3.4: Gene Expression profiles in PBMC following co-cultivated with influenza infected FNEC.

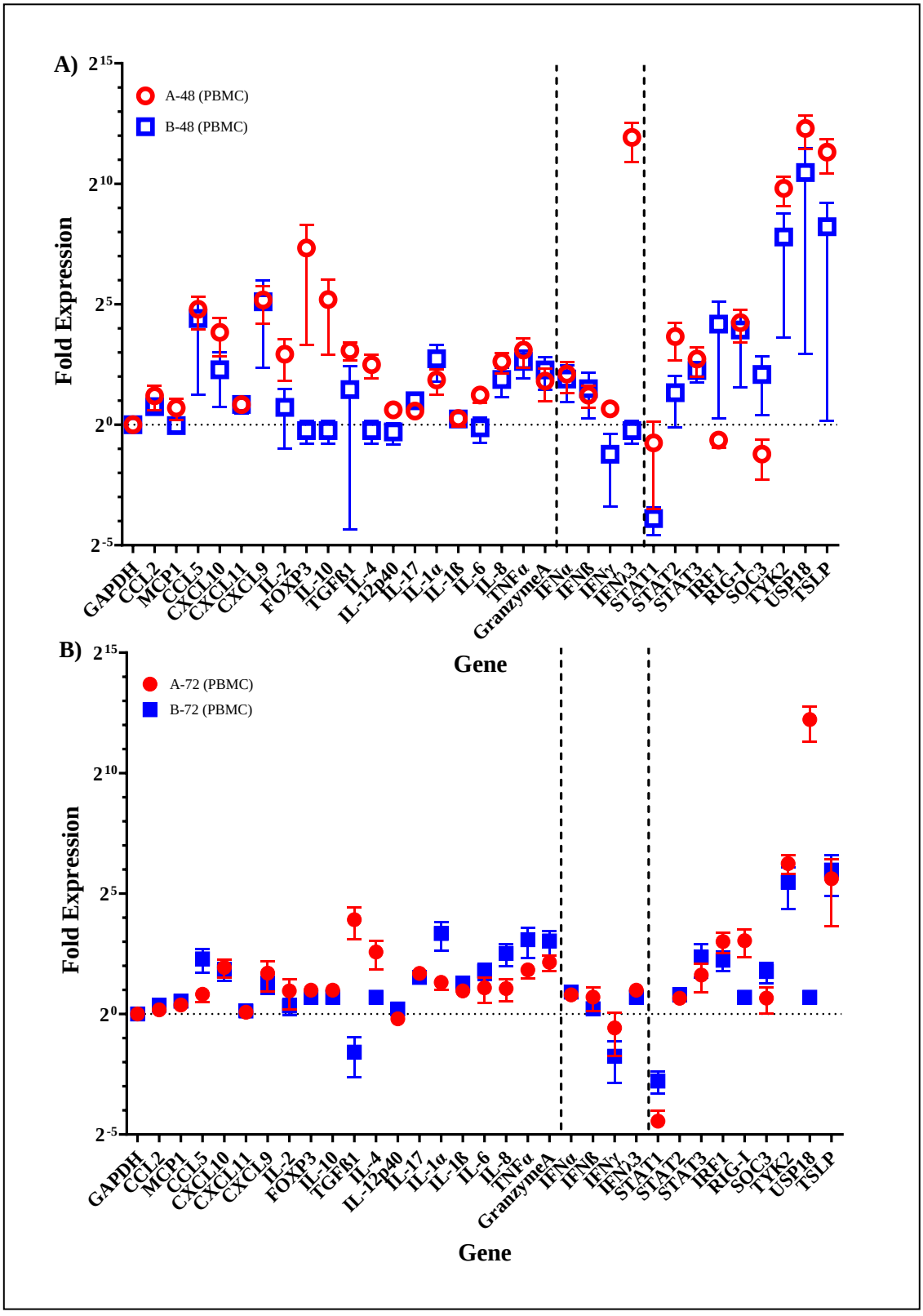

Average fold gene expression, normalized to mock FNEC inoculated, co-cultivated cultures. FNEC were inoculated with IAV (CA or KS) or IBV (BR or PH) for 24Hr prior to co-culture with ferret PBMC. IAV are represented by red circles and IBV are represented by blue squares. Panel A) Fold gene expression in PBMC at 24Hr post co-cultivation (48Hr post FNEC inoculation). Panel B) Fold gene expression in PBMC at 48hr post co-cultivation (72Hr post FNEC inoculation). Red circles (IAV) and blue circles (IBV) inoculated FNEC cultures. IFN genes are between dotted lines. Gene expression values above 2^0 are upregulated and gene expression values below 2^0 are down regulated. Genes are listed on the x-axis.

Table 3.1 Comparison of gene expression differences of IAV and IBV following PBMC-FNEC cocultivation.

GENE	P value	Mean of A-48 (PBMC)	Mean of B-48 (PBMC)	P value	Mean of A-72 (PBMC)	Mean of B-72 (PBMC)	P value	Mean of A-48 (FNEC)	Mean of B-48 (FNEC)	P value	Mean of A-72 (FNEC)	Mean of B-72 (FNEC)
GAPDH		1	1		1	1		1	1		1	1
CCL2	0.490	2.30	1.68	0.321	1.13	1.29	0.566712	2.404	2.998	0.329137	1.267	1.061
MCP1	0.241	1.62	0.97	0.470	1.30	1.45	0.233712	1.12	0.7613	0.267437	1.343	1.024
CCL5	0.785	27.66	21.22	0.111	1.77	4.89	0.272599	6.725	24.14	0.144558	2.439	5.146
CXCL10	0.270	14.28	4.85	0.780	3.82	3.44	0.246441	2.481	5.551	0.123085	1.27	3.131
CXCL11	0.986	1.78	1.79	0.854	1.05	1.09	0.794874	1.479	1.623	0.191297	1.132	0.8441
CXCL9	0.961	36.11	34.37	0.556	3.24	2.34	0.219884	17.31	47.13	0.234379	1.72	2.437
IL-2	0.214	7.61	1.65	0.456	1.95	1.26	0.285856	0.849	1.888	0.057355	0.9196	1.412
FOXP3	0.349	161.70	0.85	0.176	1.99	1.62	0.375758	4.02	88.03	0.99605	1.412	1.412
IL-10	0.273	36.58	0.85	0.176	1.99	1.62	0.385043	1.009	12.94	0.99605	1.412	1.412
TGFß1	0.146	8.47	2.75	0.084	15.10	0.33	0.852893	3.056	3.662	0.149073	0.02748	0.0002943
IL-4	0.049	5.64	0.85	0.121	5.95	1.62	0.516181	1.191	0.9769	0.99605	1.412	1.412
IL-12p40	0.059	1.53	0.81	0.124	0.87	1.16	0.996552	1.136	1.138	0.03674	0.7842	1.158
IL-17	0.324	1.48	1.99	0.386	3.21	2.87	0.339696	1.791	1.436	0.930717	2.75	2.721
IL-1α	0.431	3.63	6.67	0.112	2.48	10.16	0.089762	3.661	8.526	0.048721	2.377	11.34
IL-1ß	0.963	1.20	1.18	0.054	1.94	2.44	0.534873	1.255	1.424	0.289239	2.116	2.366
IL-6	0.034	2.35	0.91	0.255	2.12	3.44	0.150345	1.428	1.079	0.143828	0.8924	2.807
IL-8	0.316	6.16	3.68	0.101	2.08	5.70	0.121013	3.321	5.691	0.03631	2.71	6.659
TNFα	0.578	8.57	6.18	0.225	3.56	8.50	0.058092	3.412	7.231	0.11322	1.303	8.263
GranzymeA	0.629	3.51	4.84	0.251	4.44	8.18	0.229432	1.635	4.138	0.123182	2.294	7.785
IFNα	0.828	4.31	3.73	0.653	1.73	1.88	0.055457	3.595	1.258	0.718861	0.9258	0.7372
IFNß	0.802	2.34	2.82	0.444	1.63	1.17	0.680813	1.262	1.159	0.223058	1.225	0.9698
IFNγ	0.030	1.58	0.43	0.386	0.67	0.30	0.906614	1.122	1.056	0.912374	0.3046	0.273
IFNλ3	0.104	3894.00	0.85	0.176	1.99	1.62	0.999832	936.3	936	0.99605	1.412	1.412
STAT1	0.356	0.59	0.07	0.074	0.05	0.15	0.796075	0.298	0.3791	0.277294	0.07445	0.1091
STAT2	0.176	12.62	2.52	0.660	1.58	1.75	0.740824	5.521	7.507	0.795711	1.049	1.172
STAT3	0.546	6.62	4.76	0.451	3.07	5.13	0.880742	1.906	2.102	0.089475	2.131	0.1112
IRF1	0.377	0.64	18.05	0.246	8.03	4.70	0.387967	1.677	14.72	0.059084	7.911	3.473
RIG-I	0.818	18.88	15.28	0.091	8.26	1.62	0.276868	4.872	16.94	0.999362	2.147	2.146
SOCS3	0.284	0.43	4.25	0.158	1.58	3.39	0.315423	1.989	4.757	0.148935	3.155	1.865
TYK2	0.146	896.50	221.90	0.343	75.79	44.38	0.829293	134.6	158.7	0.266283	1.139	3.762
USP18	0.208	5029.00	1417.00	0.100	4782.00	1.62	0.879569	6000	6667	0.999706	3.106	3.105
TSLP	0.117	2543.00	297.30	0.786	49.03	62.81	0.728356	1118	1577	0.205793	0.3034	35.96

Mean fold gene expression following IAV (CA and KS) or IBV (BR and PH) inoculation in FNEC and cocultivation with PBMC. Fold expression compared to mock-inoculated FNEC or PBMC.

Table 3.2: Correlation between virus replication and gene expression in FNEC±PBMC.

	(A)						(B)						(C)					
	A&B (FNEC only)		A&B Cocult (FNEC)		A&B Cocult (PBMC)		A (FNEC only)		A Cocult (FNEC)		A Cocult (PBMC)		B (FNEC only)		B Cocult (FNEC)		B Cocult (PBMC)	
GENE	r	p	r	p	r	p	r	p	r	p	r	p	r	p	r	p	r	p	FUNCTION
GAPDH																			Housekeeping
CCL2	0.5		(0.0)		0.1		**1.0**	**0.0417**	0.2		0.4		0.4		0.2		0.2		Inflammatory chemokine
MCP1	0.2		(0.0)		0.6		(0.6)		**(1.0)**	**0.0417**	**1.0**	**0.0417**	0.6		**0.7**	**0.0229**	**0.7**	**0.006**	Inflammatory chemokine
CCL5	0.2		0.4		**(0.7)**	**0.0229**	(0.8)		0.4		(0.6)		0.8		0.6		0.0		Chemokine (RANTES)
CXCL10	(0.1)		0.6		**(0.7)**	**0.0347**	(0.8)		0.2		(0.8)		0.2		0.5		(0.1)		Th1 (IP-10)
CXCL11	(0.1)		(0.1)		(0.0)		(0.6)		(0.6)		0.4		0.2		(0.3)		(0.2)		Th1 (IP-9)
CXCL9	(0.0)		0.3		**(0.8)**	**0.0184**	0.0		0.8		(0.8)		(0.2)		0.4		0.2		Th1 (MIG)
IL-2	0.0		0.6		**(0.7)**	**0.0415**	0.6		0.6		(0.6)		(0.4)		0.3		(0.1)		Th2
FOXP3	0.2		(0.3)		0.1		(0.4)		0.4		(0.8)		0.8		0.4		0.4		Treg
IL-10	0.4		(0.5)		0.2		(0.4)		(0.8)		0.0		0.6		0.2		0.4		Treg
TGFß1	(0.2)		(0.4)		**0.7**	**0.0415**	(0.6)		0.2		0.8		(0.4)		(0.6)		(0.0)		Treg
IL-4	0.4		(0.1)		0.1		**1.0**	**0.0417**	(0.4)		(0.8)		0.8		0.4		**0.5**	**0.0393**	Teff
IL-12p40	0.5		(0.1)		0.0		(0.4)		**1.0**	**0.0417**	0.0		0.8		0.3		0.3		Teff
IL-17	0.3		0.1		(0.0)		0.0		(0.8)		(0.4)		0.6		**0.7**	**0.0347**	**0.6**	**0.0136**	Teff
IL-1α	**1.0**	**0.0006**	0.6		**(0.9)**	**0.0054**	0.8		**1.0**	**0.0417**	(0.8)		0.8		**0.9**	**0.0023**	0.4		Pro-inflammatory cytokine
IL-1ß	**0.8**	**0.014**	0.1		(0.1)		0.6		(0.4)		(0.4)		0.6		0.5		0.5		Pro-inflammatory cytokine
IL-6	**0.8**	**0.0109**	0.3		(0.3)		0.6		(0.6)		(0.8)		**1.0**	**0.0417**	**0.8**	**0.0109**	**0.6**	**0.0261**	Pro-inflammatory cytokine
IL-8	**0.8**	**0.014**	0.6		**(0.8)**	**0.0184**	0.8		0.8		(0.6)		0.6		**0.8**	**0.0184**	0.3		Pro-inflammatory cytokine
TNFα	**0.7**	**0.0415**	0.6		**(0.7)**	**0.0288**	0.6		0.8		(0.8)		**1.0**	**0.0417**	**0.9**	**0.0011**	0.4		Pro-inflammatory cytokine
GranzymeA	0.5		0.6		**(0.8)**	**0.014**	(0.4)		0.0		(0.8)		**1.0**	**0.0417**	**1.0**	**0.0002**	**0.5**	**0.0398**	Apoptosis
IFNα	0.3		(0.1)		**0.9**	**0.0036**	0.0		(0.6)		**1.0**	**0.0417**	0.6		0.4		**0.6**	**0.033**	Interferon (Type-I)
IFNß	**0.8**	**0.014**	(0.2)		0.4		0.8		(0.6)		(0.6)		**1.0**	**0.0417**	0.5		**0.6**	**0.031**	Interferon (Type-I)
IFNγ	0.4		(0.5)		0.3		(0.6)		0.8		0.4		0.8		(0.1)		0.1		Interferon (Type-II)
IFNλ3	**0.7**	**0.0347**	(0.3)		0.2		(0.4)		0.4		0.0		**1.0**	**0.0417**	0.4		0.4		Interferon (Type-III)
STAT1	0.2		(0.2)		(0.2)		0.0		**1.0**	**0.0417**	(0.8)		0.0		(0.5)		(0.4)		ISG (IFNγ, IFNα, IFNß)
STAT2	(0.4)		0.2		(0.5)		0.6		0.2		0.2		**(1.0)**	**0.0417**	0.0		(0.1)		ISG (IFNα, IFNß)
STAT3	(0.3)		(0.2)		**0.7**	**0.0229**	0.4		(0.8)		**1.0**	**0.0417**	**(1.0)**	**0.0417**	(0.4)		0.1		ISG (Teff)
IRF1	(0.0)		0.2		(0.5)		0.8		(0.8)		(0.8)		(0.8)		0.3		0.3		Type I (ISG)
RIG-I	(0.3)		(0.0)		(0.5)		0.2		0.8		(0.8)		(0.8)		(0.3)		(0.4)		Type I Resp
SOCS3	0.0		(0.0)		(0.2)		0.2		(0.2)		(0.4)		(0.4)		0.3		0.2		IFN (↓Reg)
TYK2	**0.7**	**0.0415**	(0.0)		0.6		**1.0**	**0.0417**	0.4		0.4		0.8		0.5		0.5		Type I (Reg)
USP18	0.5		(0.4)		(0.3)		(0.8)		0.8		(0.6)		**1.0**	**0.0417**	0.3		0.1		Type I (Reg) Type III (↑Reg)
TSLP	(0.6)		0.2		(0.5)		**(1.0)**	**0.0417**	0.4		0.0		(0.8)		0.1		(0.1)		Type I (Reg) Type III (↑Reg)

Correlations between virus replication and gene expression in co-cultures. Panel (A) All data for IAV and IBV for all cell types. (B)IAV inoculated samples representing CA and KS inoculated FNEC at 33°C. Panel (C) IBV inoculated samples representing BR and PH inoculated FNEC at 33°C. Strong correlations $r \geq 0.7$ and inverse correlations $r < -0.7$. Inverse, negative correlations are indicated in parentheses. Significance, $p<0.05$, are indicated in bold. Genetic functional groups are separated by dotted lines.

Figure 3.5: Interferon levels in basolateral compartment of influenza inoculated FNEC following co-cultivation with PBMC.

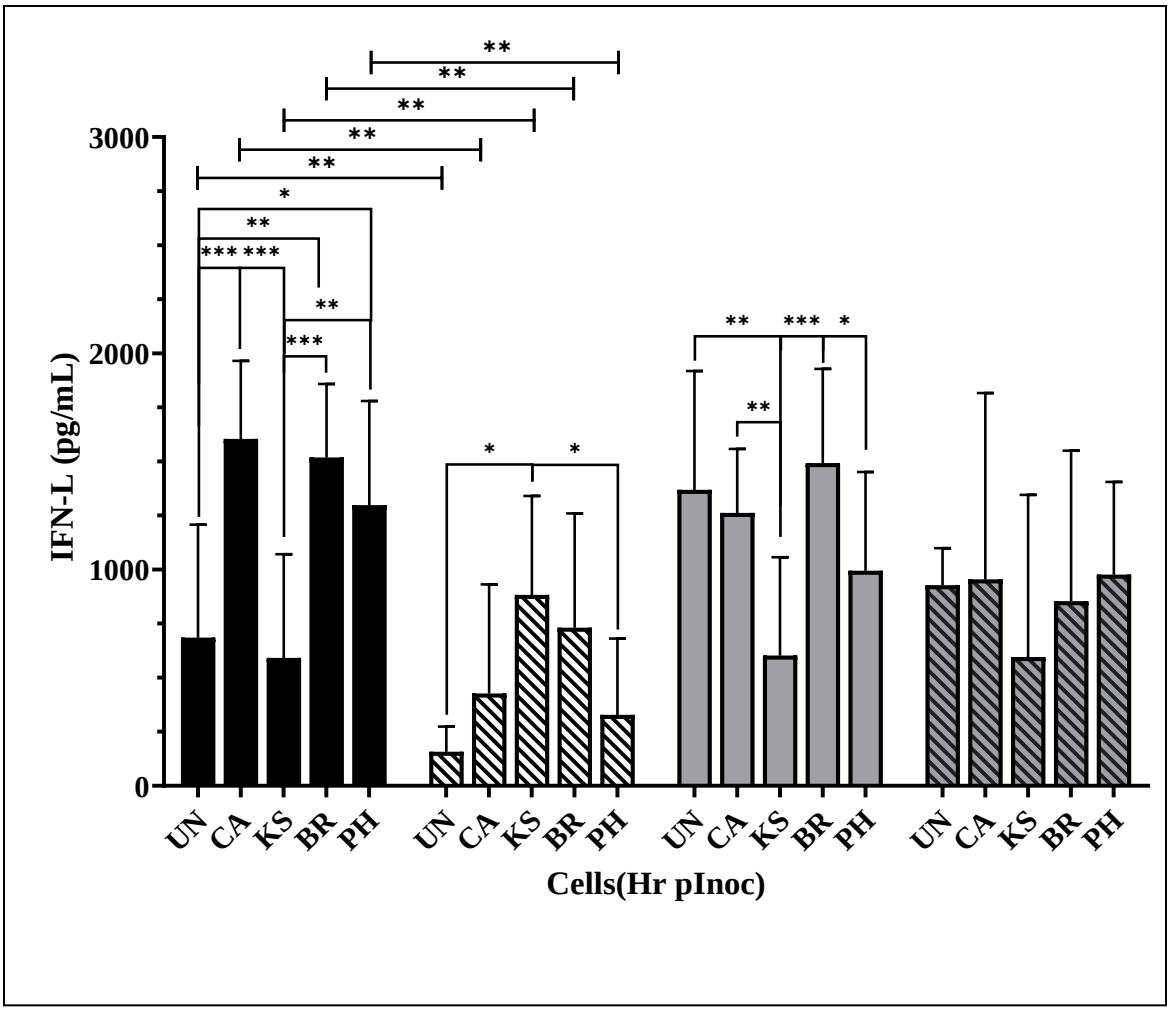

IFN-L levels in basolateral supernatants following IAV (CA, KS), IBV (BR, PH) or mock (UN) inoculation of FNEC co-cultivated with PBMC at 33°C. Forty-eight Hr post inoculation (pInoc) corresponds to 24Hr post cocultivation (FNEC/PBMC); 72Hr post pInoc corresponds to 48hr post cocultivation. 48Hr FNEC only cultures (black bars) or FNEC/PBMC coculture (black-white hatched bars). 72Hr FNEC only cultures (grey bars) or FNEC/PBMC coculture (black-grey hatched bars). Significant differences ($p<0.05$) determined for each cell type and Hr post inoculation using multiple Student's t-tests. Significant differences compared between viruses for cell types. Differences between groups (FNEC and FNEC/PBMC) determined by 2-way ANOVA (Tukey test). Significant differences ($p<0.01$) at 48Hr post inoculation only for all virus and mock groups when comparing FNEC to FNEC/PBMC cocultures.

CHAPTER 4

DELAY OF INNATE IMMUNE RESPONSES FOLLOWING INFLUENZA B INFECTION AFFECTS THE DEVELOPMENT OF A ROBUST ANTIBODY RESPONSE IN FERRETS[3]

[3] Thomas Rowe, Ashley Fletcher, Robert A. Richardson, Melissa Lange, Giuseppe A. Sautto, Greg A. Kirchenbaum, Yasuko Hatta, Gabriela Jasso, David E. Wentworth, and Ted M. Ross. Delay of innate immune responses following influenza B virus infection affects the development of a robust antibody response in ferrets. *Under review, PLoS Pathogens* (2024).

ABSTRACT

Due to its natural influenza susceptibility, clinical signs following infection, transmission, and similar sialic acid residue distribution, the ferret is the primary animal model for human influenza research. Antibodies generated following infection of ferrets with human influenza viruses are used in influenza surveillance to detect antigenic drift and cross-reactivity with vaccine viruses and circulating strains. Inoculation of ferrets, with over 1500 human clinical influenza isolates (1998 to 2019) for surveillance studies, resulted in lower serum antibody responses to 86% (387 of 448) IBV compared to 2.7% (30 of 1094) IAV. In this directed analysis, we show that the immune responses in ferrets inoculated with IAV (A/H1N1pdm09 or A/H3N2 subtype virus) were higher than IBV (B/Victoria or B/Yamagata lineage virus) and there was a delay in antibody responses by IBV. Analysis of innate gene expression in the ferret upper respiratory tract and peripheral blood indicated that IAV generated a strong inflammatory response, including an early activation of the interferon (IFN) response; whereas IBV elicited a delayed and reduced response. Additionally, serum levels of cytokines, chemokines, and IFNs were all much higher following IAV-infection than IBV-infection in ferrets. Pro-Inflammatory (MCP-1, MIP-1B, TNFA), IFN (IFNB, IFNG), Th1 (IP-10), Th2 (IL-2), and T-effector (IL-12p40) proteins were significantly higher in sera of IAV-infected than IBV-infected ferrets over twenty-eight days following challenge. Serum levels of Type-I/II/III IFNs were detected following IAV-infection throughout the 28-day period and Type-III IFN was only detected by day 28 for IBV. Early increase in IFN-lambda levels corresponded to gene expression following IAV-infection. The reduced innate immune responses detected following IBV-infection reflected the subsequent delayed and reduced

hemagglutination inhibition (HI) and neutralizing (focus reduction assay, FRA) antibodies in the sera. However, the differences in serum antibody responses elicited by IBV were not observed in antibody secreting cells in the spleen or peripheral blood. These findings help in understanding the antibody responses in humans following IBV vaccination or infection and consider potential addition of innate immunomodulators to overcome these low responses.

INTRODUCTION

Influenza A and B viruses continue to circulate and represent a major public health concern. Prevention from infection or serious complications relies on a robust adaptive immune response. Antibodies following infection or vaccination are used in surveillance assays to detect antigenic drift and make recommendations for vaccine strain selection. This study involves the use of ferrets to better understand why influenza B viruses generate weak immune responses following infection. Ferrets are an ideal model to explore immune responses to influenza virus because they are naturally susceptible to influenza including human influenza strains without the need for prior adaptation [423, 424]. Moreover, ferrets exhibit similar lung physiology and distribution of α2,3- and α2,6-linked sialic acids [425, 426]; which is the receptor for influenza virus entry. Finally, the frequency of antibody light chain isotypes in ferrets closely resembles that seen in humans [253] and further supports the use of ferrets for studying the antibody response elicited by influenza virus infection or vaccination.

Influenza A virus (IAV) and influenza B virus (IBV)-infected ferrets are used to generate antisera for influenza surveillance and to develop and improve influenza

vaccines. Over a twenty-year period from 1998 to 2019, more than 1500 antisera have been generated in ferret to IAV and IBV. In surveillance assays, such as the hemagglutination inhibition (HI) assay, reference antisera must generate a minimal titer of at least 1:160 to be able to detect antigenic variation. For IBV, 86.4% of viruses (387/448) inoculated into ferrets required a booster dose to reach the HI titer of 1:160 compared to only 2.7% (30/1094) for IAV.

Low antibody responses in humans infected with IBVs have also been observed. A cohort study conducted in Hong Kong from 2009-2014 to assess the antibody responses to B-Vic and B-Yam infections showed that <50% of PCR-confirmed individuals had detectable neutralizing antibody titers. Additionally, all B-Vic and B-Yam infected individuals with antibody responses showed low titers (<160) [427]. The effectiveness of IBV vaccine has also shown to be low, especially in children. In a study of the 2014/2015 influenza vaccine, which overall had 57% vaccine efficacy, it was shown that <20% of older children had a 4-fold rise in HI titer to influenza B following vaccination [362]. Since low antibody responses are seen in humans infected or vaccinated with IBV, and ferrets inoculated with IBVs generate much lower immune responses compared to infection with seasonal IAV, further investigation is required to identify ways to improve the immune responses to IBV.

Following exposure of the upper respiratory tract (URT) to influenza virus, the innate immune system is activated by interaction with pattern recognition receptors (PRRs) on susceptible cells. There are three different PRRs that sense influenza virus, which includes retinoic acid inducible gene I (RIG-I), Toll-like receptors (TLR3, TLR7 and TLR8) and the nucleotide binding oligomerization domain (NOD)-like receptors

[428]. Pro-inflammatory cytokines and type-I interferons are induced through RIG-I and TLR7 pathways [205]. At the site of infection (respiratory epithelial cells), TLR3 and TLR7 sense viral double-stranded and single-stranded RNA (ssRNA) respectively within the endosome while RIG-I recognizes cytosolic ssRNA or viral RNA containing 5'-triphosphate and induces type I and III interferon (IFN) responses through the transcriptional factors NF-kB and IRF by interacting with MAVS. These interactions result in the activation of NF-kB and IRF3 which result in initiating a pro-inflammatory response by the production of cytokines and chemokines as well as an interferon a type-I/III IFN response in respiratory epithelial cells. In IFN-knock out studies in mice, IFNB has been shown to be an important role in defense against IAV in lung epithelial cells, and IFNB absence results in delayed expression of IFNA thus increasing the probability that the infecting virus can overrun the innate immune response of the host [429]. The pro-inflammatory cytokines and chemokines can activate resident immune cells (innate lymphoid cells, macrophages, and dendritic cells) and recruit cells to the site of infection. Additionally, cytokines and chemokines can stimulate a T-helper 1 (Th1) response by IFNG and IL-12. They can also stimulate a T-effector response activation of STAT3 resulting in IL-6 and IL-23 secretion to further upregulate the inflammatory response [115]. These cytokines bind to the epithelial cell IFN receptors (IFNAR) or those expressed by myeloid cells causing expression of interferon stimulating genes (ISGs) and an antiviral state. In parallel, cytosolic ssRNA and DAMPs (Danger-Associated Molecular Pattern) can also interact with NLRP3 of the inflammasome complex to cause cleavage and activation of caspase-1 and induction of IL-1b and IL-18. The regulatory effects on adaptive immunity are not a result of direct action of type-III IFN (IFNL) but

rather indirectly through thymic stromal lymphopoietin (TSLP). IFNL secreted by infected respiratory epithelial cells can induce M cells to release TSLP which acts on migrating CD103+ dendritic cells (DCs) to stimulate the adaptive immune responses by enhancing CD8+ T-cell maturation and promoting germinal center reactions in the lymph node through T-follicular/helper (Tfh) cells [124]. Tfh help in B-cell survival and proliferation in germinal centers [124, 137, 193] resulting in an increase of IgG1 and IgA antibody [137]. Once these receptors are triggered by the virus, activation of several antiviral signals and production of cytokines and chemokines occurs to initiate the immune response in the host.

The humoral immune response plays a key role in immunity to influenza. This study focuses on the antibody response to influenza hemagglutinin (HA) which is the most commonly measured correlate of protection [3, 430]. Cytokine and chemokine levels in serum have been shown to correlate with increased antibody responses following vaccination and infection. Interleukin-2 (IL-2) can work together with cyclic adenosine 3' ,5'-phosphate in synergy to enhance the antibody by B-cells [147]. In elderly human subjects, IL-2 treatment enhanced antibody responses to influenza vaccination [148]. IL-2 has been shown to play an essential role in a T-helper 2 (Th2) differentiation [144] and may play a role in the adaptive immune response [149]. Inflammatory cytokine levels of IL-6 and TNFA in serum have shown a positive correlation with fold-increases in hemagglutination inhibition titers following vaccination [431]. IFN levels have also been shown to be protective and enhance antibody response following influenza infection. In mice lacking Tfh cells, which are important in humoral immunity, Th1 cells are the source of IFNG that promotes a protective IgG2 antibody response [432]. IFNL

has also been shown to increase adaptive mucosal antibodies [137]. Taken together, this study explores innate and cytokine responses following IAV and IBV infection of ferrets and their contribution to development of robust adaptive antibody responses. Understanding factors which affect the ability of influenza viruses to generate robust immune responses may aid in the testing and improvement of influenza B vaccine efficacy in humans.

MATERIALS AND METHODS

Viruses

Influenza viruses used were passaged in cells, Madin Darby Canine Kidney (MDCK), to retain antigenic similarity to the original human isolates and to avoid structural changes in the hemagglutinin which could occur from passage in eggs [377-379]. All influenza viruses were passaged in MDCK "C#" or MDCK-SIAT1 "S#" [380] cells according to established procedures [381, 382]. Representative IAV used in this study were: A/California/07/2009 "CA" (H1PDM09 subtype; passage C3) and A/Kansas/14/2017 "KS" (H3N2 subtype; passage S3). Representative IBV used in this study were: B/Brisbane/60/2008 "BR" (B-Victoria lineage; passage CXC6) and B/Phuket/3073/2013 "PH" (B-Yamagata lineage; passage C4). Viral titers were determined by focus forming assay [416] and given as log Focus Forming Units per milliliter (FFU/mL). Viral titers for virus stocks used in this study were: CA ($10^{6.64}$ FFU/mL), KS ($10^{7.00}$ FFU/mL), BR ($10^{7.17}$ FFU/mL) and PH ($10^{7.54}$ FFU/mL).

Ferret infection with influenza viruses and monitoring

All animal procedures were approved by the Institutional Animal Care and Use Committee of the Centers for Disease Control and Prevention in an Association for Assessment and Accreditation of Laboratory Animal Care International accredited facility. Male fitch ferrets (Triple F Farms, Sayre, PA), between 10 to 18 months of age and seronegative for currently circulating influenza viruses were used for infection experiments.

Four separate experiments were conducted using 18 ferrets for each virus [CA (influenza A/H1PDM09), KS (influenza A/H3N2), BR (influenza B/Victoria lineage) and PH (influenza B/Yamagata lineage)]. In each experiment ferrets were first anesthetized with an intramuscular cocktail of ketamine (15-30 mg/kg) plus xylazine (1-2 mg/kg) "KX" and challenged intranasally with 1 mL of virus (4x105 FFU/mL). The animals were monitored over 28 days post challenge for weight loss, fever, and other clinical signs (lethargy, sneezing and dyspnea). The animals were weighed on day 0 prior to influenza challenge to establish a baseline weight and then weighed daily for the first ten days post challenge followed weekly thereafter through day 28. Changes in weight were calculated as percentage loss or gain from day 0 weight. For fever calculation, a temperature transponder [IPTT-300; Bio Medic Data Systems (BMDS), Waterford, WI, USA] was programed to identify each ferret and implanted subcutaneously between the shoulder blades of each animal and read with a scanner (DAS-6007 IPTT Scanner System, BMDS). A baseline temperature (°F) was determined by the average temperature over three days prior to challenge. Temperatures were assessed over the first 10 days post challenge, then weekly and fever was determined as any temperature greater or equal to 2 degrees Fahrenheit above baseline. Ferrets were assessed daily for clinical signs within a

two-hour window between 9AM – 11AM during peak normal activity and to reduce variation due to circadian rhythms [433]. Lethargy was determined by the relative inactivity index (RII) from day 0 through day 7 post challenge; this period allowed for lethargy calculation throughout the period of active replication in the ferret respiratory tract. RII, sneezing and dyspnea were assessed each day prior to handling and sedation of the animals. Clinical signs assessment was consistent with previously established methods [325, 434].

Ferret sample collection and processing

Prechallenge and on days 1, 3, 5, 7, 10, 14, 21 and 28 post challenge, nasal wash (NW) and blood samples were collected from ferrets for virologic, genetic and antibody analysis. Animals were sedated with KX followed by flushing the nares by instillation of 2 mL nasal wash solution (PBS, 1% BSA, antibiotics), inside a class-II biosafety cabinet, and collected when expelled in a Petri dish. NW was centrifuged (5 minutes x 5000 rpm at 4°C), supernatant was stored at -80°C for virus titration and multiplex assay. One hundred microliters (uL) PBS was added NW pellets followed by 280uL AVL lysis buffer (Qiagen, Germantown, MD, USA). Two to three mL blood was collected from the cranial vena cava in an SST tube for serum separation. Serum was tested for antibodies to influenza virus, cytokines, and chemokines.

On days 1, 3, 5, 7, 10 and 28 post challenge, three ferrets were euthanized for collection of tissues, sera, and cells. These animals were first anesthetized with KX, exsanguinated, and euthanized with intracardiac injection of Euthasol™ (1 mL/kg) prior to collection of tissues, including spleen. Blood was collected in SST tubes (serum) and K2/EDTA (cell purification). Serum was separated from SST tubes by centrifugation for

10 minutes at 1500 x g at room temperature. For purification of peripheral blood mononuclear cells (PBMC), an equal volume of PBS was added to blood in K2/EDTA tubes and overlayed onto Histopaque®-1077 (Sigma, St. Louis, MO, USA). Samples were centrifuged with no brake at 900 x g for 20 minutes at room temperature. Cells were collected from the Histopaque® interface, washed with cell culture media (RPMI-1640, 10% heat-inactivated fetal bovine serum (FBS)) and treated with ammonium chloride to lyse any remaining red blood cells. The final cell pellet was resuspended in 1 mL cell culture medium. Two hundred eighty uL of AVL lysis buffer were added to 200 uL PBMC samples in RPMI-1640, 10% FBS obtained by density gradient centrifugation over ficoll-hypaque. Samples were mixed 3 to 4 times and lysate was frozen at -80°C until RNA extraction. Carrier RNA was added to each sample and RNA was extracted using EZ1 DSP kit on a Qiagen EZ1 Advanced XL extractor according to the manufacturer's instructions (Qiagen, Germantown, MD, USA). RNA was eluted in 120 uL RNase-free water and stored at -80°C until evaluated for gene expression by qRT-PCR. The remaining PBMC sample was cryopreserved in FBS, 10% DMSO and stored in the vapor phase of liquid nitrogen freezer. Splenocytes were isolated from spleens by passing tissue through a 70-micron cell strainer (Millipore-Sigma, Burlington, MA, USA) in DMEM,10% FBS, followed by lysing red blood cells with ammonium chloride. Cells were cryopreserved in FBS, 10% FBS and stored in the vapor phase of liquid nitrogen freezer until used in ELISpot assays.

Tissues and blood were collected from an additional three mock-infected ferrets and included as naïve controls.

Virus kinetics by focus forming assay (FFA)

Nasal wash (NW) samples collected from influenza virus-infected ferrets were tested for virus with a Focus Forming Assay (FFA) as previously described [416]. Briefly, ½-log serially diluted influenza viruses in virus growth medium plus trypsin (DMEM, 0.1% BSA, 1 µg/mL TPCK-treated trypsin (Sigma, St. Louis, MO, USA)) were added to confluent monolayers of MDCK-SIAT1 cells [380] in 96-well flat-bottom tissue culture plates in quadruplicate. Following a two-hour incubation at 37°C, and overlay of 1.2% Avicel RC/CL [384] (Type: RC581 NF; FMC Health and Nutrition, Philadelphia, PA, USA) in 2X MEM containing 1 µg/mL TPCK-treated trypsin, 0.1% BSA, and antibiotics] was added. Plates were incubated overnight at 37°C, 5% CO2, fixed, permeabilized, and stained with a monoclonal antibody pool to influenza A or B nucleoprotein (International Reagent Resource; www.internationalreagentresource.org). Infectious foci (spots) were visualized using TrueBlue substrate (Sera Care, Inc., Milford, MA, USA). The foci were enumerated using a CTL Bio Spot Analyzer with ImmunoCapture 6.4.87 software (Cellular Technology Ltd., Shaker Heights, OH, USA). The FFA titer was determined by multiplying sample dilution which gave between one hundred to three hundred spots by the spot number at that dilution, to obtain the Focus Forming Units per milliliter (FFU/mL). The foci in the cell control were subtracted and the number of foci remaining was multiplied by twenty to give FFU/mL. The limit of detection was $10^{2.3}$ FFU/mL.

Antibody detection by hemagglutination inhibition (HI) assay

Ferret sera were treated with receptor destroying enzyme [RDE] (Denka Co Ltd, Tokyo, Japan) and adsorbed with turkey erythrocytes (TRBC), and tested by HI assay according to established procedures [381]. Briefly, RDE-treated, and adsorbed sera were

2-fold serially diluted, starting at 1:10, in v-bottom 96-well plates followed by the addition of 4 hemagglutination units of influenza virus (CA, KS, BR, or PH). Plates were incubated at room temperature for approximately 15 minutes followed by the addition of 0.5% TRBC and mixed by gentle agitation. The TRBCs were allowed to settle for 30 minutes at room temperature. The HI titers were determined as the reciprocal of the last serum dilution which inhibited the hemagglutination of the TRBCs by the virus.

Neutralizing antibody level detection by focus reduction assay (FRA)

The Focus Reduction Assay (FRA), initially developed by the WHO collaborating Centre in London, United Kingdom, was modified and utilized in this study. MDCK-SIAT1 cells were seeded in 96-well plates in Dulbecco's Modified Eagle Medium (DMEM) containing 5% heat-inactivated FBS and antibiotics. The following day, the confluent cell monolayers were rinsed with 0.01M phosphate-buffered saline pH 7.2 (PBS), (Gibco BRL, ThermoFisher Scientific Inc., Waltham, MA, USA) followed by the addition of two-fold serially diluted RDE-treated ferret sera at 50 µL per well starting with 1:20 dilution in virus growth medium containing 1 µg/mL TPCK-treated trypsin, VGM-T [DMEM, 0.1% fraction-V bovine serum albumin (BSA), antibiotics (penicillin/streptomycin) and 1 µg/mL TPCK-treated trypsin]. Afterwards, 50 µL standardized virus in VGM-T was added to each plate or VGM-T to cell control wells. The virus stocks were standardized by FFA to determine Focus Forming Units per milliliter (FFU/mL). Following a 2-hour incubation period at 37°C, an 100 µL overlay consisting of equal volumes of 1.2% Avicel RC/CL [384] in 2X MEM containing 1 µg/mL TPCK-treated trypsin, 0.1% BSA, and antibiotics was added to each well. Plates were incubated for 18-22 hours at 37°C, 5% CO2. The overlays were removed from each

well and the monolayer was washed once with PBS to remove any residual Avicel. The plates were fixed with ice-cold 4% (w/v) paraformaldehyde in PBS (10% formalin) for 30 minutes at 4oC, followed by a PBS wash and cell permeabilization using 0.5% Triton X-100 in PBS/glycine at room temperature for 20 minutes. Plates were washed three times with PSBT (PBS, 0.1% Tween-20), incubated for 1 hour with a monoclonal antibody pool against influenza A or B nucleoprotein [435] in ELISA buffer (PBS,10% horse serum, 0.1% Tween-80). Following three washes with PBST, the cells were incubated with goat anti-mouse peroxidase-labelled IgG (Sera Care, Inc., Milford, MA, USA) in ELISA buffer for one hour at room temperature. Plates were washed three times with PBST, and infectious foci (spots) were visualized using TrueBlue substrate containing 0.03% H2O2 incubated at room temperature for 10-15 minutes. The reaction was stopped by washing five times with deionized water. Plates were dried and the foci enumerated using a CTL Bio Spot Analyzer with ImmunoCapture 6.4.87 software (Cellular Technology Ltd., Shaker Heights, OH, USA). The FRA titer was reported as the reciprocal of the highest dilution of serum corresponding to 50% foci reduction compared to the virus control (VC) minus the cell control (CC).

Antigen-specific ferret Ig ELISA

Antigen-specific Ig ELISA was performed to assess ferret Ig reactivity against recombinant hemagglutinin (rHA) expressed and purified as previously described [436] and representing the influenza A or influenza B virus strains used for infection. The ELISA was performed using previously described mouse anti-ferret antibodies [253] and similarly to previously described protocols [252]. In brief, Immulon 4HBX plates (Thermo Fisher) were coated overnight at 4°C with 1 μg/mL rHA in PBS (50 uL per

well) in a humidified chamber and the following day plates were blocked with 200 uL per well of ELISA blocking buffer for at least 1 hour at 37°C. Serum samples were 3-fold serially diluted in blocking buffer in duplicate, and plates incubated for 1 hour at 37°C. Plates were washed four times with PBS, 100 uL per well of mouse anti-ferret IgG "IgG" (mAb 11E3), or mouse anti-ferret IgKappa/IgLambda (mAb 8H9 + mAb 4B10, hereafter referred to as "totIg") each diluted to 1 µg/mL in blocking buffer, added, and incubated in a humid chamber for 1 hour at 37°C. Plates were washed five times with PBS before adding 100 uL of HRP-conjugated goat anti-mouse IgG1 (Southern Biotech, Birmingham, AL, USA) diluted 1:4000 in blocking buffer and were then incubated overnight at 4°C. Plates were then washed 5 times PBS before addition of 2,2'-azino-bis(3-ethylbenzothiazoline-6-sulfonic acid (ABTS) substrate (VWR), and incubation at 37°C for 15 minutes. Colorimetric conversion was terminated by addition of 5% SDS (50 uL per well) and absorbance was measured at 414 nm using a BioTek Epoch 2 Microplate Spectrophotometer (Agilent Technologies, Santa Clara, CA, USA). The endpoint absorbance of each sample was determined on a plate-by-plate basis where the absorbances of all the blank wells were averaged and multiplied by three. The GraphPad® Prism 10 "Interpolate a standard curve" function was utilized to generate a standard curve for each individual sample with the absorbances from the serial dilutions followed by plotting the previously calculated endpoint absorbance onto the curve to find the endpoint dilution of each sample. Duplicate ferret samples were run on separate plates in tandem.

ELISpot assay

ELISpot were performed using anti-ferret antibodies as previously described [437]. Briefly, Multi-ScreenHTS HA filter plates (EMD Millipore, Billerica, MA, USA) were coated overnight at 4°C with 25 µg/mL of rHA representing the influenza A ["CA" (H1pdm09) or "KS" (H3N2)] or influenza B ["BR" (B-Victoria lineage) or "PH" (B-Yamagata lineage)] [437] in PBS (50 µL per well). Additional plates were coated with PBS containing 5 µg/mL BSA alone. Plates were washed three times with PBS before blocking with B cell medium, prepared as previously described [437], for at least 1 h at room temperature. Serially diluted ferret PBMC or splenocytes were then incubated in ELISpot plates for 16-18 hours at 37°C, 5% CO2. ELISpot plates were then washed three times with PBS + 0.1% Triton X-100 (Sigma-Aldrich), and after an additional five washes with PBS, mouse anti-ferret IgG (mAb 11E3) and mouse anti-ferret totIg (mAb 8H9 + mAb 4B10) diluted each to 1 µg/mL in blocking buffer (PBS containing 2% BSA [Sigma-Aldrich], 1% bovine gelatin [Sigma-Aldrich], and 0.05% Tween 20 [Thermo Fisher Scientific]) was added and plates incubated for 2 h at 37°C. Plates were then washed three times with PBS + 0.1% Triton X-100 (Sigma-Aldrich), and after an additional five washes with PBS, alkaline phosphatase goat anti-mouse IgG1 (Southern Biotech, Birmingham AL, USA) diluted 1:4000 in blocking buffer was added and plated were incubated for 2 hours at 37°C. Plates were washed five times with PBS and then twice with distilled water (dH2O) before addition of 5-bromo-4-chloro-3-indolyl-phosphate/NBT (BCIP/NBT) one-step solution (Thermo Fisher Scientific) and incubation at 37°C for approximately 15 minutes. Development of the substrate was terminated by decanting solution and gently washing plates with dH2O. Plates were air dried at room

temperature before automated counting using the S6 Ultimate M2 Analyzer and the ImmunoSpot 7.0.28.5 software (Cellular Technology Ltd., Shaker Heights, OH, USA).

Gene expression in ferret cells

Ferret primers generated to pro-inflammatory (*MCP1, IL-1B, IL-6),* Th1 (*CXCL10*), Th2 (*IL-2*), T-regulatory (*TGFB1*), T-effector (*IL-4, IL-12p40, IL-17*), apoptosis (*Granzyme A*), Type-I/II/III interferons (*IFNA, IFNB, IFNG, IFNL3*), interferon responses (*STAT1, STAT2, STAT3, RIG-I, SOCS3, TSLP)* and housekeeping (*GAPDH*) genes were used to measure differences in expression levels in ferret cells. For genes using TaqMan, probes were modified with 6-FAM, fluorescein amidites (FAM) fluorophore on the 5' end and a non-fluorescent Black Hole Quencher®-1 (BHQ-1) on the 3' end. Additionally, a locked nucleic acid at adenine <LNA A> was incorporated in all probes in order to increase template binding strength for real-time PCR [387]. Primers and probes for all ferret genes were generated from published ferret sequences [5, 390, 391, 416]. All primer/probe sets used are shown in Table 2.1.

Quantitative real time PCR (qRT-PCR) was performed using an ABI 7500 Fast Dx Real-Time PCR instrument (Applied Biosystems, Waltham, MA, USA). PCR reactions were performed in a 5 uL RNA reaction volume using SYBR™GreenER™ qPCR SuperMix (Applied Biosystems) or SuperScript™ III Platinum™ One-Step qRT-PCR Kit for TaqMan reactions (InvivoGen, San Diego, CA, USA). An RT reaction for 30 minutes at 50°C, inactivation for 2 minutes at 95°C, followed by 40 amplification cycles at an annealing temperature of 50°C. Reactions were performed on three ferrets for each virus and timepoint and the values were normalized by subtracting the mean value of the cycle threshold (C_T) from that of the C_T for glyceraldehyde-3-phosphate dehydrogenase

(GAPDH) housekeeping gene (ΔC_T). The relative levels of gene expression for infected cells were determined by subtracting the individual ΔC_T values from that of average ΔC_T values of pre-infection cells ($\Delta\Delta C_T$) and expressing the final quantification values ($2^{-\Delta\Delta CT}$) as relative fold changes. Genes upregulated $>10^4$-fold (>10,000) were given a value of 10,000 and genes downregulated $<10^{-4}$-fold (<0.0001) were given a value of 0.0001.

Cytokine/chemokine levels in ferret sera by multiplex assay

Ferret serum samples were stored at -80°C until evaluated. Samples were thawed at room temperature for 30 minutes prior to testing by Luminex ferret multiplex assay. The Luminex Assay kit [Ampersand Biosciences (www.ampersandbio.com) Lake Clear, NY, USA] contained ferret-specific antibodies and proteins in a microsphere-based assay and consisted of antigen-specific antibodies covalently coupled to magnetic Luminex beads and biotinylated detection antibodies in a capture-sandwich format. All incubations were performed at room temperature in 96-well plates. Thirty uL of standard, controls, or serum samples (1:5 dilution) were added followed by ten uL of multiplexed capture-antibody microspheres and ten uL of blocking buffer to each well. The plates were sealed and incubated for 2 hours on a plate shaker. The plates were washed 3 times using the Bio-Plex Pro Wash Station [Bio-Rad (www.bio-rad.com), Hercules, CA, USA] followed by the addition of 40 uL of biotinylated detection antibody and incubated for 1 hour on a plate shaker. After incubation, 20 uL diluted streptavidin-phycoerythrin was added to each well, thoroughly mixed, and incubated for 30 minutes. Following 3 washes, the beads in the plates were resuspended in 100 uL of wash buffer. After shaking on a plate shaker for 5 minutes, the plate was then analyzed on a Luminex 200 Analyzer [Luminex Corporation (www.luminexcorp.com)], Austin, TX, USA]. The cytokine/chemokine

results were determined by extrapolating the analyte concentration from the measured mean fluorescence intensity (MFI) value using the standard curve. Results were generated and extracted using the RBM Plate Reader and Plate Viewer analysis software, respectively. Data were exported with values represented to two significant figures and analyzed in Microsoft Excel and GraphPad Prism 10 (GraphPad Software, La Jolla, CA, USA).

Type-III IFN bioassay

Interferon lambda (IFNL) levels in influenza-infected ferret serum was detected using HEK-λ reporter cells (HEK-Blue^{TM} IFN-λ cells: InvivoGen, San Diego, CA, USA) designed to monitor the activation of the JAK/STAT/ISGF3 pathway induced by type III IFNs. The HEK-λ cells were generated by stable transfection of HEK-293 cells with the human IFNLR and IL-10R receptor genes as well as the human signal transducers and activators of STAT2 and IRF9 resulting in a fully active IFNL signaling pathway. Activation of the pathway was detected since these cells harbored the secreted embryonic alkaline phosphatase (SEAP) under the control of the ISG54 promoter, which is activated by IFNL. Stimulation of the IFNL triggered the JAK/STAT/ISGF3 pathway and induced SEAP production which was measured by a colorimetric assay at 650 nm using Quanti-Blue^{TM} solution according to the manufacturer's instructions (InvivoGen, San Diego, CA, USA).

Twenty uL of sera from uninfected, IAV and IBV infected ferrets were added in triplicate wells of 96-well tissue culture plate. A tissue culture flask containing HEK-λ cell monolayers was gently rinsed once with PBS and cells were dislodged and suspended in HEK medium (DMEM, 10% FBS, antibiotics) to a concentration of $2.8x10^5$

cells/mL. 180 uL of HEK-λ cells were added to each well containing twenty uL of sample and to serially 1/2-log diluted (0.1 – 1000 ng/mL) recombinant ferret IFNL3 (Kingfisher Biotech, St. Paul, MN, USA). The plates were incubated for 20Hr at 37°C, 5%CO_2. After 20Hr, 20 uL of supernatant from the wells were transferred to a new 96-well plate and 180 uL of Quanti-Blue™ substrate was added and incubated for 2Hr at 37°C, 5%CO_2. Absorbance was read at 655nm. A sigmoidal 4-point standard curve from 0.1 to 1000 ng/mL was generated using recombinant ferret IFNL3 protein [Kingfisher Biotech (www.kingfisherbiotech.com), St. Paul, MN, USA) and unknown samples were extrapolated from the standard curve.

Statistical analysis

GraphPad Prism 10 was used for all statistical analyses (GraphPad Software, La Jolla, CA, USA). One-way ANOVA was used to determine differences over time between viruses and significance between groups was determined by 2-way ANOVA analysis. Gene expression analysis was performed from three ferrets per timepoint and outliers were identified by the Grubbs' test (α=0.05) by Extreme Studentized Deviate method for removal of a single outlier if found. Spearman (1-tailed, 95% confidence) correlation method used for comparison of virus replication to gene expression or protein concentration (multiplex or bioassay) as well as antibody levels (HI or FRA) and protein concentration. The Student's t-test (unpaired) was used to assess the statistical differences in the gene expression levels in respect to the uninfected controls and for comparing influenza A to influenza B viruses and antibody secreting cells by ELISpot. A p-value of <0.05 was considered statistically significant: * $p<0.05$, ** $p<0.01$, *** $p<0.001$, **** $p<0.0001$.

RESULTS

IAV virus replication kinetics differ from IBV and cause greater morbidity in ferrets.

Eighteen ferrets were inoculated intranasally with $4x10^5$ FFU of influenza A/H1N1pdm09 (A/California/07/2009, "CA"), A/H3N2 (A/Kansas/14/2017. "KS"), B-Victoria lineage (B/Brisbane/60/2008, "BR"), or B-Yamagata lineage (B/Phuket/3073/2013, "PH") virus. This dose of virus has been optimized and used as the standard dose for generating antiserum to human influenza clinical isolates in ferrets. The animals were monitored for clinical symptoms of influenza virus infection and lethargy for seven days post challenge. This corresponds to typical viral kinetics observed in the upper respiratory tract of ferrets infected with seasonal influenza viruses [438, 439]. Weights and temperatures were taken daily for the ten days following challenge and then weekly through day 28. Three animals were euthanized on days 1, 3, 5, 7, and 10 post challenge for collection of tissues. Throughout the challenge, nasal wash and blood samples were collected for virus titration/molecular analyses and molecular/immunological analyses respectively.

Virus replication kinetics demonstrated peak early replication in the upper respiratory tract (URT) at D1 post challenge in IAV-challenged animals and late replication at D3 in IBV-challenged animals (Figure 4.1). IAV viral replication peaked earlier on D1 post challenge (CA=$10^{5.91}$ FFU/mL, KS=$10^{5.30}$ FFU/mL) whereas IBV virus replication peaked later at D3 post challenge (BR=$10^{5.24}$ FFU/mL, PH=$10^{5.68}$ FFU/mL) in ferret URT. There was a significant difference between IAV and IBV on D1

[CA vs BR ($p<0.0001$) and vs PH ($p=0.007$); KS vs BR ($p=0.002$)]; however, by D3 IBV replication increase to equivalent levels. PH, however, replicated to higher levels than KS on D3 ($p=0.003$). CA replicated significantly higher and earlier than IBV (BR, $p<0.0001$; PH, $p=0.0236$) as well as KS ($p=0.0015$). These replication kinetics confirm greater morbidity of CA in ferrets compared to other viruses tested and complement previous findings of this virus compared to other seasonal influenza viruses [306].

Following challenge with influenza, ferrets exhibited classical clinical signs of infection including elevated temperature, weight loss, lethargy and sneezing as well as virus replication in the URT (Table 4.1). Regardless of the virus used, all animals developed fever at least +2°F over prechallenge temperature by D2 post challenge with average temperature increases being similar between IAVs (+2.5°F) and IBVs (+2.55°F). No significant differences between groups were seen (2-way ANOVA). All animals demonstrated weight loss through D7 post challenge. The maximum weight loss from prechallenge weight occurred on D3 for IBV [BR (-2.7%), PH (-4.9%)] and IAV [KS (-4.3%)]; however, CA peak weight loss occurred later on D6 (-7.6%). Significant weight loss was seen with IAV [CA ($p<0.0001$), KS ($p=0.049$)] compared to IBV (BR) over the first ten days following challenge (2-way ANOVA). Over the same period, PH weight loss was significantly greater than BR as well ($p<0.0001$). Daily temperature changes and weight loss can be found in supplemental Figure 4.S1. For activity following challenge, only IAVs showed marked lethargy compared to IBVs ranging from IAV CA having the highest relative inactivity index (RII=1.37) followed by KS (RII=1.26) then the IBVs showing minimal lethargy BR (RII=1.04) and PH (RII=1.01). Taken together, clinical signs indicate that IAVs cause greater morbidity in ferrets than IBVs.

IAV induces earlier inflammatory and interferon gene expression than IBV in ferret respiratory tract and peripheral blood.

To determine the temporal relationship between innate immune responses and development of antibodies following challenge with influenza in ferrets, we conducted a comparison of host gene expression in NW cells in the URT and PBMC in the peripheral blood using qRT-PCR (Table 4.2). Gene expression at the site of infection in the URT (Table 4.2A) show that of the nine up-regulated genes (gene expression >1 over mock challenged) on D3 post challenge, seven genes (*MCP-1, CXCL10, STAT1, STAT2, STAT3, RIG-I, and SOCS3*) corresponded to either CA or KS infection. There were only two up-regulated genes (*TGFB1* and *TSLP*) following IBV (PH) infection. Of the remaining genes which were down-regulated on D3 (N=11) from prechallenge expression, IBV down-regulated genes to a greater extent for all genes (7 of 11) except for *IL-1B, IL-6, IFNA, IFNL3*. By D5 post challenge four additional genes switched from down-regulated to up-regulated (*IL-2, IL-4, IFNG, IFNL3)* and were all following IAV (CA) challenge, indicating initiation of an adaptive effector T cell and interferon responses by IAV.

Gene expression in the peripheral blood (Table 4.2B) showed few up-regulated genes, compared to the URT, on both D3 and D5 post challenge. On D3 post challenge, five genes were up-regulated (*CXCL10, STAT2, STAT3, RIG-I, and SOCS3*). Three of these genes *(STAT2, STAT3, and RIG-I)* showed greater up-regulation following IAV infection; whereas two genes (*CXCL10 and SOCS3)* were up-regulated to a greater extent following IBV infection. Of the remaining genes which were down-regulated on D3 (N=14), IBV down-regulated genes to a greater extent for all genes (8 of 14) except for *IL-2, TGFB1,*

IL-4, IFNL3, STAT1 and TSLP. By D5 post challenge, four additional genes were upregulated (*MCP-1, TGFB1, IL-4, and IFNL3).* All of these genes were up regulated to the greatest extent by IAV. Of the original five genes which were up-regulated on D3, one gene switched from IBV to IAV (CXCL10) and two genes switched from IAV to IBV (*STAT2,* and *RIG-I*). These gene expression levels indicate that IAV resulted in an earlier innate immune response in both the URT and peripheral blood.

Serum cytokine and chemokine levels are elevated following IAV infection in ferrets.

Serum cytokine and chemokine levels in ferrets following challenge with IAV and IBV were evaluated over a one-month period. Ferret sera were tested using a multiplex assay for ferret analytes (IFNB, IFNG, IP-10, IL-2, MCP-1, MIP-1B, IL-4, IL-17, IL-12p40, IL-12p70, TNFA, IL-6 and IL-8) and by bioassay (IFNL). Significant differences (2-way ANOVA) between IAV (CA and KS) and IBV (BR and PH) were observed for several analytes (Figure 4.2). Type-I (IFNB) and Type-II (IFNG) interferons showed significantly higher levels in ferret sera following challenge with IAV compared to IBV (Figure 4.2A). Type-I IFN levels were significantly higher for KS infected animals than CA ($p=0.0152$), BR, or PH ($p<0.0001$) infected animals. KS infected animals showed significantly higher levels of type-II IFN than CA ($p=0.0401$) as well as BR and PH ($p=0.0405$ and $p=0.0431$ respectively). Type-III IFN (IFNL) was higher in IAV than IBV-infected animals; however, only significant differences were between BR and PH ($p=0.0074$) (Figure 4.2A). Additionally Th1 (IP-10), Th2 (IL-2) and Teff (IL-12p40) cytokines (Figure 4.2B, 4.2C and 4.2D respectively) were also significantly higher following IAV than IBV challenge [IP-10; CA to KS, BR, and PH ($p<0.0001$) and

KS to PH (P=0.004)], [IL-2; CA and KS to BR and PH (p<0.0001)] and [IL-12p40; CA and KS to BR and PH (p<0.0001)]. Pro-inflammatory cytokines and chemokines were also higher in IAV challenged than in IBV challenged animals. Pro-inflammatory response (Figure 4.2E) was significantly higher for: [MCP-1; CA to KS (p=0.0048) and BR and PH (p<0.0001)], [MIP-1B; KS to BR (p=0.0361)], and [TNFA; KS to BR (p=0.0468)]. Cytokine and chemokine levels over entire 28-day for each virus are shown in supplemental figure 4.S2. Data from all analytes tested in sera show that for all groups (Pro-inflammatory, Th1, Th2, Teff, and IFN), IAV challenged resulted in higher levels than IBV challenged animals.

HI and neutralizing antibody responses are delayed and reduced in ferrets challenged with IBV compared to IAV.

Serum antibody responses were compared between IAV and IBV challenged animals for 28-days. The antibody responses detected by HI (Figure 4.3A) showed clear differences between IAV (CA and KS) and IBV (BR and PH). For IAVs, infection with CA resulted in significantly greater antibody response than infection with KS (p=0.0094; 2-way ANOVA); however, for infection with IBVs no significant difference in antibody response was observed. Both IAVs showed significantly higher antibody responses to IBVs (CA vs BR/PH, p<0.0001; KS vs BR, p=0.0074 and KS vs PH, p=0.0005). By HI, sera from IAV surpassed 1:160 threshold by D7 (CA, HI=2560) and D10 (KS, HI=640) post challenge; whereas only one IBV (BR) surpassed the threshold but not until D28 post challenge (HI=201). Neutralizing antibody responses by FRA (Figure 4.3B) mimicked antibody responses seen by HI; however, due to its greater sensitivity at lower antibody concentrations (Figure 4.3C), both IBVs crossed the 1:160 threshold but not

until very late post challenge (BR on D21, FRA=320; PH on D28, FRA=186). Both IAV showed significantly higher neutralization titers compared to IBV for all viruses ($p<0.0001$); however, no statistical differences between IBV (BR and PH) were observed. Results of antibody responses in ferrets show that IAV initiated an earlier and higher functionally neutralizing antibody titer that was sustained over the 28-day period. In contrast, IBV neutralizing antibody titers were delayed and failed to reach comparable titers to IAV by D28. Both HI and neutralizing antibody (FRA) responses in ferrets following IAV or IBV infection are consistent with antibody responses seen with previously tested viruses.

To evaluate the kinetics and magnitude of the ferret Ig response elicited following IAV or IBV infection, sera collected throughout the study were assessed for reactivity against the corresponding rHA protein by ELISA (Figure 4.4). Consistent with a delay in the generation of IgG class-switched antibodies in the primary response, increased rHA-specific antibody titers were not robustly detected until Day 10 for both IAV and IBV. For antigen-specific ELISA to IgG (Figure 4.4A), similar antibody patterns were observed for each individual virus. When comparing IgG responses for IAV and IBV (Figure 4.4C), IBV showed significantly higher levels on D14 ($p=0.034$); however, by D21 antibody IgG titers to IAVs were significantly higher than to IBVs (D21 $p<0.0001$, D28 $p=0.0001$). Interestingly, when performing antigen-specific ELISA for total Ig (IgKappa and IgLambda light chains) “totIg”, individual IBVs showed higher titers than individual IAV over 28-days post challenge (Figure 4.4B). When comparing IAVs to IBVs (Figure 4.4D), significantly higher levels of totIg were observed following IBV

infection starting on D10 through D28 compared to IAV infection (D10/D14 $p<0.0001$; D21 $p=0.0011$; D28 $p=0.0003$).

Delay in serum antibody responses by IBV are not observed by antibody secreting cells.

To determine whether the delay and reduced antibody levels in serum were also observed in antibody secreting B cells, we performed ELISpot assays to detect ferret IgG or total Ig "totIg" (IgKappa and IgLambda light chains) [252] antibody secreting cells (ASC) in ferret splenocytes or PBMC on D5 and D7 post IAV and IBV challenge (Figure 4.5). In ferret splenocytes (Figure 4.5A and 5.5B) significant increases on D7 in ASC secreting IgG and totIg in IBVs (BR and PH) and IAV (KS) were detected [(IgG: BR to KS, $p=0.0038$; PH to KS, $p=0.047$); (totIg: BR to KS, $p=0.008$; PH to KS, $p=0.044$)]; however no significant increases of IBVs to IAV (CA) were detected. When comparing differences in both IAV to IBV, no significant differences were detected. Similar responses were observed in ASC from PBMC (Figure 4.5C and 5.5D) comparing IBV (PH) to IAV (KS). Even though some differences in ASC were observed with individual viruses, overall differences between IAV and IBV were absent. This is in contrast to significant differences seen between serum antibody responses by HI and FRA where IAV virus antibody responses appeared earlier and more robust than IBV following challenge. While IAV elicits potently neutralizing antibody specificities, IBV may elicit strong rHA-specific response without potent HI or FRA activity. This may be due to differences in epitope bias.

Correlations between viral loads, gene expression, antibody responses and protein levels in ferret samples.

We compared virus levels in the URT (D1, D3, and D5 post challenge) to gene expression in both cells in the NW of the URT and PBMC in the peripheral blood (Table 4.3) to determine whether there was a correlation of viral titers to innate gene expression in IAVs and IBVs. In the URT (Table 4.3A) we saw a direct correlation between type-I IFN (*IFNA, IFNB*) and gene expression and IAV viral titers; however, there was an inverse correlation with IBV. Similar correlations were also seen with Teff gene (*IL-17*) and viral titers. For Th1 (*CXCL10*) we saw the reverse; a direct correlation for IBVs and an inverse correlation for IAVs. Generally, we saw greater direct correlations between viral titers and IFN and pro-inflammatory genes with IAV (KS) than other viruses. Interestingly a direct correlation between both *IFNL* and *TSLP* gene expression and viral titers was observed for both IAV (KS) and IBV (PH) indicating that IFNL and TSLP gene expression may be linked. However, only inverse correlations for inflammatory gene (*MCP-1)* and interferon response gene (*STAT2)* showed any significance in IBV (PH). For correlations between viral titers in the URT and gene expression in PBMC (Table 4.3B), a direct correlation was achieved for type-I/II IFN (*IFNA, IFNB, IFNG)* genes in all IAVs and IBVs (*IFNA*), three of four viruses (*IFNB* – CA, KS, and BR; *IFNG* – CA, KS, and PH). A direct correlation of pro-inflammatory gene (*IL-1B*) to virus titer was also seen in all IAVs and IBVs. An inverse correlation was achieved for IFN-response genes (*STAT2* and *RIG-I*) and all IAVs and IBVs indicating that direct effects on IFN expression may result in lower virus titers. Even though only a few comparisons show significant correlations, due to a limited number of observations (D1, D3, D5), overall comparisons of URT virus titers and gene expression in NW cells and PBMC

show a trend that IAVs impact more genes with a direct correlation to pro-inflammatory and IFN responses than IBVs.

Since additional timepoints were tested (prechallenge and days 1, 3, 5, 7, 10, 14, 21 and 28 post challenge), a clearer correlation can be seen when comparing antibody levels (HI and FRA) to analyte levels in ferret sera following IAV and IBV challenge (Table 4.4). Direct correlations of serum HI (Table 4.4A) and neutralizing FRA (Table 4.4B) antibody seen for all IAVs and IBVs to Th2 (IL-2) and Teff (IL12-p40) analytes. These analytes indicate that strong adaptive (Th2 and Teff) responses are associated with increased antibody responses. Interestingly, an inverse correlation between the pro-inflammatory response (MCP-1 chemokine) was observed for all IAVs and IBVs indicating that a strong pro-inflammatory response may dampen the antibody response. Some differences in correlation are seen comparing HI and FRA to analyte levels. For instance, IFNB shows a direct correlation to HI antibody response to all IAVs and IBVs (Table 4.4A); however, by FRA, only IAV (KS) and IBV (PH) show a direct correlation (Table 4.4B). Also, Teff (IL-4) shows an inverse correlation to all IAVs and IBVs by FRA (Table 4B); however, only show an inverse correlation to 3 of 4 viruses by HI (Table 4.4A). correlations to IFNs are also seen depending on whether HI or FRA is used for the comparisons. For example, type-III IFN (IFNL) levels show direct correlation to IAV and inverse correlation to IBV using HI (Table 4.4A) ; however, by using FRA, this is not a clear distinction (Table 4.4B). Since analytes are secreted with different kinetics over the entire 28 days (Supplemental Figure 4.S2), a clearer distinction could be obtained if the window of comparisons were narrowed. Overall differences in analytes

expression as well as gene expression show differences in immune responses to IAVs and IBVs.

DISCUSSION

Influenza A and B viruses continue to circulate and present a major public health concern. Prevention from serious complications relies on a robust adaptive immune response. The ferret remains the primary animal model for influenza research due to its natural susceptibility to human influenza viruses, clinical signs following infection and ability to generate immune responses similar to those in humans. When using antisera generated in ferrets following challenge with influenza viruses, we noted that while IAVs generated robust antibody responses fourteen days post challenge, IBV challenge resulted in delayed and significantly lower antibody responses (HI titers <1:160) over the same period in almost 90% of the viruses tested. This study was designed to determine whether innate immune markers and soluble cytokines/chemokines in serum following challenge could shed light on why IBVs do not elicit an antibody response as quickly and robustly as IAVs in ferrets.

Four representative viruses were used in this study, two IAVs and two IBVs to determine innate and adaptive differences following challenge in ferrets. Initial differences in clinical signs as well as virus kinetics following IAV or IBV are apparent. Clinically, IAVs cause greater lethargy (average RII=1.31) compared to IBV (average RII=1.03), greater maximum weight loss (IAV ~6% and IBV ~4%), and more sneezing (IAV ~52%; IBV ~33%) during viremia. In addition to greater morbidity, IAVs virus replication peaked early (D1 post challenge) compared to IBV (D3 post challenge) in

ferrets. Just these observations could indicate that IAVs initiate an earlier innate immune response than IBVs which could lead to an earlier and more robust adaptive immune response. It has been shown for COVID-19 vaccination that a strong innate immune response results in an early, robust antibody response [440].

We have previously shown in ferret primary respiratory tract cells that pro-inflammatory genes and IFNs are delayed and downregulated by IBVs compared to IAVs [416]. Th1 (*CXCL10*), Th2 (*IL-2*), and Teff (*IL-4*) were also significantly up-regulated by IAV. Similar responses were seen in the URT and PBMC from IAV and IBV infected ferrets in this study. IAV (CA), in particular showed early (D3) up-regulation of Th1 (*CXCL10*), and late (D5) up-regulation of Th2 (*IL-2*) and Teff (*IL-4*) in the URT indicating a switch to a strong adaptive immune response. For IFN response in the URT, only Type-II (*IFNG*) and Type-III (*IFNL3*) IFNs were up-regulated from prechallenge levels following IAV (CA) challenge. In PBMC by D5 post challenge only Teff (*IL-4*) and Type-III IFN *(IFNL3*) were up-regulated by IAV (KS). However, early D3 up-regulation Th1 (*CXCL10*) was highest for IBV (PH) which switched to late D5 highest up-regulation for IAV (KS). Interestingly IFN response (*SOCS3*) gene, which is responsible for downregulating the IFN response was highest for IBV (BR) both early and late post challenge. This may support that IBV have greater IFN-antagonism properties than IAV. Unfortunately, due to the limited number of samples tested (3 animals per timepoint) significant differences for gene expression for all genes was not possible. Additional studies with greater samples collected and tested at each timepoint may aid in increasing the significance as was seen in our study using ferret respiratory epithelial cells. However, it is important to note that the responses seen in this study show

similar trends as observations from respiratory epithelial cells infected with IAV and IBV.

Striking differences in antibody responses to IAVs and IBVs were observed that indicate differences in the initial innate immune response may be playing an essential role in triggering a strong adaptive immune response. In both HI and neutralizing antibody tests, IAV infections generated an early, strong antibody response between day 7 to 10 post challenge, whereas IBV infections did not reach equivalent HI titers and required at least 21 to 28 days to reach titers of at least 1:160 by FRA. These experiments terminated at 28 days post challenge; it would be interesting to see if IBV antibody responses eventually reach equivalent levels to IAVs after 1 month or if peak antibody levels are reached by 28 days post challenge. Additionally, it would be important to determine how long IAV antibody titers remain elevated above 1:160 threshold. Antibodies to influenza A may persist for up 18 months or longer in humans [441-443], however, the longevity of influenza B directed antibodies has not been tested.

Even though significant suppression and delay in serum HI and neutralizing antibodies was observed, antibody responses to recombinant antigens by ELISA showed significantly higher total Ig antibodies and earlier IgG antibodies to IBV compared to IAV. Similar differences in IgG responses by ELISA compared to HI and neutralizing titers was seen by Huang *et al.* [444]. As observed in this study, a comparison of thirteen IAV/IBV strains in ferrets showed that IBV induced the weakest antibody response. Thus, a direct determination of Ig antibody levels by ELISA may not be sufficient in the development of a strong antibody response. Additionally, the four canonical antigenic sites may be detected differently by HI/FRA and ELISA. It has been demonstrated in a

study using IBV (B/Yamagata/16/1988) that the HA 120 loop appears to be the least dominant to elicit HI antibodies in mice and ferrets but contributed significantly to the total IgG responses by ELISA; conversely, the 190 helix induced substantial HI antibodies but the least dominant to elicit total IgG responses in the ferret [445].

Comparisons of ASCs in ferret splenocytes and PBMC following IAV and IBV infection revealed that although there were significant differences between antibody responses in the serum, these differences were not seen at the B-cell level. We observed the highest number of IgG and total Ig ASCs following IBV (PH) challenge and the least number of ASC following IAV (KS) challenge on day 7. IAV (CA) however, showed equivalent levels of IgG and total Ig ASC in PBMC. When comparing all IAVs (CA and KS) to all IBVs (BR and PH) there were no statistical differences in either splenocytes or PBMC. Greater differences between IAV and IBV may be seen in ASC in the mediastinal lymph nodes [214].

To determine whether there were differences in cytokine and chemokines levels in ferrets following IAV and IBV infection over 28 days, we tested sera by multi-plex or bioassay (IFNL). IAV infection resulted in significantly higher levels of Type-I/II IFNs, Th1 (IP-10), Th2 (IL-2), Teff (IL-12p40) and pro-inflammatory cytokines/chemokines (MCP-1, MIP-1B, and TNFA). These responses showed correlations to increases in antibody responses by HI and FRA. These responses indicate that strong adaptive responses are associated with robust antibody responses. This further supports our assumption that a strong innate immune response will lead to a robust antibody response.

In conclusion, the data suggest that IBVs have a greater suppression of the innate immune response than IAV and this would lead to a reduced antibody response. In this report, inflammatory and IFN gene expression is higher following IAV than IBV infection in the URT and PBMC of ferrets. Additionally, serum levels of pro-inflammatory cytokines and type I/II IFNs are significantly higher following IAV infection than IBV infection. Suppression of the IFN response is a hallmark of immune evasion by influenza [446]. Further studies adding immunoadjuvants, such as type-I or type-III IFNs to vaccines or following infection may aid in overcoming innate immunosuppression by IBVs resulting in generation of robust antibody titers leading to better protection. This may be important and beneficial in developing improved vaccines for influenza and other viruses of public health importance.

Table 4.1: Ferret clinical signs following infection with influenza A and B viruses.

Virus	**Inactivity**[a]	**Days Sneezing**	**% Weight loss**[b]	**Elevated temperature**[c]	**NW viral load**[d] **(Avg±SD Log$_{10}$ FFU/mL)**	
(Type)	(D1-7pInf)	(%)	(Day)	(Days)	D1	D3
CA	1.37	D4-D5	7.6%	+2.3°F	**6.14±0.68**	5.36±0.56
(A/H1N1pdm09)		(25%)	(D6)	(D2)		
KS	1.26	D2	4.3%	+2.7°F	**5.41±0.55**	4.10±0.92
(A/H3N2)		(80%)	(D3)	(D2,D4)		
BR	1.04	D3	2.7%	+2.7°F	4.33±0.69	**5.19±0.34**
(B-Victoria)		(27%)	(D3)	(D2)		
PH	1.01	D2	4.9%	+2.4°F	4.69±0.59	**5.70±0.27**
(B-Yamagata)		(40%)	(D3)	(D2)		

[a]Relative inactivity index "RII" (D1 – D7) post challenge. RII=$\sum_{(D1-7)}[score+1]n/\sum_{(D1-7)}n$

[b]Day post challenge of peak weight loss percentage (day) from prechallenge weight from D1 – D7 post challenge.

[c]Average elevated temperature of at least +2°F (Fever) above baseline (days post challenge elevated). Fever indicated by any temperature greater than the average baseline (D-2 to D0 prechallenge) +2°F

[d]Average viral load in ferret URT on D1 and D3 post challenge. Peak viral load in bold. Baseline = 2.3 Log$_{10}$ FFU/mL.

Figure 4.1: Viral kinetics of influenza in ferret upper respiratory tract.

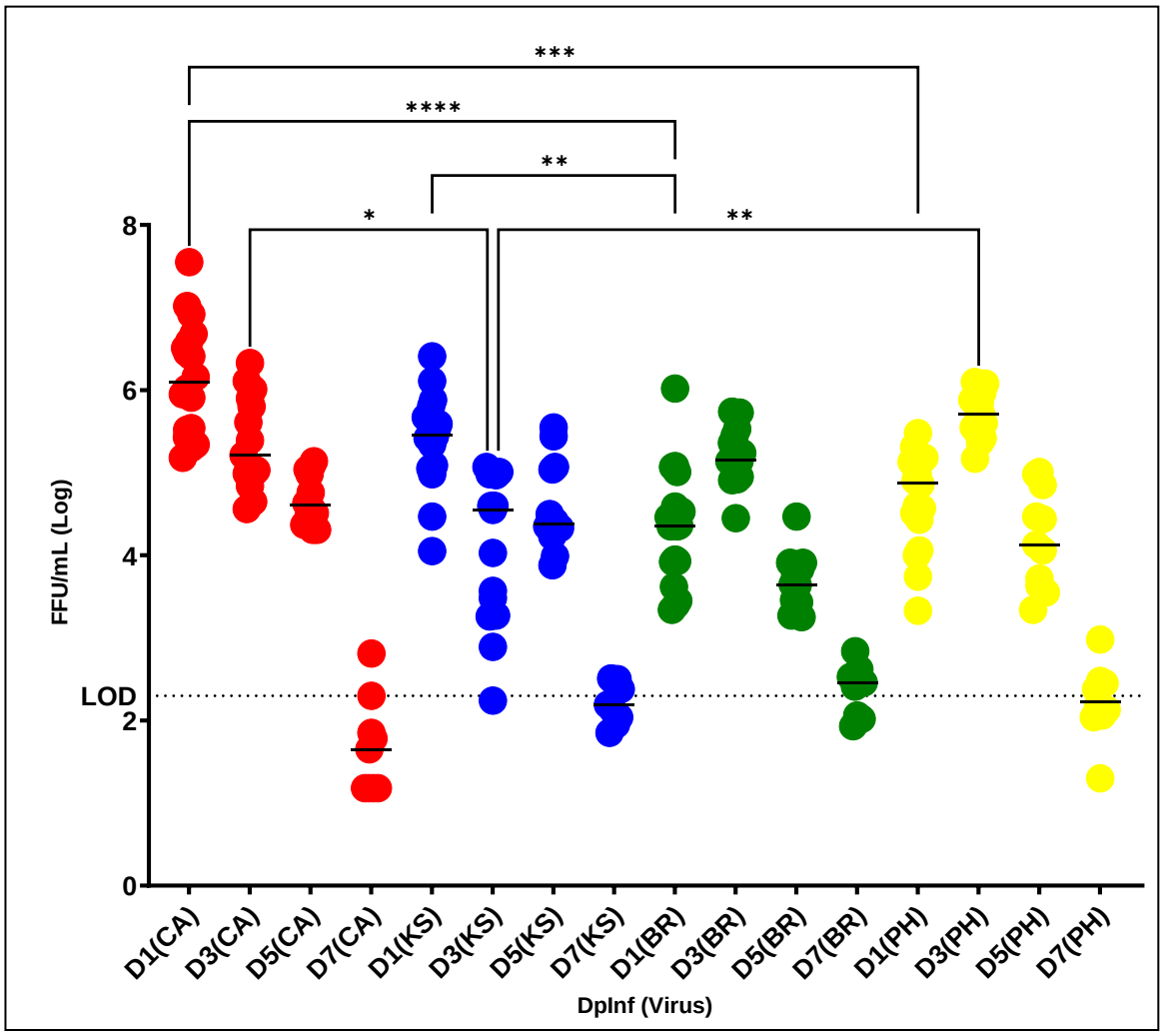

Replication kinetics of IAV [H1N1pdm09 "CA" (A/California/07/2009), H3N2 "KS" (A/Kansas/14/2017)] and IBV [B-Victoria lineage "BR" (B/Brisbane/60/2008), B-Yamagata lineage "PH" (B/Phuket/3073/2013)] in ferret upper respiratory tract. r 72Hr. A) H1N1pdm09 = red, H3N2= orange, B-Victoria = green, B-Yamagata= yellow. B) Comparison of IAV (CA/KS) and IBV (BR/PH) in black and white circles, respectively. All points are from four independent assays in FNEC conducted in triplicate. Limit of detection, indicated by a dotted line, was $10^{3.3}$ FFU/mL. Significance between groups was determined using 1-way ANOVA (Sidak's multiple comparison test).

Table 4.2: Comparison of ferret gene expression following IAV and IBV challenge in the URT and peripheral blood by qRT-PCR. A) URT (NW)

GENE	DpInf	A/H1p CA	A/H3 KS	>	p	A/H1p CA	B/Vic BR	>	p	A/H1p CA	B/Yam PH	>	p	A/H3 KS	B/Vic BR	>	p	A/H3 KS	B/Yam PH	>	p	B/Vic BR	B/Yam PH	>	p	DpInf	Highest Expression	Highest Expression
MCP1	D3	14.42	10	CA>KS		14.42	12.03	CA>BR		14.42	3.805	CA>PH		10	12.03	BR>KS		10	3.805	KS>PH		12.03	3.805	BR>PH		D3	CA	14.42
	D5	227.3	2.508	CA>KS		227.3	4.906	CA>BR		227.3	10.71	CA>PH		2.508	4.906	BR>KS		2.508	10.71	PH>KS		4.906	10.71	PH>BR		D5	CA	227.3
CXCL10	D3	28.07	25.63	CA>KS		28.07	24.3	CA>BR		28.07	21.68	CA>PH		25.63	24.3	KS>BR		**25.63**	**21.68**	**KS>PH**	**0.022598**	24.3	21.68	BR>PH		D3	CA	28.07
	D5	10.4	24.58	KS>CA		10.4	25.06	BR>CA		10.4	21.87	PH>CA		24.58	25.06	BR>KS		24.58	21.87	KS>PH		25.06	21.87	BR>PH		D5	BR	25.06
IL-2	D3	0.05262	0.02764	CA>KS		0.05262	0.01306	CA>BR		0.05262	0.006186	CA>PH		0.02764	0.01306	KS>BR		0.02764	0.006186	KS>PH		0.01306	0.006186	BR>PH		D3	CA	0.05262
	D5	19.72	0.02713	CA>KS		19.72	0.02534	CA>BR		19.72	0.104	CA>PH		0.02713	0.02534	KS>BR		0.02713	0.104	PH>KS		0.02534	0.104	PH>BR		D5	CA	19.72
TGFB1	D3	4.917	8.194	KS>CA		4.917	3.252	CA>BR		4.917	9.479	PH>CA		8.194	3.252	KS>BR		8.194	9.479	PH>KS		3.252	9.479	PH>BR		D3	PH	9.479
	D5	330.3	2.874	CA>KS		330.3	2.991	CA>BR		330.3	2.958	CA>PH		2.874	2.991	BR>KS		2.874	2.958	PH>KS		2.991	2.958	BR>PH		D5	CA	330.3
IL-4	D3	0.2227	0.01152	CA>KS		0.2227	0.01513	CA>BR		0.2227	0.01513	CA>PH		0.01152	0.01513	BR>KS		0.01152	0.01749	PH>KS		0.01513	0.01749	PH>BR		D3	CA	0.2227
	D5	86.86	0.01178	CA>KS		86.86	0.01655	CA>BR		86.86	0.01655	CA>PH		0.01178	0.01655	BR>KS		**0.01178**	**0.1082**	**PH>KS**	**0.011514**	0.01655	0.1082	PH>BR		D5	CA	86.86
IL-12p40	D3	0.007685	0.007397	CA>KS		0.005562	0.007685	BR>CA		0.005562	0.007397	PH>CA		0.008094	0.007685	KS>BR		0.008094	0.007397	KS>PH		0.007685	0.007397	BR>PH		D3	KS	0.008094
	D5	0.002085	0.00472	KS>CA		0.1048	0.002085	CA>BR		0.1048	0.00472	CA>PH		0.00362	0.002085	KS>BR		0.00362	0.00472	PH>KS		0.002085	0.00472	PH>BR		D5	CA	0.1048
IL-17	D3	0.006049	0.009264	KS>CA		0.006049	0.008696	BR>CA		0.006049	0.007609	PH>CA		0.009264	0.008696	KS>BR		0.009264	0.007609	KS>PH		0.008696	0.007609	BR>PH		D3	KS	0.009264
	D5	0.188	0.006763	CA>KS		0.188	0.00512	CA>BR		0.188	0.007672	CA>PH		0.006763	0.00512	KS>BR		0.006763	0.007672	PH>KS		0.00512	0.007672	PH>BR		D5	CA	0.188
IL-1B	D3	0.0113	0.01404	KS>CA		0.0113	0.01417	BR>CA		0.0113	0.01031	CA>PH		0.01404	0.01417	BR>KS		0.01404	0.01031	KS>PH		0.01417	0.01031	BR>PH		D3	BR	0.01417
	D5	0.8363	0.009789	CA>KS		0.8363	0.002183	CA>BR		0.8363	0.009211	CA>PH		0.009789	0.002183	KS>BR		0.009789	0.009211	KS>PH		0.002183	0.009211	PH>BR		D5	CA	0.8363
IL-6	D3	0.0149	0.02718	KS>CA		0.0149	0.027	BR>CA		0.0149	0.01235	CA>PH		0.02718	0.027	KS>BR		0.02718	0.01235	KS>PH		**0.027**	**0.01235**	**BR>PH**	**0.015947**	D3	BR	0.02718
	D5	0.4311	0.008049	CA>KS		0.4311	0.005556	CA>BR		0.4311	0.008318	CA>PH		0.008049	0.005556	KS>BR		0.008049	0.008318	PH>KS		0.005556	0.008318	PH>BR		D5	CA	0.4311
Granzyme A	D3	0.008142	0.009978	KS>CA		0.008142	0.007138	CA>BR		0.008142	0.004567	CA>PH		0.009978	0.007138	KS>BR		0.009978	0.004567	KS>PH		0.007138	0.004567	BR>PH		D3	KS	0.009978
	D5	0.4046	0.006679	CA>KS		0.4046	0.01033	CA>BR		0.4046	0.02839	CA>PH		0.006679	0.01033	BR>KS		0.006679	0.02839	PH>KS		0.01033	0.02839	PH>BR		D5	CA	0.4046
IFNA	D3	0.004703	0.006081	KS>CA		**0.004703**	**0.007637**	**BR>CA**	**0.002453**	0.004703	0.004873	PH>CA		0.006081	0.007637	BR>KS		0.006081	0.004873	KS>PH		0.007637	0.004873	BR>PH		D3	BR	0.007637
	D5	0.2634	0.003368	CA>KS		0.2634	0.002735	CA>BR		0.2634	0.003783	CA>PH		0.003368	0.002735	KS>BR		0.003368	0.003783	PH>KS		0.002735	0.003783	PH>BR		D5	CA	0.2634
IFNB	D3	0.000109	0.000147	KS>CA		0.000109	0.00011	PH>CA		0.000109	0.00011	PH>CA		0.000147	0.000135	KS>BR		0.000147	0.00011	KS>PH		0.000135	0.00011	BR>PH		D3	KS	0.000147
	D5	0.007491	0.000107	CA>KS		0.007491	0.0001	CA>BR		0.007491	0.000138	CA>PH		0.000107	0.0001	KS>BR		0.000107	0.000138	PH>KS		0.0001	0.000138	PH>BR		D5	CA	0.007491
IFNG	D3	0.01864	0.03413	KS>CA		0.01864	0.03148	BR>CA		0.01864	0.01964	PH>CA		0.03413	0.03148	KS>BR		0.03413	0.01964	KS>PH		0.03148	0.01964	BR>PH		D3	KS	0.03413
	D5	1.602	0.0108	CA>KS		1.602	0.01955	CA>BR		1.602	0.03304	CA>PH		0.0108	0.01955	BR>KS		0.0108	0.03304	PH>KS		0.01955	0.03304	PH>BR		D5	CA	1.602
IFNL3	D3	**0.09687**	**0.01167**	**CA>KS**	**0.002717**	**0.09687**	**0.0001**	**CA>BR**	**0.000093**	0.09687	0.5484	PH>CA		0.01167	0.0001	KS>BR		0.01167	0.5484	PH>KS		0.0001	0.5484	PH>BR		D3	PH	0.5484
	D5	62.48	0.001479	CA>KS		62.48	0.008139	CA>BR		62.48	0.06212	CA>PH		0.001479	0.008139	BR>KS		0.001479	0.06212	PH>KS		0.008139	0.06212	PH>BR		D5	CA	62.48
STAT1	D3	109.5	101.9	CA>KS		109.5	99.42	CA>BR		109.5	76.6	CA>PH		101.9	99.42	KS>BR		101.9	76.6	KS>PH		99.42	76.6	BR>PH		D3	CA	109.5
	D5	142.7	92.64	CA>KS		142.7	98.93	CA>BR		142.7	94.66	CA>PH		92.64	98.93	BR>KS		92.64	94.66	PH>KS		98.93	94.66	BR>PH		D5	CA	142.7
STAT2	D3	515.5	477.4	CA>KS		515.5	436.5	CA>BR		515.5	302.2	CA>PH		477.4	436.5	KS>BR		477.4	302.2	KS>PH		436.5	302.2	BR>PH		D3	CA	515.5
	D5	176.4	358.5	KS>CA		176.4	481	BR>CA		176.4	365.8	PH>CA		358.5	481	BR>KS		358.5	365.8	PH>KS		481	365.8	BR>PH		D5	BR	481
STAT3	D3	199.8	179.8	CA>KS		199.8	198.1	CA>BR		199.8	118.7	CA>PH		179.8	198.1	BR>KS		179.8	118.7	KS>PH		198.1	118.7	BR>PH		D3	CA	199.8
	D5	75.87	154.9	KS>CA		75.87	178	BR>CA		75.87	182	PH>CA		154.9	178	BR>KS		154.9	182	PH>KS		178	182	PH>BR		D5	PH	182
RIG-I	D3	3144	2450	CA>KS		3144	2235	CA>BR		3144	1567	CA>PH		2450	2235	KS>BR		2450	1567	KS>PH		2235	1567	BR>PH		D3	CA	3144
	D5	624.5	2167	KS>CA		624.5	2333	BR>CA		624.5	1684	PH>CA		2167	2333	BR>KS		2167	1684	PH>KS		**2333**	**1684**	**BR>PH**	**0.02329**	D5	BR	2333
SOCS3	D3	88.35	82.2	CA>KS		88.35	80.74	CA>BR		88.35	57.16	CA>PH		82.2	80.74	KS>BR		82.2	57.16	KS>PH		80.74	57.16	BR>PH		D3	CA	88.35
	D5	26.4	78.65	KS>CA		26.4	81.32	BR>CA		26.4	73.76	PH>CA		78.65	81.32	BR>KS		78.65	73.76	PH>KS		81.32	73.76	BR>PH		D5	BR	81.32
TSLP	D3	0.102	0.7906	KS>CA		**0.102**	**0.01724**	**CA>BR**	**0.009674**	0.102	1.37	PH>CA		0.7906	0.01724	KS>BR		0.7906	1.37	PH>KS		0.01724	1.37	PH>BR		D3	PH	1.37
	D5	2019	0.3535	CA>KS		2019	0.1043	CA>BR		2019	0.3581	CA>PH		0.3535	0.1043	KS>BR		0.3535	0.3581	KS>PH		0.1043	0.3581	PH>BR		D5	CA	2019

B) Peripheral blood (PBMC)

GENE	DpInf	A/H1p CA	A/H3 KS	>	p	A/H1p CA	B/Vic BR	>	p	A/H1p CA	B/Yam PH	>	p	A/H3 KS	B/Vic BR	>	p	A/H3 KS	B/Yam PH	>	p	B/Vic BR	B/Yam PH	>	p	DpInf	Highest Expression	Highest Expression
MCP1	D3	0.003462	0.03872	KS>CA		0.003462	0.004744	BR>CA		0.003462	0.1708	PH>CA		0.03872	0.004744	KS>BR		0.03872	0.1708	PH>KS		0.004744	0.1708	PH>BR		D3	PH	0.1708
	D5	0.009197	3.552	KS>CA		0.009197	0.01285	BR>CA		0.009197	0.003527	CA>PH		3.552	0.01285	KS>BR		3.552	0.003527	KS>PH		0.01285	0.003527	BR>PH		D5	KS	3.552
CXCL10	D3	1.392	1.2	CA>KS		1.392	1.682	BR>CA		1.392	2.066	PH>CA		1.2	1.682	BR>KS		1.2	2.066	PH>KS		1.682	2.066	PH>BR		D3	PH	2.066
	D5	1.333	1.868	KS>CA		1.333	1.699	BR>CA		1.333	1.457	PH>CA		1.868	1.699	KS>BR		1.868	1.457	KS>PH		1.699	1.457	BR>PH		D5	KS	1.868
IL-2	D3	0.1427	0.2196	KS>CA		0.1427	0.2398	BR>CA	0.038257	0.1427	0.2667	PH>CA		0.2196	0.2398	BR>KS		0.2196	0.2667	PH>KS		0.2398	0.2667	PH>BR		D3	PH	0.2667
	D5	0.06187	0.1176	KS>CA		**0.06187**	**0.1517**	**BR>CA**		0.06187	0.07544	PH>CA		0.1176	0.1517	BR>KS		0.1176	0.07544	KS>PH		**0.1517**	**0.07544**	**BR>PH**	**0.045083**	D5	BR	0.1517
TGFB1	D3	0.0389	0.2504	KS>CA		0.0389	0.1066	BR>CA		0.0389	0.3234	PH>CA		0.2504	0.1066	KS>BR		0.2504	0.3234	PH>KS		0.1066	0.3234	PH>BR		D3	PH	0.3234
	D5	0.02092	1.161	KS>CA		0.02092	0.05467	BR>CA		**0.02092**	**0.001387**	**CA>PH**	**0.027336**	1.161	0.05467	KS>BR		1.161	0.001387	KS>PH		0.05467	0.001387	BR>PH		D5	KS	1.161
IL-4	D3	0.04393	0.1008	KS>CA		0.04393	0.02243	CA>BR		0.04393	0.1548	PH>CA		0.1008	0.02243	KS>BR		0.1008	0.1548	PH>KS		0.02243	0.1548	PH>BR		D3	PH	0.1548
	D5	0.1271	2.375	KS>CA		**0.1271**	**0.01211**	**CA>BR**	**0.016924**	**0.1271**	**0.03001**	**CA>PH**	**0.006184**	2.375	0.01211	KS>BR		2.375	0.03001	KS>PH		0.01211	0.03001	PH>BR		D5	KS	2.375
IL-12p40	D3	0.05721	0.1053	KS>CA		0.05721	0.05419	CA>BR		0.05721	0.08563	PH>CA		0.1053	0.05419	KS>BR		0.1053	0.08563	KS>PH		0.05419	0.08563	PH>BR		D3	KS	0.1053
	D5	0.02812	0.3133	KS>CA		0.02812	0.02935	BR>CA		0.02812	0.04166	PH>CA		0.3133	0.02935	KS>BR		0.3133	0.04166	KS>PH		**0.02935**	**0.04166**	**PH>BR**	**0.039017**	D5	KS	0.3133
IL-17	D3	0.1321	0.289	KS>CA		0.1321	0.122	CA>BR		0.1321	0.07949	CA>PH		0.289	0.122	KS>BR		0.289	0.07949	KS>PH		0.122	0.07949	BR>PH		D3	KS	0.289
	D5	0.06729	0.2883	KS>CA		0.06729	0.09985	BR>CA		0.06729	0.1307	PH>CA		0.2883	0.09985	KS>BR		0.2883	0.1307	KS>PH		0.09985	0.1307	PH>BR		D5	KS	0.2883
IL-1B	D3	**0.1299**	**0.4085**	**KS>CA**	**0.026373**	0.1299	0.203	BR>CA		0.1299	0.1746	PH>CA		0.4085	0.203	KS>BR		0.4085	0.1746	KS>PH		0.203	0.1746	BR>PH		D3	KS	0.4085
	D5	0.1401	0.4969	KS>CA		0.1401	0.1367	CA>BR		0.1401	0.1273	CA>PH		0.4969	0.1367	KS>BR		0.4969	0.1273	KS>PH		0.1367	0.1273	BR>PH		D5	KS	0.4969
IL-6	D3	**0.06016**	**0.1755**	**KS>CA**	**0.020214**	0.06016	0.09414	BR>CA		0.06016	0.105	PH>CA		0.1755	0.09414	KS>BR		0.1755	0.105	KS>PH		0.09414	0.105	PH>BR		D3	KS	0.1755
	D5	0.04668	0.2707	KS>CA		**0.04668**	**0.07398**	**BR>CA**	**0.049178**	**0.04668**	**0.08357**	**PH>CA**	**0.018119**	0.2707	0.07398	KS>BR		0.2707	0.08357	KS>PH		0.07398	0.08357	PH>BR		D5	KS	0.2707
Granzyme A	D3	**0.05415**	**0.2944**	**KS>CA**	**0.00079**	0.05415	0.09742	BR>CA		0.05415	0.07536	PH>CA		**0.2944**	**0.09742**	**KS>BR**	**0.002837**	**0.2944**	**0.07536**	**KS>PH**	**0.008508**	0.09742	0.07536	BR>PH		D3	KS	0.2944
	D5	0.04708	0.1432	KS>CA		**0.04708**	**0.09879**	**BR>CA**	**0.022823**	0.04708	0.09694	PH>CA		0.1432	0.09879	KS>BR		0.1432	0.09694	KS>PH		0.09879	0.09694	BR>PH		D5	KS	0.1432
IFNA	D3	0.2028	0.7137	KS>CA		0.2028	0.2547	BR>CA		0.2028	0.2213	PH>CA		0.7137	0.2547	KS>BR		0.7137	0.2213	KS>PH		0.2547	0.2213	BR>PH		D3	KS	0.7137
	D5	0.1292	0.4936	KS>CA		0.1292	0.1515	BR>CA		**0.1292**	**0.223**	**PH>CA**	**0.01907**	0.4936	0.1515	KS>BR		0.4936	0.223	KS>PH		**0.1515**	**0.223**	**PH>BR**	**0.028795**	D5	KS	0.4936
IFNB	D3	0.05646	0.1551	KS>CA		0.05646	0.1251	BR>CA		0.05646	0.1382	PH>CA		0.1551	0.1251	KS>BR		0.1551	0.1382	KS>PH		0.1251	0.1382	PH>BR		D3	KS	0.1551
	D5	0.04945	0.7872	KS>CA		0.04945	0.05368	BR>CA		0.04945	0.2094	PH>CA		0.7872	0.05368	KS>BR		0.7872	0.2094	KS>PH		0.05368	0.2094	PH>BR		D5	KS	0.7872
IFNG	D3	0.07692	0.06884	CA>KS		0.07692	0.04831	CA>BR		0.07692	0.1383	PH>CA		0.06884	0.04831	KS>BR		0.06884	0.1383	PH>KS		0.04831	0.1383	PH>BR		D3	KS	0.1383
	D5	0.05607	0.3029	KS>CA		0.05607	0.03293	CA>BR		0.05607	0.0308	CA>PH		0.3029	0.03293	KS>BR		0.3029	0.0308	KS>PH		0.03293	0.0308	BR>PH		D5	KS	0.3029
IFNL3	D3	0.0001	0.000159	KS>CA		0.0001	0.0001			0.0001	0.4073	PH>CA		0.000159	0.0001	KS>BR		0.000159	0.4073	PH>KS		0.0001	0.4073	PH>BR		D3	PH	0.4073
	D5	0.0001	5.678	KS>CA		0.0001	0.0001			0.0001	0.0001			5.678	0.0001	KS>BR		5.678	0.0001	KS>PH		0.0001	0.0001			D5	KS	5.678
STAT1	D3	0.5598	0.6232	KS>CA		0.5598	0.8695	BR>CA		0.5598	0.5945	PH>CA		0.6232	0.8695	BR>KS		0.6232	0.5945	KS>PH		0.8695	0.5945	BR>PH		D3	BR	0.8695
	D5	0.5924	0.5661	KS>CA		0.5924	0.6764	BR>CA		0.5924	0.5704	PH>CA		0.5661	0.6764	BR>KS		0.5661	0.5704	PH>KS		**0.6764**	**0.5704**	**BR>PH**	**0.027588**	D5	BR	0.6764
STAT2	D3	28.42	18.77	CA>KS		28.42	26.39	CA>BR		28.42	21.51	CA>PH		18.77	26.39	BR>KS		18.77	21.51	PH>KS		26.39	21.51	BR>PH		D3	CA	28.42
	D5	19.45	8.381	CA>KS		19.45	34.1	BR>CA		**19.45**	**29.66**	**PH>CA**	**0.044549**	**8.381**	**34.1**	**BR>KS**	**0.020304**	**8.381**	**29.66**	**PH>KS**	**0.007105**	34.1	29.66	BR>PH		D5	BR	34.1
STAT3	D3	0.9295	1.532	KS>CA		0.9295	1.373	BR>CA		0.9295	1.379	PH>CA		1.532	1.373	KS>BR		1.532	1.379	KS>PH		1.373	1.379	PH>BR		D3	KS	1.532
	D5	0.9752	2.086	KS>CA		0.9752	1.174	BR>CA		0.9752	0.8461	CA>PH		2.086	1.174	KS>BR		2.086	0.8461	KS>PH		1.174	0.8461	BR>PH		D5	KS	2.086
RIG-I	D3	**43.32**	**16.37**	**CA>KS**	**0.02784**	43.32	36.59	CA>BR		**43.32**	**11.22**	**CA>PH**	**0.012321**	**16.37**	**36.59**	**BR>KS**	**0.032792**	16.37	11.22	KS>PH		**36.59**	**11.22**	**BR>PH**	**0.010406**	D3	CA	43.32
	D5	**50.22**	**7.149**	**CA>KS**	**0.00258**	50.22	51.76	BR>CA		50.22	51.89	PH>CA		**7.149**	**51.76**	**BR>KS**	**0.029414**	**7.149**	**51.89**	**PH>KS**	**0.000497**	51.76	51.89	PH>BR		D5	BR	51.89
SOCS3	D3	2.985	2.985	KS>CA		2.985	3.071	BR>CA		2.985	2.827	CA>PH		2.985	3.071	BR>KS		2.985	2.827	KS>PH		3.071	2.827	BR>PH		D3	BR	3.071
	D5	**3.451**	**1.232**	**CA>KS**	**0.01166**	3.451	4.146	BR>CA		3.451	3.741	PH>CA		**1.232**	**4.146**	**BR>KS**	**0.002316**	**1.232**	**3.741**	**PH>KS**	**0.003306**	4.146	3.741	BR>PH		D5	BR	4.146
TSLP	D3	0.008381	0.07152	KS>CA		0.008381	0.009628	BR>CA		0.008381	0.1494	PH>CA		0.07152	0.009628	KS>BR		0.07152	0.1494	KS>PH		0.009628	0.1494	PH>BR		D3	PH	0.1494
	D5	0.001205	0.7328	KS>CA		0.001205	0.009344	BR>CA		**0.001205**	**0.02397**	**PH>CA**	**0.003576**	0.7328	0.009344	KS>BR		0.7328	0.02397	KS>PH		0.009344	0.02397	PH>BR		D5	KS	0.7328

Comparison of gene expression by IAV and IBV in the (A) URT and (B) peripheral blood of ferrets on D3 and D5 post challenge by qRT-PCR. Gene expression in the URT was determined in NW cells and peripheral blood expression was determined in PBMC. Average fold-gene expression levels over pre-infection (D0) mock challenged animals for IAV (CA and KS) and IBV (BR and PH) are shown. An upregulation of expression (>1-fold) indicated in pink and a down-regulation (<1-fold) indicated in light blue. Comparisons of IAV to IAV (CA to KS), IAV to IBV (CA to BR, CA to PH, KS to BR, and KS to PH), and IBV to IBV (BR to PH) displayed and virus expression differences shown in column ">" and virus with highest level for all comparisons indicated in column "HIGHEST EXPRESSOR". Comparisons with statistical differences, using t-test, $p<0.05$ shown in "p" column. Interferon genes are grouped between dotted lines.

Figure 4.2: Cytokine and chemokine levels in ferret sera following IAV or IBV infection.

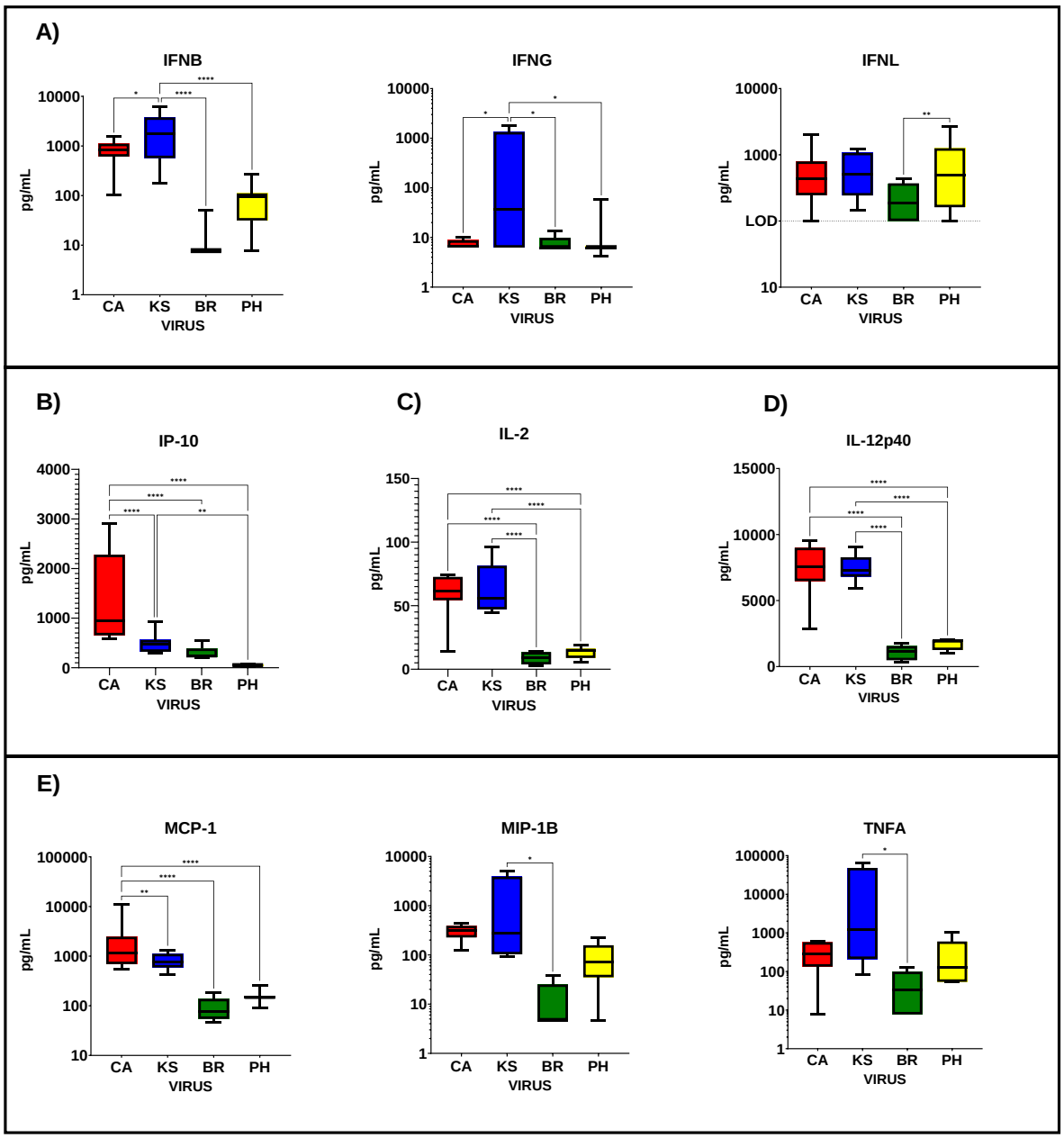

Cytokine and chemokine levels in sera following IAV (CA and KS) or IBV (BR and PH) infection (day 1 to day 28) in ferrets. Influenza A viruses: H1N1pdm09 A/California/07/2009, "CA" (red) and H3N2 A/Kansas/14/2017, "KS" (blue). Influenza B viruses: B-Victoria lineage B/Brisbane/60/2008, "BR" (Green) and B-Yamagata

lineage B/Phuket/3073/2013, “PH” (yellow). A) Type-I (IFNB), Type-II (IFNG) and Type-III (IFNL) interferons. B) Th1 chemokine (IP-10). C) Th2 cytokine (IL-2). D) Teff cytokine (IL-12p40). E) Pro-inflammatory chemokines (MCP-1 and MIP-1B) and cytokine (TNFA). 2-way ANOVA used to determine significant differences between viruses over a 28-day period.

Figure 4.3: Serum antibody responses following IAV or IBV ferret challenge.

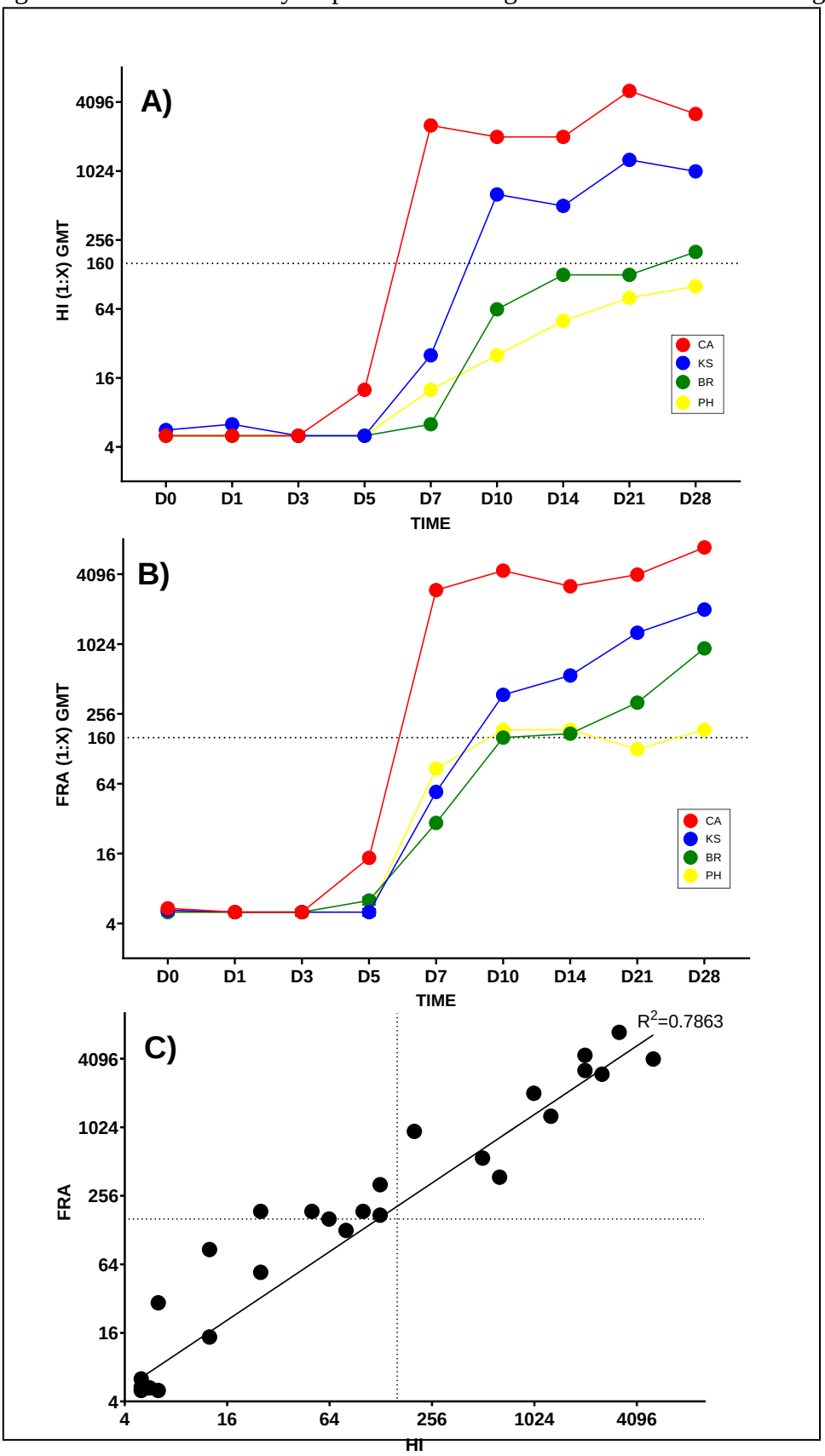

Serum antibody by HI and neutralizing antibody (FRA) levels following infection with IAV ("CA" red, "KS" blue) and IBV ("BR" green, "PH" yellow) over 28 days post challenge. Average geometric mean titer (GMT) given for HI (A) and FRA (B) tests. Values above 1:160 (dotted line) indicate robust antibody response. Correlation of HI to FRA (C).

Figure 4.4: Antigen-specific antibodies in ferret serum following IAV and IBV challenge by ELISA.

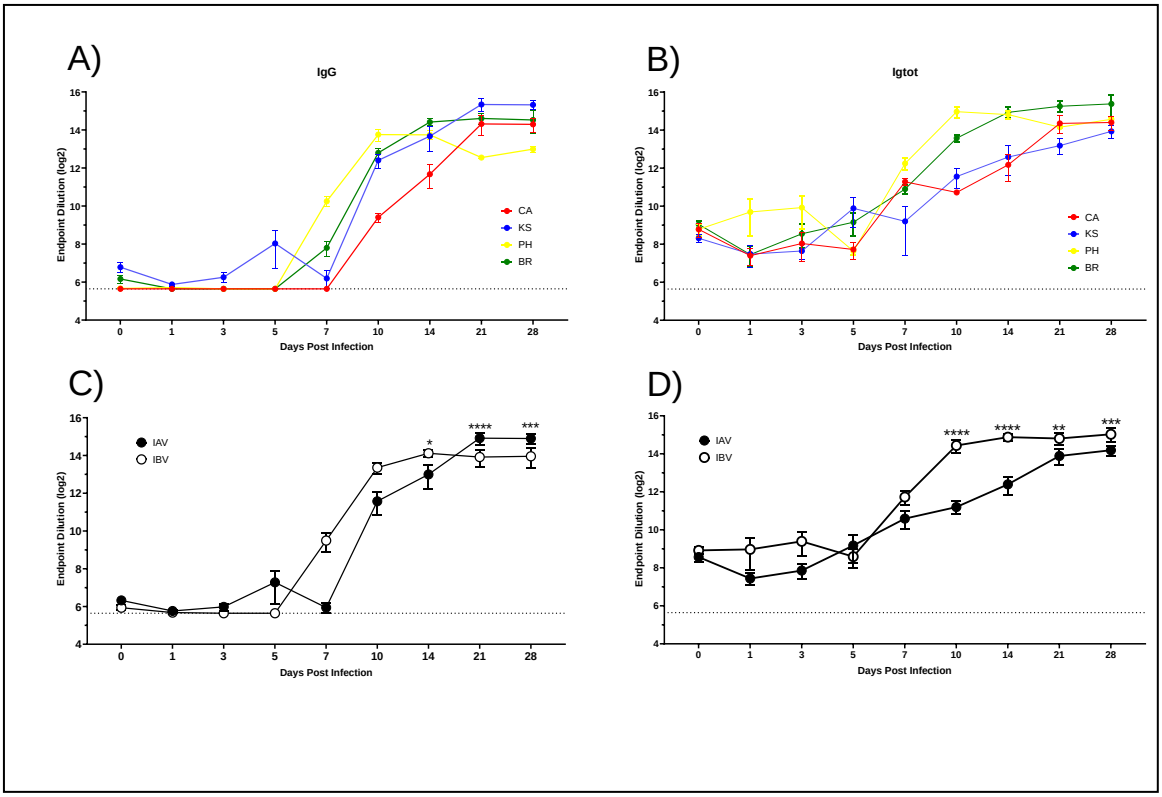

Antigen-specific antibodies in ferret sera over 28 days following infection with IAV and IBV. Antigen-specific IgG (A) and total Ig (B) to CA (red), KS (blue), BR (green) or PH (yellow) over 28 days. Comparison of IAV to IBV for antigen-specific IgG (C) and total

Ig (D). Significant differences for each timepoint determined using 2-way ANOVA. The dotted line indicates the limit of detection.

Figure 4.5: Antibody-secreting cells in ferret spleen and peripheral blood following IAV and IBV challenge.

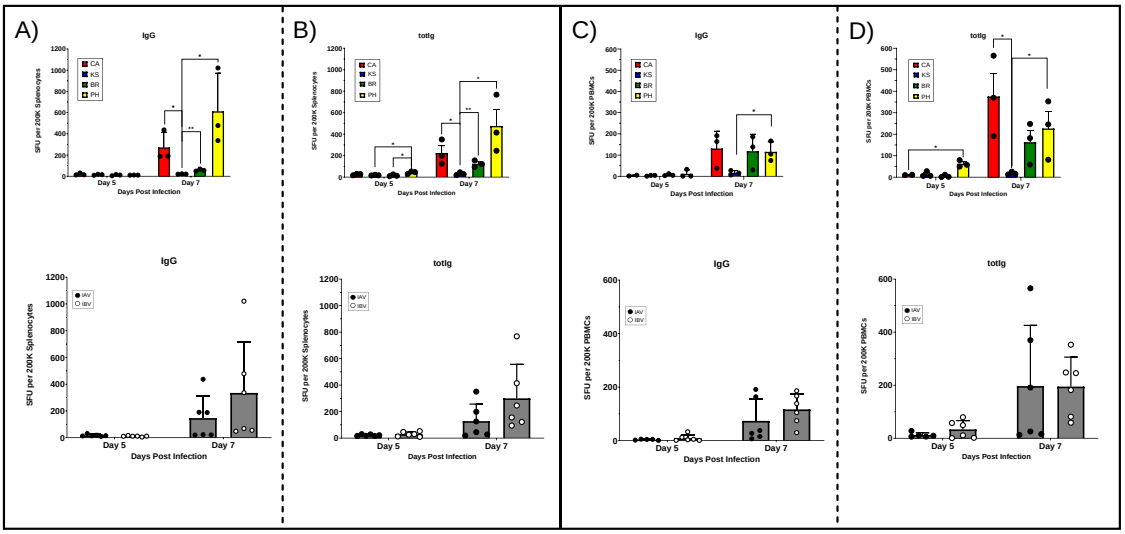

Early antibody-secreting cells (ASC) in splenocytes (A and B) and peripheral blood (PBMC) (C and D) on days 5 and 7 post challenge with IAV and IBV. ASC to following challenge with individual viruses: CA (red), KS (blue), BR (green) or PH (yellow) in splenocytes and PBMC. Panel A) top panel is individual virus IgG spot forming units (SFU) in splenocytes (significance using multiple t-tests), bottom panel comparing IgG SFU following IAV and IBV challenge (ns, t-test). Panel B) top panel is individual virus total Ig "totIg" SFU in splenocytes (significance by multiple t-tests), bottom panel comparing totIg SFU following IAV and IBV challenge (ns, t-test). Panel C) top panel is individual virus IgG SFU in PBMC (significance by multiple t-tests), bottom panel

comparing IgG SFU following IAV and IBV challenge (ns, t-test). Panel D) top panel is individual virus total totIg SFU in PBMC (significance by multiple t-tests), bottom panel comparing totIg SFU following IAV and IBV challenge (ns, t-test).

Table 4.3: Correlation between virus titer and gene expression in ferret samples.

A) VIRUS TITER (NW) VS GENE EXPRESSION (NW)		CA(H1PDM09)			KS(H3N2)			BR(B-VIC)			PH(B-YAM)		
GROUP	GENE	r	P-VALUE	SIGNIFICANCE	r	P-VALUE	SIGNIFICANCE	r	P-VALUE	SIGNIFICANCE	r	P-VALUE	SIGNIFICANCE
INFLAM.	*MCP-1*	-0.8386	0.1834	ns	-0.8274	0.1898	ns	0.9071	0.1383	ns	**-0.9993**	**0.012**	*
TH1/TH2	*CXCL10*	-0.1089	0.4653	ns	-0.9488	0.1023	ns	0.08812	0.4719	ns	0.2245	0.4279	ns
	IL-2	-0.8048	0.2023	ns	0.9268	0.1225	ns	-0.07546	0.476	ns	-0.2225	0.4286	ns
T-REG	*TGFB1*	-0.8257	0.1908	ns	0.3816	0.3754	ns	-0.07407	0.4764	ns	0.4686	0.3447	ns
T-EFF	*IL-4*	-0.8388	0.1832	ns	0.9276	0.1219	ns	-0.07451	0.4763	ns	-0.2682	0.4136	ns
	IL-12p40	0.744	0.2329	ns	0.9262	0.1231	ns	-0.06412	0.4796	ns	-0.1922	0.4384	ns
	IL-17	0.4762	0.342	ns	0.9265	0.1228	ns	-0.0723	0.477	ns	-0.2021	0.4352	ns
PRO-INFLAM.	*IL-1B*	-0.5162	0.3273	ns	0.9249	0.1241	ns	-0.06899	0.478	ns	-0.1953	0.4374	ns
	IL-6	-0.215	0.431	ns	0.9199	0.1283	ns	-0.06655	0.4788	ns	-0.1808	0.4421	ns
APOPTOSIS	*GranA*	-0.07551	0.4759	ns	0.9272	0.1222	ns	-0.07718	0.4754	ns	-0.2484	0.4201	ns
INTERFERON	*IFNA*	0.1787	0.4428	ns	0.9272	0.1222	ns	-0.0709	0.4774	ns	-0.199	0.4362	ns
	IFNB	0.7823	0.2141	ns	0.9275	0.1219	ns	-0.07433	0.4763	ns	-0.2035	0.4348	ns
	IFNG	-0.7016	0.2525	ns	0.9113	0.1351	ns	-0.06662	0.4788	ns	-0.269	0.4133	ns
	IFNL3	-0.7832	0.2136	ns	0.8926	0.1489	ns	-0.07466	0.4762	ns	0.9378	0.1129	ns
INTERFERON RESPONSE	*STAT1*	-0.9863	0.0528	ns	-0.9587	0.0918	ns	-0.08597	0.4726	ns	0.1458	0.4534	ns
	STAT2	-0.03779	0.488	ns	**-0.9921**	**0.0401**	*	-0.07283	0.4768	ns	0.1077	0.4656	ns
	STAT3	-0.05986	0.4809	ns	-0.9786	0.0659	ns	0.2315	0.4256	ns	-0.1053	0.4664	ns
	RIG-I	-0.03527	0.4888	ns	-0.9223	0.1263	ns	-0.05813	0.4815	ns	0.3091	0.4	ns
	SOCS3	-0.02618	0.4917	ns	-0.9545	0.0964	ns	0.03669	0.4883	ns	-0.9695	0.0788	ns
	TSLP	-0.7391	0.2353	ns	0.9278	0.1217	ns	-0.07472	0.4762	ns	0.9036	0.1409	ns

B) VIRUS TITER (NW) VS GENE EXPRESSION (PBMC)

GROUP	GENE	CA(H1PDM09) r	CA(H1PDM09) P-VALUE	CA(H1PDM09) SIGNIFICANCE	KS(H3N2) r	KS(H3N2) P-VALUE	KS(H3N2) SIGNIFICANCE	BR(B-VIC) r	BR(B-VIC) P-VALUE	BR(B-VIC) SIGNIFICANCE	PH(B-YAM) r	PH(B-YAM) P-VALUE	PH(B-YAM) SIGNIFICANCE
INFLAM.	*MCP-1*	0.8614	0.1696	ns	-0.1505	0.4519	ns	-0.07781	0.4752	ns	0.9457	0.1054	ns
TH1/TH2	*CXCL10*	0.9416	0.1094	ns	-0.328	0.3936	ns	-0.1038	0.4669	ns	**0.9908**	**0.0431**	*
	IL-2	0.9614	0.0887	ns	0.8566	0.1726	ns	-0.00847	0.4973	ns	**0.9968**	**0.0253**	*
T-REG	*TGFB1*	0.9706	0.0773	ns	-0.09313	0.4703	ns	-0.02421	0.4923	ns	0.9648	0.0847	ns
T-EFF	*IL-4*	0.8415	0.1817	ns	-0.05974	0.481	ns	-0.0583	0.4814	ns	0.8991	0.1443	ns
	IL-12p40	0.9633	0.0865	ns	0.8498	0.1767	ns	-0.03465	0.489	ns	0.8303	0.1882	ns
	IL-17	0.9551	0.0957	ns	0.9275	0.1219	ns	-0.04045	0.4871	ns	-0.7077	0.2497	ns
PRO-INFLAM.	*IL-1B*	0.8696	0.1644	ns	**0.9884**	**0.0485**	*	0.06249	0.4801	ns	0.8652	0.1672	ns
	IL-6	0.9165	0.131	ns	**1**	**0.0013**	**	-0.04096	0.487	ns	0.6168	0.2884	ns
APOPTOSIS	*GranA*	0.903	0.1414	ns	0.7788	0.2158	ns	-0.08171	0.474	ns	-0.6045	0.2934	ns
INTERFERON	*IFNA*	0.9327	0.1175	ns	0.8675	0.1657	ns	0.009508	0.497	ns	0.1834	0.4413	ns
	IFNB	0.887	0.1528	ns	0.4687	0.3447	ns	0.04545	0.4855	ns	-0.2012	0.4355	ns
	IFNG	0.961	0.0892	ns	0.2935	0.4052	ns	-0.05777	0.4816	ns	0.9179	0.1298	ns
	IFNL3	0.8834	0.1552	ns	-0.1174	0.4625	ns	-0.07462	0.4762	ns	0.9483	0.1028	ns
INTERFERON RESPONSE	*STAT1*	0.9318	0.1183	ns	**-1**	**0.0012**	**	0.4272	0.3595	ns	0.1257	0.4599	ns
	STAT2	-0.2512	0.4192	ns	-0.05059	0.4839	ns	-0.1903	0.4391	ns	-0.7545	0.2279	ns
	STAT3	0.8615	0.1695	ns	-0.4725	0.3433	ns	**1**	**0.0018**	**	0.936	0.1145	ns
	RIG-I	-0.9584	0.0921	ns	-0.3754	0.3775	ns	-0.3349	0.3913	ns	-0.7968	0.2065	ns
	SOCS3	0.43	0.3585	ns	-0.2935	0.4052	ns	-0.4087	0.366	ns	-0.7898	0.2102	ns
	TSLP	0.9835	0.0578	ns	0.01149	0.4963	ns	-0.07576	0.4759	ns	0.893	0.1486	ns

A) Spearman correlation of virus titer in NW to gene expression in NW cells. B) Spearman correlation of virus titer in NW vs gene expression in PBMC. Direct correlations are in pink and inverse correlations are in blue. Significant ($p<0.05$) correlations in bold.

Table 4.4: Correlations between antibody levels and protein levels in ferret sera.

B) SERUM AB TITER (FRA) VS ANALYTE																	
		CA(H1PDM09)			KS(H3N2)			BR(B-VIC)			PH(B-YAM)		
GROUP	ANALYTE	r	P-VALUE	SIGNIFICANCE	r	P-VALUE	SIGNIFICANCE	r	P-VALUE	SIGNIFICANCE	r	P-VALUE	SIGNIFICANCE
INTERFERON	IFNb	-0.1255	0.3753	ns	**0.6781**	**0.0269**	*	-0.4178	0.3333	ns	0.3281	0.1929	ns
	IFNg	-0.3889	0.1463	ns	-0.3103	0.2081	ns	0.3157	0.207	ns	0.5057	0.0833	ns
	IFNL	-0.1255	0.3753	ns	0.08476	0.4205	ns	-0.4178	0.3333	ns	0.3281	0.1929	ns
TH1/TH2	IP-10	-0.41	0.1363	ns	-0.2373	0.2711	ns	-0.2034	0.3031	ns	0.2039	0.2976	ns
	IL-2	0.4034	0.1392	ns	**0.6103**	**0.0454**	*	0.3899	0.1512	ns	**0.8335**	**0.0052**	**
CHEMOKINE	MCP-1	**-0.6444**	**0.0343**	*	**-0.8815**	**0.0017**	**	**-0.8476**	**0.0035**	**	-0.3784	0.154	ns
	MIP-1b	**-0.795**	**0.0072**	**	-0.2034	0.3031	ns	0.13	0.3733	ns	-0.1064	0.3929	ns
T-EFF	IL-4	-0.3682	0.1632	ns	-0.1187	0.3855	ns	-0.06781	0.4372	ns	-0.4256	0.1258	ns
	IL-17	**-0.7615**	**0.011**	*	-0.2034	0.3031	ns	0.2543	0.2573	ns	-0.1419	0.3579	ns
	IL-12p40	0.569	0.0576	ns	0.4577	0.1106	ns	0.4916	0.0925	ns	**0.7625**	**0.0123**	*
	IL-12p70	**-0.9121**	**0.0007**	***	-0.4238	0.1295	ns	0.3745	0.1586	ns	-0.1064	0.3929	ns
PRO-INFLAM.	TNFa	**-0.6695**	**0.0275**	*	-0.3221	0.2	ns	0.431	0.1233	ns	-0.08867	0.4119	ns
	IL-6	0.1702	0.3305	ns	-0.2373	0.2711	ns	**-0.8728**	**0.001**	***	0.2926	0.2187	ns
	IL-8	**-0.5941**	**0.0493**	*	0.5933	0.0511	ns	-0.339	0.1867	ns	0.3901	0.1456	ns

A) SERUM AB TITER (HI) VS ANALYTE			CA(H1PDM09)			KS(H3N2)			BR(B-VIC)			PH(B-YAM)		
GROUP	ANALYTE	r	P-VALUE	SIGNIFICANCE	r	P-VALUE	SIGNIFICANCE	r	P-VALUE	SIGNIFICANCE	r	P-VALUE	SIGNIFICANCE
INTERFERON	IFNb	0.01703	0.4867	ns	**0.6723**	**0.0272**	*	0.08381	0.3889	ns	0.322	0.197	ns
	IFNg	-0.2178	0.2895	ns	-0.3846	0.1517	ns	0.1876	0.3128	ns	-0.2172	0.2857	ns
	IFNL	0.01703	0.4867	ns	0.06723	0.4342	ns	-0.3592	0.4444	ns	0.322	0.197	ns
TH1/TH2	IP-10	-0.315	0.2031	ns	-0.2605	0.2476	ns	-0.2885	0.2243	ns	0.09574	0.4026	ns
	IL-2	0.2949	0.2161	ns	**0.6051**	**0.0454**	*	0.5246	0.0734	ns	**0.7659**	**0.0113**	*
CHEMOKINE	MCP-1	-0.5789	0.0544	ns	**-0.7143**	**0.0181**	*	**-0.8569**	**0.003**	**	-0.2666	0.2413	ns
	MIP-1b	-0.5363	0.0709	ns	-0.2101	0.2927	ns	0.04789	0.4537	ns	-0.2959	0.2183	ns
T-EFF	IL-4	-0.2128	0.2907	ns	0.09244	0.4082	ns	0.3262	0.1907	ns	**-0.6468**	**0.0339**	*
	IL-17	-0.4341	0.121	ns	-0.2773	0.2326	ns	0.2011	0.3012	ns	-0.2785	0.2322	ns
	IL-12p40	**0.6214**	**0.0411**	*	0.4454	0.1151	ns	0.5596	0.0595	ns	**0.6615**	**0.0303**	*
	IL-12p70	**-0.6895**	**0.0236**	*	-0.5714	0.057	ns	0.4654	0.1021	ns	-0.3307	0.1903	ns
PRO-INFLAM.	TNFa	-0.5874	0.0516	ns	-0.3866	0.1517	ns	0.498	0.0884	ns	-0.2437	0.2621	ns
	IL-6	-0.03463	0.4673	ns	-0.3109	0.2061	ns	**-0.853**	**0.0032**	**	0.1567	0.343	ns
	IL-8	-0.2639	0.2451	ns	0.5042	0.0849	ns	-0.4984	0.086	ns	**0.6267**	**0.0396**	*

A) Spearman correlation of antibody response (HI) in serum to protein (analyte) levels in serum. B) Spearman correlation of neutralizing antibody response (FRA) in serum to protein levels in serum. Direct correlations are in pink and inverse correlations are in blue. Significant ($p<0.05$) correlations in bold.

Figure 4.S1: Temperature and weight changes in ferrets following influenza challenge.

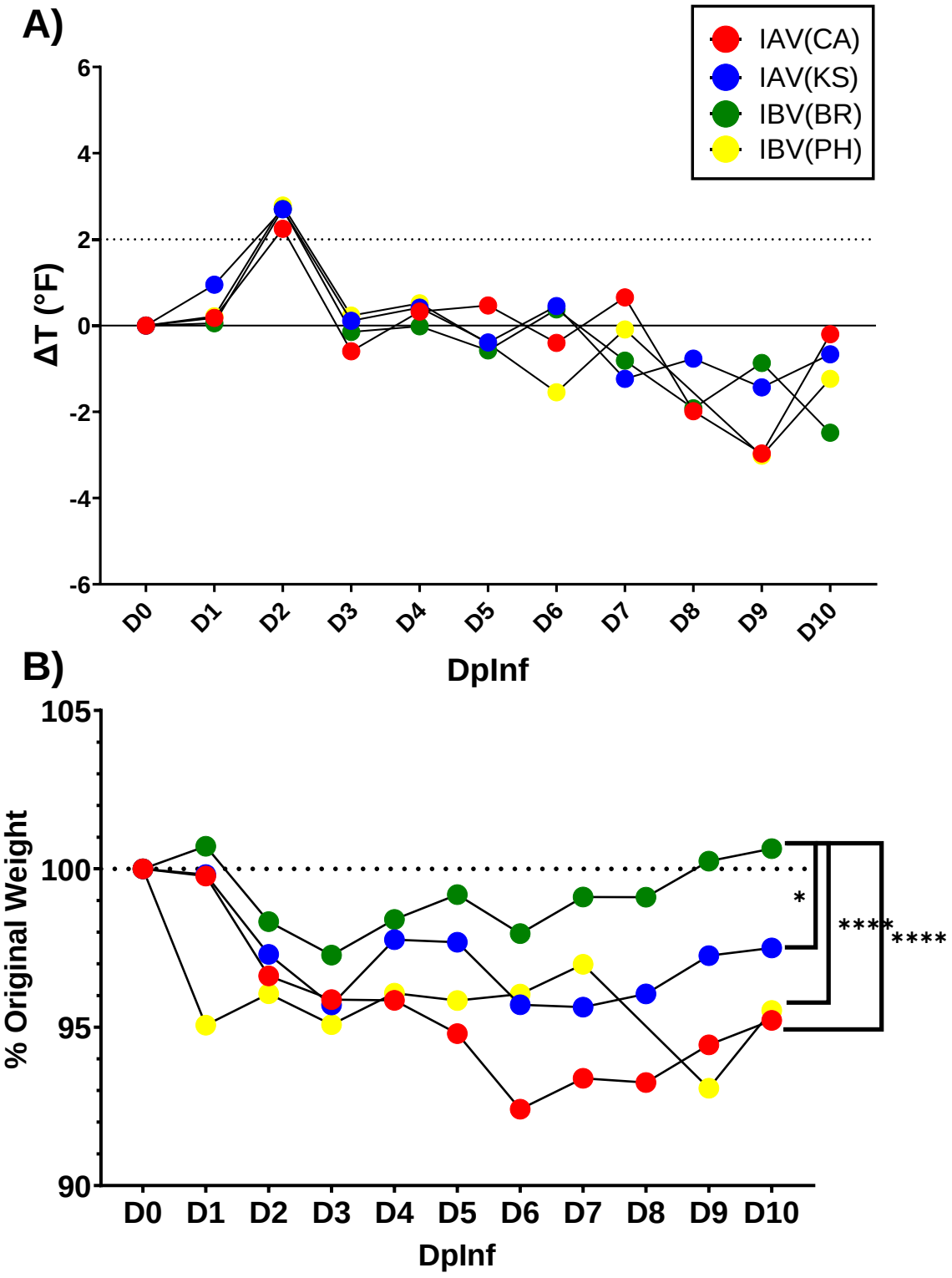

Clinical parameters in ferrets challenged with IAV and IBV. Red (IAV, H1N1pdm09 subtype, CA), blue (IAV, H3N2 subtype, KS), green (IBV, Victoria lineage, BR), yellow (IBV, Yamagata lineage, PH). A) Average body temperature changes from baseline following challenge. Fever indicated by dotted line at +2°F above baseline. B) Weight loss following challenge. Percentage of original, prechallenge, weight. Significant differences between IAV (CA/KS) and BR as well as PH and BR (2-way ANOVA).

Figure 4.S2: Kinetics of cytokine and chemokines in ferret serum following IAV and IBV challenge.

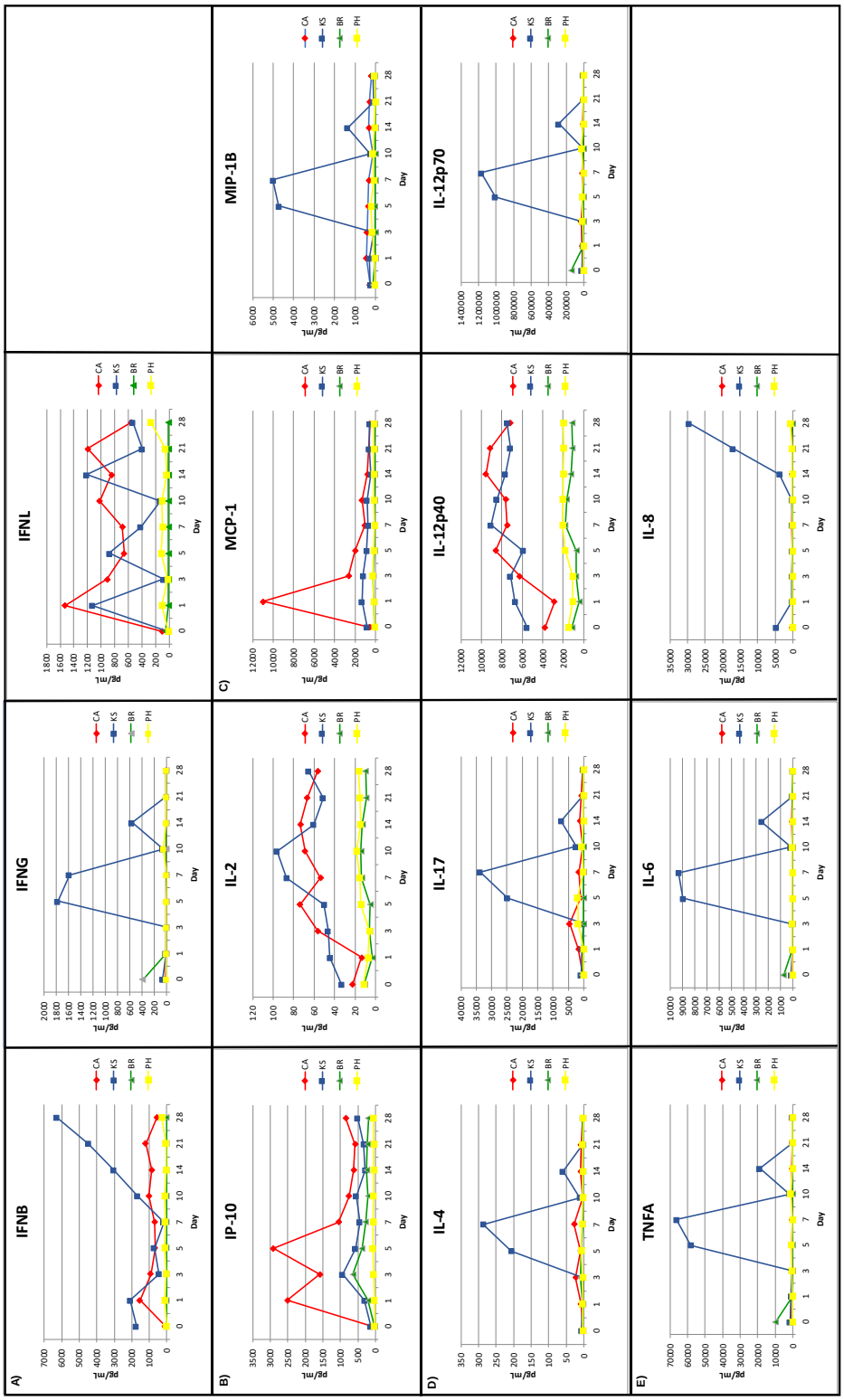

A) Interferon responses. Type-I (IFNB), Type-II (IFNG) and Type-III* (IFNL). *Bio-assay B) Th1 (IP-10) and Th2 (IL-2) response C) Pro-inflammatory chemokines (MCP-1 and MIP1B) D) Teff response (IL-4, IL-17, IL-12p40 & IL-12p70) E) Pro-inflammatory cytokine response (TNFA, IL-6, and IL-8).

CHAPTER 5

INTERFERON AS AN IMMUNOADJUVANT FOR ENHANCING ADAPTIVE RESPONSES FOLLOWING INFUENZA B INFECTION AND VACCINATION IN THE FERRET[4]

[4] Thomas Rowe, Ashley Fletcher, Pavel Svoboda, Jan Pohl, Yasuko Hatta, Gabriela Jasso, David E. Wentworth, and Ted M. Ross. Interferon as an immunoadjuvant to enhance antibody responses to influenza B infection and vaccination in the ferret. *submitted to NPJ Vaccines* (2024).

ABSTRACT

Despite annual vaccination, influenza B viruses (IBV) continue to cause significant morbidity and mortality in humans. We have found that IBV infection resulted in a weaker innate and adaptive immune response than influenza A viruses (IAV) in ferrets. To understand and overcome the weak immune responses to IBV in ferrets, we administered type-I or type-III interferon (IFN) to ferrets following infection or vaccination and evaluated their effects on the immune response. IFN signaling following viral infection plays a key role in the initial innate immune response and affects subsequent adaptive immune responses. In the respiratory tract, IFN lambda (IFNL) has regulatory effects on adaptive immunity indirectly through thymic stromal lymphopoietin (TSLP), which then acts on immune cells to stimulate the adaptive response.

Following IBV infection or vaccination, IFN treatment (IFN-Tx) upregulated gene expression of early inflammatory responses in the upper respiratory tract and robust IFN, TSLP, and inflammatory responses in peripheral blood cells. These responses were sustained following challenge or vaccination in IFN-Tx animals. Serum IFNL and TSLP levels were enhanced in IFN-Tx animals following challenge/rechallenge over mock-Tx; however, this difference was not observed following vaccination. Antibody responses in serum of IFN-Tx animals following IBV infection or vaccination increased more quickly, to higher titers, and was sustained longer than mock-Tx animals over 3 months. Following rechallenge of infected animals 3 months post treatment, antibody levels remained higher than mock-Tx. However, IFN-Tx did not have an effect on antibody responses following challenge of vaccinated animals.

A strong direct correlation was found between TSLP levels and antibody responses following challenge-rechallenge and vaccination-challenge indicating it as a useful tool for predicting adaptive immune responses following IBV infection or vaccination. The effects of IFN on strengthening both innate and adaptive responses to IBV may aid in development of more effective treatments following infection and improved influenza vaccines.

INTRODUCTION

The vast majority of influenza studies focus on influenza A viruses (IAV), however, influenza B viruses (IBV) represent nearly one quarter of all influenza infections and are generally responsible for most cases late in the influenza season [1]. Even though IBV co-circulate with IAV, much less is known about the innate and adaptive responses following IBV infection and vaccination [2, 47]. IBV are not divided into subtypes as IAV, but instead are classified into two antigenically distinct lineages: B/Yamagata and B/Victoria [11]. Some differences between IBV demographics in humans indicate that patients with Victoria lineage are generally younger (0 – 4 years, 60% versus 40% in adults; 5 – 14 years, 72% versus 28% in adults) compared to patients infected with Yamagata lineage; however, clinical presentation is equal [447]. The average vaccine effectiveness for IBV is 54% [448], however, during the 2014/2015 influenza season vaccine, it was 57%. During this period fewer than 20% of older children (9 – 17 years) had a 4-fold rise in antibody titer to the IBV component following vaccination [362].

Ferrets are the primary animal model for influenza research and vaccine studies [324, 336, 423, 449]. Therefore, ferrets were either vaccinated or infected with IBV to assess immune responses. In studies comparing multiple circulating IAV and IBV strains in ferrets, IBV induced weaker immune responses even though IBV strains replicated as well as IAV strains in the upper respiratory tract [444, 450]. In addition, live attenuated influenza virus (LAIV) vaccines elicited weaker antibodies generated to the IBV components (B-Victoria and B-Yamagata) than to the IAV components (A/H1N1pdm09 and A/H3N2) [451].

Following infection of respiratory epithelial cells, influenza viruses are recognized by the innate immune system using pattern recognition receptors (PRRs). These receptors recognize pathogen-associated molecular patterns (PAMPs) of which three classes of PRRs can recognize influenza virus infection and initiate an inflammatory response. The PRRs that recognize and activate innate signaling pathways to IAV include the toll-like receptors (TLRs), nod-like receptors (NLRs) and Retinoic acid Induced Gene 1 like receptor (RIG-I) [118]. TLR-3 is expressed in endosomes and recognizes viral double-stranded RNA which is produced during viral replication, while endosomal TLR-7 and cytoplasmic RIG-I recognize single-stranded RNA. These PAMP-PRR interactions lead to activation of several signaling pathways and to the production of type I and type-III interferons (IFNs) and inflammatory cytokines [100]. IFN signaling rapidly promotes an antiviral state by inducing IFN stimulating genes to limit viral replication and spread and induces immune responses in neighboring cells to protect them from infection [114]. The non-structural protein 1 (NS1) of IAV inhibits the IFN response. NS1 has shown to be an IFN-antagonist to dampen host IFN response and

facilitate virus replication [408]. In general, viruses avoid elements of the innate immune response, such as the IFN response, thereby allowing for increased virus replication and spread before the initiation of the adaptive immune response. The IAV NS1 inhibits type-I IFN release and can also inhibit dendritic cell (DC) maturation and function, which is important in adaptive immune responses [452]. Type-III IFN lambda (IFNL) can recruit DCs, regulate IL-10 production, and enhance type-I helper T cell responses [136]. IFNL is non-inflammatory and primarily activated in the mucosal tract and does not have the inflammatory effects seen with type-I IFNs. IFNL acts indirectly on DCs through the induction of thymic stromal lymphopoietin (TSLP) in the respiratory tract [137], thus inducing a mucosal immune response. Upon induction TSLP regulates germinal center function and antigen-specific antibody responses [138], thus having an important effect on the magnitude of the adaptive immune response.

Infection with IBV results in a delay in both innate and antibody responses in ferrets compared to IAV infection [450]. In this study, IFN was examined as an immunoadjuvant to enhance the immune responses in infected or vaccinated animals and assess protection following rechallenge with IBV. We used PEGylated ferret IFNs as potential immunoadjuvants following IBV infection or vaccination. Effects of IFNs as an alternative method to stimulate robust immune responses may be important to understanding reduced immune responses following IBV infection as well as a way to improve vaccine efficacy.

MATERIALS AND METHODS

Interferon PEGylation and testing

Polyethylene glycol (PEG) attachment to molecules, PEGylation, is considered one of the most successful techniques to enhance the therapeutic and biotechnological potential of peptides and proteins [453-455]. Recombinant ferret type-I interferon alpha (IFNA) and type-III interferon lambda 3 (IFNL3) were purchased from Kingfisher Biotech, Inc. (Saint Paul, MN, USA). IFNA and IFNL3 was PEGylated with Hydroxyl-PEG-NHS ester 5000Da (HO-PEG5K-NHS; PEG5K; Sigma-Aldrich, Milwaukee, WI, USA) and m-PEG-Lys-NHS ester 20000Da (mPEG-Lys-NHS 20000; PEG20K; BroadPharm, San Diego, CA, USA). One microgram per microliter solutions of IFNA and IFNL3 were prepared in 100 mM pH 7.2 sodium phosphate buffer. Fifteen-fold molar excess of PEGs over the molar concentration of proteins were added to protein solutions. PEGs were dissolved in dimethyl sulfoxide (DMSO). The DMSO volume did not exceed 20% of total reaction volume. The mixtures were incubated at 25°C for 1Hr. One microgram aliquots of each sample were taken and electrophoresed on 4-12% NuPAGE Bis-Tris polyacrylamide gels and stained with Imperial Protein Stain to determine the extent of protein modification. Activity of PEGylated-IFNs was determined using an IFN bioassay. The modified proteins were stored at -80°C prior to use in animal experiments.

Viruses

Influenza B-Yamagata lineage virus (B/Phuket/3073/2013, "PH") was used for infection and vaccination studies. For infection studies PH was passaged in Madin Darby Canine Kidney (MDCK) cells, to retain antigenic similarity to the original human isolates and to avoid structural changes in the hemagglutinin which could occur from passage in eggs[377-379]. The virus was passaged in MDCK cells "C#" according to established

procedures [381]. PH passage C4 was used for all challenge and rechallenge experiments. For the vaccine study, live-attenuated influenza virus B-Yamagata lineage strain B/Phuket/3073/2013-CDC-LV11B (LAIV) was developed according to established procedures [456] and passaged in embryonated chicken eggs [381]. All Viral titers, challenge/rechallenge and vaccine strain, were determined by focus forming assay and given as log focus forming units per milliliter (FFU/mL). Viral titers for challenge/rechallenge virus (PH) and vaccine strain (LAIV) used in this study were $10^{7.54}$ FFU/mL and $10^{8.93}$ FFU/mL respectively.

Ferrets and study design

All animal procedures were approved by the Institutional Animal Care and Use Committee of the Centers for Disease Control and Prevention in an Association for Assessment and Accreditation of Laboratory Animal Care International accredited facility. Male fitch ferrets (Triple F Farms, Sayre, PA), between 1.2 to 2 years of age and seronegative for currently circulating influenza viruses were used for all experiments.

Two separate experiments were conducted using 18 ferrets for each: 1) challenge-rechallenge experiment and 2) vaccination-challenge experiment.

Challenge-rechallenge experiment

In this study, we chose a representative virus (B/Phuket/3073/2013, "PH"), which in previous experiments typified the delayed and low immune responses of IBVs, for a challenge/rechallenge study. Six groups of three ferrets per group were used: Mock-challenged/mock-treated (UN-MOCK), mock-challenged/IFNA-treated (UN-IFNA), mock-challenged/IFNL3-treated (UN-IFNL), PH-challenged/mock-treated (PH-MOCK), PH-challenged/IFNA-treated (PH-IFNA), and PH-challenged/IFNL3-treated (PH-IFNL).

The ferrets were first anesthetized with an intramuscular cocktail of ketamine (15-30 mG/kG) plus xylazine (1-2 mG/kG) "KX" and challenged intranasally with 1mL of virus ($4x10^5$ FFU/mL) or PBS. Twenty-four hours post challenge ferrets were anesthetized and 1uG/kG PEGylated-IFN (IFNA or IFNL) or PBS was introduced intranasally to the appropriate groups. The animals were monitored over 28 days post challenge for weight loss, fever, and other clinical signs (lethargy, sneezing and dyspnea) of infection. The animals were weighed on day 0 prior to PH challenge to establish a baseline weight and then daily for the first ten days post challenge followed by weekly thereafter through day 28. Changes in weight were calculated as percentage loss or gain from day 0 weight. For fever calculation, a temperature transponder [IPTT-300; Bio Medic Data Systems (BMDS), Waterford, WI, USA] was programed to identify each ferret and implanted subcutaneously between the shoulder blades of each animal and read with a scanner (DAS-6007 IPTT Scanner System, BMDS). A baseline temperature (°F) was determined by the average temperature over three days prior to challenge. Temperatures were assessed over the first 10 days post challenge, then weekly and fever was determined as any temperature greater or equal to 2 degrees Fahrenheit above baseline. Ferrets were assessed daily for clinical signs within a two-hour window between 9AM – 11AM during peak normal activity and to reduce variation due to circadian rhythms [433]. Lethargy was determined by the relative inactivity index (RII) from day 0 through day 7 post challenge; this period allowed for lethargy calculation throughout the period of active replication in the ferret respiratory tract. RII, sneezing and dyspnea were assessed each day prior to handling and sedation of the animals. Clinical signs assessment was consistent with previously established methods [325, 434]. Ferrets were monitored for 12

weeks post challenge and either challenged (UN-MOCK, UN-IFNA, and UN-IFNL groups) or rechallenged (PH-MOCK, PH-IFNA, and PH-IFNL groups) intranasally with 1mL PH ($4x10^5$ FFU/mL). Ferrets were monitored for seven days post challenge/rechallenge as listed above.

Vaccination-challenge study

The live-attenuated B-Yamagata lineage strain B/Phuket/3073/2013-CDC-LV11B (LAIV) was used as the vaccine for this study. Six groups of three ferrets per group were used for the vaccination-challenge study: Mock-vaccinated/mock-treated (UN-MOCK), mock-vaccinated/IFNA-treated (UN-IFNA), mock-vaccinated/IFNL3-treated (UN-IFNL), vaccinated/mock-treated (LAIV-MOCK), vaccinated/IFNA-treated (LAIV-IFNA), and vaccinated/IFNL3-treated (LAIV-IFNL). The ferrets were first anesthetized with KX and vaccinated intranasally with 1mL LAIV ($4x10^5$ FFU/mL) or PBS. Twenty-four hours post vaccination ferrets were anesthetized and 1uG/kG PEGylated-IFN (IFNA or IFNL) or PBS was introduced intranasally to the appropriate groups. Animals were monitored as in challenge-rechallenge study. At 12 weeks post vaccination, all animals were challenged intranasally with 1mL PH ($4x10^5$ FFU/mL). Ferrets were monitored for seven days post challenge as described previously.

Ferret sample collection and processing

Pre-challenge and on days (D) 1, 3, 5, and 7 post challenge or vaccination, nasal wash (NW) was collected from ferrets for virologic and gene expression. Additional NW samples (D0, D1, D2, D5, and D7) were collected after 3 months for the challenge-rechallenge study or the vaccination-challenge study. These collection timepoints correspond to typical viral kinetics observed in the upper respiratory tract of ferrets

infected with seasonal influenza viruses [438, 439]. Animals were sedated with KX followed by flushing the nares by instillation of 2 mL nasal wash solution (PBS, 1% BSA, antibiotics), inside a class-II biosafety cabinet, and collected when expelled in a Petri dish. NW was centrifuged (5 minutes, 2500 x g at 4°C), supernatant was stored at -80°C for virus titration. One hundred microliters (uL) PBS was added to NW pellets followed by 280uL of AVL lysis buffer. Samples were mixed 3-4 times and lysate was frozen at -80°C until RNA extraction. Carrier RNA was added to each sample and RNA was extracted using EZ1 DSP kit on a Qiagen EZ1 Advanced XL extractor according to the manufacturer's instructions (Qiagen, Germantown, MD, USA). RNA was eluted in 120 uL RNase-free water and stored at -80°C until evaluated for gene expression by qRT-PCR.

Blood samples were collected for gene expression (pre-challenge, D3 and D5; re-challenge D0, D1, D3, D5) and antibody/cytokine analysis (Pre-challenge, weeks 1, 2, 4, 8, 12 and D7 post-rechallenge). Blood was collected from the cranial vena cava and transferred to an SST tube (serum for antibody and cytokine analysis) and a K2/EDTA tube (cells for gene expression). Serum was separated from SST tubes by centrifugation for 10 minutes at 1500 x g at room temperature. For purification of peripheral blood mononuclear cells (PBMC), an equal volume of PBS was added to blood in K2/EDTA tubes and overlayed onto Histopaque®-1077 (Sigma, St. Louis, MO, USA). Samples were centrifuged with no brake at 900 x g for 20 minutes at room temperature. Cells were collected from the Histopaque® interface, washed with cell culture media (RPMI-1640, 10% heat-inactivated fetal bovine serum (FBS)) and treated with ammonium chloride to lyse any remaining red blood cells. The final cell pellet was resuspended in 1 mL cell

culture medium. Two hundred eighty uL of AVL lysis buffer were added to 200 uL PBMC samples in cell culture medium obtained by density gradient centrifugation over ficoll-hypaque. Samples were mixed 3-4 times and lysate was frozen at -80°C until RNA extraction. Carrier RNA was added to each sample and RNA was extracted using EZ1 DSP kit on a Qiagen EZ1 Advanced XL extractor according to the manufacturer's instructions (Qiagen, Germantown, MD, USA). RNA was eluted in 120 uL RNase-free water and stored at -80°C until evaluated for gene expression by qRT-PCR. The remaining PBMC sample was cryopreserved in FBS, 10% DMSO and stored in the vapor phase of liquid nitrogen.

Virus kinetics assessment by Focus Forming Assay

NW samples collected from influenza virus-infected and vaccinated ferrets were tested for virus with a Focus Forming Assay (FFA), as previously described [416]. Briefly, ½-log serially diluted influenza viruses in virus growth medium plus trypsin (DMEM, 0.1% BSA, 1 uG/mL TPCK-treated trypsin (Sigma, St. Louis, MO, USA)) were added to confluent monolayers of MDCK-SIAT1 cells [380] in 96-well flat-bottom tissue culture plates in quadruplicate. Following a two-hour incubation at 37°C, and overlay of 1.2% Avicel RC/CL [384] (Type: RC581 NF; FMC Health and Nutrition, Philadelphia, PA, USA) in 2X MEM containing 1 uG/mL TPCK-treated trypsin, 0.1% BSA, and antibiotics] was added. Plates were incubated overnight at 37°C, 5% CO_2 , fixed, permeabilized, and stained with a monoclonal antibody pool to influenza B nucleoprotein (International Reagent Resource; www.internationalreagentresource.org). Infectious foci (spots) were visualized using TrueBlue substrate (Sera Care, Inc., Milford, MA, USA). The foci enumerated using a CTL Bio Spot Analyzer with ImmunoCapture 6.4.87

software (CTL, Shaker Heights, OH, USA). The FFA titer was determined by multiplying sample dilution which gave between one hundred to three hundred spots by the spot number at that dilution, to obtain the Focus Forming Units per milliliter (FFU/mL). The foci in the cell control were subtracted and number of foci remaining was multiplied by twenty to give FFU/mL. The limit of detection was $10^{1.3}$ FFU/mL.

Neutralizing antibody responses by Focus Reduction Assay

The Focus Reduction Assay (FRA), initially developed by the WHO collaborating Centre in London, United Kingdom, was modified and utilized in this study as previously described [450]. Two-fold serially diluted Receptor Destroying Enzyme – treated sera [381] from vaccinated or infected ferrets was added to 96-well plates containing Confluent MDCK-SIAT1 cells [380]. Afterwards, standardized B/Phuket/3073/2013 virus was added to each plate or media to cell control wells. The virus was standardized by FFA [416] to determine the FFU/mL. Following a 2Hr incubation, an overlay containing Avicel [384] and 1 uG/mL TPCK-treated trypsin, 0.1% BSA, and antibiotics was added to each well. Plates were incubated overnight at 37°C, 5% CO_2. The overlays were removed, washed with PBS, fixed with ice-cold 4% (w/v) paraformaldehyde in PBS (10% formalin), and permeabilized with 0.5% Triton X-100 in PBS/glycine. An incubation with primary antibody pool against influenza B nucleoprotein [435] (www.internationalreagentresource.org) was performed, washed, followed by an incubation with secondary goat anti-mouse peroxidase-labelled IgG (Sera Care, Inc., Milford, MA, USA). Plates were washed and infectious foci (spots) were visualized using TrueBlue substrate (Sera Care, Inc., Milford, MA, USA) containing 0.03% H_2O_2. Plates were rinsed with deionized water, dried, and foci enumerated using a CTL Bio Spot

Analyzer with ImmunoCapture 6.4.87 software (Cellular Technology Ltd., Shaker Heights, OH, USA). The FRA titer was reported as the reciprocal of the highest dilution of serum corresponding to 50% foci reduction compared to the virus control (VC) minus the cell control (CC).

Gene Expression in ferret cells

Ferret primers generated to pro-inflammatory (*MCP1, IL-1B, IL-6),* Th1 (*CXCL10*), Th2 directed (*IL-2*), Treg (*TGFB1*), Teff (*IL-4*, *IL-12p40*, *IL-17*), apoptosis (*Granzyme A*), Type-I/II/III interferons (*IFNA, IFNB, IFNG, IFNL3*), interferon responses (*STAT1, STAT2, STAT3, RIG-I, SOCS3, TSLP)* and housekeeping (*GAPDH*) genes were used. For genes using TaqMan, probes were modified with 6-FAM, fluorescein amidites (FAM) fluorophore on the 5' end and a non-fluorescent Black Hole Quencher®-1 (BHQ-1) on the 3' end. Additionally, a locked nucleic acid at adenine <LNA A> was incorporated in all probes in order to increase template binding strength for real-time PCR [387]. Primers and probes for all ferret genes were generated from published ferret sequences [5, 390, 391, 416]. All primers and probes used in these experiments were generated in a previous study [416]; listed in Table 2.1.

Quantitative real time PCR (qRT-PCR) was performed using an ABI 7500 Fast Dx Real-Time PCR instrument (Applied Biosystems, Waltham, MA, USA). PCR reactions were performed in a 5 microliter RNA reaction volume using SYBR™GreenER™ qPCR SuperMix (Applied Biosystems) or SuperScript™ III Platinum™ One-Step qRT-PCR Kit for TaqMan reactions (InvivoGen, San Diego, CA, USA). An RT reaction for 30 minutes at 50°C, inactivation for 2 minutes at 95°C, followed by 40 amplification cycles at an annealing temperature of 50°C. Reactions were

performed on three ferrets for each virus and timepoint and the values were normalized by subtracting the mean value of the cycle threshold (C_T) from that of the C_T for glyceraldehyde-3-phosphate dehydrogenase (GAPDH) housekeeping gene (ΔC_T). The relative levels of gene expression for infected cells were determined by subtracting the individual ΔC_T values from that of average ΔC_T values of pre-infection cells ($\Delta\Delta C_T$) and expressing the final quantification values ($2^{-\Delta\Delta CT}$) as relative fold changes. Genes upregulated $>10^4$-fold (>10,000) were given a value of 10,000 and genes downregulated $<10^{-4}$-fold (<0.0001) were given a value of 0.0001.

Assessment of cytokines and chemokines in ferret sera

Sera were collected from ferrets on day 0 (pre-challenge/vaccination) and weekly (1, 2, 4, 8, and 12) post challenge/vaccination as well as one week following 3-month re-challenge, challenge, or vaccination (R7). Samples were stored at -80°C until testing by multiplex, bioassay, or ELISA as described below. All cytokine/chemokine values were normalized to pre-challenge/vaccination (day 0) to account for basal levels of each analyte and to observe effects of IBV and adjuvants.

Type-I/II IFN (IFNB and IFNG), TH1/TH2 (IP-10 and IL-2), pro-inflammatory (MCP-1, MIP-1B, TNFA, IL-6, IL-8 and IL-23) and T-effector (IL-4, IL-17, IL-12p40, and IL-12p70) levels in ferret sera were tested using a multiplex Luminex Assay kit [Ampersand Biosciences (www.ampersandbio.com) Lake Clear, NY, USA] containing ferret-specific antibodies and proteins in a microsphere-based assay and consisting of antigen-specific antibodies covalently coupled to magnetic Luminex beads and biotinylated detection antibodies in a capture-sandwich format as previously described [416].

The assay was analyzed using a Luminex 200 Analyzer [Luminex Corporation (www.luminexcorp.com)], Austin, TX, USA]. The cytokine/chemokine results were determined by extrapolating the analyte concentration from the measured mean fluorescence intensity (MFI) value using the standard curve. Results were generated and extracted using the RBM Plate Reader and Plate Viewer analysis software, respectively. Data were exported with values represented to two significant figures and analyzed in GraphPad Prism 10 (GraphPad Software, La Jolla, CA, USA).

Ferret Type-III IFN (IFNL) was detected in serum using a HEK-Lambda reporter cell assay (HEK-Blue™ cells, InvivoGen, San Diego, CA, USA) and calculated from a standard curve using recombinant ferret IFNL3 [Kingfisher Biotech (www.kingfisherbiotech.com), St. Paul, MN, USA]. This assay was modified and tested for detection of ferret IFNL [416]. The limit of detection was 100 pg/mL.

Thymic Stromal Lymphopoietin (TSLP) was detected in ferret sera using a commercially available human TSLP Quantikine® ELISA Kit [R&D Systems (www.rndsytems.com), Minneapolis, MN, USA] according to manufacturer's instructions. Ferret TSLP protein sequence available (NCBI BLAST Accession number XP_044943037.1) showed a 62.7% sequence homology to human TSLP protein (NCBI BLAST Accession number AAH40592.1); however, the homology may be greater since the ferret sequence was of low quality.

Statistical analysis

GraphPad Prism 10 was used for all statistical analyses (GraphPad Software, La Jolla, CA, USA). One-way ANOVA was used to determine differences over time between groups and significance between groups was determined by 2-way ANOVA

analysis. Gene expression analysis was performed from three ferrets per group. Spearman (1-tailed, 95% confidence) correlation method used for comparison of protein concentration (multiplex, bioassay, or ELISA) and antibody levels (FRA) for each treatment group to observe an increase or decrease in association. Multiple Student's t tests were used to assess the statistical differences between timepoints and treatment groups. A p-value of <0.05 was considered statistically significant: * $p<0.05$, ** $p<0.01$, ***$p<0.001$, ****$p<0.0001$.

RESULTS

Virus replication kinetics is affected by timing of PEGylated-IFN administration following IBV infection in ferrets.

Recombinant ferret IFNA and IFNL3 were PEGylated and used as immunoadjuvants in challenge-rechallenge and vaccination-challenge studies. PEGylation of the proteins was successful as demonstrated by bonding patterns of PEG to ferret IFNs, as visualized by imperial and silver staining, and retained activity following storage at 4°C or freeze/thaw following storage at -80°C (supplemental figure 5.S1). Even though PEG-IFNL3 activity was determined (supplemental figure 5.S1-D), PEG-IFNA activity could not be determined using HEK-Blue™ Type I interferon reporter cells in a bioassay due to inability to detect Type I ferret IFN, as well as cross-reactivity of type-III IFNs in the assay (Supplemental figure 5.S1-C).

A preliminary study was performed to determine the optimal time to add PEG-IFN post IBV challenge, 12 adult ferrets were intranasally challenged with PH followed by intranasal treatment with PEGylated-IFNA or -IFNL at 8Hr, 24Hr or 48Hr post-

infection. Administration of IFNA at 8Hr post infection resulted in a significant reduction in influenza virus kinetics compared to addition at 24Hr ($p=0.047$) or 48Hr ($p=0.0154$) post-infection (Figure 5.1). Significant differences in virus titers were also observed at 48Hr after IFNA and IFNL addition following IBV infection ($p=0.013$). Overall, administration of IFNs at 24h post-infection was the optimal time to treat ferrets and minimize the effects on virus replication.

IFN treatment reduced morbidity in ferrets following IBV challenge and re-challenge.

The addition of PEGylated-IFN as an immunoadjuvant following influenza virus infection stimulates both innate and adaptive immune responses. Day 1 post-challenge ferrets administered PEG-IFNA or PEG-IFNL and then intranasally infected had no clinical signs or detectable 5.virus in the upper respiratory tract (URT) over 7 days of observation (Table 5.1A). Three months post challenge, animals were either rechallenged (PH groups) or challenged (UN groups) with PH and assessed for 7 days (Table 5.1B). The mock-challenged animals (UN-MOCK/IFNA/IFNL) did not have any detectable lethargy, fever, or weight loss, regardless of treatment. Following virus challenge, IFN (PH-MOCK) had signs of severe morbidity. The untreated ferrets were lethargic (RII=1.18) compared to IFNA-treated (RII=1.14) and IFNL-treated (RII=1.01) ferrets. Additionally, PH-MOCK ferrets were observed sneezing on D2 and D3 post challenge. However, although PH-IFNL treated ferrets had no observable clinical signs (RII=1.01), both the IFNL- and mock-treated ferrets developed fever at D2 post-challenge. Additionally, the IFNL treated ferrets had the greatest weight loss (3.2%) post-challenge, even though the animal activity was normal. Interestingly, no fever was observed in the

IFNA treated animals. Following challenge, IFNA treated ferrets had significantly higher viral nasal wash titers in the URT than un-treated ferrets (p=0.0223). In contrast, there was no significant difference in viral titers between PEG-IFNA and PEG-IFNL treated animals (Table 5.1A). Following rechallenge there were no significant differences in viral titers between ferrets any group (Table 5.1B). Ferrets, previously treated with IFNs, and subsequently challenged had no differences in observed clinical signs, except in MOCK treated ferrets that had fever (Table 5.1B; UN-Tx groups). Both untreated (UN-MOCK) and IFNA treated (UN-IFNA) developed fever on D2, however, no fever was observed following IFNL treatment (UN-IFNL) (supplementary Figure 5.S2 (A-D)). Taken together, IFN-treated ferrets had overall fewer signs of lethargy and had more rapid recovery from infection than untreated animals.

IFN treatment induced only an early inflammatory response in ferret URT but robust IFN and inflammatory responses in PBMC following initial IBV challenge which was sustained following rechallenge.

Differential gene expression by qRT-PCR was performed on cells of the URT (NW cells) and PBMC following IBV challenge and treatment with IFNs (Figure 5.2). For samples collected from the URT following challenge or rechallenge, IFNA-treated ferrets had the highest gene expression of TH1 (*CXCL10*) and interferon response (*SOCS3*) compared to IFNL and MOCK treated ferrets (Figure 5.2A). No detectable IFN genes (*IFNA, IFNB, IFNG, IFNL3*) were upregulated in any ferrets in the URT at D3 or D5 post-challenge. Concurrently, *SOCS3* was upregulated in all ferrets. Upon rechallenge at 3 months an early upregulation of TH1 (*CXCL10*), TH2 directed response (*IL-2*), T-effector (*IL-17*), apoptosis (*Granzyme A*), pro-inflammatory (*IL-1B*), and IFN (*IFNL3*)

genes was detected in IFN-treated ferrets and was sustained through D5 post rechallenge. IFNL-treated ferrets had, in general, strong upregulation of all genes examined.

There was upregulation of type-I/II IFNs at D3 and type-I/II/III IFNs at D5 in PBMC collected from IFN-treated ferrets (Figure 5.2B). Type-I IFN expression levels at D3 and D5 were lower in mock treated ferrets. There were equal levels of type-II IFN at D3 and type-III IFN at D5 in IFNL-treated animals. For inflammatory (*MCP-1*) and pro-inflammatory (*IL-1B*) genes, the responses were upregulated early (D3) in IFN-treated ferrets and peaked late (D5) in mock-treated ferrets. Following rechallenge at 3 months post-treatment, inflammatory, TH1, TH2 directed, IFN, and TSLP genes were all upregulated early (D1) in IFN-treated ferrets and sustained through D5. In contrast, upregulation of the same responses in mock-treated ferrets occurred at (D3), which was only transiently expressed and down-regulated by D5. IFN (*IFNL3*) gene was only upregulated at D5 (1.3-fold) in mock-treated ferrets. IFN-treated ferrets had the highest overall gene upregulation post challenge and D3/D5 post rechallenge. This overall expression was sustained following rechallenge in previously IFN-treated ferrets, whereas in mock-treated ferrets, overall gene expression was only transiently upregulated (D3) following rechallenge.

Serum cytokines and chemokines levels are elevated in IBV-infected ferrets following IFN treatment.

Ferrets challenged with IBV or treated with IFNA or IFNL for 12 weeks, and then rechallenged had elevated serum cytokine and chemokine levels one week following rechallenge (Figure 5.3). Type-I IFN (IFNB) levels were highest in IFNA-treated ferrets and lowest in untreated animals (Figure 5.3A). However, there were no differences

between the two sets of ferrets. IBV challenge did not result in differences between sets of ferrets. There was variable serum levels of Type-II IFN (IFNG) in both IBV-challenged and mock-challenged ferrets. Type-III IFN (IFNL) levels were only detectable in IFN-treated ferrets with the highest levels occurring in IFNL-treated ferrets following IBV-challenge and rechallenge. Following IBV challenge, IFN- (IFNA and IFNL) treated ferrets had the highest levels of TSLP following rechallenge.

TH1 response (IP-10), Th2 directed response (IL-2) and chemokines (MCP-1 and MIP1B) were also elevated in IFN-treated ferrets compared to untreated animals (Figure 5.2B). However, Th1 (IP-10) levels were highest untreated ferrets challenged at 3 months (7R, dotted blue line). These ferrets had inflammatory responses, such as a fever of +3.2°F temperature over baseline. T-effector responses were higher for IL-4 following IBV-challenge and IFN-treatment early at 1-week post-challenge (Figure 5.2C). In contrast, these responses were suppressed in untreated Ferrets although the levels were generally low. Cytokines, IP-10 and IL-12p40, associated with influenza severity [457, 458] were only observed in untreated ferrets challenged at 3 months (7R, dotted blue line). Pro-inflammatory levels were generally suppressed in collected sera following IBV challenge or rechallenge except for IL-8 and IL-23, which were highest following IFNA-treatment (Figure 5.2D). Serum IFNs and other cytokines and chemokines were highest in IFN-treated animals, which were consistent with gene expression observed in IFN-treated ferrets.

IFN treatment did not affect IBV-LAIV vaccine replication but reduced morbidity in ferrets following IBV challenge.

Ferrets were either vaccinated intranasally with live-attenuated influenza vaccine, B/Phuket/3073/2013-CDC-LV11B (LAIV) or mock vaccinated (UN). One day post vaccination, PEG-IFNA, PEG-IFNL or PBS (mock) was administered intranasally (3 ferrets per group). For mock-vaccinated (UN-Tx) ferrets (Table 5.2A), there was no lethargy or adverse effects of IFN treatment. Following vaccination (LAIV-Tx), there was no lethargy or fever observed, regardless of treatment. Ferrets administered IFNL (LAIV-IFNL) had little weight loss. IFN treatment did not affect LAIV replication in the URT or the virus kinetics following infection between these two sets of ferrets (p=ns, 2-way ANOVA).

IFNL treated animals showed modest weight loss following influenza virus challenge at 3 months post-vaccination. No ferrets had clinical signs of infection (supplementary Figure 5.S2 (E and F)) and little virus was detected in the nasal washes post challenge (supplementary Figure 5.S2 (G and H)). No differences in virus kinetics were observed between the two sets of ferrets (ns, 2-way ANOVA).

IFN treatment induced early IFN and inflammatory responses in ferret URT but not in PBMC following IBV-LAIV vaccination, but IFNL response was sustained following challenge.

Differential gene expression by qRT-PCR was performed on cells of the URT (NW cells) and PBMC following IBV-LAIV vaccination and treatment with IFNs (Figure 5.4). IFNA-treated ferrets had the highest expression of TH1 (*CXCL10* gene) and interferon response (*SOCS3* gene) in NW cells from the URT following vaccination and challenge compared to ferrets administered IFNL- or mock ferret groups (Figure 5.4A). These results were similar to the gene expression profiles in ferrets infected with

B/Phuket/3073/2013 (PH) in the challenge-rechallenge ferret groups. Type-I/II IFN genes were all downregulated, however, type-II(*IFNG*) and type-III (*IFNL3*) were upregulated in IFNL-treated and IFNA-treated ferrets at D3 and D5 post-vaccination. The *SOCS3* gene was upregulated in all ferrets following vaccination and challenge. IFN-treated ferrets showed persistent, highly upregulated TH1 (*CXCL10*) and IFN-response (*SOCS3*) genes following challenge. Pro-inflammatory (*MCP1)* was upregulated by D5 post vaccination and D3 post challenge in IFNA-treated ferrets but sustained in mock treated ferrets throughout vaccination and challenge.

Unlike the challenge-rechallenge study, there is an upregulation of only type-I IFNs at D3 in the PBMC collected from IFNA-treated ferrets following vaccination (Figure 5.4B). Type-III IFN (*IFNL3*) and IFN response (*TSLP*) genes were upregulated only in IFNL-treated and mock-treated ferrets post vaccination. Other inflammatory, such as TH1/TH2 directed and IFN (*IFNB, IFNG*) genes, were expressed at the highest levels in mock-treated ferrets. Following challenge at 3 months post-vaccination, IFN-treated ferrets had high and sustained expression of inflammatory (*MCP1*), type-III IFN (*IFNL3*), IFN response (*RIG-I* and *TSLP*) compared to mock-treated ferrets that had sustained expression of TH1/TH2, T-effector, and IFN (*IFNA*) genes. Unlike the sustained upregulated expression of inflammatory and IFN genes in IFN-treated animals following IBV challenge-rechallenge, responses following LAIV-vaccination and challenge had a weaker inflammatory response in IFN-treated ferrets. However, type-III IFN (*IFNL3*) and inflammatory (*MCP1*) genes were sustained in IFN-treated animals. Interestingly, mock-treated vaccinated ferrets exhibited earlier inflammatory responses post-challenge compared to mock-treated rechallenged ferrets in the challenge-

rechallenge study. In the previous study, mock-treated rechallenged ferrets had a transient inflammatory response on D3.

IFN treatment did not enhance serum cytokine and chemokine levels following IBV-LAIV vaccination and challenge in ferrets.

Serum cytokine and chemokine levels were evaluated in ferrets following IBV-LAIV vaccination and treatment with IFNA or IFNL3 for 12Wk and 1Wk following challenge [Figure 5.5]. Analyte levels were normalized to pre-vaccination (D0) levels to determine whether cytokine and chemokines were either increased or decreased from pre-vaccination levels. IFN levels were similar to levels detected over a 12-week period following vaccination in all ferrets regardless of treatment (Figure 5.5A). However, TSLP levels were consistently higher in IFNA- and IFNL-treated animals. TH1 (IP-10) responses were consistently higher in IFNA-treated ferrets following LAIV-vaccination than IFNL- or mock (PBS)-treated animals (Figure 5.5B) that was consistent with the TH1 (*CXCL10)* gene expression responses observed in ferret NW cells. The kinetics of T-effector cytokines in IFN-treated ferrets were similar to mock (Figure 5.5C). IFNA- and mock-treated animals had increases in IL-4 and IL-17 within the first 1-2 weeks post-treatment and showed similar increases post challenge, whereas IFNL-treated ferrets had lower levels of both IL-4 and IL-17. Pro-inflammatory cytokines were similar for all ferrets (Figure 5.5D). Overall, IFN-treatment did not have an enhanced effect on cytokine and chemokine levels indicated following IBV-challenge.

IFN treatment following IBV challenge generated higher neutralizing antibody titers compared to IBV alone in ferrets following challenge and rechallenge.

Ferrets were infected with IBV (PH) followed by intranasal treatment with PEGylated type-I (IFNA), type-III (IFNL) IFN, or Mock (UN) and assessed for serum neutralizing antibodies to IBV by FRA (Table 5.3). For challenge-rechallenge study, all ferrets reached geometric mean titers (GMT) of >1:160 (bold) by week 4 that fell below 1:160 threshold by 12 weeks (Table 5.3A). IFNA- and IFNL-treated animals had higher titers than mock-treated ferrets at week 4 (IFNA/IFNL3=296, Mock=235) and week 8 (IFNA=296, IFNL=235, Mock=202) post-challenge. At 1 week post rechallenge, neutralizing titers in IFNA-Tx ferrets was 1.2 times higher (GMT=1016) and in IFNL3-treated ferrets it was 1.7 times higher (GMT=1493) than mock-treated animals (GMT=871). The effects of IFN-treatment on unchallenged animals were only slightly higher than mock-treated animals following challenge 12 weeks later, however, this did not result in neutralizing titers reaching the 1:160 threshold. IFN-treatment clearly showed higher neutralizing antibody levels for 4 to 8 weeks following IBV challenge compared to mock. IFN-treatment resulted in higher antibody responses following rechallenge over mock-treatment which may indicate a more robust adaptive immune response.

IFN treatment following LAIV vaccination generated higher neutralizing antibodies compared to mock treatment but did not result in higher antibody levels following challenge.

Ferrets were vaccinated with LAIV-IBV (LAIV) followed by intranasal treatment with PEGylated type-I (IFNA), type-III (IFNL3) IFN, or Mock (UN) and assessed for serum neutralizing antibodies to IBV by FRA (Table 5.3). For the vaccination study, (Table 5.3B) ferrets treated with IFN had a geometric mean neutralizing titers (GMT) of

>1:160 by 8 weeks post vaccination (IFNA-Tx = 218, IFNL-Tx=187). Interestingly, in the absence of vaccination (UN-PH), IFN-treated animals had neutralizing antibody titers >1:160 at 1-week post-challenge, even though these animals were treated with IFN 12 weeks earlier. IFN-treated ferrets failed to attain antibody titers greater than mock-treated animals following challenge of vaccinated ferrets. IFN-treatment did not result in higher neutralizing antibodies than mock-treatment following LAIV vaccination.

Serum TSLP directly correlated and IFN inversely correlated to neutralizing Ab responses in ferrets following IBV challenge-rechallenge or LAIV vaccination-challenge.

Next, serum cytokine levels were compared to neutralizing antibody responses in ferrets following IBV challenge or IBV vaccination (Table 5.4). Correlations, that include 3Mo rechallenge or post vaccination challenge are shown in supplementary Table 5.S2. There was a direct correlation between TSLP and neutralizing antibody response in both mock-treated (r=0.77) and IFNL-treated (r=0.71) ferrets following IBV challenge-rechallenge (Table 5.S2A). There was an inverse correlation between IFNG and neutralizing antibody response following IBV challenge and IFNA-treatment (Table 5.4A). Additionally, T-effector (IL-12p40) levels, inversely correlated with antibody responses following IBV challenge, regardless of treatment. Only mock-treated and IFNL-treated ferrets had an indirect correlation to antibody levels and pro-inflammatory cytokines (TNFA and IL-6) post-challenge and rechallenge. However, IL-8 was indirectly correlated with antibody responses, regardless of treatment (Table 5.S2A).

Correlations of cytokines to neutralizing antibodies are shown in Table 5.4B that include both 3 months rechallenge or 3 months post-vaccination challenge (supplemental

Table 5.S2B). Only TSLP had a strong direct correlation to neutralizing antibody in IFN-treated ferrets either post vaccination or 3 months post-challenge (Table 5.4 and Table 5.S2B). There was a correlation between neutralizing antibody and IFNL and a strong inverse correlation (r=-0.8) to the IFNA-treated ferrets both post-vaccination and vaccination-challenge.

DISCUSSION

When characterizing the innate immune responses of IAV and IBV infection of ferret primary respiratory tract cells, the expression of pro-inflammatory genes and IFNs were delayed and downregulated by IBV strains compared to IAV strains [416]. Subsequent studies of IAV and IBV infections of ferrets confirmed that a delay in initial innate responses resulted in weak antibody responses to IBV [450]. Due to these observations, the goal of this study was to determine whether addition of IFNs, as potential immunoadjuvants, could overcome the delay in the initial innate immune responses to IBV and boost the antibody response following infection or vaccination.

To boost the immune responses to IBV, PEGylated ferret IFNA and IFNL3 were chosen in both challenge-rechallenge and vaccination-challenge studies. Intramuscular treatment of ferrets with seasonal influenza vaccine plus human PEGylated IFNA2b stimulated innate interferon stimulating genes compared to vaccine alone [391]. A previous study, using intra-muscular treatment of ferrets with influenza vaccine plus PEGylated human IFNA2b (Unitron PEG, Schering-Plough), found that 1uG/Kg was sufficient to stimulate innate interferon stimulating gene responses to IAV compared to vaccine alone [391]. Previously, the innate immune responses in the URT of ferrets was

characterized. In this study, ferret IFNs were introduced intranasally in order to assess the effects directly on cells in the URT and determine the impact on virus replication, as well as downstream adaptive immune responses. Since, live-attenuated influenza vaccines were administered intranasally, IFN was also administered intranasally. By administering both virus and vaccine mucosally, coupled with the fact that IFNL is highly expressed on epithelial cells lining the respiratory tract, the immune responses could be assessed at the site of infection [459, 460]. Since IFNs are activated following influenza virus infection and affect influenza virus replication in mice and ferrets [461-463], initially ferrets were treated with IFN at various times in order to determine the minimal effect on virus replication, while still stimulating innate immune responses. Virus replication was reduced if PEG-IFNs were added within 8Hr post-challenge. However, if PEG-IFN was added 24Hr or later post-challenge, virus replication was not affected. In this study, following IBV infection in ferrets, IFN treatment resulted in reduced morbidity compared to untreated animals. Although animals treated with IFNL had greater weight loss than untreated ferrets, a clear difference in ferret activity post-challenge and vaccination was observed even in IFNA treated animals. For animals challenged with IBV 3 months following INF treatment, only mock and IFNA treated ferrets developed fever. This was an interesting observation since animals were only treated once with IFNs more than 3 months prior to challenge; however, some residual effect on the inflammatory response by IFNL may be evident. In fact, Type-III IFN has been shown to be anti-inflammatory [464]; however the long term effects of a single treatment have not been shown.

In the URT of IBV challenged animals, IFN-treatment induced early inflammatory responses and increased IFNL expression following rechallenge, but

PBMC had high and sustained upregulation of type-I/II/III IFNs following IBV challenge and rechallenge in IFN-treated animals. In the URT, *SOCS3* was upregulated in all ferrets and has been shown to down-modulate IFN signaling in a RIG-I dependent pathway to inhibit antiviral responses and suppress the inflammatory response [465-467]. Concurrently with IFN responses, only IFN-treated animals had elevated levels of type-I/II/III IFNs throughout infection and following rechallenge. This indicates that IFN-treatment can influence both IFN gene expression and serum cytokines levels following IBV infection that are otherwise suppressed and delayed. Viral infection in the respiratory tract IFNL is required for production of virus-specific IgG1, IgA, as well as generation of antiviral CD8+ T cells [137]. The mechanism behind this response affects IFNL triggering the synthesis of TSLP in upper airway M cells, which in turn influences germinal center responses by migrating DCs, thus allowing for enhancement of mucosal immunity and IAV resistance. Following IFNL-treatment of ferrets following IBV challenge or vaccination, there were increased *IFNL3* gene expression and protein levels that correlated to an increase in *TSLP* gene expression and protein levels in PBMC. Interestingly, IFNA-treatment also increased IFNL3 expression and TSLP protein following rechallenge. This induction may be due to an alternate, unknown mechanism of TSLP activation. Innate immune responses were activated following IFN-treatment that resulted in a strong sustained antibody response for 4 – 8 weeks following challenge. By week 12 post-vaccination, these ferrets had HAI activity less than 1:160 and animals were rechallenged with IBV to observe antibody recall responses and enhancement. For untreated ferrets, antibody titers to IBV increased 8.6-fold from 12-week levels (GMT from 1:101 to 1:871), which was 1 week after re-challenge. IFNA-treated animals had

higher antibody titers following rechallenge, however, these levels only increased 6.9-fold (GMT from 1:148 to 1:1016) from 12-week levels. IFNL-treated ferrets had the greatest increase in antibody responses (17.4-fold), from a GMT of 1:86 to 1:1493) following rechallenge.

For the vaccine-challenge study in ferrets, as in the challenge-rechallenge study, vaccine replication was not affected by IFN treatment. All ferrets were protected from challenge at 12 weeks post-vaccination, regardless of treatment during the time of vaccination. However, mock-vaccinated animals treated with IFN did show less morbidity than untreated ferrets, even though a single IFN treatment was given 12 weeks prior to challenge. Unfortunately, no differences in virus replication were observed in any of the ferrets. This indicates IFN may be used prophylactically to prevent increased morbidity following influenza infection. Prophylactic treatment of people with type-I or type-III IFN reduced the severity of influenza virus and other respiratory virus induced disease [468-470]. Following viral challenge, IFN-treated ferrets had high and sustained gene expression of *IFNL3* and *TSLP* in collected PBMC. However, IFN-treatment did not enhance cytokine effects that may be due, in part, to the protective responses elicited by the vaccine. Further exploration of the residual effects of IFN-treatment need to be determined in challenge studies at time points beyond 12 weeks post-vaccination.

There was a strong correlation between TSLP levels and antibody responses following IFN-treatment of ferrets in both challenge-rechallenge and vaccination-challenge studies. This indicates a possible biomarker for assessment of antibody responses following influenza infection or vaccination. Since TSLP responses are upregulated in conjunction with IFNL at D3 to D5 in PBMC following IBV infection,

TSLP responses could be used as a tool in predicting antibody outcome. Further analysis with different influenza vaccines is necessary to determine whether these markers could be used to assess vaccine efficacy.

Even though there was a benefit of IFN treatment of 1uG/kG on the immune responses in ferrets, additional treatments, as well as testing different concentrations and routes, may result in a greater benefit of IFN and generation of a more robust immune response. The development and availability of additional ferret immune reagents, especially antibodies to ferret IgA and ferret cell surface markers, will allow for a more in-depth analysis of the immune responses in the ferret model and aid in the development of improved vaccines and therapeutics.

The initial innate responses, especially the IFN response, following influenza virus infection or vaccination is important in the development of robust adaptive immune responses to protect from subsequent infection or lessen severity of disease. As with influenza viruses, other viruses are impaired by IFN signaling, and IFN treatment is a powerful therapeutic [471-474]. Due to the anti-inflammatory characteristics of type-III IFNs and lower toxicity in humans [475], IFNL may be advantageous over IFNA, which is inflammatory and shows greater adverse effects in humans [476, 477]. SARS-CoV-2 studies indicated that lower antiviral type-I and type-III expression and elevated IL-6 expression contributed to development of COVID-19 disease [473], suggesting the use of IFNA/B and IFNL [478] or JAK/STAT inhibitors [479] as potential therapeutics. Consequently, IFN-treatment, especially IFNL, may be an important consideration for use following influenza virus infection or as a potential immunoadjuvant to increase immunity to influenza (especially for influenza B virus) and other viral infections.

Figure 5.1: PEGylated IFN optimal time of addition following IBV Challenge.

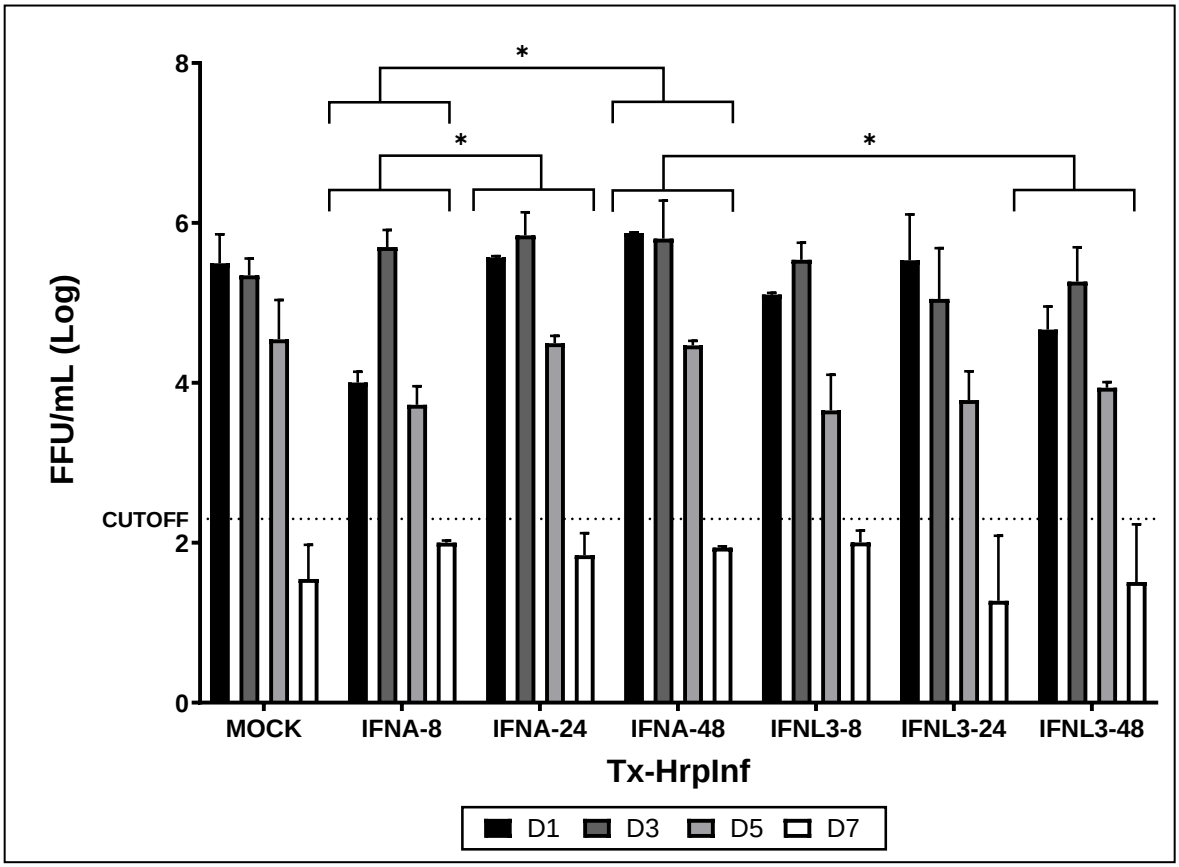

Kinetics of virus replication following IBV challenge and addition of PEGylated IFN. PEGylated IFNA added at 8Hr (IFNA-8), 24Hr (IFNA-24) or 48Hr (IFNA-48) post B/Phuket/3073/2013 challenge and compared to Mock treated group. PEGylated IFNL3 added at 8Hr (IFNL-8), 24Hr (IFNL-24) or 48Hr (IFNL-48) post challenge. Nasal wash titers determined on D1, D3, D5, and D7 post challenge (bar color indicating time of NW collection) and tested for virus Log FFU/mL by FFA. Significance between groups tested by 2-way ANOVA. Significant differences between IFNA-8 to IFNA-24 ($p=0.0470$) and IFNA-8 to IFNA-48 ($p=0.0154$) as well as IFNA-48 to IFNL-48 ($p=0.0130$). No significant differences noted between any groups with IFN added at 24Hr and no significance compared to Mock-treated group.

Table 5.1: Clinical signs and virus replication in IFN-treated ferrets following IBV challenge-rechallenge.

	Group-Tx	Inactivity[a] RII (D1-7)	Days Sneezing (%)	Average Weight loss[b] (D1-7)	Average Fever[c] (Max Day)	NW viral load[d] (Avg±SD Log_{10} FFU/mL) D1	D3	D5	D7
A)CHALLENGE	UN-MOCK	1.00	-	-	+2.1°F (D1)	N/A	N/A	N/A	N/A
	UN-IFNA	1.00	-	-	-	N/A	N/A	N/A	N/A
	UN-IFNL	1.00	-	-	-	N/A	N/A	N/A	N/A
	PH-MOCK	1.18	D2-D3 (33)	0.6%	+2.3°F (D2)	3.51±0.95	5.37±0.23	4.27±0.67	1.30±0.00
	PH-IFNA	1.14	-	1.2%	-	4.97±0.47	5.45±0.43	4.34±0.53	2.26±0.83
	PH-IFNL	1.01	-	3.2%	+2.9°F (D2)	4.82±0.31	5.38±0.02	4.03±0.06	1.80±0.86
B)CHALLENGE/ RECHALLENGE (3MO)	UN-MOCK	1.02	D2 (33)	3.3%	+3.2°F (D2)	5.50±0.36	5.34±0.21	4.54±0.49	1.55±0.43
	UN-IFNA	1.04	D2 (33)	6.6%	+2.5°F (D2)	5.32±0.42	5.42±0.38	4.83±0.28	1.74±0.16
	UN-IFNL	1.04	D2 (66)	1.6%	-	5.49±0.33	5.53±0.50	4.97±0.38	2.13±0.25
	PH-MOCK	1.05	D2-D3 (33)	0.1%	-	2.35±0.21	2.03±0.38	1.82±0.46	2.24±0.26
	PH-IFNA	1.01	-	-	-	2.12±0.40	2.57±0.33	2.35±0.34	2.42±0.44
	PH-IFNL	1.00	-	-	-	2.08±0.62	2.30±0.88	1.92±0.48	2.47±0.51

Clinical signs and virus replication in the URT of ferrets challenged with B/Phuket/3073/2013 (PH) followed by IFN treatment (or Mock) on D1 post challenge. Group designated as "UN" were mock challenged and groups designated as "PH" were challenged with IBV (PH). A) Initial challenge clinical signs and virus replication. Groups above the dotted line were mock-challenged with PBS and groups below the dotted line were challenged with PH. NW viral loads listed as N/A for mock-challenged groups. B) At 3 months post challenge, all groups were challenged (above the dotted line, UN) or rechallenged (below the dotted line, PH) with PH.

[a]Relative inactivity index "RII" (D1 – D7) post challenge. RII=$\sum_{(D1-7)}[score+1]n/\sum_{(D1-7)}n$

[b]Day post challenge of peak weight loss percentage (day) from pre-challenge weight from D1 – D7 post challenge.

[c]Average elevated temperature of at least +2°F (Fever) above baseline (days post challenge elevated). Fever indicated by any temperature greater than the average baseline (D-2 to D0 pre-challenge) +2°F.

[d]Average viral load in ferret URT on D1 through D7 post challenge. Peak viral load in bold. Baseline = 1.30 Log_{10} FFU/mL.

Figure 5.2: Gene expression in IFN-treated ferret URT and PBMC following IBV challenge-rechallenge.

A)URT

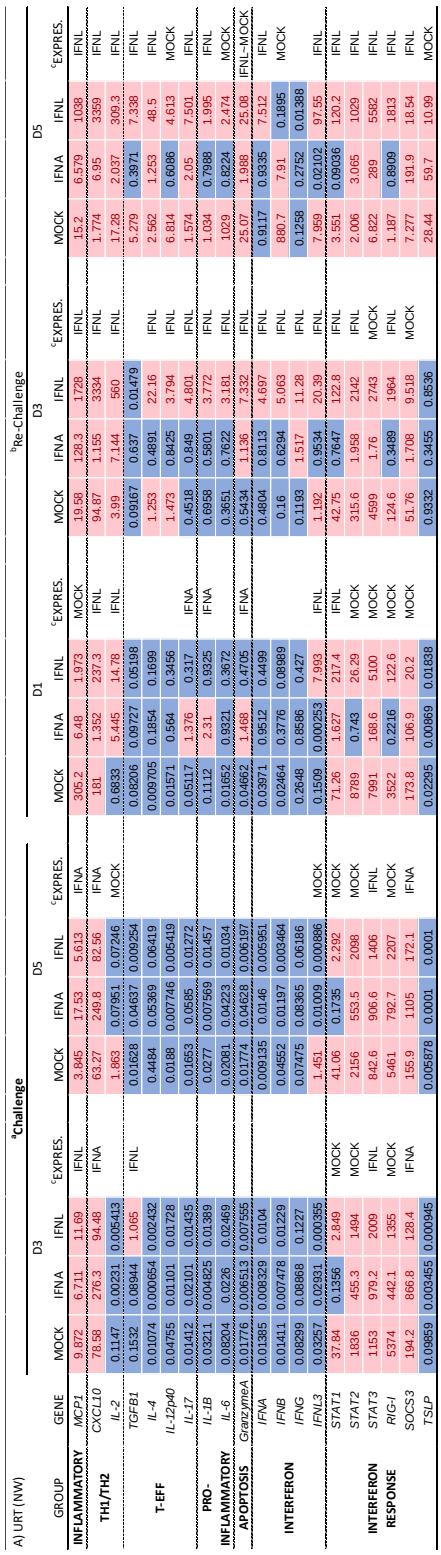

A) URT (NW)		[a]Challenge							[b]Re-Challenge									
		D3				D5			D1			D3			D5			
GROUP	GENE	MOCK	IFNA	IFNL	[c]EXPRES.	MOCK	IFNA	IFNL	[c]EXPRES.	MOCK	IFNA	IFNL	[c]EXPRES.	MOCK	IFNA	IFNL	[c]EXPRES.	MOCK	IFNA	IFNL	[c]EXPRES.
INFLAMMATORY	*MCP1*	9.872	6.711	11.69	IFNL	3.845	17.53	5.613	IFNA	305.2	6.48	1.973	MOCK	19.58	128.3	1728	IFNL	15.2	6.579	1038	IFNL
	CXCL10	78.58	276.3	94.48	IFNA	63.27	249.8	82.56	IFNA	181	1.352	237.3	IFNL	94.87	1.155	3334	IFNL	1.774	6.95	3359	IFNL
TH1/TH2	*IL-2*	0.1147	0.00231	0.005413	MOCK	1.863	0.07951	0.07246	MOCK	0.6833	5.445	14.78	IFNL	3.99	7.144	560	IFNL	17.28	2.037	309.3	IFNL
	TGFB1	0.1532	0.08944	1.065	IFNL	0.01628	0.04637	0.009254		0.08206	0.09727	0.05198		0.09167	0.637	0.01479		5.279	0.3971	7.338	IFNL
	IL-4	0.01074	0.000654	0.002432		0.4484	0.05369	0.06419		0.009705	0.1854	0.1699		1.253	0.4891	22.16	IFNL	2.562	1.253	48.5	IFNL
T-EFF	*IL-12p40*	0.04755	0.01101	0.01728		0.0188	0.007746	0.005419		0.01571	0.564	0.3456		1.473	0.8425	3.794	IFNL	6.814	0.6086	4.613	MOCK
	IL-17	0.01412	0.02101	0.01435		0.0163	0.0585	0.01272		0.05117	1.376	0.317	IFNA	0.4518	0.849	4.801	IFNL	1.574	2.05	7.501	IFNL
PRO-	*IL-1B*	0.03211	0.004825	0.01389		0.0277	0.007569	0.01457		0.1112	2.31	0.9325	IFNA	0.6958	0.5801	3.772	IFNL	1.034	0.7988	1.995	IFNL
INFLAMMATORY	*IL-6*	0.08204	0.0226	0.02469		0.02081	0.04223	0.01034		0.01652	0.9321	0.3672		0.3651	0.7622	3.181	IFNL	1029	0.8224	2.474	MOCK
APOPTOSIS	*Granzyme A*	0.01776	0.006513	0.007555		0.01774	0.04628	0.006197		0.04662	1.468	0.4705	IFNA	0.5434	1.136	7.332	IFNL	25.07	1.988	25.08	IFNL=MOCK
	IFNA	0.01385	0.008329	0.0104		0.009135	0.0146	0.005951		0.03971	0.9512	0.4499		0.4804	0.8113	4.697	IFNL	0.9117	0.9335	7.512	IFNL
	IFNB	0.01411	0.007478	0.01229		0.04552	0.01197	0.003464		0.02464	0.3776	0.08989		0.16	0.6294	5.063	IFNL	880.7	7.91	0.1895	MOCK
INTERFERON	*IFNG*	0.08299	0.08868	0.1227		0.07475	0.08365	0.06166		0.2648	0.8586	0.427		0.1193	1.517	11.28	IFNL	0.1258	0.2752	0.01388	
	IFNL3	0.03257	0.02931	0.000355	MOCK	1.451	0.01009	0.000886	MOCK	0.1509	0.000253	7.993	IFNL	1.192	0.9534	20.39	IFNL	7.959	0.02102	97.55	IFNL
	STAT1	37.84	0.1356	2.849	MOCK	41.06	0.1735	2.292	MOCK	71.26	1.627	217.4	IFNL	42.75	0.7647	122.8	IFNL	3.551	0.09036	120.2	IFNL
	STAT2	1836	455.3	1494	MOCK	2156	553.5	2098	MOCK	8789	0.743	26.29	MOCK	315.6	1.958	2142	IFNL	2.006	3.065	1029	IFNL
INTERFERON	*STAT3*	1153	979.2	2009	IFNL	842.6	906.6	1406	IFNL	7991	168.6	5100	MOCK	4599	1.76	2743	MOCK	6.822	289	5582	IFNL
RESPONSE	*RIG-I*	5374	442.1	1355	MOCK	5461	792.7	2207	MOCK	3522	0.2216	122.6	MOCK	124.6	0.3489	1964	IFNL	1.187	0.8909	1813	IFNL
	SOCS3	194.2	866.8	128.4	IFNA	155.9	1105	172.1	IFNA	173.8	106.9	20.2	MOCK	51.76	1.708	9.518	MOCK	7.277	191.9	18.54	IFNL
	TSLP	0.09859	0.003455	0.000945		0.005878	0.0001	0.0001		0.02295	0.00869	0.01838		0.9332	0.3455	0.8536		28.44	59.7	10.99	MOCK

B)PBMC

B) PBMC		[a]Challenge							[b]Re-Challenge											
		D3				D5			D1				D3				D5			
GROUP	GENE	MOCK	IFNA	IFNL	[c]EXPRES.	MOCK	IFNA	IFNL	[c]EXPRES.	MOCK	IFNA	IFNL	[c]EXPRES.	MOCK	IFNA	IFNL	[c]EXPRES.	MOCK	IFNA	IFNL	[c]EXPRES.
INFLAMMATORY	*MCP1*	41.6	3.09	26.05	IFNL	109.3	6.441	70.44	MOCK	0.3558	506.2	0.6539	IFNA	5.132	0.1041	0.7898	MOCK	0.06565	.3316	0.6273	IFNA
	CXCL10	0.4828	30.37	0.4833	IFNA	0.196	29.4	0.3442	IFNA	0.5829	1.28	1.386	IFNA=IFNL	0.6698	0.8712	1.53	IFNL	0.6564	3.291	2.783	IFNA
TH1/TH2	*IL-2*	1.61	1.263	2.49	IFNL	1.182	2.512	2.904	IFNL	0.4604	2.06	1.117	IFNA	1.72	0.2156	0.993	MOCK	0.4702	16.81	1.191	IFNA
	TGFB1	2.018	2.302	0.09398	IFNA	6.218	3.206	4.862	MOCK	0.7827	3.767	0.09269	IFNA	20.22	0.3125	1.933	MOCK	0.6026	15.9	1.565	IFNA
	IL-4	7.478	2.01	0.8149	MOCK	4.303	2.055	0.8962	MOCK	0.8862	6.195	0.7343	IFNA	6.303	0.7244	16.17	IFNL	0.2766	12.75	0.7578	IFNA
T-EFF	*IL-12p40*	1.93	57.37	6.655	IFNA	2.477	2.822	4.449	IFNL	0.4894	2.033	0.6761	IFNA	3.531	0.2504	0.9959	MOCK	1.313	10.65	1.065	IFNA
	IL-17	1.093	3.142	4.787	IFNL	1.857	3.696	3.644	IFNA=IFNL	0.4587	0.6033	1.097	IFNL	3.511	0.8372	1.019	MOCK	0.4743	10.51	1.691	IFNA
PRO-INFLAMMATORY	*IL-1B*	3.164	4.672	4.643	IFNA=IFNL	4.699	3.193	3.912	MOCK	0.5434	0.9187	1.306	IFNL	2.472	0.2186	1.205	MOCK	0.4291	9.531	1.441	IFNA
	IL-6	2.103	1.82	3.795	IFNL	2.469	2.656	3.644	IFNL	0.2677	0.7956	1.079	IFNL	2.898	0.177	0.8647	MOCK	0.3619	5.642	1.901	IFNA
APOPTOSIS	*Granzyme A*	1.105	6.653	4.691	IFNA	3.042	3.651	4.063	IFNL	0.2815	0.2996	1.583	IFNL	80.16	0.123	0.7139	MOCK	0.0838	9.21	1.494	IFNA
	IFNA	2.127	13.87	39.16	IFNL	3.815	2.352	4.473	IFNL	0.4259	0.3932	1.394	IFNL	3.949	0.2043	0.8495	MOCK	0.3471	6.936	1.532	IFNA
	IFNB	2.446	2.41	4.29	IFNL	2.488	2.7	3.175	IFNL	0.1709	0.805	1.956	IFNL	2.509	0.1985	1.408	MOCK	0.3916	6.847	2.485	IFNA
INTERFERON	*IFNG*	2.815	1.431	2.794	MOCK=IFNL	1.07	3.047	2.493	IFNA	0.6285	2.547	0.6987	IFNA	10.51	0.4902	1.719	MOCK	0.7005	26.73	1.394	IFNA
	IFNL3	0.077	0.09974	0.004948		1.637	1.275	0.00169	MOCK	0.02637	196.4	0.02196	IFNA	0.5301	0.02759	2.267	IFNL	1.264	334.3	0.03119	IFNA
	STAT1	0.7509	6.387	0.3962	IFNA	0.396	3.563	0.8028	IFNA	0.7784	0.6435	1.574	IFNL	1.559	0.6234	1.426	MOCK=IFNL	0.8806	2.804	2.483	IFNA=IFNL
	STAT2	0.1658	103	2.212	IFNA	0.3048	5.639	1.45	IFNA	0.7447	0.3113	2.024	IFNL	0.4	1.11	1.159	IFNA=IFNL	0.7082	2.057	4.432	IFNL
INTERFERON	*STAT3*	0.4677	4.166	0.5949	IFNA	0.5207	1.447	0.6459	IFNA	0.8128	0.4709	1.044	IFNL	0.6363	0.6176	0.9915		0.7627	2.184	1.711	IFNA
RESPONSE	*RIG-I*	0.5812	283.5	4.445	IFNA	0.0519	1.422	2.304	IFNL	6.979	0.9393	4.846	MOCK	0.5814	1.252	14.73	IFNL	2.094	1.001	15.68	IFNL
	SOCS3	0.4073	1119	1.436	IFNA	0.3133	60.86	1.059	IFNA	0.8341	0.429	0.9208		0.7764	0.7418	0.7683		0.7833	1.708	2.523	IFNL
	TSLP	22.95	2.764	62.84	IFNL	98.74	10.87	108.9	IFNL	0.02321	28.26	0.1173	IFNA	1.479	0.831	0.3263	MOCK	0.4759	358.1	4.149	IFNA

Average fold gene expression in IBV-infected ferrets following IFN-treatment. [a]Animals challenged with B/Phuket/3073/2013 and treated with IFNA, IFNL or mock on D1 post challenge. [b]IFNA, IFNL3 or mock treated animals rechallenged with B/Phuket/3073/2013 three months post challenge. [c]Expression (EXPRES.) indicates treatment group with highest gene expression increase at each given timepoint post challenge or re-challenge. Gene upregulation (positive fold-increase in gene expression over D0) indicated in pink and down-regulation of gene expression indicated in blue. Target gene functional groups are listed under GROUP and separated by dotted lines. A)Average fold gene expression in NW cells of the URT following IBV challenge or rechallenge. B)Average fold gene expression in PBMC following IBV challenge or rechallenge.

Figure 3: Cytokine and chemokine levels in sera of IFN-treated ferrets following IBV challenge and rechallenge.

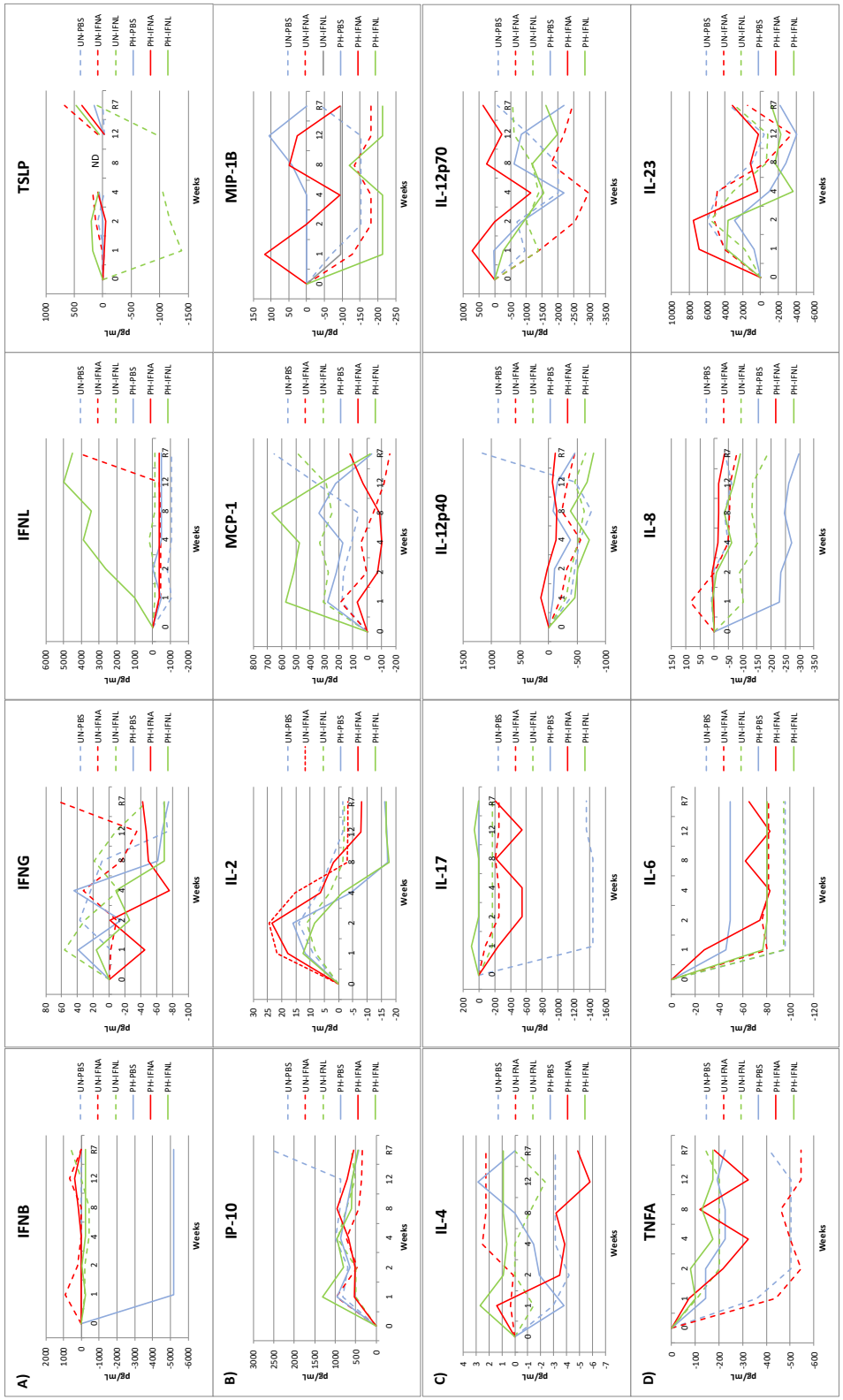

Serum cytokine and chemokine levels in IBV-infected ferrets following IFN-treatment. Mock-infected groups (UN-X) are represented by dotted lines and IBV-challenged groups (PH-X) are indicated by solid lines. Treatment groups are Mock (PBS, light blue), IFNA (red) and IFNL (green). The x-axis indicated the weeks post challenge or mock challenge (1, 2, 4, 8, 12) and after 3MO [day 7 (R7) post challenge or rechallenge]. Average pG/mL levels of analytes are shown from the following functional groups: A) Interferon responses. Type-I (IFNB), Type-II (IFNG) and Type-III* (IFNL) and Type-III IFN response cytokine (TSLP). B) TH1 (IP-10) and TH2 (IL-2) directed responses. C)Pro-inflammatory chemokines (MCP-1 and MIP-1B) D)T-effector response (IL-4, IL-17, IL-12p40 & IL-12p70) E)Pro-inflammatory cytokine response (TNFA, IL-6, IL-8, and IL-23). All levels of cytokines/chemokines are normalized to D0 and represent average increases or decreases from pre-challenge over a 12Wk period plus 1Wk (R7) challenge/rechallenge.

Table 5.2: Clinical signs and virus replication in ferrets following IBV vaccination and challenge.

	Group-Tx[a]	Inactivity[b] RII (D1-7)	Days Sneezing (%)	Average Weight loss[c] (D1-7)	Average Fever[d] (Max Day)	NW viral load[e] (Avg±SD Log_{10} FFU/mL) D1	D3	D5	D7
A) VACCINATION	UN-MOCK	1.00	-	0.8%	-	N/A	N/A	N/A	N/A
	UN-IFNA	1.00	-	-	-	N/A	N/A	N/A	N/A
	UN-IFNL	1.00	-	0.1%	-	N/A	N/A	N/A	N/A
	LAIV-MOCK	1.02	-	-	-	2.88±0.11	3.88±0.96	3.31±0.26	1.30±0.00
	LAIV-IFNA	1.04	-	-	-	2.96±0.11	4.26±0.56	4.06±0.96	1.72±0.73
	LAIV-IFNL	1.00	-	1.2%	-	3.24±0.21	5.17±0.24	3.48±0.37	1.68±0.67
B) CHALLENGE (3MO)	UN-MOCK	1.25	D2-D4 (33)	2.8%	+4.4°F (D2)	5.72±0.59	5.55±0.17	4.21±0.66	1.72±0.28
	UN-IFNA	1.01	-	4.1%	+3.5°F (D2)	5.19±0.99	5.52±0.33	3.83±0.34	1.53±0.39
	UN-IFNL	1.01	D3 (33)	1.4%	+2.3°F (D2)	5.53±0.76	5.35±0.32	4.31±0.51	2.08±0.26
	LAIV-MOCK	1.00	-	-	-	2.06±0.61	1.47±0.30	2.06±0.67	1.90±0.43
	LAIV-IFNA	1.01	-	-	-	1.54±0.42	1.74±0.38	2.93±0.33	2.36±0.62
	LAIV-IFNL	1.00	-	1.2%	-	2.07±0.88	2.02±0.87	1.60±0.38	1.92±0.53

Clinical signs and virus replication in the URT of ferrets vaccinated with live-attenuated influenza vaccine (B/Phuket/3073/2013-CDC-LV11B; "LAIV") followed by IFN treatment (or Mock) on D1 post vaccination. Group designated as "UN" were mock vaccinated and groups designated as "LAIV" were vaccinated. A) Initial vaccination clinical signs and virus replication (of LAIV). Groups above the dotted line were mock vaccinated with PBS and groups below the dotted line were vaccinated with LAIV. NW viral loads listed as N/A for mock-vaccinated groups. B) At 3 months post vaccination, all groups were challenged with PH.

[a]Relative inactivity index "RII" (D1 – D7) post challenge. RII=$\sum_{(D1-7)}[score+1]n/\sum_{(D1-7)}n$

[b]Day post challenge of peak weight loss percentage (day) from pre-vaccination or pre-challenge weight from D1 – D7 post vaccination or challenge.

[c]Average elevated temperature of at least +2°F (Fever) above baseline (days post challenge elevated). Fever indicated by any temperature greater than the average baseline (D-2 to D0 pre-challenge) +2°F

[d]Average viral load in ferret URT on D1 through D7 post challenge. Peak viral load in bold. Baseline = 1.30 Log_{10} FFU/mL.

Figure 5.4: Gene expression in ferret URT/PBMC following IBV vaccination/challenge.

A)NW

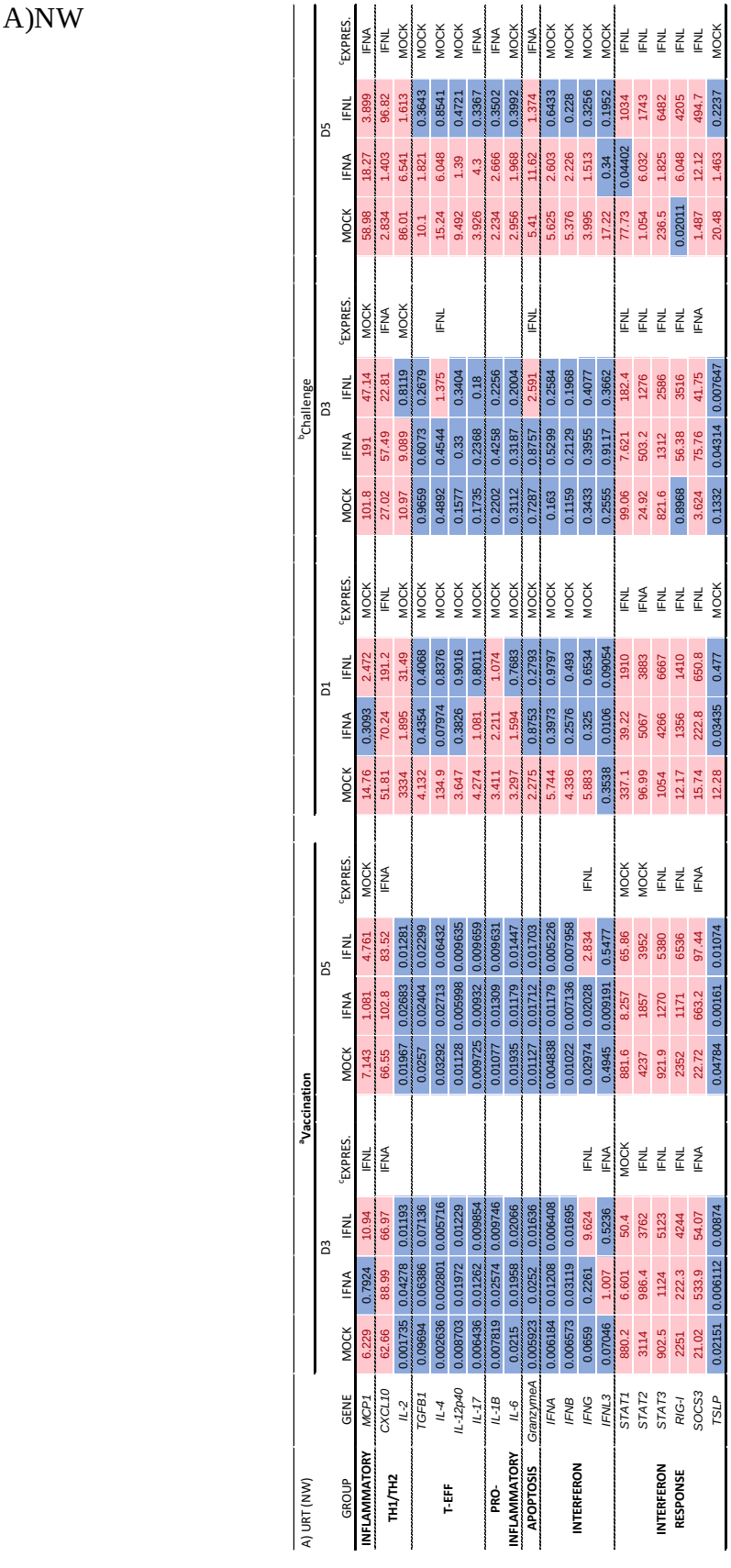

A) URT (NW)		[a]Vaccination							[b]Challenge									
		D3				D5			D1			D3			D5			
GROUP	GENE	MOCK	IFNA	IFNL	[c]EXPRES.	MOCK	IFNA	IFNL	[c]EXPRES.	MOCK	IFNA	IFNL	[c]EXPRES.	MOCK	IFNA	IFNL	[c]EXPRES.	MOCK	IFNA	IFNL	[c]EXPRES.
INFLAMMATORY	*MCP1*	6.229	0.7924	10.94	IFNL	7.143	1.081	4.761	MOCK	14.76	0.3093	2.472	MOCK	101.8	191	47.14	MOCK	58.98	18.27	3.899	IFNA
TH1/TH2	*CXCL10*	62.66	88.99	66.97	IFNA	66.55	102.8	83.52	IFNA	51.81	70.24	191.2	IFNL	27.02	57.49	22.81	IFNA	2.834	1.403	96.82	IFNL
	IL-2	0.001735	0.04278	0.01193		0.01967	0.02683	0.01281		3334	1.895	31.49	MOCK	10.97	9.089	0.8119	MOCK	86.01	6.541	1.613	MOCK
	TGFB1	0.09694	0.06386	0.07136		0.0257	0.02404	0.02299		4.132	0.4354	0.4068	MOCK	0.9659	0.6073	0.2679		10.1	1.821	0.3643	MOCK
T-EFF	*IL-4*	0.002636	0.002801	0.005716		0.03292	0.02713	0.06432		134.9	0.07974	0.8376	MOCK	0.4892	0.4544	1.375	IFNL	15.24	6.048	0.8541	MOCK
	IL-12p40	0.008703	0.01972	0.01229		0.01128	0.005998	0.009635		3.647	0.3826	0.9016	MOCK	0.1577	0.33	0.3404		9.492	1.39	0.4721	MOCK
	IL-17	0.006436	0.01262	0.009854		0.009725	0.00932	0.009659		4.274	1.081	0.8011	MOCK	0.1735	0.2368	0.18		3.926	4.3	0.3367	IFNA
PRO-INFLAMMATORY	*IL-1B*	0.007819	0.02574	0.009746		0.01077	0.01309	0.009831		3.411	2.211	1.074	MOCK	0.2202	0.4258	0.2256		2.234	2.666	0.3502	IFNA
	IL-6	0.0215	0.01958	0.02066		0.01935	0.01179	0.01447		3.297	1.594	0.7683	MOCK	0.3112	0.3187	0.2004		2.956	1.968	0.3992	MOCK
APOPTOSIS	*GranzymeA*	0.005923	0.0252	0.01636		0.01127	0.01712	0.01703		2.275	0.8753	0.2793	MOCK	0.7287	0.8757	2.591	IFNL	5.41	11.62	1.374	IFNA
	IFNA	0.006184	0.01208	0.006408		0.004838	0.01179	0.005226		5.744	0.3973	0.9797	MOCK	0.163	0.5299	0.2584		5.625	2.603	0.6433	MOCK
	IFNB	0.006573	0.03119	0.01695		0.01022	0.007136	0.007958		4.336	0.2576	0.493	MOCK	0.1159	0.2129	0.1968		5.376	2.226	0.228	MOCK
INTERFERON	*IFNG*	0.0659	0.2261	9.624	IFNL	0.02974	0.02028	2.834	IFNL	5.883	0.325	0.6534	MOCK	0.3433	0.3955	0.4077		3.995	1.513	0.3256	MOCK
	IFNL3	0.07046	1.007	0.5236	IFNA	0.4945	0.009191	0.5477		0.3538	0.0106	0.09054		0.2555	0.9117	0.3662		17.22	0.34	0.1952	MOCK
	STAT1	880.2	6.601	50.4	MOCK	881.6	8.257	65.86	MOCK	337.1	39.22	1910	IFNL	99.06	7.621	182.4	IFNL	77.73	0.04402	1034	IFNL
	STAT2	3114	986.4	3762	IFNL	4237	1857	3952	MOCK	96.99	5067	3883	IFNA	24.92	503.2	1276	IFNL	1.054	6.032	1743	IFNL
INTERFERON	*STAT3*	902.5	1124	5123	IFNL	921.9	1270	5380	IFNL	1054	4266	6667	IFNL	821.6	1312	2586	IFNL	236.5	1.825	6482	IFNL
RESPONSE	*RIG-I*	2251	222.3	4244	IFNL	2352	1171	6536	IFNL	12.17	1356	1410	IFNL	0.8968	56.38	3516	IFNL	0.02011	6.048	4205	IFNL
	SOCS3	21.02	533.9	54.07	IFNA	22.72	663.2	97.44	IFNA	15.74	222.8	650.8	IFNL	3.624	75.76	41.75	IFNA	1.487	12.12	494.7	IFNL
	TSLP	0.02151	0.006112	0.00874		0.04784	0.00161	0.01074		12.28	0.03435	0.477	MOCK	0.1332	0.04314	0.007647		20.48	1.463	0.2237	MOCK

B)PBMC

B)PBMC		[a]Vaccination							[b]Challenge									
		D3				D5			D1				D3			D5		
GROUP	GENE	MOCK	IFNA	IFNL	[c]EXPRES.	MOCK	IFNA	IFNL	[c]EXPRES.	MOCK	IFNA	IFNL	[c]EXPRES.	MOCK	IFNA	IFNL	[c]EXPRES.	MOCK	IFNA	IFNL
INFLAMMATORY	*MCP1*	3352	1.625	28.62	MOCK	3.653	0.627	3.161	MOCK	1.014	446.9	3.704	IFNA	1.923	0.3896	2.388	IFNL	0.8925	632.6	0.2043	IFNA
TH1/TH2	*CXCL10*	2.001	0.9475	0.8934	MOCK	1.447	1.182	0.7014	MOCK	1.604	1.592	0.8224	MOCK-IFNA	1.618	1.326	1.547	MOCK	1.202	1.074	0.5122	MOCK
	IL-2	7.469	0.3119	0.7133	MOCK	2.103	0.1024	0.3346	MOCK	5.382	0.1198	0.2964	MOCK	5.653	0.2431	1.111	MOCK	9.335	0.1384	0.2762	MOCK
	TGFB1	125.1	0.3571	3365	IFNL	1.007	0.1833	3376	IFNL	0.6098	0.2498	0.2519		6.092	0.4025	1.284	MOCK	1.383	0.6088	0.1801	MOCK
T-EFF	*IL-4*	5.993	0.3563	2.528	MOCK	2.858	0.3689	3.926	IFNL	2.446	0.2425	0.7022	MOCK	22.66	0.1855	2.004	MOCK	4.34	0.2206	1.392	MOCK
	IL-12p40	4.081	0.2473	1.642	MOCK	1.655	0.2036	0.4687	MOCK	0.9463	0.425	2.023	IFNL	1.826	0.3408	1.007	MOCK	1.191	0.7559	0.3941	MOCK
	IL-17	3.456	1.173	1.45	MOCK	0.7325	0.3257	0.706		1.432	0.1602	0.6648	MOCK	2.177	0.2917	1.017	MOCK	1.195	0.5018	0.4113	MOCK
PRO-INFLAMMATORY	*IL-1B*	4.413	0.6109	1.7	MOCK	1.181	0.2278	0.6551	MOCK	1.628	0.2546	0.6165	MOCK	1.985	0.3408	1.445	MOCK	1.079	0.3579	0.3339	MOCK
	IL-6	6.393	0.4363	3.047	MOCK	1.378	0.202	3.28	IFNL	1.15	0.2394	0.5465	MOCK	1.509	0.2916	0.8035	MOCK	0.886	0.3217	0.5243	
APOPTOSIS	*GranzymeA*	3.18	0.45	2.144	MOCK	0.8173	0.1263	2.726	IFNL	1.523	0.116	0.6932	MOCK	1.795	0.4003	1.467	MOCK	2.267	0.2161	0.9372	MOCK
	IFNA	5.214	6.953	11.39	IFNA	1.038	0.3173	0.7298	MOCK	1.14	0.1132	0.5393	MOCK	2.085	0.3724	1.009	MOCK	1.112	0.2401	0.3949	MOCK
	IFNB	238.3	0.5716	1.225	MOCK	1.5	0.214	0.2933	MOCK	1.059	0.2042	4.705	IFNL	2.256	0.4035	0.7116	MOCK	0.7394	0.4188	0.6982	
INTERFERON	*IFNG*	6.003	0.4156	3.994	MOCK	2.404	0.1834	0.9753	MOCK	1.694	0.2857	6.987	IFNL	1.718	0.2684	1.486	MOCK	2.418	0.7421	0.3641	MOCK
	IFNL3	869.3	0.4554	35.75	MOCK	5.499	0.144	0.5053	MOCK	0.001035	8.038	0.1164	IFNA	0.002546	4.784	0.2025	IFNA	0.5326	10.52	1.016	IFNA
	STAT1	2.464	0.4076	0.9237	MOCK	1.3	0.2992	0.747	MOCK	1.338	1.168	0.5981	MOCK	1.77	1.015	1.136	MOCK	1.208	0.4989	0.5716	MOCK
	STAT2	1.484	1.723	0.6536	MOCK-IFNA	1.469	6.061	1.4	IFNA	0.9823	1.186	1.257	IFNL	1.787	5.19	1.346	IFNA	0.6823	3.631	0.8142	IFNA
INTERFERON	*STAT3*	1.916	0.7901	1.211	M	1.347	0.5134	0.8242	MOCK	2.618	1.66	0.5314	MOCK	2.046	1.986	1.216	MOCK	1.479	1.479	0.4323	MOCK-IFNA
RESPONSE	*RIG-I*	0.8875	14	0.7971	IFNA	1.175	13.99	0.5071	IFNA	4.17	80.45	0.4348	IFNA	2.171	71.04	1.287	IFNA	3.038	58.9	1.004	IFNA
	SOCS3	1.547	2.2	0.5989	IFNA	1.562	2.019	0.573	IFNA	1.872	0.8003	0.4997	MOCK	1.194	1.196	1.291	IFNL	0.9943	0.4465	0.4229	
	TSLP	28.84	0.1422	138.5	IFNL	79.02	0.192	181.2	IFNL	0.2903	0.5829	1.093	IFNL	2.103	0.3917	0.7518	MOCK	1.852	2.081	0.01851	IFNA

Average fold gene expression in IBV-vaccinated and challenged ferrets following IFN-treatment. [a]Animals vaccinated with IBV-LAIV and treated with IFNA, IFNL or mock on D1 post vaccination. [b]IFNA, IFNL or mock treated animals challenged with B/Phuket/3073/2013 three months post vaccination. [c]Expression (EXPRES.) indicates treatment group with highest gene expression increase at each given timepoint post vaccination or challenge. Gene upregulation (positive fold-increase in gene expression over D0) indicated in pink and down-regulation of gene expression indicated in blue. Target gene functional groups are listed under GROUP and separated by dotted lines. A)Average fold gene expression in NW cells of the URT following IBV vaccination or challenge. B)Average fold gene expression in PBMC following IBV vaccination or challenge.

Figure 5.5: Cytokine/chemokine levels in sera of IFN-treated ferrets following IBV vaccination and challenge.

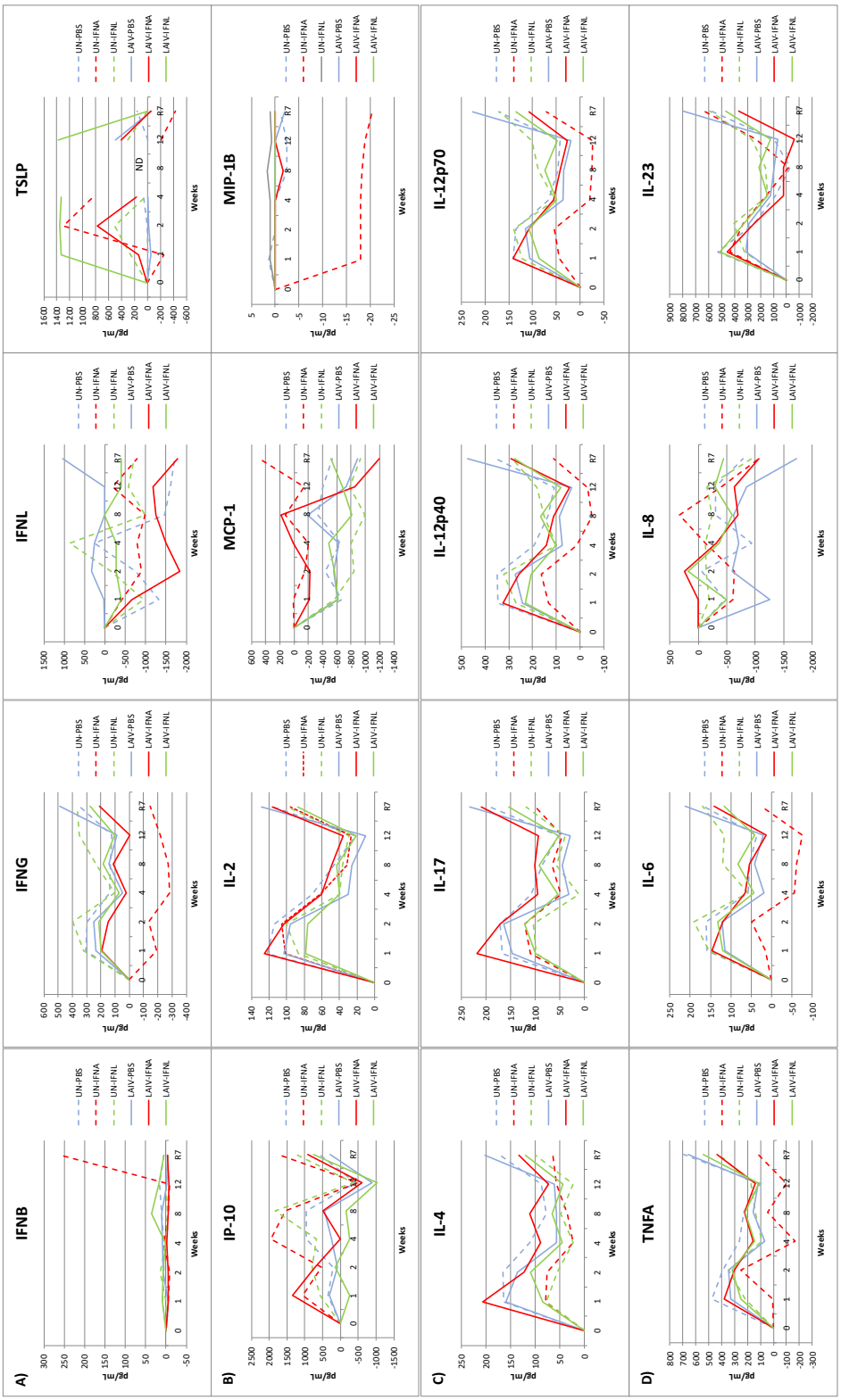

Serum cytokine and chemokine levels in IBV-vaccinated ferrets following IFN-treatment. Mock-vaccinated groups (UN-X) are represented by dotted lines and IBV-vaccinated groups (LAIV-X) are indicated by solid lines. Treatment groups are Mock (PBS, light blue), IFNA (red) and IFNL (green). The x-axis indicated the weeks post vaccination (1, 2, 4, 8, 12) and after 3MO [day 7 (R7) post challenge]. Average pG/mL levels of analytes are shown from the following functional groups: A) Interferon responses. Type-I (IFNB), Type-II (IFNG) and Type-III* (IFNL) and Type-III IFN response cytokine (TSLP). B) TH1 (IP-10) and TH2 (IL-2) directed responses. C)Pro-inflammatory chemokines (MCP-1 and MIP-1B) D)T-effector response (IL-4, IL-17, IL-12p40 & IL-12p70) E)Pro-inflammatory cytokine response (TNFA, IL-6, IL-8, and IL-23). All levels of cytokines/chemokines are normalized to D0 and represent average increases or decreases from pre-vaccination over a 12Wk period post-vaccination plus 1Wk (R7) post-challenge.

Table 5.3: Neutralizing antibody responses following IBV challenge or vaccination in ferrets treated with IFN.

A) Challenge

		Treatment[a]					
		Mock		IFNA		IFNL	
		UN-PH[b]	PH-PH[c]	UN-PH[b]	PH-PH[c]	UN-PH[b]	PH-PH[c]
Weeks post Challenge	Pre	-	5	-	5	-	5
	1	-	34	-	32	-	19
	2	-	148	-	148	-	122
	4	-	**235**	-	**296**	-	**296**
	8	-	**202**	-	**296**	-	**235**
	12	-	101	-	148	-	86
Challenge(Rechallenge)	1	93	**(871)**	118	**(1016)**	109	**(1493)**

B)Vaccination

		Treatment[d]					
		Mock		IFNA		IFNL	
		UN-PH[e]	LAIV-PH[f]	UN-PH[e]	LAIV-PH[f]	UN-PH[e]	LAIV-PH[f]
Weeks post Vaccination	Pre	-	5	-	5	-	5
	1	-	86	-	80	-	63
	2	-	93	-	127	-	80
	4	-	118	-	127	-	93
	8	-	137	-	**218**	-	**187**
	12	-	50	-	93	-	74
Challenge	1	137	**10240**	**218**	**10240**	**218**	**7525**

A)Serum neutralizing antibodies by FRA (geometric mean titer) in ferrets challenged with B/Phuket/3073/2013 and rechallenged three months (12 weeks) later with homologous virus. [a]Treatment groups include Mock (PBS), PEGylated-IFNA (IFNA), or PEGylated-IFNL3 (IFNL) on day 1 post challenge. [b]Mock-challenged group (UN-PH), followed by challenge at 3 months. All animals were treated on day 1. [c]Challenge-rechallenge group (PH-PH), challenged followed by treatment on day 1 post challenge and rechallenged at 3 months post challenge. Rechallenge titers are indicated within parentheses. Neutralizing titers >1:160 are indicated in bold. B) Serum neutralizing antibodies by FRA (geometric mean titers) in ferrets vaccinated with

B/Phuket/3073/2013-LAIV (LAIV) and challenged three months (12 weeks) later with B/Phuket/3073/2013. [d]Treatment groups include Mock (PBS), PEGylated-IFNA (IFNA), or PEGylated-IFNL3 (IFNL) on day 1 post vaccination. [e]Mock-vaccinated group (UN-PH), followed by challenge at three months. All animals were treated on day 1. [f]Vaccination-challenge group (LAIV-PH), vaccinated and treated on day 1 post vaccination and challenged at three months. Neutralizing titers >1:160 are indicated in bold.

Table 5.4: Correlations between antibody levels and protein levels in IFN-treated ferrets following IBV challenge and vaccination.

A)Challenge.

A) ANTIBODY TITER VS ANALYTE (CHALLENGE)

A) CHALLENGE

GROUP	ANALYTE	MOCK r	MOCK P-VALUE	MOCK SIGNIFICANCE	IFNA-Tx r	IFNA-Tx P-VALUE	IFNA-Tx SIGNIFICANCE	IFNL-Tx r	IFNL-Tx P-VALUE	IFNL-Tx SIGNIFICANCE
INTERFERON	IFNB	-0.6547	0.1667	ns	0.3482	0.3333	ns	-0.5071	0.1667	ns
	IFNG	0.08571	0.4597	ns	**-0.8827**	**0.0167**	*	-0.5429	0.1486	ns
	IFNL	-0.5071	0.1667	ns	-0.6742	0.1667	ns	0.6571	0.0875	ns
	TSLP[a]	0.6	0.175	ns	0.0513	0.5	ns	0.5	0.225	ns
TH1/TH2	IP-10	0.4286	0.2097	ns	**0.765**	**0.0444**	*	0.3714	0.2486	ns
	IL-2	-0.3714	0.2486	ns	0.08827	0.4444	ns	-0.4857	0.1778	ns
CHEMOKINE	MCP-1	0.2	0.3569	ns	**-0.765**	**0.0444**	*	0.4286	0.2097	ns
	MIP-1B	0.1352	0.4	ns	-0.1177	0.4056	ns	-0.3381	0.2667	ns
T-EFF	IL-4	-0.02899	0.4917	ns	-0.5591	0.1333	ns	-0.03036	0.5	ns
	IL-17				-0.4377	0.1833	ns	-0.4395	0.2	ns
	IL-12p40	-0.6	0.1208	ns	**-0.765**	**0.0444**	*	-0.6	0.1208	ns
	IL-12p70	-0.7714	0.0514	ns	-0.2648	0.3111	ns	-0.6571	0.0875	ns
PRO-INFLAM.	TNFA	**-0.8827**	**0.0222**	*	-0.6866	0.0833	ns	-0.6377	0.1	ns
	IL-6	**-0.8452**	**0.0333**	*	-0.6866	0.0833	ns	**-0.8452**	**0.0333**	*
	IL-8	**-0.8286**	**0.0292**	*	-0.5591	0.1333	ns	-0.6	0.1208	ns
	IL-23	-0.2571	0.3292	ns	0.2354	0.3278	ns	-0.6	0.1208	ns

B)Vaccination.

B) VACCINATION

B) ANTIBODY TITER VS ANALYTE (VACCINATION)

GROUP	ANALYTE	MOCK r	MOCK P-VALUE	MOCK SIGNIFICANCE	IFNA-Tx r	IFNA-Tx P-VALUE	IFNA-Tx SIGNIFICANCE	IFNL-Tx r	IFNL-Tx P-VALUE	IFNL-Tx SIGNIFICANCE
INTERFERON	IFNB	0.7714	0.0514	ns	-0.4928	0.1667	ns	0.4857	0.1778	ns
	IFNG	0.3714	0.2486	ns	0.2029	0.3556	ns	0.2571	0.3292	ns
	IFNL	0.3339	0.2667	ns	**-0.8117**	**0.0361**	*	0.3479	0.2472	ns
	TSLP[a]	-0.1	0.475	ns	**0.8721**	**0.05**	*	0.8	0.0667	ns
TH1/TH2	IP-10	0.7714	0.0514	ns	0.2029	0.3556	ns	0.08571	0.4597	ns
	IL-2	0.4286	0.2097	ns	0.2319	0.3361	ns	0.2571	0.3292	ns
CHEMOKINE	MCP-1	-0.02857	0.5	ns	0.4058	0.2167	ns	-0.4857	0.1778	ns
	MIP-1B				-0.6642	0.1667	ns			
T-EFF	IL-4	0.05798	0.4667	ns	0.3189	0.2778	ns	0.3714	0.2486	ns
	IL-17	0.5429	0.1486	ns	0.3189	0.2778	ns	0.3714	0.2486	ns
	IL-12p40	0.5429	0.1486	ns	0.2319	0.3361	ns	0.2571	0.3292	ns
	IL-12p70	0.4857	0.1778	ns	0.2319	0.3361	ns	0.3714	0.2486	ns
PRO-INFLAM.	TNFA	0.3714	0.2486	ns	0.3189	0.2778	ns	0.3714	0.2486	ns
	IL-6	0.3714	0.2486	ns	0.2319	0.3361	ns	0.3714	0.2486	ns
	IL-8	-0.08571	0.4597	ns	-0.4058	0.2167	ns	-0.4286	0.2097	ns
	IL-23	0.4286	0.2097	ns	0.2029	0.3556	ns	0.2571	0.3292	ns

Spearman non-parametric correlation (One-tailed, 95% confidence interval) were estimated to determine the relationship between neutralizing antibody response and protein levels in serum. [a]TSLP listed in interferon group due to its direct regulation by IFNL. A) Antibody correlations in challenge study for Mock-, IFNA- and IFNL-treated groups (3 animals/group). Timepoints tested include pre-challenge; weeks 1, 2, 4, 8, 12 weeks post challenge. A correlation coefficient of $r<0$ indicates an inverse correlation of antibody titer to protein levels and an $r>0$ indicates a direct correlation. Strong positive ($r>0.7$) or negative ($r<-0.7$) correlations are underlined and significant ($p<0.05$) correlations are in bold. B) Antibody correlations in vaccination study for Mock-, IFNA- and IFNL-treated groups (3 animals/group). Timepoints tested include pre-vaccination; weeks 1, 2, 4, 8, 12 weeks post vaccination. A correlation coefficient of $r<0$ indicates an inverse correlation of antibody titer to protein levels and an $r>0$ indicates a direct correlation. Significant ($p<0.05$) correlations in bold.

Figure 5.S1: PEGylation of ferret IFNs and biological activity.

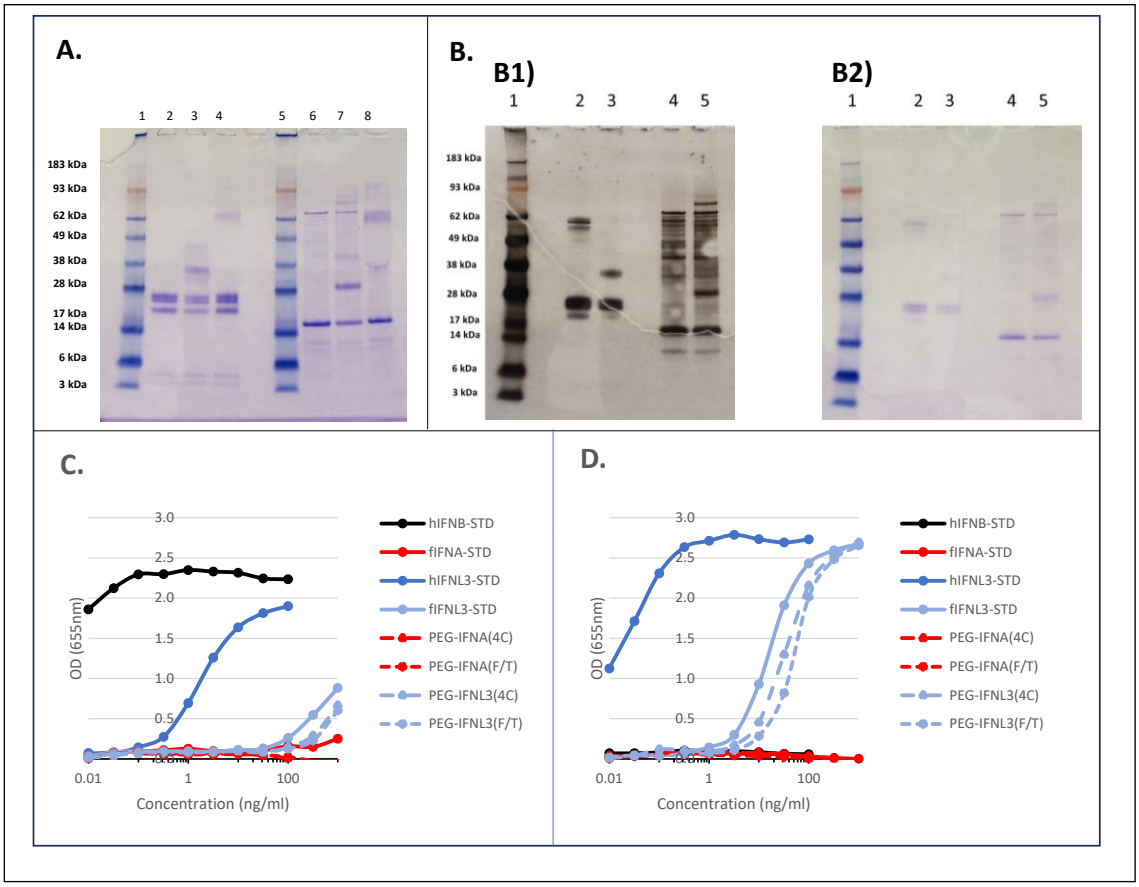

A)Comparison of PEGylation of ferret IFNA and IFNL3 by PEG-5K and PEG-20K; imperial staining. Lane designation: MW standards (1 and 5), ferret IFNA [2 (IFNA), 3 (IFNA+PEG-5K), 4 (IFNA+PEG-20K)], ferret IFNL3 [6 (IFNL3), 7 (IFNL3+PEG-5K), 8 (IFNL3+PEG-20K)] by imperial staining. 2 uG/lane added.

B)Comparison of imperial and silver staining of (PEG-5K) PEGylation of ferret IFNA and IFNL3. Silver staining (B1) and imperial staining (B2). Lane designation: mw standards (1), ferret IFNA [2 (IFNA), 3 (IFNA+PEG-5K)], ferret IFNL3 [6 (IFNL3), 7 (IFNL3+PEG-5K)]. 1 uG/lane added.

C)Type-I IFN bioassay to determine retention of activity of ferret PEGylated IFNA (IFNA+PEG-5K) and stored at 4°C or -80°C (freeze/thaw; "F/T"). Human IFNB standard

(solid black line), ferret IFNA standard (solid red line) and PEGylated IFNA stored at 4°C [PEG-IFNA(4C), long red dashed line] or stored at -80°C and thawed [PEG-IFNA(F/T), short red dashed line]. Human IFNL standard (solid dark blue line), ferret IFNL3 standard [fIFNL3-STD, solid light blue line] and PEGylated IFNL3 stored at 4°C [PEG-IFNL3(4C), long light blue dashed line] or stored at -80°C and thawed [PEG-IFNA(F/T), short, dashed light blue line].

D) Type-III IFN bioassay to determine retention of activity of ferret PEGylated IFNL3 (IFNL3+PEG-5K) and stored at 4°C or -80°C (freeze/thaw; "F/T"). Human IFNB standard (solid black line), ferret IFNA standard (solid red line) and PEGylated IFNA stored at 4°C [PEG-IFNA(4C), long red dashed line] or stored at -80°C and thawed [PEG-IFNA(F/T), short red dashed line]. Human IFNL standard (solid dark blue line), ferret IFNL3 standard [fIFNL3-STD, solid light blue line] and PEGylated IFNL3 stored at 4°C [PEG-IFNL3(4C), long light blue dashed line] or stored at -80°C and thawed [PEG-IFNA(F/T), short, dashed light blue line].

Figure 5.S2: Wt. & Temp. following IBV challenge or vaccination and IFN-treatment in

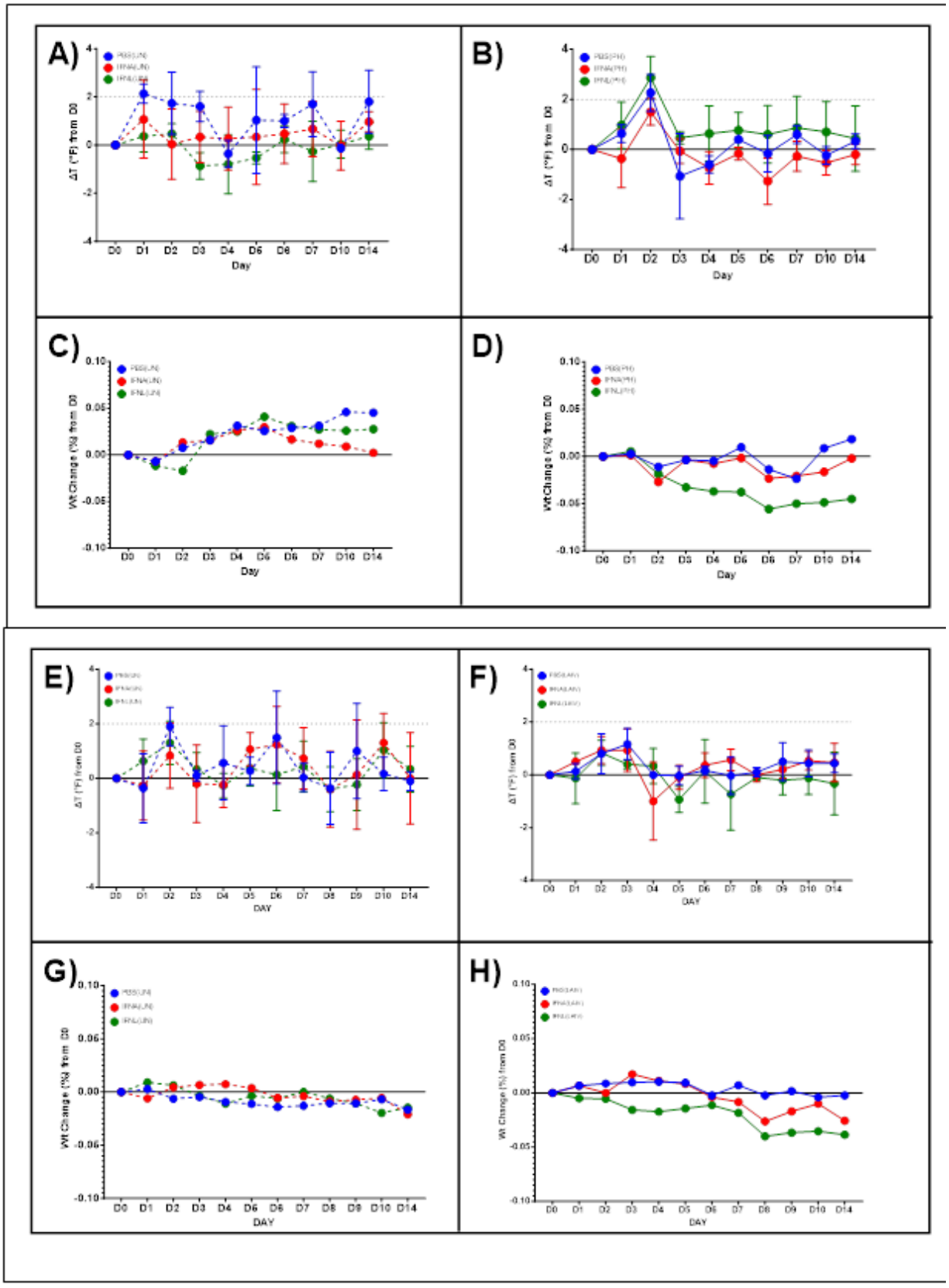

ferrets.

A – D) Challenge experiment temperature and weight changes from D0 to D14 post challenge. A) Average Change in temperature in MOCK-infected ferrets (dotted lines) treated with IFN on day 1 post mock-challenge. Groups are as follows: Untreated (blue). IFNA-treated (red), IFNL-treated (green). Dotted line at +2°F over baseline indicates fever threshold. B) IBV-infected ferrets (solid lines) treated with IFN on day 1 post challenge. Groups are as follows: Untreated (blue). IFNA-treated (red), IFNL-treated (green). Dotted line at +2°F over baseline indicates fever threshold. C) Average weight changes in ferrets mock-challenged (dotted lines) compared to day 0 weights. Changes in weight range from -10% to +10%. Untreated (blue). IFNA-treated (red), IFNL-treated (green). D) Average weight changes in ferrets challenged with IBV (solid lines) compared to pre-challenge weights. Changes in weight range from -10% to +10%. Untreated (blue). IFNA-treated (red), IFNL-treated (green).

E – H) Vaccination experiment temperature and weight changes from D0 to D14 post vaccination. E) Average Change in temperature in Mock-vaccinated ferrets (dotted lines) treated with IFN on day 1 post mock-vaccination. Groups are as follows: Untreated (blue). IFNA-treated (red), IFNL-treated (green). Dotted line at +2°F over baseline indicates fever threshold. F) IBV-vaccinated ferrets (solid lines) treated with IFN on day 1 post vaccination. Groups are as follows: Untreated (blue). IFNA-treated (red), IFNL-treated (green). Dotted line at +2°F over baseline indicates fever threshold. G) Average weight changes in ferrets mock-vaccinated (dotted lines) compared to day 0 weights. Changes in weight range from -10% to +10%. Untreated (blue). IFNA-treated (red), IFNL-treated (green). H) Average weight changes in ferrets vaccinated with IBV (solid

lines) compared to pre-vaccination weights. Changes in weight range from -10% to +10%. Untreated (blue). IFNA-treated (red), IFNL-treated (green).

Figure 5.S3: Gene expression in ferret URT and PBMC following IFN-treatment.

		[a]URT (NW)							[b]PBMC						
		D3				D5			D3				D5		
GROUP	GENE	MOCK	IFNA	IFNL	[c]EXPRES.	MOCK	IFNA	IFNL	[c]EXPRES.	MOCK	IFNA	IFNL	[c]EXPRES.	MOCK	IFNA	IFNL	[c]EXPRES.
INFLAMMATORY	*MCP1*	2.71	42.11	7.264	IFNA	3.328	1.167	3.198	MOCK	3.092	7.936	446.7	IFNL	14.69	8.359	3.285	
TH1/TH2	*CXCL10*	0.2228	3.919	1.303	IFNA	0.7754	34.4	1.062	IFNA	1.955	0.7998	0.8035	MOCK	0.7354	0.8882	0.9767	
	IL-2	9.508	6.657	2.202	MOCK	1.685	0.7676	2.769	IFNL	3.707	0.6393	0.7743	MOCK	19.63	0.7783	0.9671	MOCK
T-EFF	*TGFB1*	1.131	1.453	1.556	IFNA~IFNL	0.4563	0.2063	1.834	IFNL	1.593	65.54	69.99	IFNL	53.46	187	124.9	IFNL
	IL-4	5.387	3.113	1.379	MOCK	0.8735	0.7883	2.722	IFNL	2.783	0.7887	1.361	MOCK	29.36	0.462	1.67	MOCK
	IL-12p40	1.06	0.6088	0.8169	MOCK	0.7461	0.308	15.81	IFNL	1.532	0.5599	1.215	MOCK	8.573	18.21	1.317	IFNA
	IL-17	0.6795	0.7769	0.944		1.812	0.4869	0.4969	MOCK	9.48	0.4135	0.3472	MOCK	16.27	16.9	0.808	MOCK~IFNA
PRO-INFLAMMATORY	*IL-1B*	1.333	0.8983	1.235	MOCK~IFNL	4.688	0.4597	0.5722	MOCK	5.093	0.6117	0.6093	MOCK	10.73	1.365	1.348	MOCK
	IL-6	0.5549	1.239	1.211	IFNA~IFNL	0.7236	0.3945	0.8582		2.398	0.3832	0.6974	MOCK	8.29	0.2778	0.9716	MOCK
APOPTOSIS	*GranzymeA*	0.8606	2.31	1.623	IFNA	1.195	0.6679	0.491	MOCK	10.7	0.3259	0.3165	MOCK	9.014	1.934	1.064	MOCK
INTERFERON	*IFNA*	0.8752	1.238	1.026	IFNA	1.137	0.5508	0.503	MOCK	4.812	0.5724	0.739	MOCK	12.25	0.4962	1.113	MOCK
	IFNB	0.8238	1.076	0.6866	IFNA	1.183	0.3363	0.7095	MOCK	2.835	0.2784	0.6375	MOCK	10.27	12.63	0.9961	IFNA
	IFNG	0.6957	1.832	0.9243	IFNA	0.2261	0.4121	1.249	IFNL	1.397	0.8925	1.524	IFNL	13	0.9891	1.165	MOCK
	IFNL3	1.954	3.324	2.513	IFNA	3.525	1	236.8	IFNL	1.021	1.018	1322	IFNL	10.23	1.477	170.8	IFNL
INTERFERON RESPONSE	*STAT1*	0.0977	17.93	17.02	IFNA	2.132	906.5	3200	IFNL	2.014	0.7505	0.5504	MOCK	1.128	0.9228	0.7195	MOCK
	STAT2	0.9613	3.518	0.9951	IFNA	0.4093	88.04	2.604	IFNA	1.401	0.9501	0.6264	MOCK	0.3628	0.7776	1.425	IFNL
	STAT3	1.2	4.516	1.111	IFNA	2.869	1525	3.243	IFNA	1.54	0.6657	0.5695	MOCK	1.507	1.041	0.7678	MOCK
	RIG-I	1.238	3.113	1.397	IFNA	0.3738	21.46	1.916	IFNA	1.321	1.136	0.4259	MOCK	0.7054	0.9187	1.068	IFNL
	SOCS3	0.2403	2.643	2.007	IFNA	5.453	57.9	0.3345	IFNA	4.332	1.152	0.3378	MOCK	1.534	1.215	0.8168	MOCK
	TSLP	0.7344	0.6283	3.533	IFNL	0.053	0.1274	139.3	IFNL	0.6892	1.772	767.9	IFNL	3.993	0.02407	545.7	IFNL

Average fold gene expression in ferrets following IFN-treatment. [a]NW cells from the URT of mock-challenge/vaccinated (PBS) animals and treated with IFNA, IFNL or mock on D1 post challenge. [b]PBMC from animals mock-challenge/vaccinated (PBS) and treated with IFNA, IFNL or mock on D1 post challenge. [c]Expression (EXPRES.) indicates treatment group with highest gene expression increase at each given timepoint post challenge. Gene upregulation (positive fold-increase in gene expression over D0) indicated in pink and down-regulation of gene expression indicated in blue. Target gene functional groups are listed under GROUP and separated by dotted lines.

Table 5.S1: Correlation between antibody levels and protein levels in IFN-treated ferrets following IBV challenge and vaccination – Including 3-month challenge/rechallenge timepoint.

A) CHALLENGE - RECHALLENGE

A) ANTIBODY TITER VS ANALYTE (CHALLENGE-RECHALLENGE)			MOCK			IFNA-Tx			IFNL-Tx		
	GROUP	ANALYTE	r	P-VALUE	SIGNIFICANCE	r	P-VALUE	SIGNIFICANCE	r	P-VALUE	SIGNIFICANCE
	INTERFERON	IFNB	-0.6124	0.1429	ns	0.1134	0.4762	ns	-0.5345	0.119	ns
		IFNG	-0.3214	0.2488	ns	-0.5092	0.1246	ns	-0.6847	0.0508	ns
		IFNL	-0.5345	0.119	ns	-0.6236	0.1429	ns	0.6429	0.0694	ns
		TSLP[a]	0.7714	0.0514	ns	0.4638	0.1972	ns	0.7143	0.0681	ns
	TH1/TH2	IP-10	0.1071	0.4198	ns	0.6183	0.0738	ns	0.07143	0.4532	ns
		IL-2	-0.3929	0.1978	ns	-0.3273	0.2389	ns	-0.5406	0.1067	ns
	CHEMOKINE	MCP-1	-0.25	0.2974	ns	-0.09092	0.4262	ns	-0.1071	0.4198	ns
		MIP-1B	-0.04454	0.5	ns	-0.4312	0.1643	ns	-0.4009	0.2143	ns
	T-EFF	IL-4	0.07412	0.4476	ns	-0.6001	0.0825	ns	0.0197	0.5	ns
		IL-17				-0.09436	0.431	ns	-0.49	0.1429	ns
		IL-12p40	**-0.75**	**0.0331**	*	**-0.7456**	**0.031**	*	**-0.75**	**0.0331**	*
		IL-12p70	**-0.8469**	**0.0127**	*	0.03637	0.4778	ns	-0.6429	0.0694	ns
	PRO-INFLAM.	TNFA	**-0.8982**	**0.0071**	**	-0.4954	0.1325	ns	-0.7042	0.0524	ns
		IL-6	**-0.8018**	**0.0238**	*	-0.4954	0.1325	ns	**-0.8018**	**0.0238**	*
		IL-8	**-0.8929**	**0.0062**	**	**-0.7274**	**0.0365**	*	**-0.75**	**0.0331**	*
		IL-23	-0.3214	0.2488	ns	0.2182	0.3222	ns	-0.5	0.1333	ns

B) VACCINATION - CHALLENGE

B) ANTIBODY TITER VS ANALYTE (VACCINATION-CHALLENGE)			MOCK			IFNA-Tx			IFNL-Tx		
	GROUP	ANALYTE	r	P-VALUE	SIGNIFICANCE	r	P-VALUE	SIGNIFICANCE	r	P-VALUE	SIGNIFICANCE
	INTERFERON	IFNB	0.25	0.2974	ns	-0.2342	0.3099	ns	0.2143	0.3308	ns
		IFNG	0.6071	0.0833	ns	0.5045	0.129	ns	0.5357	0.1179	ns
		IFNL	0.593	0.0893	ns	**-0.7928**	**0.0198**	*	0	0.5155	ns
		TSLP[a]	0.3714	0.2486	ns	**0.8407**	**0.0222**	*	**0.8857**	**0.0167**	*
	TH1/TH2	IP-10	0.6786	0.0548	ns	0.3243	0.2409	ns	0.4286	0.1768	ns
		IL-2	0.6429	0.0694	ns	0.3424	0.2294	ns	0.5357	0.1179	ns
	CHEMOKINE	MCP-1	-0.3929	0.1978	ns	-0.1261	0.3988	ns	-0.2143	0.3308	ns
		MIP-1B	-0.6124	0.1429	ns	-0.4119	0.2857	ns			
	T-EFF	IL-4	0.4144	0.1786	ns	0.3964	0.1917	ns	0.6071	0.0833	ns
		IL-17	**0.7143**	**0.044**	*	0.3964	0.1917	ns	0.6071	0.0833	ns
		IL-12p40	**0.7143**	**0.044**	*	0.3424	0.2294	ns	0.5357	0.1179	ns
		IL-12p70	0.6786	0.0548	ns	0.2523	0.2909	ns	0.6071	0.0833	ns
	PRO-INFLAM.	TNFA	0.6071	0.0833	ns	0.5766	0.0937	ns	0.6071	0.0833	ns
		IL-6	0.6071	0.0833	ns	0.3424	0.2294	ns	0.3214	0.2488	ns
		IL-8	-0.4286	0.1768	ns	-0.6307	0.0706	ns	-0.4286	0.1768	ns
		IL-23	0.6429	0.0694	ns	0.3243	0.2409	ns	0.3571	0.2222	ns

Spearman non-parametric correlation (One-tailed, 95% confidence interval) were estimated to determine the relationship between neutralizing antibody response and protein levels in serum. [a]TSLP listed in interferon group due to its direct regulation by IFNL. A) Antibody correlations in Challenge-Rechallenge study for Mock-, IFNA- and

IFNL-treated groups (3 animals/group). Timepoints tested include pre-challenge; weeks 1, 2, 4, 8, 12 weeks post challenge; 1 week post re-challenge. A correlation coefficient of $r<0$ indicates an inverse correlation of antibody titer to protein levels and an $r>0$ indicates a direct correlation. Strong positive ($r>0.7$) or negative ($r<-0.7$) correlations are underlined and significant ($p<0.05$) correlations are in bold. B) Antibody correlations in Vaccination – Challenge study for Mock-, IFNA- and IFNL-treated groups (3 animals/group). Timepoints tested include pre-vaccination; weeks 1, 2, 4, 8, 12 weeks post vaccination; 1 week post challenge. A correlation coefficient of $r<0$ indicates an inverse correlation of antibody titer to protein levels and an $r>0$ indicates a direct correlation. Significant ($p<0.05$) correlations in bold.

CHAPTER 6

CONCLUSIONS AND FUTURE WORK

In this body of work, an investigation into the disparities between influenza A (IAV) and B viruses (IBV) in generating robust immune responses in ferrets were evaluated. Initial investigation of the innate immune responses in vitro at the site of infection in ferret nasal epithelial cells (FNEC) revealed glimpses in how these cells communicate with circulating immune cells. In vivo studies revealed immune deficits in ferrets following IBV infection. These deficits were evaluated through analyses of innate and adaptive responses in ferrets as well as the effects of immunoadjuvants to overcome immune deficiencies observed following IBV infection and vaccination.

Within this work ferrets were utilized for both in vitro and in vivo experiments. The ferret is a well-established animal model for studying influenza pathogenesis and vaccines. Ferrets can be directly infected with influenza from human clinical isolates without prior adaptation and are capable of transmitting these viruses to other animals and humans [318, 449, 480]. This susceptibility to influenza A and B virus infection is based on similarities in α2,6-linked sialic acid receptors in cells of the upper respiratory tract which mimics that of humans [297, 481]. This model has limitations of reagent availability for studying the innate and adaptive immune responses; however, recent advances in reagent development [368, 369], including sequencing the ferret genome [308], have allowed for exploration into innate and adaptive immune responses in ferrets

following influenza virus infection. Host responses to IBV infection are poorly understood. Immune sera generated against IBV in ferrets have mostly required a boost (with adjuvant) in order to generate sufficient antibody titers to be used as reference antisera for virus characterization studies. Since 1998 most ferrets infected at the CDC with IBV, 387/448 (86.4%), required a boost to generate hemagglutination inhibition titers of at least 1:160 compared to 30/1094 (2.7%) of ferrets infected with H1, H2 or H3 human seasonal viruses for use in surveillance assays. Additionally, ferrets infected with IBV generally presented mild clinical signs and also had lower specific antibody responses [444]. Only a few differences in the innate response to IAV and IBV infections have been assessed and one of the goals of this work was to explore these differences with additional tools as well as provide additional data to help in overcoming this gap in immune responses. Throughout this work, assays and reagents were developed to aid in understanding immune responses to influenza in the ferret. This included generating primers and probes to key innate ferret genes (*IFNL3, TGFB1, TYK2, USP18*, and *TSLP*) [416], testing and validating multiplexing assays for ferret cytokines/chemokines [416, 450, 482], preparation and testing of ferret interferon immunoadjuvants [483], and optimization of assays for detection of virus replication and neutralizing antibodies to influenza in serum [416, 450].

Within this work, improvements in isolation and differentiation of ferret nasal epithelial cells (FNEC) allowed for identification of innate genes which were delayed in expression following inoculation with IBV. During initial isolation of FNEC, contaminating fibroblasts continued to outgrow delicate respiratory epithelial cells and overtake cultures. The primary method to remove fibroblasts from respiratory epithelial

cells involves negative selection through adherence [359]. This method removes most of the fibroblasts; however, the remaining fibroblasts quickly outgrow the primary ferret respiratory epithelial cells and thus no longer contain FNEC. Since fibroblasts lacked an enzyme, D-amino oxidase [383], which could convert D-amino acids to L-amino acids, modifications to initial cell adherence steps and differentiation were performed using media containing D-valine in place of L-valine. This allowed for FNEC to outgrow any contaminating fibroblasts remaining in primary ferret epithelial cell cultures. This improvement in ex vivo culturing of ferret respiratory epithelial cells allowed for consistent cell cultures devoid of fibroblasts for IAV/IBV comparison studies as well as improved FNEC rescue from cryopreservation.

Initial in vitro studies in AIM-1 comparing differential gene expression following influenza infection of FNEC showed that although IAV and IBV replicated equally in FNEC; however, a delay in the pro-inflammatory and interferon (IFN) response was only observed with IBV. IAV infection of FNEC resulted in significant upregulation of key genes that have been correlated with downstream effects on antibody responses. Significant upregulation and duration of IFN expression by IAV between 48Hr (*IFNG*) and 72Hr (*IFNA,IFNB, IFNL3*) suggested a link between innate gene expression and adaptive immune response. Human infection [484] and vaccine [485, 486] studies confirmed a direct correlation between kinetics and magnitude of IFN responses and a robust antibody response to influenza virus infection. The FNEC studies performed also showed a significant upregulation and duration of TH1 (*CXCL10*) and apoptosis (*GRANA*) gene expression by IAV, thus showing additional innate gene expression that may affect downstream cellular adaptive immune responses. As with IFN, there is a

correlation in human serum levels of CXCL10 [487] and apoptosis gene expression [488] as biomarkers for vaccine-induced antibody responses.

Subsequent in vitro co-culture experiments in AIM-1 were performed to demonstrated that communication, or "cross talk", between cells at the site of influenza infection (FNEC) and peripheral blood cells (PBMC) may be a key component to mounting a protective immune response. Human studies with IAV-infected human nasal epithelial cells (hNEC) demonstrated that hNEC released type-I/II/III IFNs and proinflammatory cytokines which activated various cells in PBMC cocultures [421]. Within this work, an early upregulation of pro-inflammatory (*MCP-1, CXCL10, IL-6, IL-8* and *TNFA*), Teff (*IL-4)* and IFN (*IFNG* and *IFNL3*) gene expression in PBMC following cocultivation with IAV-infected FNEC (48hr post infection; 24Hr post cocultivation); but a delayed response in PBMC following cocultivation with IBV-infected FNEC (72Hr post infection; 48Hr post cocultivation) was demonstrated. Since ferret cytokine/chemokine assays were not available for AIM-1 studies, soluble factors secreted by FNEC following influenza infection could only be inferred from gene expression data. PBMC isolated from transplant patients who seroconverted to seasonal influenza vaccine, demonstrated significantly elevated levels of type I/II IFNs, and proinflammatory cytokines in supernatants following H1N1pdm09 stimulation in vitro [422]. Thus, showing that a strong IFN and pro-inflammatory response in PBMC was essential for development of a robust antibody response to influenza. Future analysis of ferret cytokine/chemokine levels in the basolateral compartment of FNEC-PBMC cocultures as well as activation of ferret PBMC cell subsets will validate findings

observed in humans and allow for a greater understanding of disparities between the immune responses of IAV and IBV.

To expand upon the initial innate immune responses observed in vitro in AIM-1, investigation whether the differences observed in FNEC would translate into reduced antibody responses to IBV in vivo. In AIM-2 experiments ferrets were inoculated with the same IAV and IBV strains used in AIM-1 experiments. Gene expression responses in the FNEC of IAV and IBV infected-ferrets confirmed responses observed in AIM-1. Type-II IFN (*IFNG*) and type-III (*IFNL3*) gene expression was highest in IAV-infected ferret nasal wash and PBMC samples respectively. Concurrent with an upregulation of IFN gene expression by IAV was an upregulation of *RIG-I*, which is associated with induction of IFN response [489]. Interestingly IFN response (*SOCS3*) gene, which is responsible for downregulating the IFN response and T-cell activation [467] was highest for IBV (BR) both early and late post challenge. This may indicate that IBV has greater IFN-antagonism properties than IAV. Future studies exploring Interferon antagonism by IBV may help in unraveling the differences to IAV. Interestingly a direct correlation between both *IFNL* and *TSLP* gene expression and viral titers was observed for both IAV and IBV indicating that IFNL and TSLP gene expression may be linked. One way in which IAV viruses evade both innate and adaptive immune responses is via their NS1 protein. Some of the innate genes affected by IAV-NS1 include: *MCP-1, IL-8*, *IFNA*, *IFNB,* and *CCR7*. IAV-NS1 has also been shown to block the production of type-I IFN in infected cells, including epithelial cells and DCs and affect DC maturation [490]. I believe that NS1 of IBV may elicit a stronger IFN antagonistic properties than IAV in FNEC thereby resulting in a delay in initiation of the innate immune response in these

cells. Infection of DCs by influenza viruses propose that IAV NS1 elicits greater IFN antagonism since it is able to evade early recognition in the cytosol since it only activates the IFN response after viral RNA synthesis, whereas IBV induces an IFN directly upon infection in the cytosol [412]. This necessitates the need for follow-up studies with NS1 mutants for IBV and compare IFN responses. Substituting IAV-NS1 with IBV-NS1 and IBV-NS1 with IAV-NS1 by intertypic reassortment or reverse genetics to produce chimeric viruses may be feasible to compare NS1 IFN antagonistic activities and effects on innate responses in FNEC following infection. This may be feasible since viral packaging signals between IAV and IBV are compatible [491].

During these studies, ferret NW and serum samples were submitted to Ampersand Biosciences (www.ampersandbio.com) to help validate their Ferret Cytokine Panel Luminex assay. This allowed for the detection of ferret cytokines and chemokines to at least 12 analytes which previously were not possible. Detection of significantly higher levels of type-I (IFNB) and type-II (IFNG) by IAV compared to IBV helped to confirm that initial gene expression differences resulted in secretion of cytokines. Additionally, the upregulated inflammatory gene expression by IAV in ferrets was confirmed by significantly higher levels of cytokines and chemokines in the serum. IBV in vivo resulted in a weaker antibody response in ferrets as seen historically. These studies confirmed the low and delayed adaptive immune responses by IBV and provide further evidence that initial innate responses, especially IFN and proinflammatory responses play a key role in developing robust antibody responses.

Since a correlation between IFN responses and subsequent antibody responses was discovered, in AIM-3 ferret IFN was utilized as an immunoadjuvant to determine

whether this could boost the weak antibody levels observed to IBV in ferrets. It was previously shown that ferrets vaccinated with seasonal influenza vaccine adjuvanted with PEGylated human IFNA2b upregulated interferon stimulating gene expression, activated antibody generation by B cells through *Ras* signaling, and showed a reduction in viral loads compared to un-adjuvanted vaccine following infection [391]. This demonstrated that innate immunomodulators may be able to enhance vaccine effectiveness by generating robust neutralizing antibody responses. However, the effects of PEG-IFN on antibody responses to the IBV component of the vaccine were not assessed nor were the animals challenged with IBV. To ensure the greatest chance of an effect of IFN as an immunoadjuvant, ferret IFNA and IFNL3 protein were generated. Since ferret IFNA and IFNL3 protein sequences were available [309] Kingfisher Biotech, Inc. (www.kingfisherbiotech.com) was contacted to generate recombinant ferret proteins. The biological activity at least for ferret IFNL3 was determined by adapting a IFNL HEK 293 cell reporter assay (www.invivogen.com) for ferret IFNL. Additionally, successful in PEGylation of both ferret IFNA and IFNL was attained for as immunoadjuvants in ferrets following IBV vaccination or infection.

IFN-treatment of ferrets following challenge with IBV resulted in reduced morbidity. IFN-treatment also upregulated both IFN and proinflammatory gene expression in PBMC which were sustained following rechallenge. Concurrent with gene expression, levels of IFNL and TSLP were highest in IFN-treated animals following challenge. For vaccination studies live-attenuated (LAIV) IBV was used followed by PEG-IFN addition since both are added intranasally. Although, IFN-treatment following LAIV vaccination did not enhance serum cytokine/chemokine levels assessed by multiplexing and IFNL

bioassays, TSLP levels were higher following IFN-treatment. For both challenge and vaccination studies, IFN-treatment did increase neutralizing antibody levels in the serum over mock-treated. A strong correlation was observed between TSLP serum levels and neutralizing antibody responses indicating its potential use as a biomarker to predict antibody responses following IBV infection or vaccination.

Within this work differences between IAV and IBV were observed in the ferret model and key markers for this disparity were found. IFN, proinflammatory and TSLP responses demonstrated relationships between initiation and maintenance of innate responses resulting in subsequent strong antibody responses. However, limitations in AIM-3 affecting the intensity of these responses were found. Primarily the size of the ferret groups (N=3 animals/group) limited the statistical power of these experiments. Additional experiments increasing group sizes to at least 6 animals/group would show clearer differences in key responses as were observed in the in vitro studies. This would allow for a clearer correlation to what is observed in humans. Due to logistical and budgetary constraints as well as to follow up on historical observations in ferrets for generation of antibodies to influenza viruses and vaccines, only male ferrets were used in this work. Future studies comparing male and female ferrets are warranted to determine whether sex differences play a role in the reduced responses that were observed within this work using male ferrets. Recently female mice were less susceptible to IBV than male mice; however female mice mounted more robust and broader antibody responses against IBV following B-LAIV vaccination than male [492]. In previous comparison studies female mice showed a greater breadth of antibodies to IAV (A/California/2009

virus) vaccine due to greater numbers and activity of germinal center B cells than in males [493].

I believe this body of work has added important observations and tools for influenza research, especially IBV. Successful development and testing of important ferret gene primer sets to innate genes, including *IFNL3* and *TSLP*, will allow for a better understanding of immune responses following influenza infection or vaccination. Ferret IFNA and IFNL are now commercially available and have been successfully PEGylated and could be used as immunoadjuvants for influenza or other respiratory infections which generate weak immune responses. The type-III IFN reporter assay has been adapted for use in testing ferret serum and nasal secretions. Addition of ferret cytokine multiplex assay will allow for measuring immune biomarkers for their effect on antibody responses and vaccine efficacy for influenza and other respiratory viruses. These assays are now commercially available. Addition of optimized and sensitive focus forming assay (FFA) and focus reduction assay (FRA) for testing influenza virus replication and neutralizing antibody responses. By adding additional immune reagents and assays for detection of immune responses, this will aid in the usefulness and importance of the ferret model for influenza. Ferrets are similar in their presentation of disease following infection with influenza as well as their immune responses. A main advantage of this model is that ferrets are susceptible to infection and can transmit human and avian influenza viruses isolated directly from the host. Ferrets do not require adaptation of these viruses in order to infect and cause disease in the animals.

Future studies to further elucidate disparities between IAV and IBV observed in this work should address several areas. Since immune responses to IBV are reduced, this

could be due to mammals being the potential reservoir for these viruses. IBV may persist in mammals and alter immune functions in order to be maintained in the population. For example, the Sooty mangabey (SM) has been proposed as the animal reservoir for simian immunodeficiency virus (SIV). The immune responses of the SM are suppressed and the animals do not develop disease following SIV infection. Additionally, immune activation is suppressed as noted by reduced IFNA production by plasmacytoid dendritic cells. However, when a Rhesus macaque is infected with SIV, the immune system is activated and the animal develops disease [27]. The SM also may be a reservoir for yellow fever virus with decreases TLR7 signaling, transient antibody responses and reduced IFNA and DC activation following infection. Whereas, the Rhesus macaque develops severe disease and death following infection with the same virus, indicate of a robust inflammatory response [27]. Hallmarks of reservoirs for several zoonotic emerging RNS viruses include variations in innate signaling, anti-inflammatory innate immune responses, aberrant IFN responses, and weak or transient antibody responses in the animal reservoir [494]. Immune pressure for IBV (slower and less mutation rates than IAV) and may also represent an added justification for mammals as the reservoir for these viruses. Ferrets show these same responses to IBV and may represent a model for another mammalian reservoir to IBV. Comparisons of virus mutations and quasi species frequencies using next generation sequencing of input and viruses in ferret nasal washes following infection may support reduced immune pressures and responses by IBV.

Effects of age may also be an important consideration for IBV. Since only adult ferrets were used in this body of work, future studies comparing immune responses in younger animals will be beneficial to determine whether similar responses are observed

in younger animals. Since children have greater morbidity and mortality to IBV compared to IAV infections, their immunological development may play a role in their responses to IBV in this age group. Several factors in early life immune responses are different from adults and include: 1) neonatal CD4+ and CD8+ T cells produce decreased IFNγ and TNFα upon exposure to pathogenic bacteria, 2) cord blood contains increased CD4+CD25+ regulatory T cells (Treg) that may inhibit adaptive immune responses, 3) Increased levels of IL-4/IL-10/IL-13/ TGFß in cord blood compared to adults, and 4) neonatal plasma inhibits TLR-mediated generation of pro-inflammatory cytokines [31]. Treg effects on anti-influenza antibody responses have shown that TGFß as well as CD4+Foxp3+ Treg cells may act as checkpoints between antibody production after vaccination as shown by lower antibody titers to influenza B component in a human vaccine study of healthy young adults 35.6±12.5 years [32]. These early life immune responses are biased against pro-inflammatory responses while favoring immune suppression which may take time to mature into adult responses thus allowing IBV to cause severe morbidity and mortality in younger populations due to innate and adaptive immune disparities.

Exploring the effects of IFN on enhancing immune responses to influenza may help in understanding how to overcome weak antibody levels observed following IBV infection and vaccination. Augmentation of IFN to IBV vaccines may “jump start” the innate immune responses prior to suppression by IBV NS1 protein or some other mechanism. Future studies to determine whether similar enhancement of adaptive immune responses can be ascertained following IAV infection and vaccination may show that this effect may be beneficial any influenza virus or vaccine which fails to generate a

robust immune response or if this enhancement is restricted to IBV. Finally, IFN levels in the sera or gene expression kinetics may be used as predictors of vaccine efficacy or as a diagnostic tool for disease progression. Taken together, this work has shown the value of the ferret model in assessing immune responses following influenza vaccination and infection. Continued development and availability of additional reagents for ferrets will be beneficial to unraveling immune processes following infection with new and emerging respiratory viruses and aid in the development of improved countermeasures quickly to address public health needs.

REFERENCES

1. Mosnier, A., et al., *Ten influenza seasons in France: distribution and timing of influenza A and B circulation, 2003-2013.* BMC Infect Dis, 2015. **15**: p. 357.
2. Koutsakos, M., et al., *Knowns and unknowns of influenza B viruses.* Future Microbiol, 2016. **11**(1): p. 119-35.
3. Trombetta, C.M. and E. Montomoli, *Influenza immunology evaluation and correlates of protection: a focus on vaccines.* Expert Rev Vaccines, 2016. **15**(8): p. 967-76.
4. Black, S., et al., *Hemagglutination inhibition antibody titers as a correlate of protection for inactivated influenza vaccines in children.* Pediatr Infect Dis J, 2011. **30**(12): p. 1081-5.
5. Maines, T.R., et al., *Local innate immune responses and influenza virus transmission and virulence in ferrets.* J Infect Dis, 2012. **205**(3): p. 474-85.
6. Organization, W.H. *Influenza (Seasonal) Key Facts*. 2024 [cited 2024; Available from: https://www.who.int/news-room/fact-sheets/detail/influenza-(seasonal).
7. Fields, B.N., D.M. Knipe, and P.M. Howley, *Fields Virology*. 6 ed. Vol. 1. 2013, Philadelphia: Lippincott Williams & Wilkins.
8. Tong, S., et al., *A distinct lineage of influenza A virus from bats.* Proc Natl Acad Sci U S A, 2012. **109**(11): p. 4269-74.

9. Tong, S., et al., *New world bats harbor diverse influenza A viruses.* PLoS Pathog, 2013. **9**(10): p. e1003657.

10. Yang, W., T. Schountz, and W. Ma, *Bat Influenza Viruses: Current Status and Perspective.* Viruses, 2021. **13**(4).

11. Rota, P.A., et al., *Cocirculation of two distinct evolutionary lineages of influenza type B virus since 1983.* Virology, 1990. **175**(1): p. 59-68.

12. Paget, J., et al., *Has influenza B/Yamagata become extinct and what implications might this have for quadrivalent influenza vaccines?* Euro Surveill, 2022. **27**(39).

13. Koutsakos, M., et al., *Influenza lineage extinction during the COVID-19 pandemic?* Nat Rev Microbiol, 2021. **19**(12): p. 741-742.

14. Dawood, F.S., et al., *Emergence of a novel swine-origin influenza A (H1N1) virus in humans.* N Engl J Med, 2009. **360**(25): p. 2605-15.

15. Smith, G.J., et al., *Origins and evolutionary genomics of the 2009 swine-origin H1N1 influenza A epidemic.* Nature, 2009. **459**(7250): p. 1122-5.

16. Abdelwhab, E.M. and T.C. Mettenleiter, *Zoonotic Animal Influenza Virus and Potential Mixing Vessel Hosts.* Viruses, 2023. **15**(4).

17. Tran, D., et al., *Hospitalization for Influenza A Versus B.* Pediatrics, 2016. **138**(3).

18. Bodewes, R., et al., *Recurring influenza B virus infections in seals.* Emerg Infect Dis, 2013. **19**(3): p. 511-2.

19. Ran, Z., et al., *Domestic pigs are susceptible to infection with influenza B viruses.* J Virol, 2015. **89**(9): p. 4818-26.

20. Chang, C.P., et al., *Influenza virus isolations from dogs during a human epidemic in Taiwan.* Int J Zoonoses, 1976. **3**(1): p. 61-4.

21. Pandrea, I., et al., *Into the wild: simian immunodeficiency virus (SIV) infection in natural hosts.* Trends Immunol, 2008. **29**(9): p. 419-28.

22. Apetrei, C., et al., *Direct inoculation of simian immunodeficiency virus from sooty mangabeys in black mangabeys (Lophocebus aterrimus): first evidence of AIDS in a heterologous African species and different pathologic outcomes of experimental infection.* J Virol, 2004. **78**(21): p. 11506-18.

23. Souquiere, S., et al., *Simian immunodeficiency virus types 1 and 2 (SIV mnd 1 and 2) have different pathogenic potentials in rhesus macaques upon experimental cross-species transmission.* J Gen Virol, 2009. **90**(Pt 2): p. 488-499.

24. Kornfeld, C., et al., *Antiinflammatory profiles during primary SIV infection in African green monkeys are associated with protection against AIDS.* J Clin Invest, 2005. **115**(4): p. 1082-91.

25. Easterbrook, J.D. and S.L. Klein, *Immunological mechanisms mediating hantavirus persistence in rodent reservoirs.* PLoS Pathog, 2008. **4**(11): p. e1000172.

26. Schountz, T. and J. Prescott, *Hantavirus immunology of rodent reservoirs: current status and future directions.* Viruses, 2014. **6**(3): p. 1317-35.

27. Mandl, J.N., et al., *Distinctive TLR7 signaling, type I IFN production, and attenuated innate and adaptive immune responses to yellow fever virus in a primate reservoir host.* J Immunol, 2011. **186**(11): p. 6406-16.

28. Cohen, C., et al., *Severe influenza-associated respiratory infection in high HIV prevalence setting, South Africa, 2009-2011.* Emerg Infect Dis, 2013. **19**(11): p. 1766-74.

29. Centers for Disease, C. and Prevention, *Influenza-associated pediatric deaths--United States, September 2010-August 2011.* MMWR Morb Mortal Wkly Rep, 2011. **60**(36): p. 1233-8.

30. CDC. *Seasonal Influenza Vaccine Effectiveness, 2017-2018*. 2018 [cited 2019 November 17]; Available from: https://www.cdc.gov/flu/vaccines-work/2017-2018.html.

31. Belderbos, M.E., et al., *Plasma-mediated immune suppression: a neonatal perspective.* Pediatr Allergy Immunol, 2013. **24**(2): p. 102-13.

32. Wang, S.M., et al., *The regulatory T cells in anti-influenza antibody response post influenza vaccination.* Hum Vaccin Immunother, 2012. **8**(9): p. 1243-9.

33. Pekarek, M.J. and E.A. Weaver, *Existing Evidence for Influenza B Virus Adaptations to Drive Replication in Humans as the Primary Host.* Viruses, 2023. **15**(10).

34. Zhao, C. and J. Pu, *Influence of Host Sialic Acid Receptors Structure on the Host Specificity of Influenza Viruses.* Viruses, 2022. **14**(10).

35. Long, J.S., et al., *Publisher Correction: Host and viral determinants of influenza A virus species specificity.* Nat Rev Microbiol, 2019. **17**(2): p. 124.

36. Long, J.S., et al., *Host and viral determinants of influenza A virus species specificity.* Nat Rev Microbiol, 2019. **17**(2): p. 67-81.

37. Caini, S., et al., *The epidemiological signature of influenza B virus and its B/Victoria and B/Yamagata lineages in the 21st century.* PLoS One, 2019. **14**(9): p. e0222381.

38. Wang, Y.F., et al., *Characterization of glycan binding specificities of influenza B viruses with correlation with hemagglutinin genotypes and clinical features.* J Med Virol, 2012. **84**(4): p. 679-85.

39. Laporte, M., et al., *Hemagglutinin Cleavability, Acid Stability, and Temperature Dependence Optimize Influenza B Virus for Replication in Human Airways.* J Virol, 2019. **94**(1).

40. Conenello, G.M., et al., *A Single N66S Mutation in the PB1-F2 Protein of Influenza A Virus Increases Virulence by Inhibiting the Early Interferon Response In Vivo.* J Virol.

41. Jagger, B.W., et al., *An overlapping protein-coding region in influenza A virus segment 3 modulates the host response.* Science, 2012. **337**(6091): p. 199-204.

42. Lutz Iv, M.M., et al., *Key Role of the Influenza A Virus PA Gene Segment in the Emergence of Pandemic Viruses.* Viruses, 2020. **12**(4).

43. Chen, X., et al., *Host Immune Response to Influenza A Virus Infection.* Front Immunol, 2018. **9**: p. 320.

44. Yuan, W. and R.M. Krug, *Influenza B virus NS1 protein inhibits conjugation of the interferon (IFN)-induced ubiquitin-like ISG15 protein.* EMBO J, 2001. **20**(3): p. 362-71.

45. Koutsakos, M., et al., *Downregulation of MHC Class I Expression by Influenza A and B Viruses.* Front Immunol, 2019. **10**: p. 1158.

46. Dou, D., et al., *Influenza A Virus Cell Entry, Replication, Virion Assembly and Movement.* Front Immunol, 2018. **9**: p. 1581.

47. van de Sandt, C.E., et al., *Influenza B viruses: not to be discounted.* Future Microbiol, 2015. **10**(9): p. 1447-65.

48. Rogers, G.N., et al., *Single amino acid substitutions in influenza haemagglutinin change receptor binding specificity.* Nature, 1983. **304**(5921): p. 76-8.

49. Matrosovich, M.N., et al., *Avian influenza A viruses differ from human viruses by recognition of sialyloligosaccharides and gangliosides and by a higher conservation of the HA receptor-binding site.* Virology, 1997. **233**(1): p. 224-34.

50. Nicholls, J.M., et al., *Evolving complexities of influenza virus and its receptors.* Trends Microbiol, 2008. **16**(4): p. 149-57.

51. Imai, M. and Y. Kawaoka, *The role of receptor binding specificity in interspecies transmission of influenza viruses.* Curr Opin Virol, 2012. **2**(2): p. 160-7.

52. Ito, T., et al., *Molecular basis for the generation in pigs of influenza A viruses with pandemic potential.* J Virol, 1998. **72**(9): p. 7367-73.

53. Walther, T., et al., *Glycomic analysis of human respiratory tract tissues and correlation with influenza virus infection.* PLoS Pathog, 2013. **9**(3): p. e1003223.

54. Jia, N., et al., *Glycomic characterization of respiratory tract tissues of ferrets: implications for its use in influenza virus infection studies.* J Biol Chem, 2014. **289**(41): p. 28489-504.

55. Karakus, U., M.O. Pohl, and S. Stertz, *Breaking the Convention: Sialoglycan Variants, Coreceptors, and Alternative Receptors for Influenza A Virus Entry.* J Virol, 2020. **94**(4).

56. Guo, H., et al., *Kinetic analysis of the influenza A virus HA/NA balance reveals contribution of NA to virus-receptor binding and NA-dependent rolling on receptor-containing surfaces.* PLoS Pathog, 2018. **14**(8): p. e1007233.

57. Roy, A.M., et al., *Early stages of influenza virus entry into Mv-1 lung cells: involvement of dynamin.* Virology, 2000. **267**(1): p. 17-28.

58. Rust, M.J., et al., *Assembly of endocytic machinery around individual influenza viruses during viral entry.* Nat Struct Mol Biol, 2004. **11**(6): p. 567-73.

59. Sieczkarski, S.B. and G.R. Whittaker, *Influenza virus can enter and infect cells in the absence of clathrin-mediated endocytosis.* J Virol, 2002. **76**(20): p. 10455-64.

60. de Vries, E., et al., *Dissection of the influenza a virus endocytic routes reveals macropinocytosis as an alternative entry pathway.* PLoS Pathog, 2011. **7**(3): p. e1001329.

61. Pinto, L.H., L.J. Holsinger, and R.A. Lamb, *Influenza virus M2 protein has ion channel activity.* Cell, 1992. **69**(3): p. 517-28.

62. Imai, M., et al., *Influenza B virus BM2 protein is a crucial component for incorporation of viral ribonucleoprotein complex into virions during virus assembly.* J Virol, 2004. **78**(20): p. 11007-15.

63. Yoshimura, A. and S. Ohnishi, *Uncoating of influenza virus in endosomes.* J Virol, 1984. **51**(2): p. 497-504.

64. Bui, M., G. Whittaker, and A. Helenius, *Effect of M1 protein and low pH on nuclear transport of influenza virus ribonucleoproteins.* J Virol, 1996. **70**(12): p. 8391-401.

65. Harrison, S.C., *Viral membrane fusion.* Virology, 2015. **479-480**: p. 498-507.

66. Baudin, F., et al., *Structure of influenza virus RNP. I. Influenza virus nucleoprotein melts secondary structure in panhandle RNA and exposes the bases to the solvent.* EMBO J, 1994. **13**(13): p. 3158-65.

67. Eisfeld, A.J., G. Neumann, and Y. Kawaoka, *At the centre: influenza A virus ribonucleoproteins.* Nat Rev Microbiol, 2015. **13**(1): p. 28-41.

68. Fodor, E., *The RNA polymerase of influenza a virus: mechanisms of viral transcription and replication.* Acta Virol, 2013. **57**(2): p. 113-22.

69. Plotch, S.J., et al., *A unique cap(m7GpppXm)-dependent influenza virion endonuclease cleaves capped RNAs to generate the primers that initiate viral RNA transcription.* Cell, 1981. **23**(3): p. 847-58.

70. Poon, L.L., et al., *Direct evidence that the poly(A) tail of influenza A virus mRNA is synthesized by reiterative copying of a U track in the virion RNA template.* J Virol, 1999. **73**(4): p. 3473-6.

71. Jorba, N., R. Coloma, and J. Ortin, *Genetic trans-complementation establishes a new model for influenza virus RNA transcription and replication.* PLoS Pathog, 2009. **5**(5): p. e1000462.

72. York, A. and E. Fodor, *Biogenesis, assembly, and export of viral messenger ribonucleoproteins in the influenza A virus infected cell.* RNA Biol, 2013. **10**(8): p. 1274-82.

73. Ayllon, J. and A. Garcia-Sastre, *The NS1 protein: a multitasking virulence factor.* Curr Top Microbiol Immunol, 2015. **386**: p. 73-107.

74. Satterly, N., et al., *Influenza virus targets the mRNA export machinery and the nuclear pore complex.* Proc Natl Acad Sci U S A, 2007. **104**(6): p. 1853-8.

75. Eisfeld, A.J., et al., *RAB11A is Essential for Influenza Genome Transport to the Plasma Membrane.* J Virol, 2011.

76. Paterson, D. and E. Fodor, *Emerging roles for the influenza A virus nuclear export protein (NEP).* PLoS Pathog, 2012. **8**(12): p. e1003019.

77. Gerber, M., et al., *Selective packaging of the influenza A genome and consequences for genetic reassortment.* Trends Microbiol, 2014. **22**(8): p. 446-55.

78. Duhaut, S.D. and J.W. McCauley, *Defective RNAs inhibit the assembly of influenza virus genome segments in a segment-specific manner.* Virology, 1996. **216**(2): p. 326-37.

79. Chou, Y.Y., et al., *One influenza virus particle packages eight unique viral RNAs as shown by FISH analysis.* Proc Natl Acad Sci U S A, 2012. **109**(23): p. 9101-6.

80. Muramoto, Y., et al., *Hierarchy among viral RNA (vRNA) segments in their role in vRNA incorporation into influenza A virions.* J Virol, 2006. **80**(5): p. 2318-25.

81. Liang, Y., Y. Hong, and T.G. Parslow, *cis-Acting packaging signals in the influenza virus PB1, PB2, and PA genomic RNA segments.* J Virol, 2005. **79**(16): p. 10348-55.

82. Lakdawala, S.S., E. Fodor, and K. Subbarao, *Moving On Out: Transport and Packaging of Influenza Viral RNA into Virions.* Annu Rev Virol, 2016. **3**(1): p. 411-427.

83. Sherry, L., et al., *Identification of cis-acting packaging signals in the coding regions of the influenza B virus HA gene segment.* J Gen Virol, 2016. **97**(2): p. 306-315.

84. Lingwood, D. and K. Simons, *Lipid rafts as a membrane-organizing principle.* Science, 2010. **327**(5961): p. 46-50.

85. Nayak, D.P., et al., *Influenza virus morphogenesis and budding.* Virus Res, 2009. **143**(2): p. 147-61.

86. Zhang, J., A. Pekosz, and R.A. Lamb, *Influenza virus assembly and lipid raft microdomains: a role for the cytoplasmic tails of the spike glycoproteins.* J Virol, 2000. **74**(10): p. 4634-44.

87. Noton, S.L., et al., *Identification of the domains of the influenza A virus M1 matrix protein required for NP binding, oligomerization and incorporation into virions.* J Gen Virol, 2007. **88**(Pt 8): p. 2280-2290.

88. Jarsch, I.K., F. Daste, and J.L. Gallop, *Membrane curvature in cell biology: An integration of molecular mechanisms.* J Cell Biol, 2016. **214**(4): p. 375-87.

89. Basak, S., M. Tomana, and R.W. Compans, *Sialic acid is incorporated into influenza hemagglutinin glycoproteins in the absence of viral neuraminidase.* Virus Res, 1985. **2**(1): p. 61-8.

90. Palese, P., et al., *Characterization of temperature sensitive influenza virus mutants defective in neuraminidase.* Virology, 1974. **61**(2): p. 397-410.

91. Summerfield, A. and K.C. McCullough, *Dendritic Cells in Innate and Adaptive Immune Responses against Influenza Virus.* Viruses, 2009. **1**(3): p. 1022-34.

92. Sanders, C.J., P.C. Doherty, and P.G. Thomas, *Respiratory epithelial cells in innate immunity to influenza virus infection.* Cell Tissue Res, 2011. **343**(1): p. 13-21.

93. Chan, R.W., et al., *Tissue tropism of swine influenza viruses and reassortants in ex vivo cultures of the human respiratory tract and conjunctiva.* J Virol, 2011.

94. Zeng, H., et al., *Tropism and infectivity of influenza virus, including highly pathogenic avian H5N1 virus, in ferret tracheal differentiated primary epithelial cell cultures.* J Virol, 2013. **87**(5): p. 2597-607.

95. Ganesan, S., A.T. Comstock, and U.S. Sajjan, *Barrier function of airway tract epithelium*. Tissue Barriers, 2013. **1**(4): p. e24997.

96. Cohen, M., et al., *Influenza A penetrates host mucus by cleaving sialic acids with neuraminidase.* Virol J, 2013. **10**: p. 321.

97. Yang, X., et al., *A beneficiary role for neuraminidase in influenza virus penetration through the respiratory mucus.* PLoS One, 2014. **9**(10): p. e110026.

98. Chang, W.C., et al., *Lack of the pattern recognition molecule mannose-binding lectin increases susceptibility to influenza A virus infection.* BMC Immunol. **11**(1): p. 64.

99. Benne, C.A., et al., *Interactions of surfactant protein A with influenza A viruses: binding and neutralization.* J Infect Dis, 1995. **171**(2): p. 335-41.

100. Tripathi, S., M.R. White, and K.L. Hartshorn, *The amazing innate immune response to influenza A virus infection.* Innate Immun, 2015. **21**(1): p. 73-98.

101. Ioannidis, I., et al., *Toll-like receptor expression and induction of type I and type III interferons in primary airway epithelial cells.* J Virol, 2013. **87**(6): p. 3261-70.

102. Diebold, S.S., et al., *Innate antiviral responses by means of TLR7-mediated recognition of single-stranded RNA.* Science, 2004. **303**(5663): p. 1529-31.

103. Loo, Y.M. and M. Gale, Jr., *Immune signaling by RIG-I-like receptors.* Immunity, 2011. **34**(5): p. 680-92.

104. Dai, J., et al., *Regulation of IFN regulatory factor-7 and IFN-alpha production by enveloped virus and lipopolysaccharide in human plasmacytoid dendritic cells.* J Immunol, 2004. **173**(3): p. 1535-48.

105. Iwasaki, A. and P.S. Pillai, *Innate immunity to influenza virus infection.* Nat Rev Immunol, 2014. **14**(5): p. 315-28.

106. Matsumoto, M., et al., *Subcellular localization of Toll-like receptor 3 in human dendritic cells.* J Immunol, 2003. **171**(6): p. 3154-62.

107. Chen, Y., et al., *Toll-like receptor 3 (TLR3) regulation mechanisms and roles in antiviral innate immune responses.* J Zhejiang Univ Sci B, 2021. **22**(8): p. 609-632.

108. Onomoto, K., K. Onoguchi, and M. Yoneyama, *Regulation of RIG-I-like receptor-mediated signaling: interaction between host and viral factors.* Cell Mol Immunol, 2021. **18**(3): p. 539-555.

109. Saito, T. and M. Gale, Jr., *Differential recognition of double-stranded RNA by RIG-I-like receptors in antiviral immunity.* J Exp Med, 2008. **205**(7): p. 1523-7.

110. Rehwinkel, J., et al., *RIG-I detects viral genomic RNA during negative-strand RNA virus infection.* Cell, 2010. **140**(3): p. 397-408.

111. Pang, I.K., P.S. Pillai, and A. Iwasaki, *Efficient influenza A virus replication in the respiratory tract requires signals from TLR7 and RIG-I.* Proc Natl Acad Sci U S A, 2013. **110**(34): p. 13910-5.

112. Lee, N., et al., *Role of human Toll-like receptors in naturally occurring influenza A infections.* Influenza Other Respir Viruses, 2013. **7**(5): p. 666-75.

113. Pothlichet, J., et al., *Study of human RIG-I polymorphisms identifies two variants with an opposite impact on the antiviral immune response.* PLoS One, 2009. **4**(10): p. e7582.

114. Mifsud, E.J., M. Kuba, and I.G. Barr, *Innate Immune Responses to Influenza Virus Infections in the Upper Respiratory Tract.* Viruses, 2021. **13**(10).

115. Zelaya, H., et al., *Respiratory Antiviral Immunity and Immunobiotics: Beneficial Effects on Inflammation-Coagulation Interaction during Influenza Virus Infection.* Front Immunol, 2016. **7**: p. 633.

116. Denney, L., et al., *Epithelial-derived TGF-beta1 acts as a pro-viral factor in the lung during influenza A infection.* Mucosal Immunol, 2018. **11**(2): p. 523-535.

117. Peiro, T., et al., *Neutrophils drive alveolar macrophage IL-1beta release during respiratory viral infection.* Thorax, 2018. **73**(6): p. 546-556.

118. Tavares, L.P., M.M. Teixeira, and C.C. Garcia, *The inflammatory response triggered by Influenza virus: a two edged sword.* Inflamm Res, 2017. **66**(4): p. 283-302.

119. Isaacs, A. and J. Lindenmann, *Virus interference. I. The interferon.* Proc R Soc Lond B Biol Sci, 1957. **147**(927): p. 258-67.

120. Isaacs, A., J. Lindenmann, and R.C. Valentine, *Virus interference. II. Some properties of interferon.* Proc R Soc Lond B Biol Sci, 1957. **147**(927): p. 268-73.

121. Sutton, R.N.P. and D.A.J. Tyrrell, *Some Observations on Interferon Prepared in Tissue Cultures.* British Journal of Experimental Pathology, 1962. **42**(2): p. 99-105.

122. Asselin-Paturel, C., et al., *Mouse type I IFN-producing cells are immature APCs with plasmacytoid morphology.* Nat Immunol, 2001. **2**(12): p. 1144-50.

123. Denney, L. and L.P. Ho, *The role of respiratory epithelium in host defence against influenza virus infection.* Biomed J, 2018. **41**(4): p. 218-233.

124. Ye, L., D. Schnepf, and P. Staeheli, *Interferon-lambda orchestrates innate and adaptive mucosal immune responses.* Nat Rev Immunol, 2019. **19**(10): p. 614-625.

125. Zhou, Z., et al., *Type III interferon (IFN) induces a type I IFN-like response in a restricted subset of cells through signaling pathways involving both the Jak-STAT pathway and the mitogen-activated protein kinases.* J Virol, 2007. **81**(14): p. 7749-58.

126. Bolen, C.R., et al., *Dynamic expression profiling of type I and type III interferon-stimulated hepatocytes reveals a stable hierarchy of gene expression.* Hepatology, 2014. **59**(4): p. 1262-72.

127. Betakova, T., et al., *Cytokines Induced During Influenza Virus Infection.* Curr Pharm Des, 2017. **23**(18): p. 2616-2622.

128. Baumgarth, N. and A. Kelso, *In vivo blockade of gamma interferon affects the influenza virus-induced humoral and the local cellular immune response in lung tissue.* J Virol, 1996. **70**(7): p. 4411-8.

129. Graham, M.B., et al., *Response to influenza infection in mice with a targeted disruption in the interferon gamma gene.* J Exp Med, 1993. **178**(5): p. 1725-32.

130. Steimle, V., et al., *Regulation of MHC class II expression by interferon-gamma mediated by the transactivator gene CIITA.* Science, 1994. **265**(5168): p. 106-9.

131. Yokozeki, H., et al., *Interferon-gamma differentially regulates CD80 (B7-1) and CD86 (B7-2/B70) expression on human Langerhans cells.* Br J Dermatol, 1997. **136**(6): p. 831-7.

132. Bauvois, B., et al., *Types I and II interferons upregulate the costimulatory CD80 molecule in monocytes via interferon regulatory factor-1*. Biochem Pharmacol, 2009. **78**(5): p. 514-22.

133. Ma, X., et al., *The interleukin 12 p40 gene promoter is primed by interferon gamma in monocytic cells.* J Exp Med, 1996. **183**(1): p. 147-57.

134. Hillyer, P., et al., *Expression profiles of human interferon-alpha and interferon-lambda subtypes are ligand- and cell-dependent.* Immunol Cell Biol, 2012. **90**(8): p. 774-83.

135. Boulant, S., et al., *Editorial: Type III interferons: Emerging roles beyond antiviral barrier defense.* Front Immunol, 2022. **13**: p. 1030812.

136. Hemann, E.A., et al., *Interferon-lambda modulates dendritic cells to facilitate T cell immunity during infection with influenza A virus.* Nat Immunol, 2019. **20**(8): p. 1035-1045.

137. Ye, L., et al., *Interferon-lambda enhances adaptive mucosal immunity by boosting release of thymic stromal lymphopoietin.* Nat Immunol, 2019. **20**(5): p. 593-601.

138. Domeier, P.P., Z.S.M. Rahman, and S.F. Ziegler, *B cell- and T cell-intrinsic regulation of germinal centers by thymic stromal lymphopoietin signaling.* Sci Immunol, 2023. **8**(79): p. eadd9413.

139. Oslund, K.L., et al., *Synergistic up-regulation of CXCL10 by virus and IFN gamma in human airway epithelial cells.* PLoS One, 2014. **9**(7): p. e100978.

140. Neville, L.F., G. Mathiak, and O. Bagasra, *The immunobiology of interferon-gamma inducible protein 10 kD (IP-10): a novel, pleiotropic member of the C-X-C chemokine superfamily.* Cytokine Growth Factor Rev, 1997. **8**(3): p. 207-19.

141. Cole, A.M., et al., *Cutting edge: IFN-inducible ELR- CXC chemokines display defensin-like antimicrobial activity.* J Immunol, 2001. **167**(2): p. 623-7.

142. Hayney, M.S., et al., *Serum IFN-gamma-induced protein 10 (IP-10) as a biomarker for severity of acute respiratory infection in healthy adults.* J Clin Virol, 2017. **90**: p. 32-37.

143. Bermejo-Martin, J.F., et al., *Th1 and Th17 hypercytokinemia as early host response signature in severe pandemic influenza.* Crit Care, 2009. **13**(6): p. R201.

144. Zhu, J., et al., *Stat5 activation plays a critical role in Th2 differentiation.* Immunity, 2003. **19**(5): p. 739-48.

145. McKinstry, K.K., et al., *Effector CD4 T-cell transition to memory requires late cognate interactions that induce autocrine IL-2.* Nat Commun, 2014. **5**: p. 5377.

146. McKinstry, K.K., et al., *Memory CD4 T cell-derived IL-2 synergizes with viral infection to exacerbate lung inflammation.* PLoS Pathog, 2019. **15**(8): p. e1007989.

147. Dennig, D., et al., *Interleukin-2 may enhance or inhibit antibody production by B cells depending on intracellular cAMP concentrations.* Immunology, 1992. **77**(2): p. 251-5.

148. Provinciali, M., et al., *Adjuvant effect of low-dose interleukin-2 on antibody response to influenza virus vaccination in healthy elderly subjects.* Mech Ageing Dev, 1994. **77**(2): p. 75-82.

149. Bendickova, K. and J. Fric, *Roles of IL-2 in bridging adaptive and innate immunity, and as a tool for cellular immunotherapy.* J Leukoc Biol, 2020. **108**(1): p. 427-437.

150. Singh, S., D. Anshita, and V. Ravichandiran, *MCP-1: Function, regulation, and involvement in disease.* Int Immunopharmacol, 2021. **101**(Pt B): p. 107598.

151. Dessing, M.C., et al., *Monocyte chemoattractant protein 1 contributes to an adequate immune response in influenza pneumonia.* Clin Immunol, 2007.

152. Menten, P., A. Wuyts, and J. Van Damme, *Macrophage inflammatory protein-1*. Cytokine Growth Factor Rev, 2002. **13**(6): p. 455-81.

153. Memoli, M.J., et al., *The natural history of influenza infection in the severely immunocompromised vs nonimmunocompromised hosts.* Clin Infect Dis, 2014. **58**(2): p. 214-24.

154. Fritz, R.S., et al., *Nasal cytokine and chemokine responses in experimental influenza A virus infection: results of a placebo-controlled trial of intravenous zanamivir treatment.* J Infect Dis, 1999. **180**(3): p. 586-93.

155. Cook, D.N., et al., *Requirement of MIP-1 alpha for an inflammatory response to viral infection.* Science, 1995. **269**(5230): p. 1583-5.

156. Miyauchi, K., et al., *Influenza virus infection expands the breadth of antibody responses through IL-4 signalling in B cells.* Nat Commun, 2021. **12**(1): p. 3789.

157. Murphy, K. and C. Weaver, *The adaptive immune response*, in *Janeway's Immunobiology*. 2017, Garland Science: New York. p. 345-398.

158. Graham, M.B. and T.J. Braciale, *Resistance to and recovery from lethal influenza virus infection in B lymphocyte-deficient mice.* J Exp Med, 1997. **186**(12): p. 2063-8.

159. Mills, K.H.G., *IL-17 and IL-17-producing cells in protection versus pathology.* Nat Rev Immunol, 2023. **23**(1): p. 38-54.

160. Wang, X., et al., *A critical role of IL-17 in modulating the B-cell response during H5N1 influenza virus infection.* Cell Mol Immunol, 2011. **8**(6): p. 462-8.

161. Komastu, T., D.D. Ireland, and C.S. Reiss, *IL-12 and viral infections.* Cytokine Growth Factor Rev, 1998. **9**(3-4): p. 277-85.

162. Khader, S.A., et al., *Interleukin 12p40 is required for dendritic cell migration and T cell priming after Mycobacterium tuberculosis infection.* J Exp Med, 2006. **203**(7): p. 1805-15.

163. Aste-Amezaga, M., et al., *Molecular mechanisms of the induction of IL-12 and its inhibition by IL-10.* J Immunol, 1998. **160**(12): p. 5936-44.

164. Monteiro, J.M., C. Harvey, and G. Trinchieri, *Role of interleukin-12 in primary influenza virus infection.* J Virol, 1998. **72**(6): p. 4825-31.

165. Gu, Y., et al., *The Mechanism behind Influenza Virus Cytokine Storm*. Viruses, 2021. **13**(7).

166. Murphy, K. and C. Weaver, *The induced responses of innate immunity*, in *Janeway's Immunobiology*. 2017, Garland Science: New York. p. 77-137.

167. Rincon, M., *Special issue on interleukin-6 (IL-6).* Int J Biol Sci, 2012. **8**(9): p. 1225-6.

168. Rincon, M., *Interleukin-6: from an inflammatory marker to a target for inflammatory diseases.* Trends Immunol, 2012. **33**(11): p. 571-7.

169. Topley, N., et al., *Activation of inflammation and leukocyte recruitment into the peritoneal cavity.* Kidney Int Suppl, 1996. **56**: p. S17-21.

170. Guo, L., et al., *Role of CXCL5 in Regulating Chemotaxis of Innate and Adaptive Leukocytes in Infected Lungs Upon Pulmonary Influenza Infection.* Front Immunol, 2021. **12**: p. 785457.

171. Kohli, K., V.G. Pillarisetty, and T.S. Kim, *Key chemokines direct migration of immune cells in solid tumors.* Cancer Gene Ther, 2022. **29**(1): p. 10-21.

172. Zhang, W., et al., *CXCL5/CXCR2 axis in tumor microenvironment as potential diagnostic biomarker and therapeutic target.* Cancer Commun (Lond), 2020. **40**(2-3): p. 69-80.

173. Zhang, J., et al., *Two waves of pro-inflammatory factors are released during the influenza A virus (IAV)-driven pulmonary immunopathogenesis.* PLoS Pathog, 2020. **16**(2): p. e1008334.

174. Jones, S.A., *Directing transition from innate to acquired immunity: defining a role for IL-6.* J Immunol, 2005. **175**(6): p. 3463-8.

175. Lauder, S.N., et al., *Interleukin-6 limits influenza-induced inflammation and protects against fatal lung pathology.* Eur J Immunol, 2013. **43**(10): p. 2613-25.

176. Karnowski, A., et al., *B and T cells collaborate in antiviral responses via IL-6, IL-21, and transcriptional activator and coactivator, Oct2 and OBF-1.* J Exp Med, 2012. **209**(11): p. 2049-64.

177. Matsukura, S., et al., *Expression of IL-6, IL-8, and RANTES on human bronchial epithelial cells, NCI-H292, induced by influenza virus A.* J Allergy Clin Immunol, 1996. **98**(6 Pt 1): p. 1080-7.

178. Adachi, M., et al., *Expression of cytokines on human bronchial epithelial cells induced by influenza virus A.* Int Arch Allergy Immunol, 1997. **113**(1-3): p. 307-11.

179. Fitzpatrick, D.R., D.J. Peroni, and H. Bielefeldt-Ohmann, *The role of growth factors and cytokines in the tumorigenesis and immunobiology of malignant mesothelioma.* Am J Respir Cell Mol Biol, 1995. **12**(5): p. 455-60.

180. Khabar, K.S., et al., *The alpha chemokine, interleukin 8, inhibits the antiviral action of interferon alpha.* J Exp Med, 1997. **186**(7): p. 1077-85.

181. Hayden, F.G., et al., *Local and systemic cytokine responses during experimental human influenza A virus infection. Relation to symptom formation and host defense.* J Clin Invest, 1998. **101**(3): p. 643-9.

182. Skoner, D.P., et al., *Evidence for cytokine mediation of disease expression in adults experimentally infected with influenza A virus.* J Infect Dis, 1999. **180**(1): p. 10-4.

183. Dinarello, C.A., *Biologic basis for interleukin-1 in disease.* Blood, 1996. **87**(6): p. 2095-147.

184. Lopez-Castejon, G. and D. Brough, *Understanding the mechanism of IL-1beta secretion.* Cytokine Growth Factor Rev, 2011. **22**(4): p. 189-95.

185. Dinarello, C.A., *The biology of interleukin 1 and comparison to tumor necrosis factor.* Immunol Lett, 1987. **16**(3-4): p. 227-31.

186. Segura, E., et al., *Human inflammatory dendritic cells induce Th17 cell differentiation.* Immunity, 2013. **38**(2): p. 336-48.

187. Bawazeer, A.O., et al., *Interleukin-1beta exacerbates disease and is a potential therapeutic target to reduce pulmonary inflammation during severe influenza A virus infection.* Immunol Cell Biol, 2021. **99**(7): p. 737-748.

188. Tang, C., et al., *Interleukin-23: as a drug target for autoimmune inflammatory diseases.* Immunology, 2012. **135**(2): p. 112-24.

189. McKenzie, B.S., R.A. Kastelein, and D.J. Cua, *Understanding the IL-23-IL-17 immune pathway.* Trends Immunol, 2006. **27**(1): p. 17-23.

190. Kudva, A., et al., *Influenza A inhibits Th17-mediated host defense against bacterial pneumonia in mice.* J Immunol, 2011. **186**(3): p. 1666-1674.

191. Khan, T., et al., *Membrane-bound IL-12 and IL-23 serve as potent mucosal adjuvants when co-presented on whole inactivated influenza vaccines.* Virol J, 2014. **11**: p. 78.

192. Scheeren, F.A., et al., *Thymic stromal lymphopoietin induces early human B-cell proliferation and differentiation.* Eur J Immunol, 2010. **40**(4): p. 955-65.

193. Crotty, S., *T follicular helper cell differentiation, function, and roles in disease.* Immunity, 2014. **41**(4): p. 529-42.

194. Merad, M., et al., *The dendritic cell lineage: ontogeny and function of dendritic cells and their subsets in the steady state and the inflamed setting.* Annu Rev Immunol, 2013. **31**: p. 563-604.

195. Gutierrez-Martinez, E., et al., *Cross-Presentation of Cell-Associated Antigens by MHC Class I in Dendritic Cell Subsets.* Front Immunol, 2015. **6**: p. 363.

196. ten Broeke, T., R. Wubbolts, and W. Stoorvogel, *MHC class II antigen presentation by dendritic cells regulated through endosomal sorting.* Cold Spring Harb Perspect Biol, 2013. **5**(12): p. a016873.

197. Dolan, B.P., K.D. Gibbs, Jr., and S. Ostrand-Rosenberg, *Dendritic cells cross-dressed with peptide MHC class I complexes prime CD8+ T cells.* J Immunol, 2006. **177**(9): p. 6018-24.

198. Dolan, B.P., K.D. Gibbs, Jr., and S. Ostrand-Rosenberg, *Tumor-specific CD4+ T cells are activated by "cross-dressed" dendritic cells presenting peptide-MHC class II complexes acquired from cell-based cancer vaccines.* J Immunol, 2006. **176**(3): p. 1447-55.

199. Nakayama, M., *Antigen Presentation by MHC-Dressed Cells.* Front Immunol, 2014. **5**: p. 672.

200. Guermonprez, P., et al., *Antigen presentation and T cell stimulation by dendritic cells.* Annu Rev Immunol, 2002. **20**: p. 621-67.

201. Jego, G., et al., *Plasmacytoid dendritic cells induce plasma cell differentiation through type I interferon and interleukin 6.* Immunity, 2003. **19**(2): p. 225-34.

202. Heer, A.K., et al., *TLR signaling fine-tunes anti-influenza B cell responses without regulating effector T cell responses.* J Immunol, 2007. **178**(4): p. 2182-91.

203. de Groen, R.A., et al., *IFN-lambda is able to augment TLR-mediated activation and subsequent function of primary human B cells.* J Leukoc Biol, 2015. **98**(4): p. 623-30.

204. Joo, S., et al., *Critical role of TSLP-responsive mucosal dendritic cells in the induction of nasal antigen-specific IgA response.* Mucosal Immunol, 2017. **10**(4): p. 901-911.

205. Bahadoran, A., et al., *Immune Responses to Influenza Virus and Its Correlation to Age and Inherited Factors.* Front Microbiol, 2016. **7**: p. 1841.

206. Scott, G.H. and R.J. Sydiskis, *Responses of mice immunized with influenza virus by serosol and parenteral routes.* Infect Immun, 1976. **13**(3): p. 696-703.

207. Gerhard, W., et al., *Role of the B-cell response in recovery of mice from primary influenza virus infection.* Immunol Rev, 1997. **159**: p. 95-103.

208. Vono, M., et al., *Maternal Antibodies Inhibit Neonatal and Infant Responses to Vaccination by Shaping the Early-Life B Cell Repertoire within Germinal Centers.* Cell Rep, 2019. **28**(7): p. 1773-1784 e5.

209. Zaman, K., et al., *Effectiveness of Maternal Influenza Immunization in Mothers and Infants.* N Engl J Med, 2008.

210. Kantor, A.B. and L.A. Herzenberg, *Origin of murine B cell lineages.* Annu Rev Immunol, 1993. **11**: p. 501-38.

211. Baumgarth, N., et al., *B-1 and B-2 cell-derived immunoglobulin M antibodies are nonredundant components of the protective response to influenza virus infection.* J Exp Med, 2000. **192**(2): p. 271-80.

212. De Silva, N.S. and U. Klein, *Dynamics of B cells in germinal centres.* Nat Rev Immunol, 2015. **15**(3): p. 137-48.

213. Tangye, S.G., *To B1 or not to B1: that really is still the question!* Blood, 2013. **121**(26): p. 5109-10.

214. Lam, J.H. and N. Baumgarth, *The Multifaceted B Cell Response to Influenza Virus.* J Immunol, 2019. **202**(2): p. 351-359.

215. Sealy, R., et al., *Antibody response to influenza infection of mice: different patterns for glycoprotein and nucleocapsid antigens.* Immunology, 2003. **108**(4): p. 431-9.

216. Chiu, C., et al., *B cell responses to influenza infection and vaccination.* Curr Top Microbiol Immunol, 2015. **386**: p. 381-98.

217. Mettelman, R.C., E.K. Allen, and P.G. Thomas, *Mucosal immune responses to infection and vaccination in the respiratory tract.* Immunity, 2022. **55**(5): p. 749-780.

218. Ho, A.W., et al., *Lung CD103+ dendritic cells efficiently transport influenza virus to the lymph node and load viral antigen onto MHC class I for presentation to CD8 T cells.* J Immunol, 2011. **187**(11): p. 6011-21.

219. Whitmire, J.K., J.T. Tan, and J.L. Whitton, *Interferon-gamma acts directly on CD8+ T cells to increase their abundance during virus infection.* J Exp Med, 2005. **201**(7): p. 1053-9.

220. Pipkin, M.E., et al., *Interleukin-2 and inflammation induce distinct transcriptional programs that promote the differentiation of effector cytolytic T cells.* Immunity, 2010. **32**(1): p. 79-90.

221. Egli, A., et al., *IL-28B is a key regulator of B- and T-cell vaccine responses against influenza.* PLoS Pathog, 2014. **10**(12): p. e1004556.

222. Rudd-Schmidt, J.A., J.A. Trapani, and I. Voskoboinik, *Distinguishing perforin-mediated lysis and granzyme-dependent apoptosis.* Methods Enzymol, 2019. **629**: p. 291-306.

223. Brincks, E.L., et al., *The Magnitude of the T Cell Response to a Clinically Significant Dose of Influenza Virus Is Regulated by TRAIL.* J Immunol, 2011.

224. Brincks, E.L., et al., *CD8 T cells utilize TRAIL to control influenza virus infection.* J Immunol, 2008. **181**(7): p. 4918-25.

225. Legge, K.L. and T.J. Braciale, *Lymph node dendritic cells control CD8+ T cell responses through regulated FasL expression.* Immunity, 2005. **23**(6): p. 649-59.

226. Grant, E.J., et al., *Human influenza viruses and CD8(+) T cell responses.* Curr Opin Virol, 2016. **16**: p. 132-142.

227. Pizzolla, A., et al., *Resident memory CD8(+) T cells in the upper respiratory tract prevent pulmonary influenza virus infection.* Sci Immunol, 2017. **2**(12).

228. McKinstry, K.K., et al., *Memory CD4+ T cells protect against influenza through multiple synergizing mechanisms.* J Clin Invest, 2012. **122**(8): p. 2847-56.

229. Lukens, M.V., et al., *Respiratory syncytial virus-induced activation and migration of respiratory dendritic cells and subsequent antigen presentation in the lung-draining lymph node.* J Virol, 2009. **83**(14): p. 7235-43.

230. Pape, K.A., et al., *Inflammatory cytokines enhance the in vivo clonal expansion and differentiation of antigen-activated CD4+ T cells.* J Immunol, 1997. **159**(2): p. 591-8.

231. Aleebrahim-Dehkordi, E., et al., *T helper type (Th1/Th2) responses to SARS-CoV-2 and influenza A (H1N1) virus: From cytokines produced to immune responses.* Transpl Immunol, 2022. **70**: p. 101495.

232. Zhu, J., H. Yamane, and W.E. Paul, *Differentiation of effector CD4 T cell populations (*).* Annu Rev Immunol, 2010. **28**: p. 445-89.

233. Lamb, J.R., et al., *Antigen-specific human T lymphocyte clones: viral antigen specificity of influenza virus-immune clones.* J Immunol, 1982. **128**(3): p. 1428-32.

234. Mukherjee, S., et al., *IL-17-induced pulmonary pathogenesis during respiratory viral infection and exacerbation of allergic disease.* Am J Pathol, 2011. **179**(1): p. 248-58.

235. Lu, C., et al., *Memory regulatory T cells home to the lung and control influenza A virus infection.* Immunol Cell Biol, 2019. **97**(9): p. 774-786.

236. Jandl, C., C. Loetsch, and C. King, *Cytokine Expression by T Follicular Helper Cells.* Methods Mol Biol, 2017. **1623**: p. 95-103.

237. Jain, A. and C. Pasare, *Innate Control of Adaptive Immunity: Beyond the Three-Signal Paradigm*. J Immunol, 2017. **198**(10): p. 3791-3800.

238. Rastogi, I., et al., *Role of B cells as antigen presenting cells.* Front Immunol, 2022. **13**: p. 954936.

239. Severinson, E., *Identification of the IgG1 Induction Factor (Interleukin 4).* Front Immunol, 2014. **5**: p. 628.

240. Purkerson, J.M. and P.C. Isakson, *Interleukin 5 (IL-5) provides a signal that is required in addition to IL-4 for isotype switching to immunoglobulin (Ig) G1 and IgE.* J Exp Med, 1992. **175**(4): p. 973-82.

241. Stavnezer, J. and J. Kang, *The surprising discovery that TGF beta specifically induces the IgA class switch.* J Immunol, 2009. **182**(1): p. 5-7.

242. Bossie, A. and E.S. Vitetta, *IFN-gamma enhances secretion of IgG2a from IgG2a-committed LPS-stimulated murine B cells: implications for the role of IFN-gamma in class switching.* Cell Immunol, 1991. **135**(1): p. 95-104.

243. Klein, U. and R. Dalla-Favera, *Germinal centres: role in B-cell physiology and malignancy.* Nat Rev Immunol, 2008. **8**(1): p. 22-33.

244. Lambrecht, B.N. and H. Hammad, *Lung dendritic cells in respiratory viral infection and asthma: from protection to immunopathology.* Annu Rev Immunol, 2012. **30**: p. 243-70.

245. Moltedo, B., et al., *Unique type I interferon responses determine the functional fate of migratory lung dendritic cells during influenza virus infection.* PLoS Pathog, 2011. **7**(11): p. e1002345.

246. Zografou, C., A.G. Vakrakou, and P. Stathopoulos, *Short- and Long-Lived Autoantibody-Secreting Cells in Autoimmune Neurological Disorders.* Front Immunol, 2021. **12**: p. 686466.

247. Coffey, F., B. Alabyev, and T. Manser, *Initial clonal expansion of germinal center B cells takes place at the perimeter of follicles.* Immunity, 2009. **30**(4): p. 599-609.

248. Pereira, J.P., L.M. Kelly, and J.G. Cyster, *Finding the right niche: B-cell migration in the early phases of T-dependent antibody responses.* Int Immunol, 2010. **22**(6): p. 413-9.

249. Wong, J., et al., *Sequencing B cell receptors from ferrets (Mustela putorius furo).* PLoS One, 2020. **15**(5): p. e0233794.

250. Wong, J., et al., *Improving immunological insights into the ferret model of human viral infectious disease.* Influenza Other Respir Viruses, 2019. **13**(6): p. 535-546.

251. Murphy, K. and C. Weaver, *Antigen recognition by B-cell and T-cell receptors/Generation of lymphocyte antigen receptors*, in *Janeway's Immunobiology*. 2017, Garland Science: New York. p. 139-212.

252. Kirchenbaum, G.A., et al., *Infection of Ferrets with Influenza Virus Elicits a Light Chain-Biased Antibody Response against Hemagglutinin.* J Immunol, 2017. **199**(11): p. 3798-3807.

253. Kirchenbaum, G.A. and T.M. Ross, *Generation of Monoclonal Antibodies against Immunoglobulin Proteins of the Domestic Ferret (Mustela putorius furo).* J Immunol Res, 2017. **2017**: p. 5874572.

254. Vidarsson, G., G. Dekkers, and T. Rispens, *IgG subclasses and allotypes: from structure to effector functions.* Front Immunol, 2014. **5**: p. 520.

255. Schroeder, H.W., Jr. and L. Cavacini, *Structure and function of immunoglobulins.* J Allergy Clin Immunol, 2010. **125**(2 Suppl 2): p. S41-52.

256. El-Madhun, A.S., R.J. Cox, and L.R. Haaheim, *The effect of age and natural priming on the IgG and IgA subclass responses after parenteral influenza vaccination.* J Infect Dis, 1999. **180**(4): p. 1356-60.

257. Frasca, D., et al., *Effects of age on H1N1-specific serum IgG1 and IgG3 levels evaluated during the 2011-2012 influenza vaccine season.* Immun Ageing, 2013. **10**(1): p. 14.

258. Manenti, A., et al., *Comparative analysis of influenza A(H3N2) virus hemagglutinin specific IgG subclass and IgA responses in children and adults after influenza vaccination.* Vaccine, 2017. **35**(1): p. 191-198.

259. Hammarstrom, L., et al., *Subclass restriction pattern of antigen-specific antibodies in donors with defective expression of IgG or IgA subclass heavy chain constant region genes.* Clin Immunol Immunopathol, 1987. **45**(3): p. 461-70.

260. Pakkanen, S.H., et al., *Expression of homing receptors on IgA1 and IgA2 plasmablasts in blood reflects differential distribution of IgA1 and IgA2 in various body fluids.* Clin Vaccine Immunol, 2010. **17**(3): p. 393-401.

261. Maurer, M.A., et al., *Glycosylation of Human IgA Directly Inhibits Influenza A and Other Sialic-Acid-Binding Viruses.* Cell Rep, 2018. **23**(1): p. 90-99.

262. Reynolds, H.Y., *Immunoglobulin G and its function in the human respiratory tract.* Mayo Clin Proc, 1988. **63**(2): p. 161-74.

263. Lamere, M.W., et al., *Contributions of Antinucleoprotein IgG to Heterosubtypic Immunity against Influenza Virus.* J Immunol, 2011.

264. Lamere, M.W., et al., *Regulation of anti-nucleoprotein IgG by systemic vaccination and its effect on influenza virus clearance.* J Virol, 2011.

265. Crisci, E., et al., *Review: influenza virus in pigs.* Mol Immunol, 2013. **55**(3-4): p. 200-11.

266. Swearengen, J.R., *Choosing the right animal model for infectious disease research.* Animal Model Exp Med, 2018. **1**(2): p. 100-108.

267. F.D.A. *Overview of the Animal Model Qualification Program*. Available from: https://www.fda.gov/drugs/animal-model-qualification-program-amqp/overview-animal-model-qualification-program.

268. Ibricevic, A., et al., *Influenza virus receptor specificity and cell tropism in mouse and human airway epithelial cells.* J Virol, 2006. **80**(15): p. 7469-80.

269. Rigoni, M., et al., *The mouse model is suitable for the study of viral factors governing transmission and pathogenesis of highly pathogenic avian influenza (HPAI) viruses in mammals.* Vet Res, 2010. **41**(5): p. 66.

270. Bright, R.A., et al., *Mechanisms of pathogenicity of influenza A (H5N1) viruses in mice.* Avian Dis, 2003. **47**(3 Suppl): p. 1131-4.

271. Rowe, T., et al., *Neurological manifestations of avian influenza viruses in mammals.* Avian Dis, 2003. **47**(3 Suppl): p. 1122-6.

272. Kamal, R.P., J.M. Katz, and I.A. York, *Molecular determinants of influenza virus pathogenesis in mice.* Curr Top Microbiol Immunol, 2014. **385**: p. 243-74.

273. Choi, E.J., et al., *The effect of mutations derived from mouse-adapted H3N2 seasonal influenza A virus to pathogenicity and host adaptation.* PLoS One, 2020. **15**(1): p. e0227516.

274. Prokopyeva, E., et al., *Experimental Infection Using Mouse-Adapted Influenza B Virus in a Mouse Model.* Viruses, 2020. **12**(4).

275. Staeheli, P., et al., *Influenza virus-susceptible mice carry Mx genes with a large deletion or a nonsense mutation.* Mol Cell Biol, 1988. **8**(10): p. 4518-23.

276. Samet, S.J. and S.M. Tompkins, *Influenza Pathogenesis in Genetically Defined Resistant and Susceptible Murine Strains*Yale J Biol Med, 2017. **90**(3): p. 471-479.

277. Alberts, R., et al., *Gene expression changes in the host response between resistant and susceptible inbred mouse strains after influenza A infection.* Microbes Infect, 2010. **12**(4): p. 309-18.

278. Yang, Y.T. and C.A. Evans, *Hypothermia in mice due to influenza virus infection.* Proc Soc Exp Biol Med, 1961. **108**: p. 776-80.

279. Wong, J.P., et al., *Development of a murine hypothermia model for study of respiratory tract influenza virus infection.* Lab Anim Sci, 1997. **47**(2): p. 143-7.

280. Matsuoka, Y., E.W. Lamirande, and K. Subbarao, *The mouse model for influenza.* Curr Protoc Microbiol, 2009. **Chapter 15**: p. Unit 15G 3.

281. Matute-Bello, G., et al., *An official American Thoracic Society workshop report: features and measurements of experimental acute lung injury in animals.* Am J Respir Cell Mol Biol, 2011. **44**(5): p. 725-38.

282. Xu, T., et al., *Acute Respiratory Distress Syndrome Induced by Avian Influenza A (H5N1) Virus in Mice.* Am J Respir Crit Care Med, 2006.

283. Aeffner, F., B. Bolon, and I.C. Davis, *Mouse Models of Acute Respiratory Distress Syndrome: A Review of Analytical Approaches, Pathologic Features, and Common Measurements.* Toxicol Pathol, 2015. **43**(8): p. 1074-92.

284. Traylor, Z.P., F. Aeffner, and I.C. Davis, *Influenza A H1N1 induces declines in alveolar gas exchange in mice consistent with rapid post-infection progression from acute lung injury to ARDS.* Influenza Other Respi Viruses, 2012.

285. Edenborough, K.M., B.P. Gilbertson, and L.E. Brown, *A mouse model for the study of contact-dependent transmission of influenza A virus and the factors that govern transmissibility.* J Virol, 2012.

286. van der Laan, J.W., et al., *Animal models in influenza vaccine testing.* Expert Rev Vaccines, 2008. **7**(6): p. 783-93.

287. Tamura, S., T. Tanimoto, and T. Kurata, *Mechanisms of broad cross-protection provided by influenza virus infection and their application to vaccines.* Jpn J Infect Dis, 2005. **58**(4): p. 195-207.

288. Kiros, T.G., et al., *The Importance of Animal Models in the Development of Vaccines.* Innovation in Vaccinology, 2012: p. 251-64.

289. Bouvier, N.M. and A.C. Lowen, *Animal Models for Influenza Virus Pathogenesis and Transmission.* Viruses, 2010. **2**(8): p. 1530-1563.

290. Lowen, A.C., et al., *The guinea pig as a transmission model for human influenza viruses.* Proc Natl Acad Sci U S A, 2006. **103**(26): p. 9988-92.

291. Pica, N., et al., *Transmission of Influenza B viruses in the Guinea Pig.* J Virol, 2012.

292. Steel, J., et al., *Transmission of pandemic H1N1 influenza virus and impact of prior exposure to seasonal strains or interferon treatment.* J Virol, 2010. **84**(1): p. 21-6.

293. Lowen, A.C., et al., *Blocking interhost transmission of influenza virus by vaccination in the guinea pig model.* J Virol, 2009. **83**(7): p. 2803-18.

294. Bushnell, R.V., et al., *Serological characterization of guinea pigs infected with H3N2 human influenza or immunized with hemagglutinin protein.* Virol J, 2010. **7**: p. 200.

295. Lemaitre, J., et al., *Non-human primate models of human respiratory infections.* Mol Immunol, 2021. **135**: p. 147-164.

296. Karlsson, E.A., et al., *Influenza virus infection in nonhuman primates.* Emerg Infect Dis, 2012. **18**(10): p. 1672-5.

297. Hemmink, J.D., C.J. Whittaker, and H.A. Shelton, *Animal Models in Influenza Research.* Methods Mol Biol, 2018. **1836**: p. 401-430.

298. Bodewes, R., G.F. Rimmelzwaan, and A.D. Osterhaus, *Animal models for the preclinical evaluation of candidate influenza vaccines.* Expert Rev Vaccines, 2010. **9**(1): p. 59-72.

299. Carroll, T.D., et al., *Interferon-induced expression of MxA in the respiratory tract of rhesus macaques is suppressed by influenza virus replication.* J Immunol, 2008. **180**(4): p. 2385-95.

300. Rimmelzwaan, G.F., et al., *A single dose of an ISCOM influenza vaccine induces long-lasting protective immunity against homologous challenge infection but fails to protect Cynomolgus macaques against distant drift variants of influenza A (H3N2) viruses.* Vaccine, 2001. **20**(1-2): p. 158-63.

301. Safronetz, D., et al., *Pandemic swine-origin H1N1 influenza A virus isolates show heterogeneous virulence in macaques.* J Virol, 2011. **85**(3): p. 1214-23.

302. Rimmelzwaan, G.F., et al., *Pathogenesis of influenza A (H5N1) virus infection in a primate model.* J Virol, 2001. **75**(14): p. 6687-91.

303. Baskin, C.R., et al., *Early and sustained innate immune response defines pathology and death in nonhuman primates infected by highly pathogenic influenza virus.* Proc Natl Acad Sci U S A, 2009.

304. Rimmelzwaan, G.F., et al., *Induction of protective immunity against influenza virus in a macaque model: comparison of conventional and iscom vaccines.* J Gen Virol, 1997. **78 (Pt 4)**: p. 757-65.

305. Rimmelzwaan, G.F., et al., *A primate model to study the pathogenesis of influenza A (H5N1) virus infection.* Avian Dis, 2003. **47**(3 Suppl): p. 931-3.

306. Rowe, T., et al., *Modeling host responses in ferrets during A/California/07/2009 influenza infection.* Virology, 2010. **401**(2): p. 257-65.

307. Smith, W., C. H. Andrewes, and P. P. Laidlaw, *A virus obtained from influenza patients.* Lancet, 1933. **2**: p. 66-68.

308. Peng, X., et al., *The draft genome sequence of the ferret (Mustela putorius furo) facilitates study of human respiratory disease.* Nat Biotechnol, 2014. **32**(12): p. 1250-5.

309. Leon, A.J., et al., *Sequencing, annotation, and characterization of the influenza ferret infectome.* J Virol, 2013. **87**(4): p. 1957-66.

310. Prince, G.A. and D.D. Porter, *The pathogenesis of respiratory syncytial virus infection in infant ferrets.* Am J Pathol, 1976. **82**(2): p. 339-52.

311. Stittelaar, K.J., et al., *Ferrets as a Novel Animal Model for Studying Human Respiratory Syncytial Virus Infections in Immunocompetent and Immunocompromised Hosts.* Viruses, 2016. **8**(6).

312. Thormar, H., P.D. Mehta, and H.R. Brown, *Comparison of wild-type and subacute sclerosing panencephalitis strains of measles virus. Neurovirulence in ferrets and biological properties in cell cultures.* J Exp Med, 1978. **148**(3): p. 674-91.

313. Mascoli, C.C., et al., *Further studies on the neonatal ferret model of infection and immunity to and attenuation of human parainfluenza viruses.* Dev Biol Stand, 1976. **33**: p. 384-90.

314. MacPhail, M., et al., *Identification of small-animal and primate models for evaluation of vaccine candidates for human metapneumovirus (hMPV) and implications for hMPV vaccine design.* J Gen Virol, 2004. **85**(Pt 6): p. 1655-1663.

315. Martina, B.E., et al., *Virology: SARS virus infection of cats and ferrets.* Nature, 2003. **425**(6961): p. 915.

316. Zhao, Y., et al., *Ferrets: A powerful model of SARS-CoV-2.* Zool Res, 2023. **44**(2): p. 323-330.

317. Belser, J.A., J.A. Pulit-Penaloza, and T.R. Maines, *Ferreting Out Influenza Virus Pathogenicity and Transmissibility: Past and Future Risk Assessments in the Ferret Model.* Cold Spring Harb Perspect Med, 2020. **10**(7).

318. Belser, J.A., et al., *Complexities in Ferret Influenza Virus Pathogenesis and Transmission Models.* Microbiol Mol Biol Rev, 2016. **80**(3): p. 733-44.

319. Xu, Q., et al., *Influenza H1N1 A/Solomon Island/3/06 virus receptor binding specificity correlates with virus pathogenicity, antigenicity and immunogenicity in ferrets.* J Virol, 2010. **84**(10): p. 4936-45.

320. Kirkeby, S., C.J. Martel, and B. Aasted, *Infection with human H1N1 influenza virus affects the expression of sialic acids of metaplastic mucous cells in the ferret airways.* Virus Res, 2009.

321. Maines, T.R., et al., *Lack of transmission of H5N1 avian-human reassortant influenza viruses in a ferret model.* Proc Natl Acad Sci U S A, 2006. **103**(32): p. 12121-6.

322. Yen, H.L., et al., *Neuraminidase inhibitor-resistant influenza viruses may differ substantially in fitness and transmissibility.* Antimicrob Agents Chemother, 2005. **49**(10): p. 4075-84.

323. Munster, V.J., et al., *Pathogenesis and Transmission of Swine-Origin 2009 A(H1N1) Influenza Virus in Ferrets.* Science, 2009.

324. Enkirch, T. and V. von Messling, *Ferret models of viral pathogenesis.* Virology, 2015. **479-480**: p. 259-70.

325. Zitzow, L.A., et al., *Pathogenesis of avian influenza A (H5N1) viruses in ferrets.* J Virol, 2002. **76**(9): p. 4420-9.

326. Tumpey, T.M., et al., *A two-amino acid change in the hemagglutinin of the 1918 influenza virus abolishes transmission.* Science, 2007. **315**(5812): p. 655-9.

327. Sun, X., et al., *Disease phenotype of a ferret CFTR-knockout model of cystic fibrosis.* J Clin Invest, 2010. **120**(9): p. 3149-60.

328. Yan, Z., et al., *Ferret and pig models of cystic fibrosis: prospects and promise for gene therapy.* Hum Gene Ther Clin Dev, 2015. **26**(1): p. 38-49.

329. Rioux, M., et al., *The Intersection of Age and Influenza Severity: Utility of Ferrets for Dissecting the Age-Dependent Immune Responses and Relevance to Age-Specific Vaccine Development.* Viruses, 2021. **13**(4).

330. Bissel, S.J., et al., *Age-Related Pathology Associated with H1N1 A/California/07/2009 Influenza Virus Infection.* Am J Pathol, 2019. **189**(12): p. 2389-2399.

331. Meliopoulos, V., et al., *Diet-induced obesity impacts influenza disease severity and transmission dynamics in ferrets.* bioRxiv, 2023.

332. Vazquez-Pagan, A. and S. Schultz-Cherry, *Serological Responses to Influenza Vaccination during Pregnancy.* Microorganisms, 2021. **9**(11).

333. Baker, P., et al., *Development of a ferret model of maternal antibody passive transfer to suckling neonates.* The Journal of Immunology, 2023. **210**(1_Supplement): p. 224.12-224.12.

334. Horman, W.S.J., et al., *The Dynamics of the Ferret Immune Response During H7N9 Influenza Virus Infection.* Front Immunol, 2020. **11**: p. 559113.

335. Cameron, C.M., et al., *Gene expression analysis of host innate immune responses during Lethal H5N1 infection in ferrets.* J Virol, 2008. **82**(22): p. 11308-17.

336. Oh, D.Y. and A.C. Hurt, *Using the Ferret as an Animal Model for Investigating Influenza Antiviral Effectiveness.* Front Microbiol, 2016. **7**: p. 80.

337. Strickland, B.A., et al., *Species-specific transcriptomic changes upon respiratory syncytial virus infection in cotton rats.* Sci Rep, 2022. **12**(1): p. 16579.

338. Boukhvalova, M.S. and J.C. Blanco, *The cotton rat Sigmodon hispidus model of respiratory syncytial virus infection.* Curr Top Microbiol Immunol, 2013. **372**: p. 347-58.

339. Yim, K., et al., *Efficacy of trivalent inactivated influenza vaccines in the cotton rat Sigmodon hispidus model.* Vaccine, 2011.

340. Ottolini, M.G., et al., *The cotton rat provides a useful small-animal model for the study of influenza virus pathogenesis.* J Gen Virol, 2005. **86**(Pt 10): p. 2823-2830.

341. Eichelberger, M.C., *The cotton rat as a model to study influenza pathogenesis and immunity.* Viral Immunol, 2007. **20**(2): p. 243-9.

342. Blanco, J.C., et al., *Modeling Human Respiratory Viral Infections in the Cotton Rat (Sigmodon hispidus).* J Antivir Antiretrovir, 2014. **6**: p. 40-42.

343. Lindenmann, J., *Resistance of mice to mouse-adapted influenza A virus.* Virology, 1962. **16**: p. 203-4.

344. Horisberger, M.A., P. Staeheli, and O. Haller, *Interferon induces a unique protein in mouse cells bearing a gene for resistance to influenza virus.* Proc Natl Acad Sci U S A, 1983. **80**(7): p. 1910-4.

345. Pillai, P.S., et al., *Mx1 reveals innate pathways to antiviral resistance and lethal influenza disease.* Science, 2016. **352**(6284): p. 463-6.

346. Haller, O. and G. Kochs, *Mx genes: host determinants controlling influenza virus infection and trans-species transmission.* Hum Genet, 2020. **139**(6-7): p. 695-705.

347. Haller, O., P. Staeheli, and G. Kochs, *Interferon-induced Mx proteins in antiviral host defense.* Biochimie, 2007.

348. Ward, L.E., *Handling the cotton rat for research.* Lab Anim (NY), 2001. **30**(5): p. 45-50.

349. Eichelberger, M.C., G.A. Prince, and M.G. Ottolini, *Influenza-induced tachypnea is prevented in immune cotton rats, but cannot be treated with an anti-inflammatory steroid or a neuraminidase inhibitor.* Virology, 2004. **322**(2): p. 300-7.

350. Trias, E.L., et al., *Comparison of airway measurements during influenza-induced tachypnea in infant and adult cotton rats.* BMC Pulm Med, 2009. **9**: p. 28.

351. Blanco, J.C., et al., *The cotton rat: an underutilized animal model for human infectious diseases can now be exploited using specific reagents to cytokines, chemokines, and interferons.* J Interferon Cytokine Res, 2004. **24**(1): p. 21-8.

352. Curlee, J.F. and D.M. Cooper, *Cotton Rat*, in *The Laboratory Rabbit, Guinea Pig, Hamster, and Other Rodents*, M.A. Suckow, K.A. Stevens, and R.A. Wilson, Editors. 2012, Elsevier Inc. p. 1105-1113.

353. Ali, M.J., et al., *Transmissibility of influenza viruses in hamsters.* Arch Virol, 1982. **72**(3): p. 187-97.

354. Mills, J., V. Chanock, and R.M. Chanock, *Temperature-sensitive mutants of influenza virus. I. Behavior in tissue culture and in experimental animals.* J Infect Dis, 1971. **123**(2): p. 145-57.

355. Abou-Donia, H., R. Jennings, and C.W. Potter, *Growth of influenza A viruses in hamsters.* Arch Virol, 1980. **65**(2): p. 99-107.

356. Potter, C.W. and R. Jennings, *The hamster as a model system for the study of influenza vaccines.* Postgrad Med J, 1976. **52**(608): p. 345-51.

357. Reeve, P., B. Gerendas, and H. Walzl, *Growth of some attenuated influenza viruses in hamster tracheal organ cultures.* Med Microbiol Immunol, 1978. **166**(1-4): p. 141-50.

358. Iwatsuki-Horimoto, K., et al., *Syrian Hamster as an Animal Model for the Study of Human Influenza Virus Infection.* J Virol, 2018. **92**(4).

359. Zeng, H., et al., *Tropism and Infectivity of a Seasonal A(H1N1) and a Highly Pathogenic Avian A(H5N1) Influenza Virus in Primary Differentiated Ferret Nasal Epithelial Cell Cultures.* J Virol, 2019. **93**(10).

360. Chakrabarti, A.K., et al., *Host gene expression profiling in influenza A virus-infected lung epithelial (A549) cells: a comparative analysis between highly pathogenic and modified H5N1 viruses.* Virol J, 2010. **7**: p. 219.

361. Paul Glezen, W., et al., *The burden of influenza B: a structured literature review*. Am J Public Health, 2013. **103**(3): p. e43-51.

362. Petrie, J.G., et al., *The Household Influenza Vaccine Effectiveness Study: Lack of Antibody Response and Protection Following Receipt of 2014-2015 Influenza Vaccine.* Clin Infect Dis, 2017. **65**(10): p. 1644-1651.

363. Tenforde, M.W., et al., *Effect of Antigenic Drift on Influenza Vaccine Effectiveness in the United States-2019-2020.* Clin Infect Dis, 2021. **73**(11): p. e4244-e4250.

364. Mir, H., I. Haq, and P.A. Koul, *Poor Vaccine Effectiveness against Influenza B-Related Severe Acute Respiratory Infection in a Temperate North Indian State (2019-2020): A Call for Further Data for Possible Vaccines with Closer Match.* Vaccines (Basel), 2021. **9**(10).

365. van Riel, D., et al., *Human and Avian Influenza Viruses Target Different Cells in the Lower Respiratory Tract of Humans and Other Mammals.* Am J Pathol, 2007.

366. Hirst, G.K., *Studies on the Mechanism of Adaptation of Influenza Virus to Mice.* J Exp Med, 1947. **86**(5): p. 357-66.

367. Xu, L., et al., *Adaption of seasonal H1N1 influenza virus in mice.* PLoS One, 2011. **6**(12): p. e28901.

368. Albrecht, R.A., et al., *Moving Forward: Recent Developments for the Ferret Biomedical Research Model.* mBio, 2018. **9**(4).

369. DiPiazza, A.T., et al., *Analyses of Cellular Immune Responses in Ferrets Following Influenza Virus Infection.* Methods Mol Biol, 2018. **1836**: p. 513-530.

370. Prevention, C.f.D.C.a. *Weekly U.S. Influenza Surveillance Report*. 2023 [cited 2023; Available from: https://www.cdc.gov/flu/weekly/.

371. Wedekind, A., D. Fritzsch, and A. Kroger, *Add on the next level-the time point of the type I IFN response orchestrates the immune response.* Cell Mol Immunol, 2020. **17**(8): p. 791-793.

372. Teijaro, J.R., *Type I interferons in viral control and immune regulation.* Curr Opin Virol, 2016. **16**: p. 31-40.

373. Friend, S.L., et al., *A thymic stromal cell line supports in vitro development of surface IgM+ B cells and produces a novel growth factor affecting B and T lineage cells.* Exp Hematol, 1994. **22**(3): p. 321-8.

374. Ray, R.J., et al., *Characterization of thymic stromal-derived lymphopoietin (TSLP) in murine B cell development in vitro.* Eur J Immunol, 1996. **26**(1): p. 10-6.

375. Yadava, K., et al., *TSLP promotes influenza-specific CD8+ T-cell responses by augmenting local inflammatory dendritic cell function.* Mucosal Immunol, 2013. **6**(1): p. 83-92.

376. Oslund, K.L. and N. Baumgarth, *Influenza-induced innate immunity: regulators of viral replication, respiratory tract pathology & adaptive immunity.* Future Virol, 2011. **6**(8): p. 951-962.

377. Robertson, J.S., et al., *Structural changes in the haemagglutinin which accompany egg adaptation of an influenza A(H1N1) virus.* Virology, 1987. **160**(1): p. 31-7.

378. Park, Y.W., et al., *Comparison of antigenic mutation during egg and cell passage cultivation of H3N2 influenza virus.* Clin Exp Vaccine Res, 2020. **9**(1): p. 56-63.

379. Gambaryan, A.S., J.S. Robertson, and M.N. Matrosovich, *Effects of egg-adaptation on the receptor-binding properties of human influenza A and B viruses.* Virology, 1999. **258**(2): p. 232-9.

380. Matrosovich, M., et al., *Overexpression of the alpha-2,6-sialyltransferase in MDCK cells increases influenza virus sensitivity to neuraminidase inhibitors.* J Virol, 2003. **77**(15): p. 8418-25.

381. World Health, O., *Manual for the laboratory diagnosis and virological surveillance of influenza*. 2011, World Health Organization: Geneva.

382. Lin, Y., et al., *The characteristics and antigenic properties of recently emerged subclade 3C.3a and 3C.2a human influenza A(H3N2) viruses passaged in MDCK cells.* Influenza Other Respir Viruses, 2017. **11**(3): p. 263-274.

383. Hongpaisan, J., *Inhibition of proliferation of contaminating fibroblasts by D-valine in cultures of smooth muscle cells from human myometrium.* Cell Biol Int, 2000. **24**(1): p. 1-7.

384. Matrosovich, M., et al., *New low-viscosity overlay medium for viral plaque assays.* Virol J, 2006. **3**: p. 63.

385. Oh, D.Y., et al., *MDCK-SIAT1 cells show improved isolation rates for recent human influenza viruses compared to conventional MDCK cells.* J Clin Microbiol, 2008. **46**(7): p. 2189-94.

386. Matrosovich, M., et al., *New low-viscosity overlay medium for viral plaque assays.* Virol J, 2006. **3**(1): p. 63.

387. Ballantyne, K.N., R.A. van Oorschot, and R.J. Mitchell, *Locked nucleic acids in PCR primers increase sensitivity and performance.* Genomics, 2008. **91**(3): p. 301-5.

388. Manukian, G., *Regulatory T cell response during influenza infection and vaccination in the ferret*, in *School of Medicine*. 2013, Tulane University. p. 179.

389. Camp, J.V., et al., *De-novo transcriptome sequencing of a normalized cDNA pool from influenza infected ferrets.* PLoS One, 2012. **7**(5): p. e37104.

390. Carolan, L.A., et al., *TaqMan real time RT-PCR assays for detecting ferret innate and adaptive immune responses.* J Virol Methods, 2014. **205**: p. 38-52.

391. Fang, Y., et al., *Molecular characterization of in vivo adjuvant activity in ferrets vaccinated against influenza virus.* J Virol, 2010. **84**(17): p. 8369-88.

392. Matsukura, S., et al., *Expression of RANTES by normal airway epithelial cells after influenza virus A infection.* Am J Respir Cell Mol Biol, 1998. **18**(2): p. 255-64.

393. Pharo, E.A., et al., *Host-Pathogen Responses to Pandemic Influenza H1N1pdm09 in a Human Respiratory Airway Model.* Viruses, 2020. **12**(6).

394. Wang, J., et al., *Innate immune response to influenza A virus in differentiated human alveolar type II cells.* Am J Respir Cell Mol Biol, 2011. **45**(3): p. 582-91.

395. Yan, Y., et al., *Human nasal epithelial cells derived from multiple subjects exhibit differential responses to H3N2 influenza virus infection in vitro.* J Allergy Clin Immunol, 2016. **138**(1): p. 276-281 e15.

396. Garcia-Sastre, A., et al., *Influenza A virus lacking the NS1 gene replicates in interferon-deficient systems.* Virology, 1998. **252**(2): p. 324-30.

397. Nogales, A., et al., *Functional Characterization and Direct Comparison of Influenza A, B, C, and D NS1 Proteins in vitro and in vivo.* Front Microbiol, 2019. **10**: p. 2862.

398. Zhao, C., et al., *Interferon-induced ISG15 pathway: an ongoing virus-host battle.* Trends Microbiol, 2013. **21**(4): p. 181-6.

399. Makela, S.M., et al., *RIG-I Signaling Is Essential for Influenza B Virus-Induced Rapid Interferon Gene Expression.* J Virol, 2015. **89**(23): p. 12014-25.

400. Jiang, J., et al., *Robust Lys63-Linked Ubiquitination of RIG-I Promotes Cytokine Eruption in Early Influenza B Virus Infection.* J Virol, 2016. **90**(14): p. 6263-6275.

401. Vangeti, S., M. Yu, and A. Smed-Sorensen, *Respiratory Mononuclear Phagocytes in Human Influenza A Virus Infection: Their Role in Immune Protection and As Targets of the Virus.* Front Immunol, 2018. **9**: p. 1521.

402. Wilson, J.L., et al., *The Influenza B Virus Victoria and Yamagata Lineages Display Distinct Cell Tropism and Infection-Induced Host Gene Expression in Human Nasal Epithelial Cell Cultures.* Viruses, 2023. **15**(9).

403. Jiao, P., et al., *Robust induction of interferon and interferon-stimulated gene expression by influenza B/Yamagata lineage virus infection of A549 cells.* PLoS One, 2020. **15**(4): p. e0231039.

404. Hewitt, R.J. and C.M. Lloyd, *Regulation of immune responses by the airway epithelial cell landscape.* Nat Rev Immunol, 2021. **21**(6): p. 347-362.

405. Comer, D.M., J.S. Elborn, and M. Ennis, *Comparison of nasal and bronchial epithelial cells obtained from patients with COPD*. PLoS One, 2012. **7**(3): p. e32924.

406. Sposito, B., et al., *The interferon landscape along the respiratory tract impacts the severity of COVID-19.* Cell, 2021. **184**(19): p. 4953-4968 e16.

407. Zhu, F., et al., *H1N1 Influenza Virus-Infected Nasal Mucosal Epithelial Progenitor Cells Promote Dendritic Cell Recruitment and Maturation.* Front Immunol, 2022. **13**: p. 879575.

408. Garcia-Sastre, A., *Induction and evasion of type I interferon responses by influenza viruses.* Virus Res, 2011. **162**(1-2): p. 12-8.

409. Wang, W. and R.M. Krug, *The RNA-binding and effector domains of the viral NS1 protein are conserved to different extents among influenza A and B viruses.* Virology, 1996. **223**(1): p. 41-50.

410. Dauber, B., G. Heins, and T. Wolff, *The influenza B virus nonstructural NS1 protein is essential for efficient viral growth and antagonizes beta interferon induction.* J Virol, 2004. **78**(4): p. 1865-72.

411. Schreiber, A., et al., *Type I interferon antagonistic properties of influenza B virus polymerase proteins.* Cell Microbiol, 2020. **22**(2): p. e13143.

412. Osterlund, P., et al., *Incoming influenza A virus evades early host recognition, while influenza B virus induces interferon expression directly upon entry.* J Virol, 2012. **86**(20): p. 11183-93.

413. Jia, D., et al., *Influenza virus non-structural protein 1 (NS1) disrupts interferon signaling.* PLoS One, 2010. **5**(11): p. e13927.

414. Hsu, A.C., et al., *Human influenza is more effective than avian influenza at antiviral suppression in airway cells.* Am J Respir Cell Mol Biol, 2011. **44**(6): p. 906-13.

415. Duong, E., et al., *Type I interferon activates MHC class I-dressed CD11b(+) conventional dendritic cells to promote protective anti-tumor CD8(+) T cell immunity.* Immunity, 2022. **55**(2): p. 308-323 e9.

416. Rowe, T., et al., *Differential interferon responses to influenza A and B viruses in primary ferret respiratory epithelial cells.* J Virol, 2024. **98**(2): p. e0149423.

417. Betts, R.J., et al., *Influenza A virus infection results in a robust, antigen-responsive, and widely disseminated Foxp3+ regulatory T cell response.* J Virol, 2012. **86**(5): p. 2817-25.

418. Sun, J., et al., *Effector T cells control lung inflammation during acute influenza virus infection by producing IL-10.* Nat Med, 2009. **15**(3): p. 277-84.

419. Krakauer, T., *Stimulant-dependent modulation of cytokines and chemokines by airway epithelial cells: cross talk between pulmonary epithelial and peripheral blood mononuclear cells.* Clin Diagn Lab Immunol, 2002. **9**(1): p. 126-31.

420. Rennard, S.I., et al., *Airway epithelial cells: functional roles in airway disease.* Am J Respir Crit Care Med, 1994. **150**(5 Pt 2): p. S27-30.

421. Luukkainen, A., et al., *A Co-culture Model of PBMC and Stem Cell Derived Human Nasal Epithelium Reveals Rapid Activation of NK and Innate T Cells Upon Influenza A Virus Infection of the Nasal Epithelium*. Front Immunol, 2018. **9**: p. 2514.

422. Egli, A., et al., *Effect of Immunosuppression on T-Helper 2 and B-Cell Responses to Influenza Vaccination.* J Infect Dis, 2015. **212**(1): p. 137-46.

423. Belser, J.A., J.M. Katz, and T.M. Tumpey, *The ferret as a model organism to study influenza A virus infection.* Dis Model Mech, 2011. **4**(5): p. 575-9.

424. Maher, J.A. and J. DeStefano, *The ferret: an animal model to study influenza virus.* Lab Anim (NY), 2004. **33**(9): p. 50-3.

425. Jayaraman, A., et al., *Decoding the distribution of glycan receptors for human-adapted influenza A viruses in ferret respiratory tract.* PLoS One, 2012. **7**(2): p. e27517.

426. Ng, P.S., et al., *Ferrets exclusively synthesize Neu5Ac and express naturally humanized influenza A virus receptors.* Nat Commun, 2014. **5**: p. 5750.

427. Lau, Y.C., et al., *Variation by lineage in serum antibody responses to influenza B virus infections.* PLoS One, 2020. **15**(11): p. e0241693.

428. Pang, I.K. and A. Iwasaki, *Inflammasomes as mediators of immunity against influenza virus.* Trends Immunol, 2011. **32**(1): p. 34-41.

429. Koerner, I., et al., *Protective role of beta interferon in host defense against influenza A virus.* J Virol, 2007. **81**(4): p. 2025-30.

430. Cox, N.J. and K. Subbarao, *Influenza.* Lancet, 1999. **354**(9186): p. 1277-82.

431. Kang, M., et al., *The impact of pre-existing influenza antibodies and inflammatory status on the influenza vaccine responses in older adults.* Influenza Other Respir Viruses, 2023. **17**(7): p. e13172.

432. Miyauchi, K., et al., *Protective neutralizing influenza antibody response in the absence of T follicular helper cells.* Nat Immunol, 2016. **17**(12): p. 1447-1458.

433. Stockman, E.R., H.E. Albers, and M.J. Baum, *Activity in the ferret: oestradiol effects and circadian rhythms.* Anim Behav, 1985. **33**(Pt 1): p. 150-4.

434. Belser, J.A., et al., *A Guide for the Use of the Ferret Model for Influenza Virus Infection.* Am J Pathol, 2020. **190**(1): p. 11-24.

435. Walls, H.H., et al., *Characterization and evaluation of monoclonal antibodies developed for typing influenza A and influenza B viruses.* J Clin Microbiol, 1986. **23**(2): p. 240-5.

436. Ecker, J.W., et al., *High-Yield Expression and Purification of Recombinant Influenza Virus Proteins from Stably-Transfected Mammalian Cell Lines.* Vaccines (Basel), 2020. **8**(3).

437. Sautto, G.A., et al., *A Computationally Optimized Broadly Reactive Antigen Subtype-Specific Influenza Vaccine Strategy Elicits Unique Potent Broadly Neutralizing Antibodies against Hemagglutinin.* J Immunol, 2020. **204**(2): p. 375-385.

438. Laurie, K.L., et al., *Interval Between Infections and Viral Hierarchy Are Determinants of Viral Interference Following Influenza Virus Infection in a Ferret Model.* J Infect Dis, 2015. **212**(11): p. 1701-10.

439. Pulit-Penaloza, J.A., et al., *Kinetics and magnitude of viral RNA shedding as indicators for Influenza A virus transmissibility in ferrets.* Commun Biol, 2023. **6**(1): p. 90.

440. Shen, C.F., et al., *Innate Immune Responses of Vaccinees Determine Early Neutralizing Antibody Production After ChAdOx1nCoV-19 Vaccination.* Front Immunol, 2022. **13**: p. 807454.

441. Kitphati, R., et al., *Kinetics and longevity of antibody response to influenza A H5N1 virus infection in humans.* Clin Vaccine Immunol, 2009.

442. Skountzou, I., et al., *Influenza virus-specific neutralizing IgM antibodies persist for a lifetime.* Clin Vaccine Immunol, 2014. **21**(11): p. 1481-9.

443. Krammer, F., *The human antibody response to influenza A virus infection and vaccination.* Nat Rev Immunol, 2019. **19**(6): p. 383-397.

444. Huang, S.S., et al., *Comparative analyses of pandemic H1N1 and seasonal H1N1, H3N2, and influenza B infections depict distinct clinical pictures in ferrets.* PLoS One, 2011. **6**(11): p. e27512.

445. Sun, W., et al., *Antibody Responses toward the Major Antigenic Sites of Influenza B Virus Hemagglutinin in Mice, Ferrets, and Humans.* J Virol, 2019. **93**(2).

446. Schmolke, M. and A. Garcia-Sastre, *Evasion of innate and adaptive immune responses by influenza A virus.* Cell Microbiol, 2010. **12**(7): p. 873-80.

447. Socan, M., et al., *A comparison of the demographic and clinical characteristics of laboratory-confirmed influenza B Yamagata and Victoria lineage infection.* J Clin Virol, 2014. **61**(1): p. 156-60.

448. McLean, H.Q. and E.A. Belongia, *Influenza Vaccine Effectiveness: New Insights and Challenges.* Cold Spring Harb Perspect Med, 2021. **11**(6).

449. Matsuoka, Y., E.W. Lamirande, and K. Subbarao, *The ferret model for influenza.* Curr Protoc Microbiol, 2009. **Chapter 15**: p. Unit 15G 2.

450. Rowe, T., et al., *Delay of innate immune responses following influenza B virus infection affects the development of a robust antibody response in ferrets.* (Submitted) PLoS Pathogens, 2024.

451. Rudenko, L., et al., *Rationale for vaccination with trivalent or quadrivalent live attenuated influenza vaccines: Protective vaccine efficacy in the ferret model.* PLoS One, 2018. **13**(12): p. e0208028.

452. Fernandez-Sesma, A., et al., *Influenza virus evades innate and adaptive immunity via the NS1 protein.* J Virol, 2006. **80**(13): p. 6295-304.

453. Harris, J.M. and R.B. Chess, *Effect of pegylation on pharmaceuticals.* Nat Rev Drug Discov, 2003. **2**(3): p. 214-21.

454. Veronese, F.M. and A. Mero, *The impact of PEGylation on biological therapies.* BioDrugs, 2008. **22**(5): p. 315-29.

455. Turecek, P.L., et al., *PEGylation of Biopharmaceuticals: A Review of Chemistry and Nonclinical Safety Information of Approved Drugs.* J Pharm Sci, 2016. **105**(2): p. 460-475.

456. Shcherbik, S., et al., *Implementation of new approaches for generating conventional reassortants for live attenuated influenza vaccine based on Russian master donor viruses.* J Virol Methods, 2016. **227**: p. 33-9.

457. Wang, S.M., et al., *Immunophenotype expressions and cytokine profiles of influenza A H1N1 virus infection in pediatric patients in 2009.* Dis Markers, 2014. **2014**: p. 195453.

458. Gounder, A.P., et al., *Interferon induced protein 35 exacerbates H5N1 influenza disease through the expression of IL-12p40 homodimer.* PLoS Pathog, 2018. **14**(4): p. e1007001.

459. Lazear, H.M., T.J. Nice, and M.S. Diamond, *Interferon-lambda: Immune Functions at Barrier Surfaces and Beyond.* Immunity, 2015. **43**(1): p. 15-28.

460. Donnelly, R.P. and S.V. Kotenko, *Interferon-lambda: a new addition to an old family.* J Interferon Cytokine Res, 2010. **30**(8): p. 555-64.

461. Killip, M.J., E. Fodor, and R.E. Randall, *Influenza virus activation of the interferon system.* Virus Res, 2015. **209**: p. 11-22.

462. Klinkhammer, J., et al., *IFN-lambda prevents influenza virus spread from the upper airways to the lungs and limits virus transmission.* Elife, 2018. **7**.

463. Kugel, D., et al., *Intranasal administration of alpha interferon reduces seasonal influenza A virus morbidity in ferrets.* J Virol, 2009. **83**(8): p. 3843-51.

464. Andreakos, E., I. Zanoni, and I.E. Galani, *Lambda interferons come to light: dual function cytokines mediating antiviral immunity and damage control.* Curr Opin Immunol, 2019. **56**: p. 67-75.

465. Pothlichet, J., M. Chignard, and M. Si-Tahar, *Cutting edge: innate immune response triggered by influenza A virus is negatively regulated by SOCS1 and SOCS3 through a RIG-I/IFNAR1-dependent pathway.* J Immunol, 2008. **180**(4): p. 2034-8.

466. Pauli, E.K., et al., *Influenza A virus inhibits type I IFN signaling via NF-kappaB-dependent induction of SOCS-3 expression.* PLoS Pathog, 2008. **4**(11): p. e1000196.

467. Carow, B. and M.E. Rottenberg, *SOCS3, a Major Regulator of Infection and Inflammation.* Front Immunol, 2014. **5**: p. 58.

468. Treanor, J.J., et al., *Intranasally administered interferon as prophylaxis against experimentally induced influenza A virus infection in humans.* J Infect Dis, 1987. **156**(2): p. 379-83.

469. Bennett, A.L., et al., *Low-dose oral interferon alpha as prophylaxis against viral respiratory illness: a double-blind, parallel controlled trial during an influenza pandemic year.* Influenza Other Respir Viruses, 2013. **7**(5): p. 854-62.

470. Johnston, S.L., *IFN Therapy in Airway Disease: Is Prophylaxis a New Approach in Exacerbation Prevention?* Am J Respir Crit Care Med, 2020. **201**(1): p. 9-11.

471. Channappanavar, R., et al., *Dysregulated Type I Interferon and Inflammatory Monocyte-Macrophage Responses Cause Lethal Pneumonia in SARS-CoV-Infected Mice.* Cell Host Microbe, 2016. **19**(2): p. 181-93.

472. Channappanavar, R., et al., *IFN-I response timing relative to virus replication determines MERS coronavirus infection outcomes.* J Clin Invest, 2019. **129**(9): p. 3625-3639.

473. Blanco-Melo, D., et al., *Imbalanced Host Response to SARS-CoV-2 Drives Development of COVID-19.* Cell, 2020. **181**(5): p. 1036-1045 e9.

474. Woo, A.S.J., R. Kwok, and T. Ahmed, *Alpha-interferon treatment in hepatitis B.* Ann Transl Med, 2017. **5**(7): p. 159.

475. Steen, H.C. and A.M. Gamero, *Interferon-lambda as a potential therapeutic agent in cancer treatment.* J Interferon Cytokine Res, 2010. **30**(8): p. 597-602.

476. Sleijfer, S., et al., *Side effects of interferon-alpha therapy.* Pharm World Sci, 2005. **27**(6): p. 423-31.

477. Davidson, S., et al., *IFNlambda is a potent anti-influenza therapeutic without the inflammatory side effects of IFNalpha treatment.* EMBO Mol Med, 2016. **8**(9): p. 1099-112.

478. Samuel, C.E., *Interferon at the crossroads of SARS-CoV-2 infection and COVID-19 disease.* J Biol Chem, 2023. **299**(8): p. 104960.

479. Eskandarian Boroujeni, M., et al., *Dysregulated Interferon Response and Immune Hyperactivation in Severe COVID-19: Targeting STATs as a Novel Therapeutic Strategy.* Front Immunol, 2022. **13**: p. 888897.

480. Francis, T., Jr., *Transmission of Influenza by a Filterable Virus.* Science, 1934. **80**(2081): p. 457-9.

481. van Riel, D., et al., *Human and avian influenza viruses target different cells in the lower respiratory tract of humans and other mammals.* Am J Pathol, 2007. **171**(4): p. 1215-23.

482. Rowe, T., et al., *Delay of innate immune responses following influenza B virus infection affects the development of a robust antibody response in ferrets.* (In preparation), 2024.

483. Rowe, T., et al., *Interferon as an immunoadjuvant to enhance antibody responses to influenza B infection and vaccination in the ferret.* (Submitted) NPJ Vaccines, 2024.

484. Zhai, Y., et al., *Host Transcriptional Response to Influenza and Other Acute Respiratory Viral Infections--A Prospective Cohort Study.* PLoS Pathog, 2015. **11**(6): p. e1004869.

485. Cao, R.G., et al., *Differences in antibody responses between trivalent inactivated influenza vaccine and live attenuated influenza vaccine correlate with the kinetics and magnitude of interferon signaling in children.* J Infect Dis, 2014. **210**(2): p. 224-33.

486. Bucasas, K.L., et al., *Early patterns of gene expression correlate with the humoral immune response to influenza vaccination in humans.* J Infect Dis, 2011. **203**(7): p. 921-9.

487. Goncalves, E., et al., *Innate gene signature distinguishes humoral versus cytotoxic responses to influenza vaccination.* J Clin Invest, 2019. **129**(5): p. 1960-1971.

488. Furman, D., et al., *Apoptosis and other immune biomarkers predict influenza vaccine responsiveness.* Mol Syst Biol, 2013. **9**: p. 659.

489. Liu, G., et al., *Inhibition of Ongoing Influenza A Virus Replication Reveals Different Mechanisms of RIG-I Activation.* J Virol, 2019. **93**(6).

490. Lopez, C.B., et al., *Type I interferon induction pathway, but not released interferon, participates in the maturation of dendritic cells induced by negative-strand RNA viruses.* J Infect Dis, 2003. **187**(7): p. 1126-36.

491. Baker, S.F., et al., *Influenza A and B virus intertypic reassortment through compatible viral packaging signals.* J Virol, 2014. **88**(18): p. 10778-91.

492. Cardenas-Garcia, S., et al., *Impact of sex on humoral immunity with live influenza B virus vaccines in mice.* NPJ Vaccines, 2024. **9**(1): p. 45.

493. Ursin, R.L., et al., *Greater Breadth of Vaccine-Induced Immunity in Females than Males Is Mediated by Increased Antibody Diversity in Germinal Center B Cells.* mBio, 2022. **13**(4): p. e0183922.

494. Mandl, J.N., et al., *Reservoir host immune responses to emerging zoonotic viruses.* Cell, 2015. **160**(1-2): p. 20-35.

APPENDICES

APPENDIX A – ISOLATION AND CULTURE OF FERRET PRIMARY RESPIRATORY EPITHELIAL CELLS

ANIMALS AND REAGENTS

Animals

Male, fitch ferrets (*Mustela putorius* furo) 8-12Mo age – FFF Farms, Sayre, PA USA

Isolation Medium (D-Val)

[MEM (D-Val), 5% FBS, 1mM NEAA, 1mM Na-pyruvate, 25mM HEPES, antibiotics] – *For negative selection of fibroblasts*

- **437.5mL** – MEM (D-Val) (BioSource Cat#MBS653430).
- **25mL** – Dialyzed Fetal Bovine Serum, NOT heat inactivated (Gibco Cat#26400044) *Dialyzed at 10K mw cutoff to remove amino acids, including any L-Valine.*
- **12.5mL** – 1M HEPES (Gibco Cat#15630-080) *To prevent pH fluctuations during feeding and culture manipulation outside incubator and to provide additional buffering against lactate and CO_2 during cell growth.*
- **10mL** – 100mM non-essential amino acids "NEAA" (Gibco Cat#11140-050) *NEAA = Alanine, asparagines, aspartic acid, glycine, glutamic acid, proline, and serine - reduces the metabolic burden on the cells allowing for an increase in cellular proliferation.*

- **10mL** – 100mM Na-pyruvate (Gibco Cat#11360-070) A*n intermediary organic acid metabolite in glycolysis and the first of the Embden Myerhoff pathway that can pass readily into or out of the cell. Thus, its addition to tissue culture medium provides both an energy source and a carbon skeleton for anabolic processes. Its addition may help in maintaining certain specialized cells, may help when cloning and may be necessary when the serum concentration is reduced in the medium*.
- **5mL** – 100X Penicillin/Streptomycin [10,000U/mL Penicillin, 10,000µg/mL Streptomycin] (Gibco Cat#15140-122)
- Filter through 0.2µM pore size and store @2-8°C for up to 1Mo

Epithelial Cell Medium (+ supplements) – "ECM+"

[DMEM/F-12, 5% FBS, 1mM NEAA, 1mM Na-pyruvate, 25mM HEPES, antibiotics, 0.14µg/mL RA, Growth Factors (Lonza)] – *For differentiation of respiratory epithelial cells.*

- **223.7mL** – MEM, (Gibco#11095-080)
- **223.7mL** – Ham's F-12 (Gibco#11765-054)
- **25mL** – Characterized Fetal Bovine Serum, NOT heat inactivated (Hyclone Cat# SH3007103.03)
- **12.5mL** – 1M HEPES (Gibco Cat#15630-080)
- **5mL** – 100mM NEAA (Gibco Cat#11140-050)
- **5mL** – 100mM Na-pyruvate (Gibco Cat#11360-070)
- **5mL** – 100X Penicillin/Streptomycin (Gibco Cat#15140-122)
- Filter through 0.2µM pore size and add supplements and RA

- **12µL** – Retinoic Acid "RA" @6.02µg/µL in DMSO; (Sigma Cat#R2625) – *For cell differentiation to mucociliary, mucous and prevent development of stratified squamous cells and cornified apical layer*.
- **Supplements**– BEGM SingleQuots (Lonza Cat#CC-4175) – *add all except RA component*
    - Hydrocortisone – 0.5mL – *supports growth and differentiation of epithelial cells.*
    - Gentamicin/amphotericin B – 0.5mL = *antibiotic/antifungal*
    - Triiodothyroine "T_3" – 0.5mL *regulates membrane transport, differentiation and constitution of cell surface.*
    - Epinephrine – 0.5mL *Required for mucus production with IL-13.*
    - Transferrin – 0.5mL *Can be a mitogen and responsible for iron transport.*
    - Bovine pituitary extract "BPE" -2.0mL *Enhances cell growth.*
    - Recombinant human epidermal growth factor "rhEGF" – 0.5mL *Mitogen for epithelial and fibroblastic cells; synergizes with IGF-1/TGFß.*
    - Insulin – 0.5mL *for glucose uptake and oxidation; amino acid uptake; glyconeogenesis.*
- Wrap bottle in foil and keep in dark @2-8°C. Use within 2 weeks. DO NOT HEAT IN WATERBATH, ALLOW TO REACH ROOM TEMPERATURE BEFORE USE. BEST TO KEEP PROTECTED FROM LIGHT.

RBC Lysing Solution

(0.15M NH_4Cl, 10mM $KHCO_3$, 1mM EDTA) – *For removal of contaminating erythrocytes.*

- **4.01g** – Ammonium Chloride; NH_4Cl FW=53.49g/Mol (Ward Scientific Cat#470300-196)
- **0.5g** – Potassium Bicarbonate; $KHCO_3$ FW=100.11g/Mol (VWR Cat#0889-500G)
- **0.146g** – Ethylenediaminetetraacetic acid; EDTA FW=292.23g/Mol (Acros Cat#118432500)
- q.s. to 500mL with dIH_2O
- pH to 7.3 with 1N NaOH
- Filter through 0.2µM pore size and store @2-8°C

2X Freezing Medium

[ECM+, 30mM HEPES, 10% FBS, 10% DMSO]; Make fresh – *for cryopreservation of respiratory epithelial cells*

- **7.76 mL** – ECM+ (medium)
- **0.3 mL** – 1M HEPES (Gibco Cat#15630-080)
- **1.0 mL** – Characterized Fetal Bovine Serum, NOT heat inactivated (Hyclone Cat# SH30071.03)
- **1.0 mL** – DMSO (Sigma #D2438). Add slowly on ice.

PART I – COLLECTION OF TISSUES

Collection of Ferret Nasal Turbinates & Trachea

- Anesthetize ferret(s) with 0.5mL KAX (3:1:1 – ketamine, atropine, xylazine)
- Once fully sedated (absence of pedal reflex following "toe-pinch"), exsanguinate animal via IC stick and save sera

- Euthanize animal with 1mL euthanasia solution/kg and verify death by auscultation or pneumothorax
- Nasal Turbinate (NT) collection
    - Excise ~1cm segment of muzzle to reveal cross-section of nasal cavity
    - Use forceps and curette to dislodge and forcibly extract fragments of NT tissue (ventral, dorsal and ethmoid nasal turbinates) and place in 10mL cold MEM (D-Val) + antibiotics (Pen/Strep) "NO FBS OR OTHER SUPPLEMENTS" in 50mL conical tube (on ice)
- Trachea (Tr) collection
    - Wet fur with 70% EtOH and wipe excess with clean KimWipe
    - Cut longitudinal incision through fur from larynx to below the diaphragm
    - Use forceps and scalpel to peel back skin/fur from body cavity
    - Remove ribcage by transecting ribs at costochondral junctions bilaterally and cutting away any pleural attachments
    - Excise Tr with scissors from below the larynx to the major bronchi
        - Avoid esophagus during manipulations of the trachea
    - Rinse Tr with Ca^{++}/Mg^{++} free HBSS from Tr to remove extraneous tissue and blood
    - Remove any attached muscle and tissue
    - Cut longitudinally and place in 15mL cold MEM (D-Val) + antibiotics (Pen/Strep) "NO FBS OR OTHER SUPPLEMENTS" in 50mL conical tube (on ice)

PART II – ISOLATION OF CELLS

Primary Incubation of FNEC/FTEC

Digestion – D0

- Prepare **Dissociation Enzyme Solution**
    - In 50ml Conical tube
        - Add 70µg Pronase (Roche Cat#10165921001)
        - Add 1 vial (10,000 Units) DNase I (Roche Cat#04536282001)
        - Add 49.5mL cold MEM (D-Val)
        - Add 0.5mL 100X Pen/Strep
    - Vortex until dissolved
- Decant MEM (D-Val) from tissues
- Add 25ml **Dissociation Enzyme Solution** to each tube containing tissue (NT and Tr)
- Incubate tubes for 2 days @2-8°C

Collagen Coating plates/flasks

- Prepare **Collagen solution**
    - Prepare 60% EtOH in 50mL conical tube
        - 30mL 100% EtOH
        - 20ml dIH_2O
    - Add 0.5ml rat tail collagen @3.57mg/mL (Corning Cat#354236)
    - Mix by vortexing
- Coating of 12-well Transwell plates (Corning Cat#3460)
    - Add 100µL/well **Collagen solution** in BSC
    - Leave overnight in BSC with lid off

- Next day – Sterilize plate by UV for 30min in BSC and replace lid
- Store plate(s) @2-8°C for up to 4 weeks in Ziploc bag

- Coating of tissue culture flasks
  - Add **Collagen solution** to each flask in BSC and rock back and forth to coat
    - T25 = 1mL
    - T75 = 3mL
    - T175 = 5mL
  - Close flask(s) and incubate on level surface for 60min at RT
  - Aspirate **Collagen solution**
  - Rinse flask(s) 3X with Ca^{++}/Mg^{++} free HBSS (T75 = 5mL/wash; T175=10mL/wash)
  - Leave flasks uncapped in BSC overnight to dry
  - Next day -Sterilize by UV for 30min in BSC and replace cap
  - Cap flask(s) and store in Ziploc bag at 2-8°C for up to 2 weeks

Primary Incubation – Day 2

- Collect single cell suspension
  - Stop digestion by adding 2.5mL dialyzed FBS to 50mL tube containing tissue
  - Filter cell suspensions through 70µm cell strainer (Falcon Cat#352350) into new 50mL conical tube
  - Pellet cells by centrifugation (600 x g, 10min, 4°C)
  - Decant media from cell pellet

- Resuspend pellet in 30mL **Isolation Medium (D-Val)**

- Remove Fibroblasts
  - Transfer cell suspension to two 150mm x 21mm Petri dishes
  - Incubate 2Hr @37°C, 5%CO_2
  - Save supernatant to 50mL conical tube and discard Petri dishes
- P1 Cell Culture
  - Pellet cells by centrifugation (600 x g, 10min, 4°C)
  - Resuspend pellet in 3mL **Isolation Medium (D-Val)**
  - Count cells and adjust to $1x10^5$ cells/cm^2
    - T175 → $1x10^5$ cells/cm^2 x 175cm^2 = $1.75x10^7$ cells
    - Need $1.75x10^7$ cells/50mL →$3.5x10^5$ cells/mL
  - Add 50mL cell suspension to each collagen-coated 175cm^2 flask
  - Incubate at 37°C/5% CO_2 until confluent; replace with 50mL fresh **Isolation medium (D-Val)** every 2-3 days and culture until confluent

PART II – CRYOPRESERVATION OF PRIMARY CELLS (PASSAGE: P1)

<u>Freezing (P1) FNEC/FTEC</u>

- 2X wash monolayer with PBS
- Add 10mL/ 175cm^2 flask pre-warmed 0.05% trypsin, 0.02% EDTA (Gibco Cat#25300-054)
- Rock flask to coat and incubate @37°C/5% CO_2 until cells detached (~10min)
- Add 10mL **Isolation Medium (D-Val)** to inactivate trypsin
- Transfer cell suspension to 50mL conical tube and pellet cells by centrifugation (600 x g, 10min, 4°C)

- Resuspend pellet in 3mL **Isolation Medium (D-Val)** and keep on ice
- Count cells and adjust concentration to ~$4x10^6$ cells/mL with **Isolation Medium (D-Val)**
- Determine number of vials to freeze (~$4x10^6$ cell/vial) and add 1mL cold **2X Freezing Media** to 2mL cryovials based on number of vials to freeze
- Add 1mL/vial cell suspension and invert to mix
- Transfer vials to "Mr. Frosty" freezing can containing isopropanol
- Place Mr. Frosty at -80°C and leave overnight
- Transfer cells to vapor phase of liquid nitrogen freezer (-150 to -190 °C)

Thawing FNEC/FTEC

- Slowly warm vial in 37°C water bath until just thawed
- Add cell suspension to 50mL tube
- Slowly, drop-wise add 10mL **ECM+** media to tube and gently mix while adding
- Pellet cells by centrifugation (600 x g, 10min, RT)
- Resuspend pellet in 1-2mL **ECM+** media and count cells
- Adjust cell number to $5x10^4$ cells/cm^2
    - 12-well Transwell = 1.12 cm^2/well → $5x10^4$ cells/cm^2 x 1.12cm^2/well = $5.6x10^4$ cells/well
        - Need 0.5mL/well cells → $1.2x10^5$ cells/mL
    - 24-well Transwell = 0.33cm^2/well → $5x10^4$ cells/cm^2 x 0.33cm^2/well = $1.65x10^4$ cells/well
        - Need 0.25mL/well cells → $6.6x10^4$ cells/mL

Amplification/Differentiation of FNEC/FTEC

Amplification

- Seed 12-well Transwell plates
    - *Need 3 plates/virus+ Extra for cell control (for cell count determination prior to infection)*
        - Seed extra 4 wells for counting and other characterization
        - Seed 24-well plate (6-wells)
    - Add 1mL **ECM+** media to basolateral side of each well
    - Add 0.5mL/well (fresh/thawed FNEC or FTEC @$1.2x10^5$cells/mL in **ECM+**)
- Seed 24-well Transwell plates
    - Need 6 wells/cell type/ferret
        - Seed 24-well plate (6-wells) for IFA and confocal microscopy
    - Add 0.5mL **ECM+** media to basolateral side of each well
    - Add 0.25mL/well (fresh/thawed FTEC @$6.6x10^4$cells/mL in **ECM+**)
- Incubate cells at 37°C/5% CO_2 until confluent and resistance >800Ω/cm^2 – ~6-7 days
    - 12- well → ~900Ω
    - 24-well → ~270Ω for 24-well
- Change media on apical/basolateral side every 2 – 3 days with fresh **ECM+**
    - 12-well
        - Apical = 0.5mL
        - Basolateral =1.0mL
    - 24-well

- Apical = 0.25mL
- Basolateral = 0.5mL

Differentiation

- Once resistance >800Ω/cm^2, culture as air-liquid interface (ALI)
- ALI culture
  - Remove media from apical side of culture
  - Remove media from basolateral side of culture
  - Add **ECM+** media ONLY to basolateral side of culture
    - 12-well = 1mL
    - 24-well = 0.5mL
  - Exchange basolateral media every 2 – 3 days with fresh **ECM+** media
- Observe cells for ciliary movement
- If mucus deposits observed in wells, rinse apical side of wells with Ca^{++}/Mg^{++} free HBSS
- Once ciliary movement detected (~4 weeks post ALI culture), cells are ready for infection/characterization
- Cells can be maintained as ALI for several months

APPENDIX B – INFECTION OF FERRETS WITH SEASONAL INFLUENZA VIRUSES

1.0 Purpose

1.1 This document describes the procedure for bleeding and inoculation of ferrets with Biosafety Level 2 influenza viruses and exsanguination for generation of immune sera.

2.0 Definitions

2.1 AALAS – American Association for Laboratory Animal Science

2.2 BSC – Biosafety Cabinet

2.3 HI – Hemagglutination Inhibition

2.4 NGS – NextGen Sequencing

2.5 NW – Nasal Wash

2.6 PCR – Polymerase Chain Reaction

2.7 PPE – Personal Protective Equipment

2.8 PBS – Phosphate Buffered Saline

2.9 QAR – Quiet, Alert and Responsive

2.10 IACUC – Institutional Animal Care and Use Committee

2.11 BMBL – Biosafety in Microbiological and Biomedical Laboratories

2.12 KX solution – Ketamine//Xylazine mixture. Used as an injectable anesthetic in the ferret.

2.12.1 Ketamine - General anesthetic; however, it does not cause muscle relaxation. Decreases respiration.

2.12.2 Xylazine (Rompun) – Used as an anesthetic adjunct with ketamine to act as a muscle relaxant and visceral analgesic. Causes a reduction in heart rate (bradycardia) and reduced nasal secretions.

3.0 Safety Precautions

3.1 Prior to working with influenza-inoculated animals, proper training must be conducted to minimize risk of possible exposure. Training should include:

3.1.1 Hands-on training of handling of ferrets by a trained veterinarian and/or trained laboratory supervisor.

3.1.2 Completion of all IACUC-required animal courses. (Minimally AALAS "Working with the IACUC" and "Introduction to Ferrets" courses).

3.1.3 Handling of virological agents will be performed in class II certified BSC with strict adherence to biological safety guidelines set forth in the BMBL.

3.1.4 Compliance with animal safety guidelines as described by the Institutional Biosafety Committee.

4.0 Materials[1]

4.1 Virus: Allantoic fluid from influenza-infected embryonated chicken eggs or Tissue Culture Virus Supernatant (known infectious titer is optimal).

4.2 Ferrets (Juvenile male ferrets <2yr age; Triple F Farms, Sayre PA).

4.3 Caging

4.3.1 Naïve ferret caging – Standard ferret cages (www.allentowninc.com) in portable, laminar flow clean room enclosure (Lab Products, Seaford, DE).

4.3.2 Inoculated ferret caging – Individually ventilated caging system, HEPA-filtered (www.allentowninc.com)

4.4 Diluent – PBS or 95% physiological saline.

4.5 **Anesthesia** (options):

4.5.1 **"KX" solution** – Ketamine/Xylazine (3:1 ratio mixture) @ 15-30 mg/kg & 1-2 mg/kg respectively or other IACUC approved anesthetic. Note: primary anesthesia choice.

4.5.1.1 Ketamine-HCl (100 mg/ml) – Zetamine™, injectable. (Vetone) Cat# 501072. http://www.vetone.net/

4.5.1.2 Xylazine (20 mg/ml) – Anased®, injectable. (Akorn Inc.) NDC: 59399-110-20. http://www.akorn.com/

4.5.2 **"KM" solution** – Ketamine/Medetomidine (3:0.05 ratio mixture) @15-30 mg/kg & 0.05 mg/kg respectively

4.5.2.1 Ketamine-HCl (100 mg/ml) – Zetamine™, injectable. (Vetone) Cat# 501072. http://www.vetone.net/

4.5.2.2 Medetomidine-HCl (1.0 mg/ml) – injectable (Modern Veterinary Therapeutics, LLC.) http://modernveterinarytherapeutics.com/

4.5.3 **"KD" solution** – Ketamine/Dexmedetomidine (3:0.05 ratio mixture) @15-30 mg/kg & 0.025 mg/kg respectively

4.5.3.1 Ketamine-HCl (100 mg/ml) – Zetamine™, injectable. (Vetone) Cat# 501072. http://www.vetone.net/

4.5.3.2 Dexmedetomidine-HCl (0.5 mg/ml) – injectable (Modern Veterinary Therapeutics, LLC.) DIN 02483947 http://modernveterinarytherapeutics.com/

4.5.4 **Anesthesia Reversal** agent – For reversal of xylazine component of anesthesia

4.5.4.1 Atipamezole-HCl (5mg/ml) – Revertidine™, injectable (Modern Veterinary Therapeutics, LLC.) NDC: 015914-008-01 http://modernveterinarytherapeutics.com/

4.5.4.2 Use at 0.25mg/kg

4.6 Euthanasia solution (Pentobarbitol, Beuthanasia-D or equivalent) @ 1mg/kg.

4.7 9ml serum separation tubes (for exsanguination).

4.8 3ml serum separation tubes (for pre-bleeds and test bleeds).

4.9 2.0ml cryogenic vials – external thread, Corning Cat#430659.

4.10 3.6ml Cryotube – internal thread, Nunc® Cat#377267

4.11 5ml polystyrene, round-bottom, snap-cap tube (for HI screening).

4.12 22 or 23G 1" needles (for blood collection).

4.13 18G 1.5" needles (for euthanasia administration).

4.14 18-21G 1.5" vacutainer needles and holders (for exsanguination).

4.15 1ml tuberculin syringes (for blood collection and anesthesia).

4.16 3cc, luer lock syringes (for blood collection and euthanasia solution).

4.17 25G, 26G, or 27G 3/8" needles for administration of anesthesia.

4.18 16Gx1¼" Catheter – For nasal wash collection (Excel International, Cat# 26730).

4.19 NW diluent – PBS, 1% BSA, penicillin (100 U/ml), streptomycin (100 µg/ml), gentamicin (50 µg/ml).

4.19.1 Prepare 2mL aliquots and freeze at ≤-20°C.

4.19.2 Thaw vial for each NW collected at time of use.

4.20 Sterile Petri dishes (100 x 15 mm) – for nasal wash collection.

4.21 NW processing solutions

4.21.1 0.5M EDTA – Store at 15 – 25°C

4.21.2 0.5M EGTA – Store at 15 – 25°C

4.21.3 DNAse I (1 U/uL) – Prepare 5uL aliquots and freeze at ≤-70°C

4.21.3.1 Thaw vial immediately before use.

4.22 Sterile Petri dishes (100 x 15 mm) – for nasal wash collection.

4.23 Benchtop Centrifuge.

4.24 Blue absorbent pads.

[1]Or equivalent materials/reagents may be used following qualification.

5.0 Procedure

5.1 **Prepare Anesthesia (KX) solution** – **(**Prepare fresh at time of use).

5.1.1 Determine the number of animals to anesthetize and measure the following volumes of each component and mix in a 50ml conical tube:

5.1.1.1 Ketamine (100mg/ml) – 0.3ml/ferret.

5.1.1.2 Xylazine (20mg/ml) – 0.1ml/ferret.

5.1.2 Attach 25G-27G 3/8" needle to 1ml tuberculin syringe.

5.1.3 Fill syringe with ~0.3-0.35ml KX per ferret. (*NOTE: 0.2-0.25mL sufficient for ~1kG ferret*)

5.1.4 Set aside until use.

5.2 **Pre-bleed**

5.2.1 Anesthetize ferret with KX solution by inoculation into the muscle of thigh. *Note: handle all conscious ferrets with animal handling gloves.*

5.2.1.1 Approximately 0.25 ml of KX (3:1 ratio by volume) is sufficient for anesthesia for ~1Kg animal.

5.2.1.2 Ensure that the animal is adequately anesthetized by testing the pedal withdrawal reflex, pinching foot pad on hind feet. If the foot pad pinch causes a response, either wait until no response or administer additional anesthesia (~0.1 – 0.2ml) and re-test before starting the procedure.

5.2.2 Check ferret ear tag to verify that the ferret ID

5.2.3 Lay ferret in supine position with the head closest to you. Collect 1 – 2 ml of blood, using a 22-23G, 1" needle attached to a tuberculin or 3cc syringe, from the cranial vena cava or subclavian artery (Reference 10.1) and transfer to a 3 ml serum separator tube.

5.2.4 Label tube to identify ferret ID, "Pre-bleed" and date drawn and place in zip-loc bag.

5.2.5 Place ferret in individual cage in supine position, with head toward front of cage, close and secure cage. Place cage in rack insuring it is locked into position.

5.2.5.1 Monitor ferret(s) until Monitor until animal achieves sternal recumbency and is QAR.

5.2.6 Transport tubes in a biohazard marked container to BSL-2 laboratory for processing.

5.2.7 Allow blood to clot at room temperature and centrifuge within 2 hours of collection.

5.2.8 Centrifuge blood at room temperature, 2500rpm (1500 x G) for 15 minutes using a Benchtop Centrifuge.

5.2.9 Transfer 0.1 – 0.2mL of supernatant (sera) into a 5ml snap-cap tube for prescreening HI assay and transfer remaining sera into a 3.6mL cryotube for storage. Label tubes with ferret number and date of pre-bleed.

5.2.10 Transport sera in biohazard marked container to freezer (-20°C to -30°C). Store 3.6ml tube for HI testing.

5.3 **Inoculation of ferrets with Influenza A or Influenza B viruses**

Note: All procedures below are to be performed inside a certified class II biosafety cabinet. All personnel must wear appropriate PPE.

5.3.1 PRIOR TO INOCULATION

5.3.1.1 Virus stock to be used must pass PCR virus exclusivity testing.

5.3.1.2 Virus stock sequence must not have detectable polymorphisms of >5%.

5.3.1.3 Virus stock must have titration data (EID_{50}, $TCID_{50}$., PFU or FFU).

5.3.2 Inoculation with Influenza viruses.

5.3.2.1 Ideally dilute virus to ~$4x10^5$ infectious units ($TCID_{50}$, PFU, FFU, or EID_{50}) in PBS.

5.3.2.1.1 Dilution Calculation (Example virus stock = $1x10^6$ FFU/ml):

$C_1V_1 = C_2V_2$

C_1 = Known concentration (i.e. $1x10^6$ FFU/ml)

V_1 = Unknown

C_2 = concentration needed (i.e. $4x10^5$ FFU/ml)

V_2 = 1ml (volume of inoculum needed)

$V_1 = C_2V_2 / C_1$ → (4x10^5 FFU/ml x 1ml) / ($1x10^6$ FFU/ml)

$V_2 = 4x10^5 / 1x10^6 = 0.4$ ml

Need 1ml inoculum, therefore; 0.4ml virus + 0.6ml PBS

OR

Dilution = Titer needed / Stock virus titer

= $4x10^5$ FFU / $1x10^6$ FFU

= 0.4 or 1:2.5 dilution (1/0.4)

Inoculum = 0.4ml virus + 0.6ml PBS

5.3.2.2 Using a 1ml syringe, inoculate anesthetized ferret intranasally with 1ml of diluted virus by instilling dropwise into each nare (~0.5 ml/nare), while holding ferret's head with nose tilted up; alternating between the two nares. *NOTE: Allow the ferret to inhale the virus between drops and apply carefully to avoid sneezing.*

5.3.2.3 Return ferret to cage and place in supine position with head toward front of cage. Monitor until animal achieves sternal recumbency and is QAR.

5.4 **Monitoring of ferrets**

5.4.1 Collect NW sample on day 3 post infection to assess viral replication and potential mutations.

5.4.2 Anesthetize ferrets according to step 5.2.1

5.4.3 Load ~2ml cold **NW diluent** in 3.0 CC syringe connected to catheter.

5.4.4 Collect nasal wash by instilling NW diluent into ferret nostril (~1.0 ml/nostril) and collecting expelled sneeze in Petri dish (Figure 2) in certified BSC:

5.4.5 Keep NW on ice for processing.

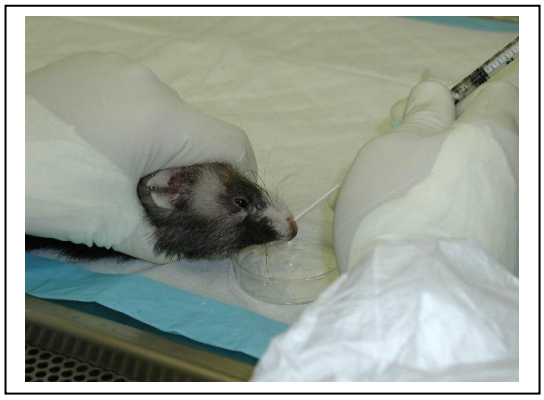

Figure 2: Collection of nasal wash from anesthetized ferret.

5.5 **Processing of NW sample for RNA isolation and NGS**

5.5.1 DNAse treat NW sample(s)

5.5.1.1 Transfer ~100uL NW sample + 110uL PBS to tube containing 5uL DNase I [1 u/uL]

5.5.1.2 Incubate for 30min @ 37°C

5.5.1.3 Inactivate DNAse

5.5.1.4 Add 8 uL PBS to tube

5.5.1.5 Add 28 uL 0.5M EDTA to tube

5.5.1.6 Add 28 uL 0.5M EGTA to tube

5.5.2 Lysis of sample

5.5.2.1 Add 280 uL AVL buffer to DNAse treated NW sample

5.5.2.2 Vortex and transfer to 2° - 8°C refrigerator and submit for NGS.

5.5.3 Retain remainder of sample for determination of viral load by FFA.

5.5.4 Optional: Collect additional ferret clinical information (i.e. Temperature, nasal discharge, activity, weight loss) as applicable.

6.0 Exsanguination of Ferrets

NOTE: Ferrets inoculated with influenza A or B viruses are exsanguinated approximately two weeks post inoculation, or one week post boost date if applicable. Prepare anesthesia according to step 5.1.

6.2 Anesthetize ferret with KX solution by inoculation into the muscle of thigh and record time and volume. *Note: handle all conscious ferrets with animal handling gloves.*

6.2.1 Approximately 0.3 ml of KX (3:1 ratio by volume) is sufficient for anesthesia for ~1Kg animal.

6.2.2 Ensure that the animal is adequately anesthetized by testing the pedal withdrawal reflex, pinching foot pad on hind feet. If the foot pad pinch causes a response, either wait until no response or administer additional anesthesia (~0.1 – 0.2ml) and re-test before starting the procedure.

6.3 Check ferret ear tag to verify that the ferret ID number matches the number given on animal cage card. If ear tag is missing, identify by other visual means as indicated on animal cage card. Check ferret ear tag and make sure it matches both cage card and experimental cage card.

6.4 Exsanguinate anesthetized ferret using cardiac puncture (Reference 7.1).

6.4.1 Place the ferret in dorsal recumbency and, using an 18G 1.5" vacutainer needle in holder, insert the needle in the cephalad near the xyphoid cartilage towards the heart at a 30° angle (with bevel up). See figure 3.

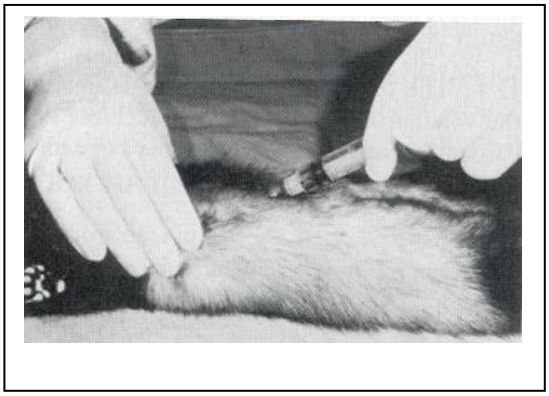

Figure 3: Cardiac puncture in an anesthetized ferret.

6.4.2 Insert empty 9 ml serum separator tube into vacutainer holder and allow filling with blood. Remove tube when full and repeat collection with new tubes until animal exsanguinated. NOTE: Adjusting the syringe and massaging of the chest may be necessary to maximize blood collection.

6.4.3 Label all tubes with the serum lot number before exsanguinating additional ferret(s).

6.4.4 Euthanize ferret by direct intracardiac injection of ~1ml euthanasia solution using an 18G 1.5" needle fitted to a 1 – 3cc syringe. NOTE: Try to draw blood into syringe to insure correct cardiac placement.

6.4.5 Verify that ferret is euthanized by absence of respiration/heartbeat, double-bag carcass in biohazard bag, transport in a leak-proof container, and place in designated dead animal freezer.

6.4.6 Transport tubes in a biohazard marked container to BSL-2 laboratory for processing.

6.4.7 Allow blood to clot at room temperature and centrifuge within 2 hours of collection.

6.4.8 Centrifuge blood at room temperature, 2500rpm (1500 x G) for 15 minutes using a Benchtop Centrifuge.

6.4.9 Pool sera in 50ml centrifuge tube and prepare 3 – 3.5ml aliquots in 3.6ml cryotubes.

6.4.10 Transport sera in biohazard marked container to freezer (-20°C to -30°C). Store 3.6ml tubes in -30°C±10°C freezer

7.0 References

7.1 Brown, C., Blood collection from the cranial vena cava of the ferret. Lab Anim (NY), 2006. 35(9): p. 23-4.

7.2 Fox, J.G., Biology and Diseases of the Ferret. 2nd ed. 1998, Baltimore: Lippincott Williams & Wilkins

7.3 Mabry, J.; Rowe, T.; Blanchard, E.; and Xu, X. Development of a HEPA-Filtered Caging System for Ferrets: Thinking Outside the Metal Box. Lab. Anim. Sci. Prof. 2013. 1(3): p. 41 – 44.

7.4 Rowe, T., et al., Modeling host responses in ferrets during A/California/07/2009 influenza infection. Virol., 2010. 401: p. 257-265

7.5 Zitzow, L.A., et al., Pathogenesis of avian influenza A (H5N1) viruses in ferrets. J Virol, 2002. 76(9): p. 4420-9

APPENDIX C – ASSESSMENT OF CLINICAL SIGNS OF SEASONAL INFLUENZA INFECTION IN FERRETS

INTRODUCTION

Once inoculated with virus, daily observations of ferrets provide critical information regarding the health of the animals, which is considered when evaluating the overall kinetics of influenza infection as well as the effects of countermeasures such as vaccines or antivirals. Ferrets are an outbred model and as such it is important to observe multiple ferrets throughout the duration of an experiment to best assess the presence and severity of any parameters of disease due to viral infection.

PURPOSE

The purpose of this procedure is to describe the observations taken after inoculation of ferrets with influenza virus.

DEFINITIONS

- Biosafety Level (BSL) – A series of work practices and facility engineering requirements to contain infectious materials to the work area and minimize risk of exposure to personnel and the work area. BSL is ranked from BSL-1 to BSL-4, with BSL-4 being the most stringent.
- ABSL-2 – Animal Biosafety Level 2
- AALAS – American Association for Laboratory Animal Science
- IACUC – Institutional Animal Care and Use Committee
- BSC – Biosafety Cabinet

CRITICAL EQUIPMENT

- Scale capable of measuring 500g to 2500g

- Seca Corp 334 Mobile digital baby scale (Fisher Scientific Cat#NC1798765)

- Temperature transponder reader
- DAS-6007 IPTT Scanner System (Bio Medic Data Systems)

MATERIALS

- Ferret Temperature Transponders
    - IPTT-300 Implantable Programmable Temperature Transponder (100/box)

SAFETY PRECAUTIONS

- Follow safety guidelines required as described in the Biosafety in Microbiological and Biomedical Laboratories (BMBL).
- Leather ferret handling gloves must be used when manipulating ferrets that are not anesthetized.

PROCEDURE

- Assessment of lethargy:
    - Before manipulating the animals in any way, observe the activity level of the ferrets.
    - Healthy ferrets are generally alert and playful and will move to the front of their cage if you approach.
    - Ferrets that are feeling unwell may become lethargic (drowsy or sluggish); appearance and severity of lethargy correlates with virus pathogenicity.
    - Each ferret should be given a lethargy score daily, based on the following scale:
        - 0 = alert and playful
        - 1 = alert but playful only when stimulated
        - 2 = alert but not playful when stimulated
        - 3 = neither alert nor playful

- At the end of each experiment, based on the daily scores for each animal in a group, a Relative Inactivity Index (RII) may be calculated.

- Daily measurement of temperatures:
  - Similar to humans, ferrets will run a fever when infected with certain influenza virus strains. Although temperatures can fluctuate substantially in ferrets, sustained elevated temperatures post-inoculation correlate with virus pathogenicity.
  - Record the temperature of each ferret on a daily basis prior to anesthesia, preferably at the same time of day to minimize variation.
  - Establish the baseline temperature for each ferret (average of all daily temperatures recorded pre- inoculation).
  - Compare the daily temperature readings recorded post-inoculation and subtract each value from the baseline temperature value for that specific ferret.
  - Results may be reported as the number of degrees Celsius or degrees Fahrenheit above baseline for each individual ferret.
- Daily measurement of weight:
  - Ferrets that are unwell generally eat less and experience weight loss. Ensure that co-housed ferrets are of similar size so that a dominance issue does not affect the weight of a small animal.
  - Weigh each ferret individually on a daily basis, preferably at the same time of day to minimize variation.
  - Establish the baseline weight for each ferret prior to inoculation.
  - Compare the daily weight readings recorded post-inoculation and divide each value from the baseline weight value.
  - Results may be reported as the percentage of weight change compared to baseline for each individual ferret.
- General observations:

- Observe for and record any of the following clinical indicators of virus infection:
    - Sneezing: similar to humans, ferrets will often sneeze when infected with certain influenza viruses. *NOTE: the presence/absence of sneezing must be recorded prior to the administration of Ketamine, as this drug can induce sneezing independent of viral infection.*
    - Nasal discharge: similar to humans, ferrets will often experience a runny nose when infected with certain influenza viruses. Look for the presence of a crusty or runny nose. Nosebleeds may occur infrequently. NOTE: the presence/absence of nasal discharge must be recorded prior to the administration of Ketamine, as this drug can induce sneezing independent of viral infection.
    - Anorexia: in addition to weight loss, observe the levels of food and water for each cage to assess if the ferrets are eating and drinking. Coordinate food and water replenishment with animal staff so that this parameter may be monitored.
    - Alopecia: Ferrets that are stressed and not eating may shed excessive amounts of fur; heightened levels of hair loss should be recorded if this occurs.
    - Dyspnea (difficult or labored breathing): Decreased pulmonary function due to viral infection may result in abnormal respiration. Observe the breathing of each ferret and record if the ferret is gasping, wheezing, hyper/hypoventilating, open-mouth breathing, etc.
    - Diarrhea: Observe the ferret as well as the ferret cage for evidence of diarrhea and record if present.

- Ocular discharge: Infection with some influenza viruses may result in ocular discharge. Check the area around each eye of the ferret and record the presence of ocular inflammation, runny or crusty discharge.
- Neurological signs: Some highly pathogenic influenza viruses are neurotropic and can result in the development of neurological signs in the ferret. If any ferret displays torticollis (abnormal head tilt), hind limb paresis/paralysis, or other neurological symptoms, the ferret should be euthanatized.

- Notes:
- All clinical observations should be recorded and the euthanasia criteria described in the approved IACUC protocol should be consulted to determine at which point (if necessary) unscheduled euthanasia should be performed.
- In addition to the parameters listed above, be alert for other health conditions of ferret unrelated to viral infection that could nonetheless adversely affect the results of the experiment. If ferrets are pair- housed, make sure the cohabitating ferrets are not fighting excessively as this could lead to scratches or bites that could become infected. Watch for open sores or abnormal tumors/growths, as well as faulty feeders and water bottles that could inhibit unrestricted access to food and water.

Attachment A: Individual Ferret Clinical Assessment Form

Ferret Clinical Score Sheet

Project: _____

GROUP: _____ **Date of Challenge:** _____ **Concentration:** _____

Animal #: _____ **Virus:** _____ **Volume/Route:** _____

IACUC#: _____ **LOT#** _____ **SAMPLE ID:** _____

TIMEPOINT pINF:	-2	-1	0	1	2	3	4	5	6	7	8	9	10	14		
Date																
Time																
No abnormalities																
Weight (g)																
Temp (°F)																
Activity Score *																
Nasal Discharge ¥																
Sneezing																
Coughing																
Ocular Discharge																
Inappetant/anorexic																
Diarrhea¤																
Neurologic signs																
Other (List below)																
Initials:																

*Activity Score:
0 = alert and playful
1 = alert but playful only when stimulated
2 = alert but not playful when stimulated
3 = neither alert nor playful when stimulated

¥ Nasal Discharge:
S = serous P = purulent
Indicate S or P AND
B = bilateral L = left R = right

¤ Neurological Signs: (Note other abnormalities not listed)
P = Paralysis Indicate P AND -> L = Left R = Right
S= Seizures H= Hind F=Front
T=Torticollis

APPENDIX D – TREATMENT OF ANTISERUM WITH RECEPTOR DESTROYING ENZYME (RDE) AND ADSORPTION WITH RBCS

1. PURPOSE

1.1. To remove non-specific inhibitors: Animal and human sera contain various sialic acid containing glycans that may bind to the hemagglutinin (HA) of influenza virus and inhibit the binding of influenza-specific anti-HA antibodies.

1.2. To remove non-specific agglutinins: when non-specific agglutinins are present in serum, agglutination occurs due to the interaction of the non-specific agglutinins with RBCs. This is independent from the hemagglutination that occurs through the interaction of the influenza virus and the RBC and can lead to masking of the correct results if not removed.

2. DEFINITIONS

2.1. Alsever's Solution: An isotonic, balanced salt solution. Used as an anticoagulant/blood preservative for storage of whole blood at refrigerated temperatures.

2.2. BMBL: Biosafety in Microbiological and Biomedical Laboratories.

2.3. PBS: Phosphate Buffered Saline

2.4. PPE: Personal Protective Equipment

2.5. Q.S.: Quantity sufficient, the amount needed.

2.6. RBC: Red Blood Cell.

2.7. RDE: Receptor Destroying Enzyme

3. MATERIALS EQUIPMENT AND REAGENTS[1]

3.1. Receptor Destroying Enzyme (Denka Seiken, catalog #370013); US distributor: [Accurate Scientific (www.accuratechemical.com), catalog #YCC340-122]

3.2. Physiological (0.85%) saline, sterile

3.3. Phosphate buffered saline (PBS) 0.01 M, pH 7.2 – Mg^{++}/Ca^{++} free PBS

3.4. Turkey Red blood cells in anticoagulant (i.e. Alsever's solution)

3.5. Gauze, sterile

3.6. Sterile, conical tubes with caps – 15 and 50 ml

3.7. Water bath(s) – 37±1°C and 56±1°C

3.8. Benchtop, refrigerated, centrifuge

3.9. Refrigerator, 2-8ºC

[1]*Or equivalent*

4. PROCEDURE

4.1. Removal of Non-specific inhibitors by RDE treatment

4.1.1. Reconstitute lyophilized RDE as indicated on the vial with physiological (0.85%) saline.

4.1.2. Add 3 volumes of RDE to 1 volume of the sera to be treated into a sterile 15 ml or 50 ml conical tube (Example: 0.3 ml of sera to 0.9 ml RDE).

4.1.3. Transfer the label containing antisera information (Strain name, lot #, date of harvest) to the conical tube and record the volume of sera being treated on the tube.

4.1.4. Incubate overnight in a 37°C water bath (12 – 24 Hr).

4.1.5. Remove tube from the 37°C water bath and incubate in a 56°C water bath for 30 minutes to inactivate the RDE.

4.1.6. Remove from water bath and allow treated sera to cool to room temperature.

4.1.7. Add 6 volumes of physiological saline (Example: add 1.8 ml saline, to the tube containing 0.3 ml sera and 0.9 ml RDE). *NOTE: The final dilution of RDE treated antisera will be 1:10.*

4.1.8. If non-specific inhibitors are not removed, see ALTERNATIVE METHODS TO REMOVE NONSPECIFIC INHIBITORS FROM SERA FOR USE IN ASSAYS USING RBCS.

4.2. Removal of Non-specific agglutinins by adsorption with RBCs

4.2.1. Filter turkey RBCs through sterile gauze into a 50ml conical tube.

4.2.2. Add PBS to RBCs and wash two times using benchtop centrifuge (300 x g for 5 min @4°C). *(Alternate method: Add filtered RBC's and PBS into 50 ml conical tube, mix and place at 4°C overnight to allow RBCs to settle.).*

4.2.3. Draw off PBS supernatant; do not disturb the RBC pellet.

4.2.4. Add 1 volume of packed RBCs to 20 volume RDE treated antisera and mix by inversion.

4.2.5. Incubate at 4°C for 60 minutes or room temperature for 30 minutes.

4.2.6. Centrifuge at 300 x g for 5 minutes at 4°C.

4.3. Aliquot treated sera

4.3.1. Carefully draw off supernatant and dispense sera into sterile 3.5ml tubes.

4.3.2. Label tubes with the following information: “Treated Animal type X Antisera”, strain name and subtype, lot #, date of RDE treatment, and date of RBC adsorption.

APPENDIX E – ANTIGEN DETECTION BY HEMAGGLUTINATION ASSAY

1. PURPOSE

1.1. Hemagglutination (HA) test procedure for quantification of influenza hemagglutination titer in samples containing influenza virus.

2. DEFINITIONS

2.1. RBC: Red blood cell

2.1.1. GPRBC: guinea pig red blood cell

2.1.2. TRBC: turkey red blood cell

2.2. HA: Hemagglutination – the agglutination, binding, of red blood cells.

2.3. v/v: volume to volume.

2.4. BSC: Class II Biosafety Cabinet

3. MATERIALS EQUIPMENT AND REAGENTS[1]

3.1. Refrigerated centrifuge

3.2. Turkey Blood in Alsever's (Lampire Biological Laboratories, Pipersville, PA, USA)

3.3. Guinea Pig Blood, Citrated (Lampire Biological Laboratories, Pipersville, PA, USA)

3.4. Phosphate buffered saline (PBS) 0.01 M, pH 7.2 – Mg^{++}/Ca^{++} free

3.5. Influenza virus strains grown in tissue culture, eggs, or from infected animals

3.6. Gauze pads, sterile

3.7. Hemacytometer and coverslips or cell counter

3.8. Trypan blue stain, 0.4%

3.9. 50 ml conical centrifuge tubes

3.10. 96 well V-bottom or U-bottom microtiter plates (Nunc)

3.11. Pipette tips and multichannel pipettor

3.12. Mechanical plate shaker

[1]*Or equivalent*

4. PROCEDURE

4.1. Standardized red blood cell (RBC) preparation

Note: *Cells should **not** be vortexed or shaken at any point during this procedure. This could result in hemolysis of cells.*

4.1.1. Visually inspect and ensure cells do not appear to be hemolyzed. Do **not** use if cells appear to be hemolyzed (supernatant is dark pink or red in color and cells are clumped).

4.1.2. TRBCs are received as individual lots and must be pooled prior to preparation.

4.1.3. GPRBCs are purchased and received pooled.

4.2. Washing TRBCs

4.2.1. Obtain at least three different lots of turkey erythrocytes.

4.2.1.1. Visually inspect to confirm cells do not appear to be hemolyzed.

4.2.2. Filter ~5mL of each lot of TRBCs through sterile gauze into a single 50mL sterile conical centrifuge tube.

4.2.3. Add PBS to the 50mL conical centrifuge tube and bring the solution up to a total volume of ~50mL.

4.2.4. Gently invert tube until TRBCs are fully resuspended.

4.2.5. Centrifuge the 50mL tube at 4˚C for 10 minutes at 300 x g.

4.2.6. Aspirate and discard the supernatant and white buffy layer (if present) without disturbing the packed TRBCs.

4.2.7. Perform a second wash by repeating steps 4.2.3– 4.2.6.

4.3. Washing GPRBCs

4.3.1. Obtain pooled guinea pig erythrocytes.

4.3.2. Visually inspect to confirm cells do not appear to be hemolyzed.

4.3.3. Filter ~2 – 5mL of GPRBCs through sterile gauze into 50mL sterile conical centrifuge tube.

4.3.4. Add PBS to the 50mL conical centrifuge tube and bring the solution up to a total volume of ~50mL.

4.3.5. Gently invert tube until GPRBCs are fully re-suspended.

4.3.6. Centrifuge the 50mL tube at 4˚C for 10 minutes at 500 x g

4.3.7. Aspirate and discard the supernatant and white buffy layer (if present) without disturbing the packed GPRBCs.

4.3.8. Perform a second wash by repeating steps 4.3.4 – 4.3.7.

4.4. The required concentrations for RBC types are captured in Table 1 below:

Table 1

Required RBC Concentrations

RBC Type	Percentage (%)	Concentration (cells/mL)	Tolerance
TRBC	0.5	4.0 x 10e7	± 0.5 x 10e7
GPRBC	0.75	6.0 x 10e7	± 0.5 x 10e7

4.5. Identify the concentration of the washed RBC suspension and adjust to the required concentrations noted in Table 1, using one of the two methods below:

4.6. Concentration Adjustment via Packed Cells (Volume-to-Volume)

4.6.1. Identify the desired volume of standardized RBCs. This is $\mathbf{V_2}$.

4.6.2. Find required concentration in percentage, as identified in Table 1, based on RBC type. This value is $\mathbf{P_{RBC}}$.

4.6.3. Calculate required volume of packed RBCs. This is $\mathbf{V_1}$.

$$\mathbf{V_1 = P_{RBC} V_2}$$

4.6.4. Proceed to step 4.8.

4.7. Concentration Adjustment via Cell Counting (Hemacytometer)

4.7.1. Add PBS to the 50mL conical tube containing washed RBCs and bring the solution up to a volume of ~50mL.

4.7.2. Gently invert or swirl until RBCs are re-suspended.

4.7.3. Use cell counter to determine concentration (cells/mL) of the RBC suspension. This value is $\mathbf{C_1}$.

4.7.4. Using Table 1, identify the required concentration, based on RBC type. This value is $\mathbf{C_2}$.

4.7.5. Determine desired volume of standardized RBCs. This value will be based on planned usage of the RBC solution. This value is $\mathbf{V_2}$.

4.7.6. Use formula: $\mathbf{C_1V_1=C_2V_2}$ to calculate the volume of washed RBCs needed. This value is $\mathbf{V_1}$:

$$\boldsymbol{V1 = \frac{C2V2}{C1}}$$

4.7.7. Proceed to step 4.8.

4.8. Calculate the volume of PBS needed, using the following formula:

4.8.1. $\mathbf{V_2 - V_1}$ = PBS volume needed

4.8.2. Using a sterile container, transfer calculated volume of RBCs, $\mathbf{V_1}$, into determined amount of PBS. This total volume should equal $\mathbf{V_2}$.

4.8.3. Confirm adjustment using cell counter.

4.8.4. If needed, continue readjusting using cell counting, as noted in 4.7.

4.9. HA Assay (Fig.1) — Performed in a BSC if using live virus.

4.9.1. Add 50µL PBS per well to a V bottom plate from row 2 through 12.

4.9.2. Add 100µL of virus to a well of the first row and perform 2-fold serial dilutions using 50µL across row, discard 50µL from last well.

4.9.3. Add 50µL of either TRBCs or GPRBC's to each well.

4.9.4. Tap plates to mix or use mechanical plate shaker.

4.9.5. Incubate plates at room temperature, 30 min for TRBCs or 60 min for GPRBCs.

Note: To assist in interpretation one well of the plate can be used as an RBC control. This well should contain only 50 µL of PBS and 50 µL of red blood cells.

4.10. Interpret and record the results

4.10.1. If using a V-bottom plate, read plates by tilting at a 45° to 60° angle.

4.10.1.1. No Agglutination - Wells in which RBCs settle into a pellet and “run” or “tear” when the plate is tilted (Fig. 2). If using GPRBC’s, the absence of hemagglutination will appear as a "halo" or circle of settled cells in the bottom of the wells (if using U-bottom plate).

4.10.1.2. Agglutination – Wells in which the RBCs form a “lattice” and do not settle exhibit hemagglutination.

4.10.1.3. The RBC control should be completely settled either as a compact button or "halo" (Fig. 2).

4.10.2. The highest dilution of virus that causes complete hemagglutination is considered the HA titration end point. For example, if the last dilution showing complete agglutination is 1:128, then the HA titer is the reciprocal of the dilution which is 128.

Fig.1 Schematic for HA Titrations

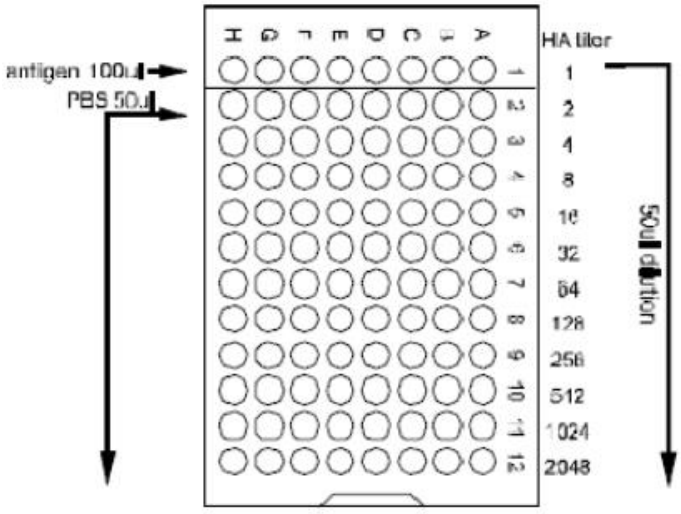

Figure 2. Typical Agglutination Patterns

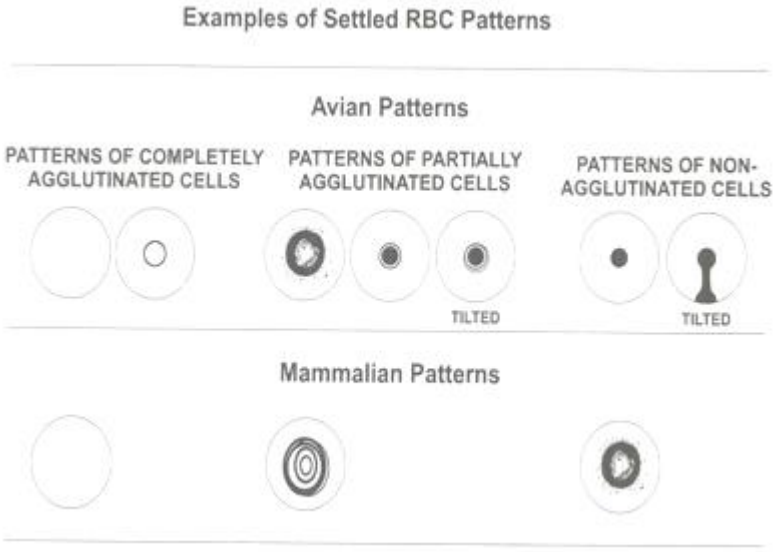

5. REFERENCES

5.1. WHO Global Influenza Surveillance Network: Manual for the laboratory diagnosis and virological surveillance of influenza (2011). (http://www.who.int/influenza/resources/documents/manual_diagnosis_surveillance_influenza/en/) ISBN 9789241548090

APPENDIX F – HEMAGGLUTINATION INHIBITION ASSAY

1. OBJECTIVE

1.1. This SOP describes the hemagglutination inhibition (HI) test procedure for identification and characterization of influenza viruses as well as antibody responses in sera to influenza virus HA.

2. DEFINITIONS

2.1. **BMBL –** Biosafety in Microbial and Biological Laboratories

2.2. **BSL-3 enhanced –** Biosafety Level 3 laboratory requiring additional respiratory protection to protect personnel against aerosols (See BMBL reference)

2.3. **PBS –** Phosphate buffered saline

2.4. **RBC –** Red blood cell

2.4.1. CRBC – Chicken Red Blood Cells (Avian)

2.4.2. GPRBC – Guinea Pig Red Blood Cells (Mammalian)

2.4.3. HUMRBC – Human Red Blood Cells (Mammalian Type "O")

2.4.4. TRBC – Turkey Red Blood Cells (Avian)

2.5. **HA –** Hemagglutination

2.6. **HA unit –** The minimum amount (dilution) of virus needed to agglutinate an equal volume of a standardized RBC suspension

2.7. **HI –** Hemagglutination Inhibition

2.8. **HPAI –** Highly Pathogenic Avian Influenza

2.9. **RDE –** Receptor Destroying Enzyme. Used to remove nonspecific hemagglutination inhibitors existing in serum samples.

2.10. **V/V –** Volume to volume. Volume per unit volume.

3. SAFETY

3.1. Adhere to the following health and safety requirements when conducting experiments with BSL-2 influenza viruses:

3.1.1. Wear a lab coat, gloves, and safety glasses/goggles.

3.1.2. Perform all steps with infectious virus in a certified biosafety cabinet.

3.1.3. Discard solid waste in biohazard bags for autoclaving and disposal.

3.1.4. Treat all liquid waste with fresh disinfectant and process appropriately.

3.1.5. Decontaminate all work surfaces and equipment with disinfectant (preferably with 10% bleach solution or other approved disinfectant followed by 70% ethanol) prior to and after use.

3.2. For highly pathogenic avian influenza (HPAI) – BSL-3 enhanced:

3.2.1. Wear appropriate personal protective equipment according to established entry-exit procedures.

3.2.2. Follow HPAI safety procedures.

4. EQUIPMENT AND REAGENTS[1]

4.1. ***Water bath*:** 37°C±2°C /56°C±2°C

4.2. ***Refrigerator*:** 2°C – 8°C

4.3. ***Freezers*:** -20°C±10°C

4.4. Bench top centrifuge

4.5. ***Biosafety Cabinet*:** Class II (certified)

4.6. ***Avian blood*:** turkey (TRBC) or chicken (CRBC) in Alsever's solution or appropriate anticoagulant

4.7. ***Mammalian blood*:** guinea pig (GPRBC) or human type "O" (HUMRBC) in Alsever's solution or appropriate anticoagulant

4.8. ***Phosphate buffered saline (PBS)*:** 0.01M pH ~7.2

4.9. ***Receptor destroying enzyme (RDE)*:** commercially available (Denka Seiken, Japan). US Distributor, Accurate Scientific.

4.10. **Influenza virus strains:** grown in tissue culture or eggs.

Note: can be live virus or inactivated

4.11. 96 well V bottom microtiter plates

4.12. ***Gauze (sterile)***

4.13. ***Assorted tubes*:** (15ml and 50ml as needed)

4.14. ***Pipet tips*:** recommend filter plug tips

4.15. Assorted pipets

4.16. ***Disinfectant*:** 10% freshly prepared bleach solution,

70% ethanol, or other approved disinfectant

4.17. Mechanical Plate Shaker

[1]*Or Equivalent*

5. PROCEDURE

5.1 Preparation of serum with RDE

5.1.1. Reconstitute the RDE according to manufacturer specifications.

5.1.2. Add 3 vol RDE to 1 vol serum (0.3ml RDE + 0.1ml serum). Incubate 12-18 hours at 37°C.

5.1.3. Heat 56°C for 30 min. Add 6 volumes physiological saline. (Additional 0.6ml saline to 0.4ml of RDE and sera)

5.1.4. Store treated sera samples at ≤-20°C.

5.2. Removal of nonspecific agglutinins

NOTE: Treated sera may contain substances that will nonspecifically agglutinate RBCs. These agglutinins can be removed with the following procedure.

5.2.1. To one volume of packed RBCs, add 20 volumes of RDE-treated serum.

5.2.2. Mix thoroughly and incubate at 4°C, mixing at intervals to resuspend cells.

5.2.3. After 1 hour, centrifuge at 300 x g for 5 minutes.

5.2.4. Carefully remove the adsorbed serum without disturbing the packed cells.

5.2.5. Discard packed cells and keep the serum.

5.2.6. Store serum at ≤-20°C.

5.3. Standardization of Red Blood Cells (RBCs)

5.3.1. If using CRBCs or TRBCs, the final concentration for HA/HI should be a 0.5% v/v concentration. A higher concentration of 0.75% v/v for GPRBC and HUMRBCs improves reading. Although most laboratories have a procedure for standardization of cells, the following procedure is used at the WHO Collaborating Center as an example.

5.3.2. Filter a volume of blood (10 to 45 ml) through gauze, and centrifuge ~300 x g for 5 min. (~500 x g for mammalian red blood cells).

5.3.3. Aspirate supernatant and resuspend cells in 50ml PBS (pH 7.2 to 7.4). *Note: Swirl gently to mix; do not vortex.*

5.3.4. Centrifuge at ~300 x g for 5 min. (~500 x g for mammalian red blood cells) to obtain packed cells. Aspirate supernatant.

5.3.5. Repeat wash (steps 7.3.2 – 7.3.3) with PBS until

supernatant is clear. *Note: Use minimal number of washes to reduce hemolysis.*

5.3.6. Dilute the packed cells to appropriate concentration based on packed cell volume (0.5% v/v for Avian RBCs, 0.75% v/v for Mammalian RBCs). The concentration can be checked and adjusted.

5.4. HA Titration of Control Reference Antigens and Test viruses

5.4.1. The HA antigens should be titrated before every HI test.

5.4.2. Add 50µl of PBS to wells #2 through 10 of each lettered row on a microtiter plate.

5.4.3. Add 100µl of each antigen to the first well of the lettered row which will be diluted.

5.4.4. Two or more RBCs control wells can be prepared in any wells at rows 11 and 12 by adding 50µl of PBS. These wells serve as indicators of a complete settling pattern without antigen.

5.4.5. Make serial two-fold dilutions of each antigen, transferring 50µl from well to well and discarding the final 50µl after row 10. The 2-fold dilutions will be 1:1 through 1:512.

5.4.6. Add 50µl of RBC suspension to each well on plate. Mix by using a mechanical shaker or by manually agitating

the plates.

5.4.7. Incubate the plates at room temperature (22 to 25°C.) for 30 min if using avian cells, but 60 min for mammalian RBCs to allow complete settling of cells.

5.4.8. Record the results and interpret.

5.4.8.1. Hemagglutination occurs when the RBCs are in suspension after the RBC control has settled completely. This is usually recorded using a "+" symbol. An “o” or “-“ symbol is used to record the absence of hemagglutination when a compact button on the bottom of the wells is formed; this button will run if the plate is tilted. This is the case with avian RBCs, however with guinea pig or human type O RBCs, the absence of hemagglutination will appear as a "halo" or circle of settled cells in the bottom of the wells. The RBC control should be completely settled either as a compact button or "halo".

5.4.8.2. The highest dilution of virus that causes complete hemagglutination is considered the HA titration end point. For example, if the last dilution showing complete agglutination is 1:128, then the HA titer is the reciprocal of the

dilution which is 128.

5.5. Preparation of Standardized Antigen for HI Test and "Back Titration" Procedure

5.5.1. Determine the volume of standardized antigen needed for the HI test.

5.5.2. The standard for the HI test is 4 HA units of antigen added to serially diluted antisera.

5.5.2.1. 25µl of antigen is added for each well of the HI test, a virus dilution that contains 4 HA units/25µl or 8 HA units/50µl is needed. Calculate the antigen dilution by dividing the HA titer, which is based on 50µl, and dividing by 8. For example, an HA titer of 128 divided by 8 is 16. Mix 1 part of virus with 15 parts PBS to obtain the desired volume of standardized antigen (Ex: add 0.1 ml antigen to 1.5 ml of PBS). Calculate and prepare dilution. Keep a record of the dilution prepared.

5.5.3. Perform a "back titration" to verify units by performing a second HA test, if an antigen does not titer 8, it must be adjusted accordingly by adding more antigen to increase units or by diluting to decrease units.

5.5.4. Record results.

5.5.5. Figure 1 is a schematic for RBC settling patterns of Avian and Mammalian RBCs.

5.6. Typical agglutination patterns

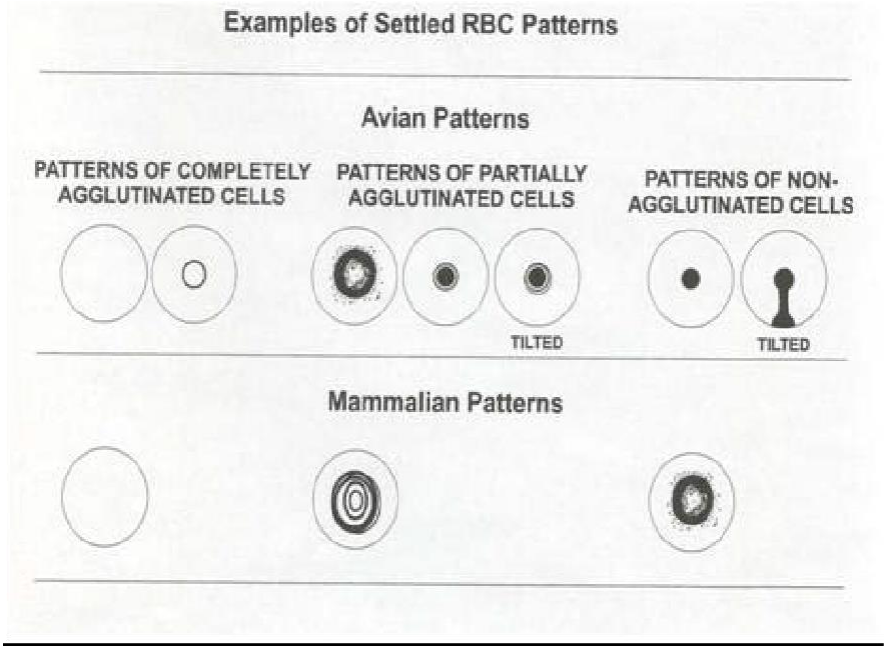

Figure 1: Typical Agglutination Patterns

6. HI TEST

6.1. Plate set up

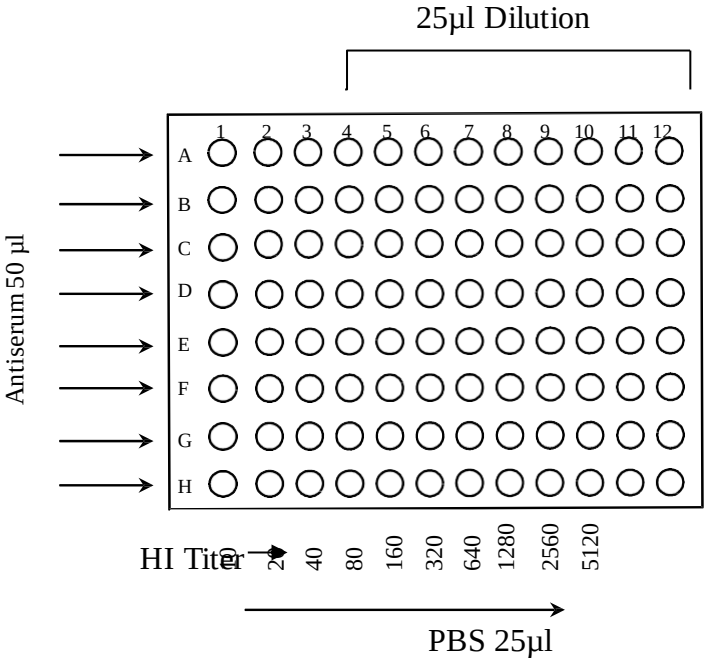

Figure 2: HI Plate Setup

6.2. Add PBS to plates

6.2.1. Add 25µl of PBS to rows 2 through 10.

6.2.2. Cover plates and maintain in humid environment to minimize evaporation. *NOTE: Evaporation can be minimized by covering plates with moistened laboratory wipes.*

6.3. Sera dilution

6.3.1. 50µl RDE treated serum (1:10) is added to the first well of the plate.

6.3.2. Transfer 25µl to second row and continue 2-fold serial dilutions across plate in wells.

6.3.3. Appropriate control sera are used.

6.4. Virus addition

6.4.1. 25µl of the virus solution (adjusted to 8HAU/50µl) is added to every well containing sera.

6.4.2. Tap to mix plate or use plate mixer.

6.4.3. The plate is incubated for 15 minutes at room temperature.

6.4.4. *Note: perform back titration to confirm virus.*

6.5. RBC addition

6.5.1. Add 50µl of standardized RBCs to every well.

6.5.2. Plates are gently tapped to mix samples or use plate mixer.

6.5.3. Cover plates and leave at room temperature.

6.5.3.1. Avian RBCs incubate for at least 30 minutes.

6.5.3.2. Mammalian RBCs incubate for at least 60 minutes.

6.6. Analysis

6.6.1. Read plates by tilting at a 45° to 60° angle.

6.6.1.1. No Agglutination (HI) - Wells in which RBCs settle into a pellet and "run" or "tear" when the plate is tilted.

6.6.1.2. Agglutination – wells in which the RBCs form a "lattice" and do not settle exhibit hemagglutination.

6.6.2. The highest dilution of sera that causes complete

inhibition of hemagglutination (HI) is considered the HI titration endpoint. The HI titer is the reciprocal of the serum dilution in the last well with complete inhibition.

7. REFERENCES

7.1. WHO Global Influenza Surveillance Network: Manual for the laboratory diagnosis and virological surveillance of influenza (2011).

7.2. (www.who.int/publications/i/item/manual-for-the-laboratory-diagnosis-and-virological-surveillance-of-influenza) ISBN 9789241548090

7.3. Biosafety in Microbiological and Biomedical laboratories (BMBL) 5th edition, L.C. Chosewood and D.E. Wilson, eds. CDC, US Department of Health and Human Services (2009)

APPENDIX G – I NFLUENZA VIRUS TITRATION BY FOCUS FORMING ASSAY

INTRODUCTION

The Focus Forming Assay (FFA) is a highly sensitive, quick and convenient method for virus titration in a 96-well format. The influenza virus FFA is performed in 96 well tissue culture plates using a colloidal suspension overlay (Avicel). Viruses are titrated by serial dilution on susceptible MDCK cells, infectious foci (spots) are visualized, and the amount of virus is determined by antibody directed to influenza NP protein within the cell. Foci (spots) are counted through the use of an automated BioSpot reader and calculated as log focus forming units (FFU)/mL. This assay is applicable from one to forty plates.

The FFA is an improvement over the standard plaque assay. The plaque assay is time-consuming and relies on the ability of viruses to lyse cells and form plaques. These plaques require several days to form and may be small or difficult to distinguish. Additionally, the assay is based on the formation of plaques under semisolid overlay, which is laborious and at times, difficult to visualize.

DEFINITIONS

- BSC- Biological Safety Cabinet.
- BMBL – Biosafety in Microbiological and Biomedical Laboratories (https://www.cdc.gov/labs/BMBL.html).

- BSA – Bovine Serum Albumin.
- CAS# - Also referred to as CAS Registry Number (CASRN). A unique chemical identifier assigned by the Chemical Abstracts Service (CAS) to every chemical substance described in the open scientific literature.
- Cat# – Catalog Number. Vendor product identifier.
- DMEM – Dulbecco's Modified Eagle's Medium.
- ELISA – Enzyme-linked immunosorbent assay.
- FBS – Fetal Bovine Serum. [Heat inactivated (30min, 56°C)].
- FFU – Focus Forming Unit.
- IRR – International Reagent Resource (www.internationalreagentresource.org).
- MDCK – Madin Darby Canine Kidney.
    - MDCK-ATL – Madin Darby Canine Kidney – Atlanta (CDC) clone. Item FR-926 distributed through International Reagent Resource (www.internationalreagentresource.org). See *Maintenance and Passage of Madin Darby Canine Kidney Cells (*SOP-029) for culture conditions.
    - MDCK-L – Madin Darby Canine Kidney-London cell line. Item FR-58 distributed through International Reagent Resource (www.internationalreagentresource.org). See *Maintenance and Passage of Madin Darby Canine Kidney Cells (SOP-029) for culture conditions.*
    - MDCK-SIAT1 – Madin Darby Canine Kidney – cells overexpress α2,6 sialic acid receptors (Requires G418 supplement to medium when

culturing). Item FR-1380 distributed through International Reagent Resource (www.influenzareagentresource.org). See *Maintenance and Passage of MDCK-SIAT-1 Cells* (SOP-282) for culture conditions].

- MEM – Modified Eagle's Medium.
- PBS – Phosphate Buffered Saline.
- RT – Room temperature (15 – 25°C).
- SDS – Safety Data Sheet. Also known as Material Safety Data Sheet (MSDS). Contains chemical hazard, exposure and disposal information.
- TPCK – L-1-tosylamido-2-phenylethyl chloromethyl ketone. Used to remove contaminating chymotrypsin activity.
- uL – Micro liters.
- VGM – Virus growth medium.
- VGM-T – Virus growth medium + 1ug/mL TPCK-Trypsin.
- v/v – Volume per unit volume.

SAFETY PRECAUTIONS

- Appropriate Personal Protective Equipment (PPE) is required while handling chemicals or infectious material. This includes but is not restricted to gloves, goggles, gowns, chemical hoods, and biosafety cabinets. (According to the BMBL, www.cdc.gov/biosafety/publications/bmbl5/index.htm).
- Perform all manipulations with live influenza virus inside a certified Class II biological safety cabinet.

- Fixative (4% formalin)
    - Paraformaldehyde solid (powder) is harmful if inhaled, may cause respiratory irritation and cancer.
    - When preparing fixative, perform all work with paraformaldehyde powder in a certified chemical fume hood wearing proper PPE, including gloves, safety glasses, and laboratory coat.
    - Discard fixative (4% formalin) as chemical waste according to local and federal guidelines. *Do NOT discard down sink.*
    - Dispose of used fixative according to chemical hygiene plan and all applicable federal and state guidelines.
    - Refer to SDS for proper protection and exposure guidelines (CAS# 30525-89-4) of paraformaldehyde.
- Hydrogen Peroxide (30%) – CAS# 7722-84-1
    - Corrosive – causes severe skin burns and eye damage.
    - When using, wear gloves, gown or liquid impervious laboratory coat, and eye protection.
    - Avoid release of stock solution (30%) to the environment and dispose of unused material according to Federal and state guidelines.

CRITICAL EQUIPMENT

- Certified, Class II biological safety cabinet.
- Water bath, 37±2°C and 56±2°C.
- Incubator(s), 37±2°C with 5±2% CO_2.

- Magnetic stir plate with stir bars (for Avicel and 10X permeabilization buffer preparation).
- 12-channel aspiration manifold (Drummond Cat#3-000-096) connected to vacuum apparatus.
- P1000 and P200 multi-channel (12) pipettors.
- Inverted microscope for the observation of cells.
- Freezer, -80°C±10°C (for virus, TPCK-trypsin storage) and -20°C±10°C (for serum, antibiotics, and 1° antibody storage).
- 4°C refrigerator, (Range 2° - 8°C).
- Automated plate washer –405^{TM} LS, BioTek (Winooski, VT) www.biotek.com
- CTL BioSpot Analyzer – CTL (Shaker Heights, OH) www.immunospot.com
- ImmunoCapture 6.4.87 software – CTL (Shaker Heights, OH) www.immunospot.com

REAGENTS[1] – and preparation

- **Influenza Virus:** Virus obtained from original specimen, tissue sample from infected animal, or amplified from cells or eggs.
- **Cells:** MDCK-SIAT1, MDCK-L or MDCK-ATL (Low passage; <30).
- **Phosphate Buffered Saline (PBS):** 0.01M, pH7.2 (Mg^{2+}/Ca^{2+} free) CDC Cat# 4539.
- **TPCK-Trypsin:** Sigma Cat# T1426 [adjusted to 2mg/mL in DMEM, filter-sterilized (0.2uM), and stored in aliquots at ≤-80°C±10°C].

- **Culture medium:** DMEM, 5% FBS, antibiotics [Refer to SOP QC-140 for preparation]

    1..1. 940 mL DMEM – Gibco Cat.# 11965.

    1..2. 10 mL 100X Antibiotics (100 U/mL Penicillin, 100ug/mL Streptomycin solution) – Gibco Cat.# 15140.

    1..3. 50 mL FBS, heat inactivated – Gibco Cat# 16000-044.

    1..4. Sterilize through a 1000 mL, 0.2 uM pore filter unit and store at 2 – 8°C for up to 1 month.

- **Virus Growth Medium (VGM):** DMEM, 0.1% BSA, antibiotics

    1..1. 488.4 mL DMEM – Gibco Cat.# 11965

    1..2. 5 mL 100X Antibiotics (100 U/mL Penicillin, 100ug/mL Streptomycin solution) – Gibco Cat.# 15140

    1..3. 6.6 mL 7.5% BSA – Gibco Cat.# 15260

    1..4. Sterilize through a 500 mL, 0.2 um pore filter unit and store at 2 – 8°C for up to 1 month.

- **1.2% Avicel:** FMC BioPolymer, Type: RC-581 NF

    1..1. Avicel – 12g

    1..2. q.s. to 1L with deionized, filtered water

    1..3. Stir for 1 - 2 hour on a magnetic stir plate

    1..4. Sterilize by autoclaving 250°F for 20min (slow exhaust cycle)

1..5. May store at room temperature for up to 1 year

- **<u>2X DMEM</u>:** 2X MEM, Gibco Cat# 11935 or prepare as follows:

1..1. 26.76 g DMEM powder – Gibco Cat# 12100

1..2. 7.4 g $NaHCO_3$ (Sodium Bicarbonate)

1..3. q.s. to 1L with endotoxin-free water

1..4. Adjust pH to 7 – 7.4

1..5. Sterilize through 0.2uM filter

1..6. Dispense aseptically and store at 2-8°C for up to 1 month

- **<u>OVERLAY</u>:** (prepare 11 mL/plate to account for dead volume):

1..1. DMEM, 0.1% BSA,0.6% Avicel, 1ug/mL TPCK-Trypsin, antibiotics

1..2. For 11 mL (prepare fresh and keep at 37°C until use):

1..2.1. 5.1 mL – 2X MEM or 2X DMEM

1..2.2. 0.3 mL – 7.5% BSA

1..2.3. 0.1 mL – 100X Antibiotics (Penicillin/Streptomycin)

1..2.4. 5.5 mL – 1.2% Avicel

1..2.5. 5.5 uL – TPCK-Trypsin (@2mg/mL stock)

- **<u>FIXATIVE</u>:** 4% Formalin

1..1. 40 g – Paraformaldehyde, $HO(CH_2O)_nH$ (Acros Organics Cat# 169650025)

1..2. q.s. to 1 L with 0.01M PBS, pH 7.2 (Mg^{2+}/Ca^{2+} free)

1..3. Heat in water bath, with periodic swirling, to dissolve paraformaldehyde (~56 – 60°C for several hours until dissolved).

1..4. Filter through 0.2uM filter

1..5. May store at 2 – 8°C for up to 3 months

- **PBS WASH BUFFER:** 0.01M, pH7.2 (Mg^{2+}/Ca^{2+} free)

1..1. 7.11.1. 10X PBS stock and dilute 1/10 with deionized water.

1..2. 7.11.2. Or 0.01M,
pH7.2
(Mg^{2+}/Ca^{2+} free)
PBS

- **PERMEABILIZATION BUFFER (10X)*:** 5% Triton X-100 in PBS/Glycine

1..1. 1.5 g – Glycine, NH_2CH_2COOH (Sigma Cat# G7126)

1..2. 95.0 mL – 0.01M PBS, pH 7.2 (Mg^{2+}/Ca^{2+} free)

1..3. 5.0 mL – Triton X-100 (Sigma Cat# T8787)

1..4. Stir on stir plate at
room temperature
until dissolved .

1..5. May store up to 1 year at room temperature.

1..6. *Working solution, dilute 1:10 in PBS.

- **ELISA BUFFER:** 10% Horse Serum, 0.1% Tween-80 in PBS

    1..1. 80.0 mL – Horse Serum (Heat inactivated), Sigma Cat# H1138

    1..2. 720.0 mL – 0.01M PBS, pH 7.2 (Mg^{2+}/Ca^{2+} free)

    1..3. 0.8 mL – Tween-80 (Sigma Cat# P8074)

    1..4. May store up to 1 month at 2 – 8°C

- **WASH BUFFER:** PBS, 0.05% v/v Tween-20

    1..1. To 1 L 0.01M PBS, pH 7.2 (Mg^{2+}/Ca^{2+} free) add 0.5 mL Tween-20 (Sigma Cat# P7949).

    1..2. Or use 10X PBS/Tween Stock and dilute 1/10 with deionized water.

- **1° ANTIBODY:** *Dilute to* optimal *concentration in ELISA buffer*

    1..1. *Influenza A:*

        1..1.1. mouse anti-A/NP mAb pool – IRR Cat# FR-794 or FR-1217. Use @1:2000 in ELISA buffer (e.g. 50 uL of 1° Antibody in 100mL of ELISA Buffer).

    1..2. *Influenza B:*

        1..2.1. mouse anti-B/NP mAb (B2 clone) – CDC Cat# PS508b (Lot# 10-039b). Use @1:2000 in ELISA buffer (e.g. 50 uL of 1° Antibody in 100mL of ELISA Buffer).

- or

1..2.2. mouse anti-B/NP mAb pool – IRR Cat# FR-829 or FR-1218. Use @1:2000 in ELISA buffer (e.g. 50 uL of 1° Antibody in 100mL of ELISA Buffer).

- **2° ANTIBODY:** *Dilute to optimal concentration in ELISA buffer*

1..1. Goat anti-mouse IgG, peroxidase labeled – Sera Care Cat# 5220-0460. Use @1:2000 in ELISA buffer. (e.g. 50 uL of 2° Antibody in 100mL of ELISA Buffer).

- **SUBSTRATE:** True Blue peroxidase, 0.03% H_2O_2 (5 mL/plate) ***MAKE IMMEDIATELY BEFORE USE***

1..1. True Blue (Sera Care Cat# 5510-0030) – 50mL [3,3',5,5'-tetramethylbenzidine (TMB) substrate]

1..2. Hydrogen Peroxide (30%, Sigma Cat# 216763) – 0.05mL (to oxidize TMB to form blue chromogenic product and to block endogenous peroxidase activity in cells)

- **STOP SOLUTION:** Tap or deionized water.

[1]Or Equivalent manufacturer may be used following quality control testing.

MATERIALS[1]

- 96-well, flat-bottom, tissue culture polystyrene microtiter plates (Corning Cat# 3598) or Immulon 2HB (Thermo Cat# 3455) plates.

- 96-well Clear V-Bottom 2 mL Polypropylene Deep Well Plate (Costar Cat# 3960) [96-well V-Bottom 2mL block].
- Disposable reagent reservoirs [Integra Biosciences; 10mL (Cat# 4337), 25mL (Cat# 4312) and 100mL (Cat# 4322)]. (www.integra-biosciences.com).
- Sterile capped tubes
- Assorted sterile pipettes (2mL, 5mL, 25mL, 50mL), pipetting device, and tips (200uL and 1000uL).
- Lint-free wipes (to blot plates prior to drying). Leica Cat#3803240. (www.LeicaBiosystems.com).

[1]Or Equivalent manufacturer may be used following testing.

PROCEDURE

- **CELL PREPARATION**

  1..1. Obtain MDCK cells and adjust concentration to 2.5 – 3x10^5 cells/mL in **culture medium.**

  1..2. Add 100µl cells/well to 96-well tissue culture plate(s) and incubate overnight in humidified 37°C, 5% CO_2 incubator. Plates can be stacked a maximum of 5 plates/stack and should not be disturbed once placed in incubator.

- **VIRUS TITRATION – FFU DETERMINATION** (Day 1) – To be completed under sterile conditions

  1..1. View plates under a light microscope to observe confluency.

NOTE: The cell monolayer must be 100% confluent and cells must be tightly packed (round not elongated) before using and ≤30 passages – see patterns below

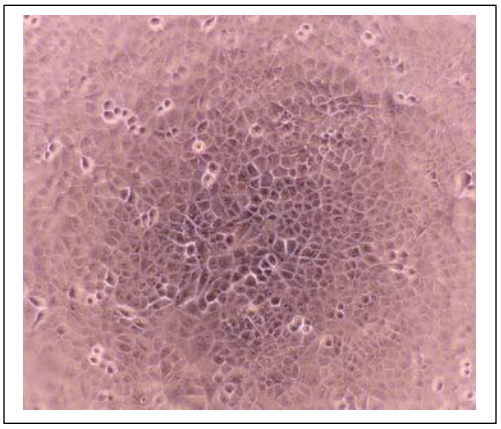

OPTIMAL – Cells confluent, packed

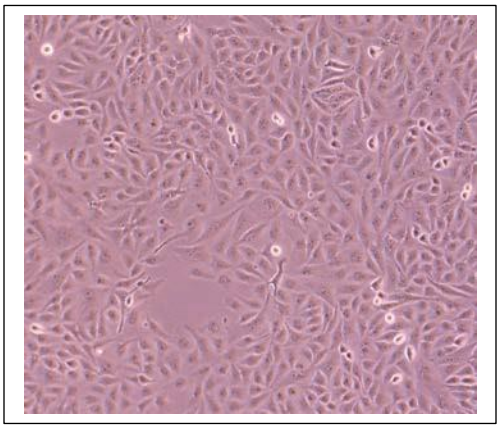

NOT Optimal – Not confluent, spindle-shaped

1..2. If cells are acceptable, aspirate media from plates using a 12-channel aspiration manifold, being mindful not to disturb cell monolayer.

1..3. Wash plate(s) twice with PBS (~100uL/well/wash) using a 12-channel aspiration manifold to aspirate. Do not disturb cell monolayer.

1..4. Aspirate PBS and add 50uL/well VGM-T [(VGM + 1ug/mL TPCK-trypsin) (e.g. 250uL TPCK-trypsin @ 2mg/mL in 500mL VGM)] to all wells.

1..5. Return plate(s) to 37°C, 5% CO2 incubator in stacks no higher than 5 plates.

1..6. Perform serial dilutions (½ Log10) of virus(es) in 96-well V-

Bottom 2mL block (1-virus/row).

1..6.1. Add 500 uL VGM-T to columns 1-12.

1..6.2. Remove 50 uL VGM-T from column 1.

1..6.3. Add 50 uL of virus for each position in column 1. (i.e. A1=Virus #1, B1=Virus #2, C1=Virus #3…H1=Virus #8.)

1..6.4. Perform serial ½ log10 dilutions (10^1, $10^{1.5}$, 10^2, $10^{2.5}$….10^6) [i.e. approximate 3-fold dilutions] by transferring 230 uL from column 1 to column 2, mix by pipette 3-4 times and dispose of tips. Repeat step until column 11. Changing tips between dilutions.

1..6.5. Remove 230 uL from column 11 and dispose.

1..6.6. Retrieve washed plates from step 1..5. in incubator.

1..6.7. For each cell plate, transfer 50 uL per row from V-Bottom 2mL block to cell plate in quadruplicate. [i.e. row A (Virus #1) → rows A-D & row B (Virus #2) → E-H]. Repeat for remaining virus(es) at 2 viruses/cell plate. See Figure 1 for cell plate configuration.

Figure 1: Virus titration cell plate configuration (2 viruses/plate).

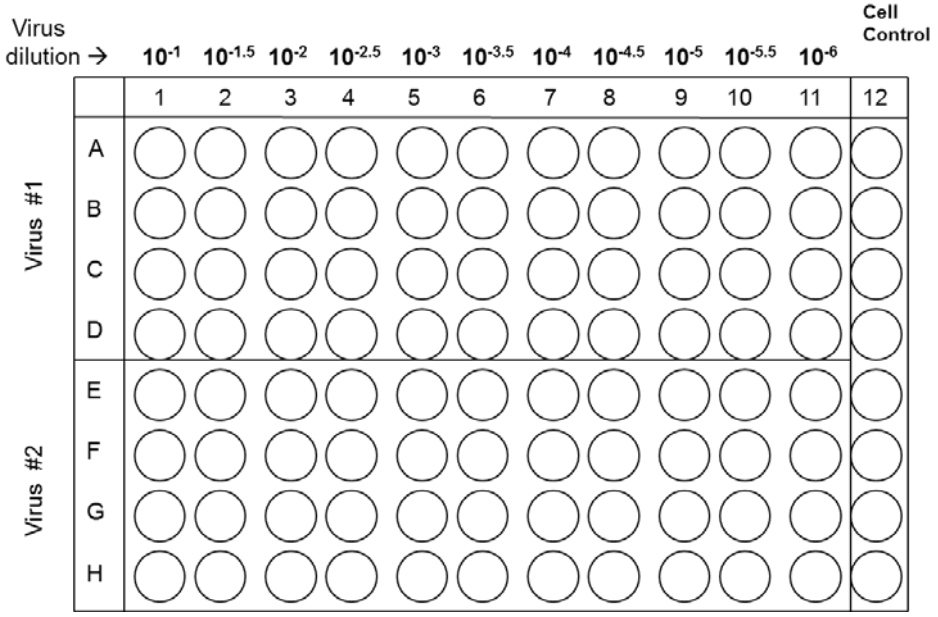

1..7. Incubate plate(s), in stacks no higher than 5 plates, undisturbed at 37°C, 5% CO2 for 2Hr±15min to allow virus to infect cells.

1..8. Prepare OVERLAY in sterile bottle (11 mL/plate), maintain at 37°C water bath, and mix well by inversion just before addition to cell plate. Refer to 7.10 for preparation instructions.

1..9. Add 100uL OVERLAY to all wells of cell plate(s) using 12-channel pipettor.

1..10. Return plates to incubator and incubate plates at 37°C, 5%CO2 overnight (18 – 22 hours). Do NOT shake or disturb plates.

- **ELISA (Day 2) – *Perform all steps prior to fixation in a BSC***

1..1. Retrieve plates from incubator and aspirate supernatant (overlay + media) from wells using 12- channel aspiration manifold. *Avoid disrupting cell monolayer*.

1..2. Wash plates once with 100ul/well PBS and aspirate. *Avoid disrupting cell monolayer.*

1..3. Add 100µl/well of chilled **FIXATIVE** to cells. *Refer to step 7.11 for preparation instructions.*

1..4. Incubate plates at 2-8°C for 30 – 40 mins, undisturbed.

1..5. Aspirate fixative using 12-channel manifold. (Discard waste as chemical waste) *After this step, working in a BSC is no longer required*.

1..6. Wash plate(s) twice with PBS (200 – 300 uL/well), aspirating between each wash, using an automated plate washer. *All PBS should be removed from wells following wash.*

1..6.1. Alternatively, can be performed manually using a 12-channel pipettor.

NOTE*: Plates can be stored in 100 uL PBS and placed in sealed bag at 2 – 8°C (for up to 3 days) or continue to 9.3.7. immediately.*

1..7. Add 100 uL/well of **1X PERMEABILIZATION BUFFER** to cell plate(s). *Refer to 7.13 for preparation instructions.*

1..8. Incubate for 20-30 min at RT, undisturbed.

1..9. Wash plate(s) 3X with **WASH BUFFER** (200 – 300 uL/well), aspirating between each wash, using an automated plate washer. *Refer to 7.15 for preparation instructions.*

1..10. Add 50µl/well of diluted **1° ANTIBODY** to all wells of 96 well plate(s). (e.g. 50 uL of 1° Antibody in 100mL of **ELISA BUFFER**.) *Refer to 7.16 for preparation instructions.*

1..11. Incubate at RT for 1 hour (or in sealed bag at 2°C – 8°C overnight), undisturbed.

1..12. Wash plate(s) 3X with **WASH BUFFER** (200 – 300 uL/well), aspirating between each wash, using an automated plate washer. *Refer to 7.15 for preparation instructions.*

1..13. Add 50 uL/well of diluted **2° ANTIBODY** to all wells of 96 well plate(s). (e.g. 50 uL of 2° Antibody in 100mL of **ELISA BUFFER**.) *Refer to 7.17 for preparation instructions*

1..14. Incubate at RT for 1 hour, undisturbed.

1..15. Wash plate(s) 3X with **WASH BUFFER** (200 – 300 uL/well), aspirating between each wash, using an automated plate washer. *Refer to 7.15 for preparation instructions*.

1..16. Add 50 uL/well of **SUBSTRATE**.(e.g. 10 uL of 30% H_2O_2

in 10mL of True Blue) . *Refer to 7.18 for preparation instructions.*

1..17. Incubate at RT for 10-15 min, undisturbed.

1..18. To stop the reaction, wash plate(s) 5X with cold tap water or deionized water using automated plate washer.

1..19. Blot excess water with lint free wipes and air-dry face down on BSC vent. Wipe bottom of plate(s) with 70% EtOH to clean. (*store in a dark place if not read same day*).

1..20. Scan and count full plate using ImmunoCapture program on CTL and analyze.

1..21. Determine FFU.

1..21.1. The FFU is determined as the average number of Foci at the dilution of each test virus that yields an easily countable number (600 $\pm$ 400).

1..21.2. FFU/mL of viral stock = #Foci(spots) /volume (uL) x 1000 uL/1mL x Dilution

Ex: 253 Foci (spots) in an inoculum of 50 uL at a dilution of 10^4

- FFU/mL = 253/50uL
- To convert to FFU/mL, multiply by

1000; FFU/mL = 5.06 FFU/uL x 1000 uL/1mL = $5.06x10^3$ FFU/mL

- Multiply by Dilution; $5.06x10^3$ x 10^4 = **$5.06x10^7$ FFU/mL or $1x10^{7.70}$ FFU/mL**

REFERENCES

- Biosafety in Microbiological and Biomedical Laboratories (BMBL), 5th Edition (2009). HHS Publication N. (CDC) 21-1112. http://www.cdc.gov/biosafety/publications/bmbl5/index.htm
- Matrosovich et al. Overexpression of the α-2,6-Sialyltransferase in MDCK Cells Increases Influenza Virus Sensitivity to Neuraminidase Inhibitors. J.Virol. 77:8418 (2003).
- Matrosovich et al. New low viscosity overlay medium for viral plaque assays. Virology Journal 3:63 (2006).
- Rowe, T., et al., *Differential interferon responses to influenza A and B viruses in primary ferret respiratory epithelial cells.* J Virol, 2024. **98**(2): p. e0149423.

FIXATIVE OPTIONS: COMPARISONS OF ALTERNATIVE FIXATIVES

- Fixative comparison – Testing of alternative fixatives w/ H3N2 viruses

1..1. 4% Formaldehyde w/v - @4°C, 30Min ±Permeabilization step

1..2. 95%MeOH/5%Acetic acid - @-20°C, 1Hr ±Permeabilization

step

1..3. 80% Acetic acid in PBS - @-20°, 30Min ±Permeabilization step

1..4. 70% EtOH - @-20°C and @ 4°C, 30Min ±Permeabilization step

- Results – 70% EtOH ±Permeabilizaton works equally well as 4% Formaldehyde solution and could be used as a less toxic method to reduce chemical hazards.
- Comparison FFU titers of different fixatives ±permeabilization step:

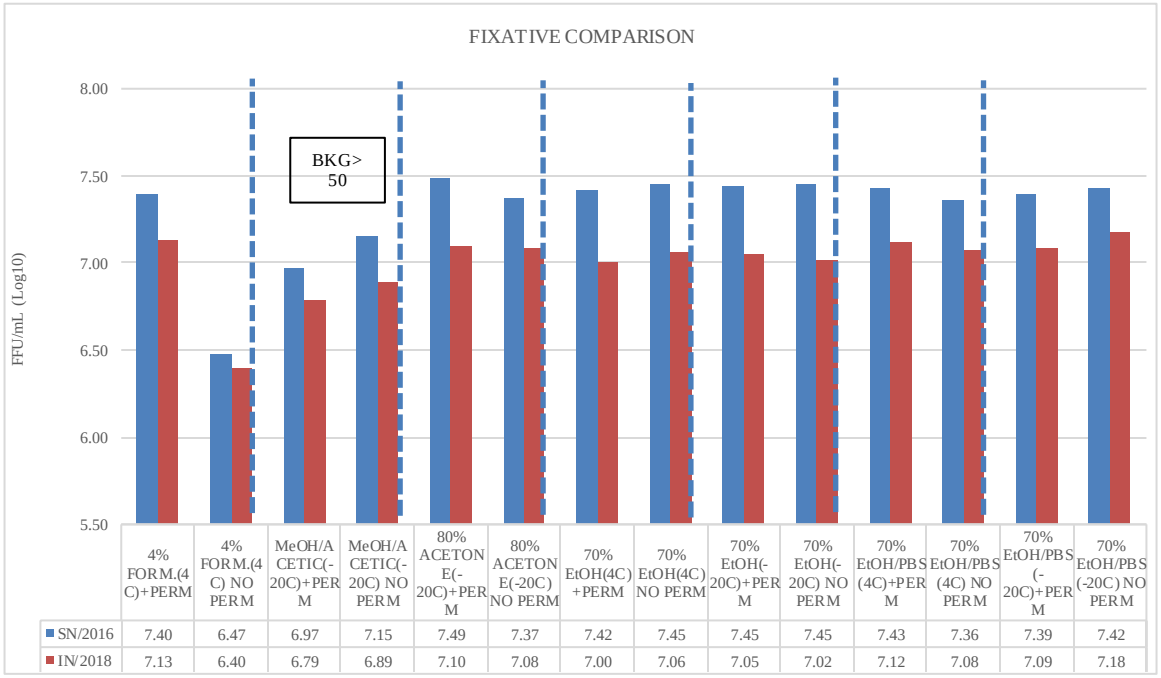

	4% FORM.(4C)+PERM	4% FORM.(4C) NO PERM	MeOH/ACETIC(-20C)+PERM	MeOH/ACETIC(-20C) NO PERM	80% ACETONE(-20C)+PERM	80% ACETONE(-20C) NO PERM	70% EtOH(4C)+PERM	70% EtOH(4C) NO PERM	70% EtOH(-20C)+PERM	70% EtOH(-20C) NO PERM	70% EtOH/PBS (4C)+PERM	70% EtOH/PBS (4C) NO PERM	70% EtOH/PBS (-20C)+PERM	70% EtOH/PBS (-20C) NO PERM
SN/2016	7.40	6.47	6.97	7.15	7.49	7.37	7.42	7.45	7.45	7.45	7.43	7.36	7.39	7.42
IN/2018	7.13	6.40	6.79	6.89	7.10	7.08	7.00	7.06	7.05	7.02	7.12	7.08	7.09	7.18

OVERLAY OPTIONS: COMPARISON OF ALTERNATIVE OVERLAY TO AVICEL

- Overlay comparison – 1.2% Avicel and 1.2% Cellulose (Sigma, Cat#435244)
- Fixative = 4% w/v Formaldehyde; +Permeabilization
- Results – 1.2% Cellulose results in ~$10^{0.5}$ FFU/mL fewer foci than Avicel with similar morphology and may potentially be used as an alternative if Avicel is unavailable.
- FFU/mL comparing H3N2 and B-Yam viruses using Avicel or Cellulose overlay

VIRUS#	VIRUS	SUBTYPE	PASSAGE	FFU/ml 10^XX	AVG CC	COMMENTS
1	A/KANSAS/14/2017	H3N2	S3(11/18/2019)	7.54	3	AVICEL-POS CTRL (EXPECTED=7.06)
2	A/SINGAPORE/INFIMH-16-0019/2016	H3N2	C1S3/S4(09/12/2018)	8.01	4	AVICEL-EXPECTED=7.73
3	A/INDIANA/08/2018	H3N2	QMC2S1(03/12/2019)	7.51	2	AVICEL-EXPECTED=7.11
4	B/PHUKET/3073/2013	B-YAM	E4/E2(07/26/2019)	8.44	5	AVICEL-EXPECTED=8.32
1	A/KANSAS/14/2017	H3N2	S3(11/18/2019)	7.11	6	CELLULOSE-POS CTRL (EXPECTED=7.06)
2	A/SINGAPORE/INFIMH-16-0019/2016	H3N2	C1S3/S4(09/12/2018)	7.46	9	CELLULOSE-EXPECTED=7.73
3	A/INDIANA/08/2018	H3N2	QMC2S1(03/12/2019)	7.00	3	CELLULOSE-EXPECTED=7.11
4	B/PHUKET/3073/2013	B-YAM	E4/E2(07/26/2019)	8.37	12	CELLULOSE-EXPECTED=8.32

APPENDIX H – NEUTRALIZING ANTIBODY DETECTION BY FOCUS REDUCTION ASSAY

PURPOSE

1.1. The influenza virus Focus Reduction Assay (FRA) is performed in 96 well tissue culture plates and the amount of virus used in the reduction assay is pre-determined by virus titration. To overcome the pitfalls of other overlays, a suspension of microcrystalline cellulose Avicel RC/CL is used as the overlay in the assay. Approximately 600 Focus Forming Units (FFU) of virus is incubated with two-fold serial dilutions of anti-sera overnight and virus reduction (neutralization) titer is reported as the reciprocal of the highest dilution of serum corresponding to 50% Foci reduction compared to the virus control. Foci (spots) are calculated by using an automated BioSpot reader.

2. DEFINITIONS

2.1. BMBL – Biosafety in Microbiological and Biomedical Laboratories (reference)

2.2. BSA – Bovine Serum Albumin

2.3. CAS# - Also referred to as CAS Registry Number (CASRN). A unique chemical identifier assigned by the Chemical Abstracts Service (CAS) to every chemical substance described in the open scientific literature.

2.4. Cat# – Catalog Number. Vendor product identifier.

2.5. DMEM – Dulbecco's Modified Eagles Medium

2.6. ELISA – Enzyme-linked immunosorbent assay

2.7. FFU – Focus Forming Units

2.8. IRR – International Reagent Resource (www.internationalreagentresource.org)

2.9. MDCK – Madin Darby Canine Kidney

2.9.1. MDCK-L – Madin Darby Canine Kidney-London cell line. Item FR-58 distributed through the IRR (www.internationalreagentresource.org)

2.9.2. MDCK-SIAT1 – Madin Darby Canine Kidney – containing overexpression of α2,6 sialic acid receptors (Requires G418 supplement to medium when culturing). Item FR-1380 distributed through the IRR (www.internationalreagentresource.org)

2.10. MEM – Modified Eagle's Medium

2.11. PBS – Phosphate Buffered Saline

2.12. Q.S. – As much as will suffice, Sufficient quantity. Latin- quantum satis

2.13. RDE – Receptor Destroying Enzyme

2.14. RT – Room temperature (15 – 25°C)

2.15. SDS – Safety Data Sheet. Also known as Material Safety Data Sheet (MSDS). Contains chemical hazard, exposure, and disposal information.

2.16. TPCK – L-1-tosylamido-2-phenylethyl chloromethyl ketone. Used to remove contaminating chymotrypsin activity.

2.17. VGM – Virus growth medium

2.18. VGM-T – Virus growth medium + 1µg/ml TPCK-Trypsin

2.19. v/v – Volume per unit volume

3. CRITCAL EQUIPMENT

3.1. Class II biological safety cabinet

3.2. Magnetic stir plate

3.3. Water baths, 37°C and 56°C

3.4. Incubator, 37°C with 5% CO_2

3.5. Inverted microscope for the observation of cells

3.6. Freezer, -80°C±10°C (for virus storage) and -20°C±10°C (for serum storage)

3.7. Automatic plate washer

3.8. 4°C refrigerator, Range 2° - 8°C

3.9. CTL-BioSpot S6 Macro Analyzer or ELISpot reader

4. **SUPPLIES**[1]

4.1. 96-well, flat-bottom, tissue culture polystyrene microtiter plates (Corning Cat# 3598) or Immulon 2HB (Thermo Cat# 3455) plates

4.2. 96-well V-Bottom 2ml block (Costar Cat# 3960)

4.3. Disposable reagent reservoirs [Integra Biosciences; 10mL (Cat# 4337), 25mL (Cat# 4312) and 100mL (Cat# 4322)]. (www.integra-biosciences.com)

4.4. Sterile capped tubes

4.5. Assorted sterile pipettes, pipetting device, and tips

4.6. Automatic plate washer – ELx405, BioTek (Santa Clara, CA, USA) www.agilent.com

4.7. CTL BioSpot Analyzer – CTL (Shaker Heights, OH, USA) www.immunospot.com

4.8. ImmunoCapture 6.4.87 software – CTL (Shaker Heights, OH, USA) www.immunospot.com

[1]*Or Equivalent manufacturer may be used following testing.*

5. REAGENTS[1]

5.1. **Influenza Virus**: Original specimen or amplified virus (minimum of $4x10^3$ FFU/mL)

5.2. **RDE treated sera**: Refer to – TREATMENT OF ANTISERUM WITH RECEPTOR DESTROYING ENZYME (RDE) AND ADSORPTION WITH RBCS.

5.3. **Cells**: MDCK-SIAT1, MDCK-London or MDCK-ATL (Low passage; <30)

5.4. **Geneticin (G418)**: Gibco Cat# 10131 @50mg/ml stock solution (adjust to 1mg/ml in culture medium; dilute 1:50); for use with MDCK-SIAT1 cell culture. *Note: G418 is not needed in assay media; only for culture of cells (cell passage).*

5.5. **Phosphate Buffered Saline (PBS)**: 0.01M, pH7.2 (Mg2+/Ca2+ free)

5.6. **TPCK-Trypsin**: Sigma Cat# T1426 (adjusted to 2mg/ml in DMEM, filter-sterilized, and stored in aliquots at ≤-70°C)

5.7. **Culture medium**: DMEM, 5% FBS, antibiotics

5.7.1. 470 ml DMEM – Gibco Cat.# 11965

5.7.2. 5 ml 100X Antibiotics (100 U/ml Penicillin, 100µg/ml Streptomycin solution) – Gibco Cat.# 15140

5.7.3. 25 ml Fetal bovine serum, heat inactivated – Corning Cat#35-015

5.7.4. Sterilize through 0.2 µM pore filter and store at 2°C - 8°C for up to 1 month

5.8. **Virus Growth Medium (VGM)**: DMEM, 0.1% BSA, antibiotics

5.8.1. 488.4 ml DMEM – Gibco Cat.# 11965

5.8.2. 5.0 ml 100X Antibiotics (100 U/ml Penicillin, 100µg/ml Streptomycin solution) – Gibco Cat.# 15140

5.8.3. 6.6 ml 7.5% BSA – Gibco Cat.# 15260

5.8.4. Sterilize through 0.2 µm pore filter and store at 4°C for up to 1 month

5.9. **1.2% Avicel**: FMC BioPolymer, Type: RC-581 NF

5.9.1. Avicel – 1.2g

5.9.2. q.s. to 100ml with distilled water

5.9.3. Stir for 1 hour on a magnetic stir plate

5.9.4. Sterilize by autoclaving 250°F for 20min (slow exhaust cycle)

5.9.5. May store at room temperature for up to 1 year

5.10. **2X DMEM**: 2X MEM, Gibco Cat# 11935 or prepare as follows:

5.10.1. 26.76 g DMEM powder – Gibco Cat# 12100

5.10.2. 7.4 g $NaHCO_3$ (Sodium Bicarbonate)

5.10.3. q.s. to 1L with endotoxin-free water

5.10.4. Adjust pH to 7 – 7.4

5.10.5. Sterilize through 0.2µM filter

5.10.6. Dispense aseptically and store in 4°C refrigerator

5.11. **Overlay: (10ml/plate)**: DMEM, 0.1% BSA,0.6% Avicel, 1ug/ml TPCK-Trypsin, antibiotics

5.11.1. For 100ml:

5.11.2. 46.3 ml – 2X MEM or 2X DMEM

5.11.3. 2.7 ml – 7.5% BSA

5.11.4. 1.0 ml – 100X Antibiotics (Penicillin/Streptomycin)

5.11.5. 50 ml – 1.2% Avicel

5.11.6. 0.05 ml – TPCK-Trypsin

5.12. **Fixative** : 4% w/v formaldehyde solution (10% Formalin)

5.12.1. 40 g – Paraformaldehyde, $HO(CH2O)_nH$ (Acros Organics Cat# 169650010)

5.12.2. q.s. to 1 L with 0.01M PBS, pH 7.2 (Mg2+/Ca2+ free)

5.12.3. Heat in water bath to dissolve paraformaldehyde (~56 – 60°C for several hours)

5.12.4. Filter through 0.2µM filter

5.12.5. May store at 4°C for up to 3 months

5.13. **10X Permeabilization buffer***: 5% Triton X-100 in PBS/Glycine

5.13.1. 1.5 g – Glycine, NH2CH2COOH (Sigma Cat# G7126)

5.13.2. 95.0 ml – 0.01M PBS, pH 7.2 (Mg2+/Ca2+ free)

5.13.3. 5.0 ml – Triton X-100 (Sigma Cat# T8787)

5.13.4. May store up to 1 year at room temperature

*Working solution, dilute 1:10 in PBS.

5.14. **ELISA Buffer**: 10% Horse Serum, 0.1% Tween-80 in PBS

5.14.1. 40.0 ml – Horse Serum (Heat inactivated), Sigma Cat# H1138

5.14.2. 360.0 ml – 0.01M PBS, pH 7.2 (Mg2+/Ca2+ free)

5.14.3. 0.4 ml – Tween-80 (Sigma Cat# P8074)

5.14.4. May store up to 1 month at 4°C

5.15. **Wash Buffer**: PBS, 0.05% v/v Tween – 20

5.15.1. To 1 L 0.01M PBS, pH 7.2 (Mg2+/Ca2+ free) add 0.5 ml Tween-20 (Sigma Cat# P7949)

5.15.2. Or use 10X PBS/Tween Stock and dilute 1/10 with deionized water.

5.16. **1° Antibody**: Dilute to optimal concentration in ELISA buffer

5.16.1. Influenza A:

5.16.1.1. mouse anti-A/NP mAb pool – IRR Cat# FR-1217 (Lot# 61791379 use @1:2000 in ELISA buffer)

5.16.2. Influenza B:

5.16.2.1. mouse anti-B/NP mAb (B2 clone) – CDC Cat# PS508b (Lot# 10-039b use @1:2000 in ELISA buffer)

or

5.16.2.2. mouse anti-B/NP mAb pool – IRR Cat# FR-1218

5.17. **2° Antibody**: Dilute to optimal concentration in ELISA buffer

5.17.1. Goat anti-mouse IgG, peroxidase labeled – KPL Cat# 474-1802 (Lot# 111098 use @1:2000 in ELISA buffer)

5.18. **Substrate**: True Blue peroxidase, 0.03% H_2O_2 (5ml/plate) MAKE IMMEDIATELY BEFORE USE

5.18.1. True Blue (Sera Care Cat# 5510-0030) – 50ml [3,3',5,5'-tetramethylbenzidine (TMB) substrate]

5.18.2. Hydrogen Peroxide (30%, Sigma Cat# 216763) – 0.05ml

5.19. **Stop Solution**: Tap or deionized water

[1]Or equivalent manufacturer may be used following quality control testing.

6. PROCEDURE

6.1. DAY 1:

6.1.1. Obtain MDCK cells and adjust concentration to 2.5 – 3x10^5 cells/ml in culture medium.

6.1.2. Add 100µl cells/well to 96-well tissue culture plate and incubate overnight in humidified 37°C, 5% CO_2 incubator.

NOTE: The cell monolayer must be confluent and cells must be tightly packed (round not elongated) before using and ≤30 passages.

6.2. DAY 2:

6.2.1. Perform two-fold serial dilutions of RDE treated serum (not adsorbed with red blood cells) in VGM-T. Starting from 1:40 by transferring half of the volume from row to row in 96-well V-Bottom 2 ml block.

6.2.2. For columns 1-10, 50 µl aliquots of 1:20 RDE treated serum are added to the first row (A). 50 µl aliquots of 1:40 RDE treated sera are added to the second row (B). 50 µl aliquots of 1:2560 RDE treated serum are added to the eighth row (H). Columns 11 and 12 are used for virus control and cell control respectively (See Figure 2 for suggested setup). (Note: For each virus/serum combination, the assay is performed in duplicate so each plate can test one virus with five anti-sera.)

6.2.3. Adjust virus concentration to 1.2x10^4 FFU/ml (corresponds to 600 FFU/50µl) in VGM-T (Need ~6ml/plate). ***NOTE: If <10µl of virus is need, first perform 1:100 dilution in VGM-T (10µl virus + 990µl VGM-T) and use. Ex. If you need 8µl virus → perform 1:100 dilution first → use 800µl of 1:100.***

Ex. For 2 plates using stock virus at $2x10^6$ FFU/ml:

FFU of stock virus needed = FFU Needed ($1.2x10^4$ FFU/ml) x #ml needed (12ml)

= $44x10^5$ FFU virus needed

Stock virus = $2x10^6$ FFU/ml, therefore → FFU Needed/FFU of stock

$$\frac{44x10^5 \text{ FFU}}{2x10^6 \text{FFU/ml}} = 0.072\text{ml virus in 12ml}$$

6.2.4. Add 50 µl of the virus to each well of the plate except for the cell control column (column 12). For virus control column (column 11). Add 50 µl of the virus to position A11, B11, C11 and D11, and add 50 µl 1/2 diluted virus to position E11, F11, G11 and H11 (Figure 3).

6.2.5. Add 50 µl of VGM-T to each well of the cell control column (column 12).

Figure 3. Typical Focus Reduction plate set-up.

A – 5 Sera/Plate (in duplicate)

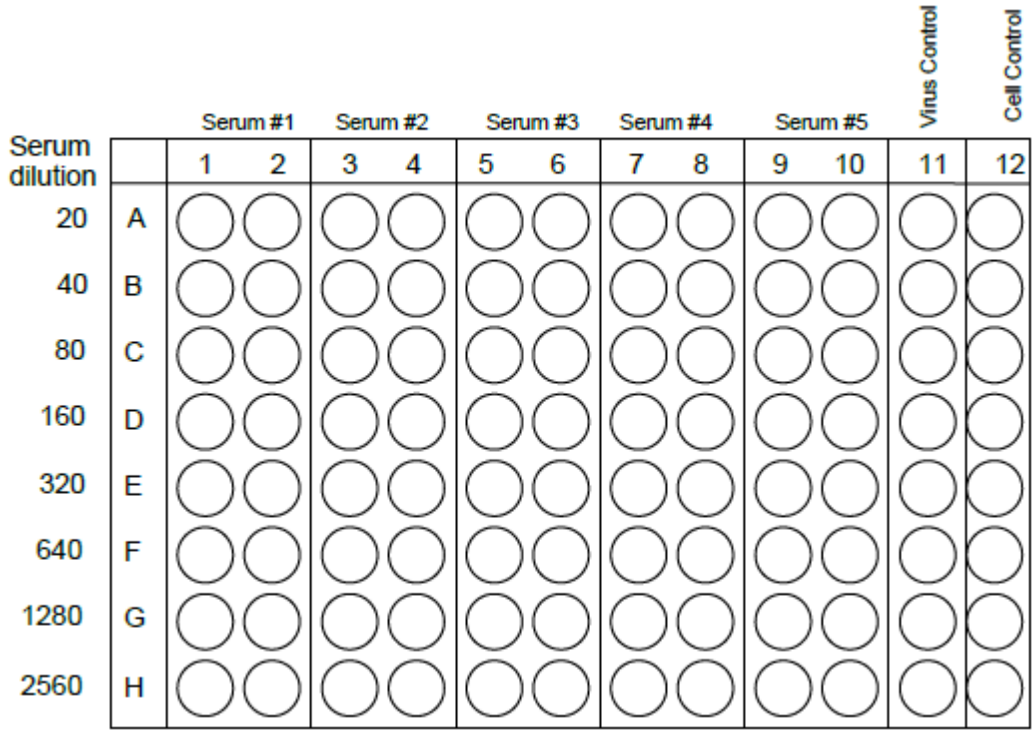

B – 8 Sera/Plate (run duplicate plates)

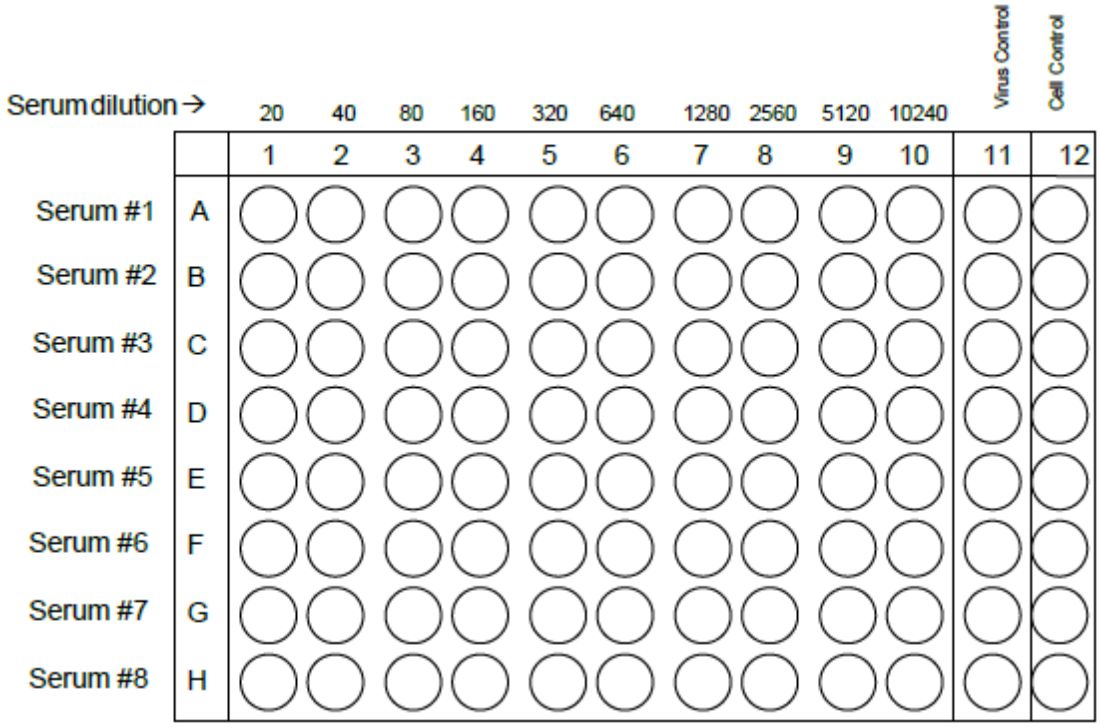

6.2.6. Incubate plate(s) at 37°C, 5% CO_2 for 2 hours to allow virus to infect cells.

6.2.7. Make up the overlay (10ml/plate) and mix well just before addition.

6.2.8. Add overlay (100µl to each well) and incubate at 37°C, 5%CO_2 overnight (18 – 22 hours) undisturbed.

6.3. DAY 3:

6.3.1. Aspirate medium from all wells.

6.3.2. Wash wells 1X with PBS (100µl/well and aspirate.

6.3.3. Add ice-cold **fixative** (100µl/well). Incubate at 4°C for 30 mins.

6.3.4. Aspirate fixative (discard as chemical waste) and wash plate twice with PBS (100µl/well).

NOTE: *Plates can be stored in PBS at 4°C or processed immediately.*

6.3.5. Add 1X permeabilization buffer (100µl/well).

6.3.6. Incubate at RT for 20-30 mins.

6.3.7. Wash plate(s) 3X with wash buffer on automatic plate washer.

6.3.8. Add diluted 1° Antibody (50µl/well) to all wells of 96 well plate(s).

6.3.9. Incubate at RT for 1 hour (or 4°C overnight).

6.3.10. Wash plate(s) 3X with wash buffer on automatic plate washer.

6.3.11. Add diluted 2° Antibody (50µl/well) to all wells of 96 well plate(s).

6.3.12. Incubate at RT for 1 hour.

6.3.13. Wash plate(s) 3X with wash buffer on automatic plate washer.

6.3.14. Add substrate (50µl/well).

6.3.15. Incubate at RT for 10 mins.

6.3.16. To stop the reaction, rinse plate(s) 5X with cold tap water or deionized water.

6.3.17. Dry plate and store in a dark place.

6.3.18. Scan the plate by using ImmunoCapture program.

6.3.19. Count the foci by using CTL BioSpot Analyzer.

6.4. USE OF IMMUNOSPOT ANALYZER TO SCAN THE PLATES

6.4.1. Optimize for assay. Typical counting parameters are listed.

6.4.2. Specify a plate type. Simply click on the proper plate type. “96 well costar-bottom light only” will be selected for the Focus Reduction Neutralization Assay.

6.4.3. Set the plate name and destination folder. Place the plate carefully on the tray, load the plate, and specify the folder into which the scan results will be stored.

6.4.4. Set the scan options. The Preselect Wells button calls up the Plate Navigator, which allows you to specify which wells should be scanned. "Auto Center for Each Well" is selected, and the software will attempt to individually center each of the wells within the camera's field of view.

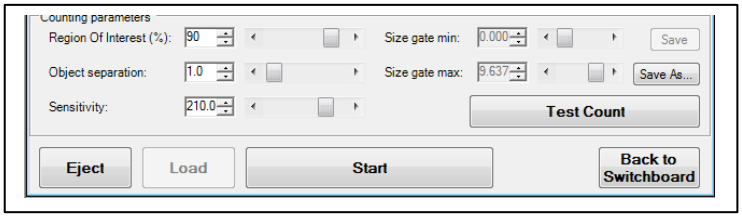

6.4.5. Counting Parameters

6.4.6. Capture Format Selection

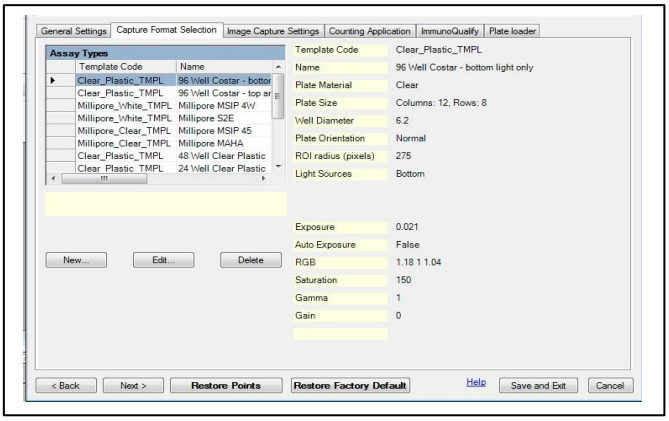

6.4.7. Image Capture Settings

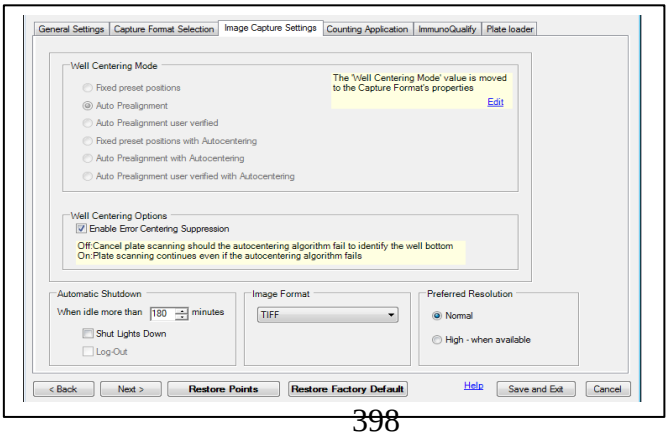

6.4.8. Counting Application

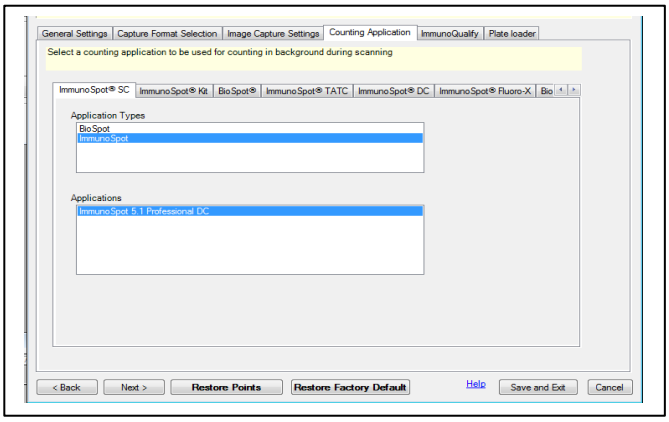

6.4.9. Start the plate scan.

6.4.10. Plates are stored as Excel files which can be imported into spreadsheet and analyzed using parameters in DATA ANALYSIS

6.5. USE OF BIOSPOT TO COUNT FOCI

6.5.1. Select the plates to be counted. Load all the plates to be analyzed by selecting the "Load plate(s)" button near the top of the screen.

6.5.2. Set the counting parameters. Click on the "Load parameters" button. We have the option of loading previously recorded spot recognition parameters, sensitivity 100, 150, 176 and 200. These parameters are stored in templates, which can be loaded from "Template repository".

6.5.3. Start the counting process.

6.6. DATA ANALYSIS

6.6.1. **Cell control (CC) and virus control (VC)** – Calculations are determined for each plate individually. The cell control should be counted ≤20, and the virus control should be counted between 200 and 1600 spots.

6.6.2. **Serum Titer** – Virus reduction is reported as the reciprocal of the highest dilution

of serum corresponding to 50% foci number reduction compared to virus control.

6.6.2.1. **50% Reduction =** (AVG VC – AVG CC)/2